MDC E0681

FIELD REPAIR OF COATED COLUMBIUM THERMAL PROTECTION SYSTEMS (TPS)

FINAL REPORT

MCDONNELL DOUGLAS ASTRONAUTICS COMPANY - EAST

MCDONNELL DOUGLAS CORPORATION

COPY NO. 2

FIELD REPAIR OF COATED COLUMBIUM THERMAL PROTECTION SYSTEMS (TPS)

MDC E0681

15 SEPTEMBER 1972

FINAL REPORT

PREPARED BY
JOHN D. CULP

SUBMITTED TO
NASA – MARSHALL SPACE FLIGHT CENTER
UNDER CONTRACT NO. NAS 8-26121

MCDONNELL DOUGLAS ASTRONAUTICS COMPANY • EAST
Saint Louis, Missouri 63166 (314) 232-0232

MCDONNELL DOUGLAS CORPORATION

ABSTRACT

The purpose of the program was to define the requirements for field repair of coated columbium panels; to develop simple, effective repair methods; and to prove the structural integrity of the developed repairs.

The initial technical consideration was to define the requirements for field repair coating. Probable causes of damage were identified and testing was conducted which established that coatings have a significant tolerance to local damage. It was further established by structural panel specimen testing that unrepaired coating damage on the skin was not of structural significance.

The major task was to develop field repair coating methods. The following types of repair methods have been developed, proven reliable, and are ready for use on an operational system:

- o replacement of the fused slurry silicide coating by a short processing cycle using a focused radiant spot heater
- o repair of the coating by a glassy matrix ceramic composition which is painted or sprayed over the defective area
- o repair of the protective coating by plasma spraying molybdenum disilicide over the damaged area employing portable equipment.

Each of the repair methods meets the criterion of being applied quickly and easily in the field and has the protective ability to prevent oxidation for over 100 reuse cycles.

A technical objective was to prove that the developed repair methods were able to protect the columbium panels for over 100 reuse cycles in a test sequence which imposed the environmental parameters expected to be experienced during actual service. The primary evaluation consisted of reentry flight simulation testing in which coated panels with repaired skins were subjected to the temperatures, air pressures, and loads of reentry. After each series of reentry profile cycles, the panels were subjected to a static boost load equivalent to a limit load. Finally, the panels were subjected to a simulated boost acoustic fatigue loading test.

The final task of the program was to produce two full-size (20 by 20-inch) rib stiffened panels with repair coating on the skin. Each of the panels had a total of 20 individual repair sites. This demonstrated that quality flight hardware could be produced and that the field repairs could be satisfactorily applied to full-size flight hardware.

FOREWORD

This is the final report for the Field Repair Program conducted under Contract NAS8-26121. The program was conducted between June 1970 and October 1972. Mr. James Carter, of Marshall Space Flight Center, was the technical contract monitor and Mr. John Culp of McDonnell Douglas Astronautics Company - East was the study leader. The contributions of the following individuals are acknowledged: R. G. Gregory, Strength Analysis and Rib Stiffened Panel Optimization Study; J. R. Suhre, Structural Dynamics; F. S. Pogorzelski, Panel Fabrication; E. J. Settlemoir, Damage Tolerance Testing and Ceramic Repair Coating Development; E. Malakelis, Diffusion Barrier Application Studies; G. Wille, Plasma Needle Repairs; M. B. Munsell and D. N. Drennan, Profile Evaluation of Panel Specimens; W. E. Noonan, Acoustic Testing; H. S. Ingham, of Metco, Plasma Sprayed Repair Development; and B. Reznik and G. Pepino of Sylvania, Lamp Repair Development.

TABLE OF CONTENTS

TABLE OF CONTENTS (Continued)

TABLE OF CONTENTS (Continued)

TABLE OF CONTENTS (Continued)

LIST OF PAGES

1. INTRODUCTION

Coated columbium could be used effectively as a thermal protection system material for the Space Shuttle or other multimission hypersonic reentry vehicles. Although the coatings are hard and tenacious, some local coating damage must be anticipated with a functionally operational system. It is important for economic and schedular reasons that such local coating damage be capable of rapid and easy repair in the field. The purpose of this program was to provide reliable, practical, and efficient field repair methods.

The initial problem, that of considering the requirements for field repair, was divided into the following efforts:

a) to determine the damage tolerance of coated columbium and demonstrate the type of damage which would require repair

b) to examine the worst case in which critical damage was not repaired.

Probable damage causes were identified, and damage tolerance testing was conducted for each cause in order to describe the types of physical evidence of coating disturbance serious enough to require repair. The effect on the structural integrity of panels with unrepaired critical damage was ascertained by testing panel specimens in a simulated reentry environment to determine the structural implications of unrepaired damage to panel skins.

The major emphasis of the program was on development of field repair methods and procedures. The approach to field repair development was to divide the effort into 1) repairs effected by replacing the fused slurry silicide coating, and 2) repairs effected by adding a new material over the damage site. In replacing the fused slurry silicide coating, attention focused on methods which could be accomplished rapidly and easily in the field and which would not necessitate reproducing the involved, complicated original coating process sequence. For repairs effected by adding a secondary material to the defect area, emphasis was placed on ceramic composition repairs and plasma sprayed repairs, both of which could be accomplished readily in the field. Conventional testing and evaluation procedures were employed in development of the repairs. The final evaluation of the repair systems employed rib stiffened panel specimens of representative size, 3 by 12 inches, which were tested under projected environmental service conditions. The flight simulation testing included alternate exposure sequences of boost acoustic loads, static critical loads, and simultaneous reentry conditions of

temperature, air pressure, and bending stress as a function of reentry time. Testing was conducted through 110 mission cycles to establish the operational readiness of the repair systems.

The final activity of the program was to construct full-size flight quality columbium hardware and demonstrate that each of the repairs was applicable to actual hardware. A highly efficient rib stiffened panel design with 0.010-inch thick skins was selected. Panels of both Cb-752 and C-129Y columbium alloys were fabricated and coated. A total of twenty repair sites were applied to defect areas intentionally cut into the skin coating for each panel. Repairs were effected and the panels were submitted to NASA for evaluation.

2. MATERIAL SELECTION AND PROCUREMENT

Two columbium base alloys, Cb-752 and C-129Y, were designated as the substrates for development and evaluation of the field repair coatings. These alloys have good strength at both room and elevated temperatures, can be fabricated readily into typical hardware configurations, and are weldable. The Cb-752 was purchased from Fansteel Metallurgical Corporation and the C-129Y from Wah Chang-Albany. Vendor certified chemical analyses of the final sheet product were:

Element	Percent by Weight	
	Cb-752	C-129Y
Carbon	0.0092	0.0050
Oxygen	0.0044	0.0110
Hydrogen	0.0005	0.0004
Nitrogen	0.0070	0.0056
Iron	0.0010	0.0050
Silicon	0.0010	0.0050
Molybdenum	0.174	0.0125
Titanium	0.005	0.004
Yttrium	--	0.12
Hafnium	--	10.05
Tantalum	0.43	0.37
Tungsten	9.80	9.40
Zirconium	2.65	0.39
Columbium	Balance	Balance

The vendor certified transverse physical properties of the sheet material were:

Property	Cb-752	C-129Y
Room temperature tensile (lb/in^2)		
ultimate	79,000	89,700
yield	59,000	74,000
% elongation	31	30.5
2200°F tensile (lb/in^2)		
ultimate	27,000	---
yield	25,000	---
% elongation	95	---
ASTM grain size	8	9.5

The interstitial contents and mechanical property values of the Cb-752 and the C-129Y fall within the range of what is considered typical.

Coatings designated for use were the Sylvania R-512E system for the Cb-752 alloy and the VAC-HYD VH-109 system for the C-129Y. Both are fused slurry silicide coatings with different chemical compositions. In many cases, the fused slurry silicide coatings show better oxidation life properties on one alloy than another. There was evidence available at the time of coating selection to indicate that the coatings chosen for the respective alloys were the longest life coatings available.

There was a clear advantage to employing two coating/alloy systems in the program, since the applicability of the developed repairs would not necessarily be restricted to one system. There were several times within the program in which the two alloys or coatings exhibited significantly different properties. The simultaneous testing of two systems was invaluable in identifying characteristics attributable to either the alloy or the coating. Thus, the technical base of the program was broadened greatly.

3. SPECIMEN FABRICATION AND COATING

Test hardware was required throughout the program to develop and evaluate field repair systems. Simple sheet material coupons and rib stiffened panels were employed. The rib stiffened design was selected to represent typical flight hardware since it was weight efficient, could be reliably coated, and was easy to inspect.

3.1 COUPONS - Coupons, 2 by 2 inches and 1 by 2 inches in size, were prepared from 0.020-inch sheet material of both Cb-752 and C-129Y alloy materials. All coupons were used to determine the damage tolerance of coated columbium, to develop field repairs, and to evaluate oxidation resistance of candidate repair systems. The Cb-752 coupons were fused slurry silicide coated with the R-512E composition by Sylvania to a nominal total coating thickness of 3 mils per surface.

The initial group of 2 by 2-inch coupons of the C-129Y alloy was coated by VAC-HYD with the VH-109 system. A nominal total coating thickness of 3.0 mils per surface (dimensional change of 2.0 mils per surface) was requested. The coupons received had an average dimensional change of 7.4 mils total (assuming one-half the coating on each surface not valid in this case) and many coupons were severely warped. Metallographic examination of these coupons revealed that the thicker, concave side had an average thickness of 5.5 mils and the thinner, convex surface had an average thickness of 3.7 mils. By comparing substrate thicknesses before and after coating, the amount of metal consumed in producing these coatings was determined to be 3.4 mils. The uneven and excessively thick coatings were reported to VAC-HYD, with a concern expressed for the critical rib stiffened panel specimens which were to be coated. In a cooperative effort to correct this problem, VAC-HYD personnel obtained a supply of the same heat of C-129Y from Wah Chang, prepared 40 duplicate coupons, and applied the VH-109 coating. This second group of specimens was not warped and had a smoother and generally improved appearance when compared with the initial set of coupons. The coating thickness was found to be approximately equal on both sides of the coupon; the average total coating thickness (measured metallographically) was 3.5 mils per surface and the average dimensional change thickness was 2.3 mils per surface. Subsequent groups of coupons had acceptable coating thicknesses with a dimensional change thickness of 3.0 to 3.5 mils per surface.

3.2 RIB STIFFENED PANEL SPECIMENS (1 by 4 INCHES) - Rib stiffened panel specimens were required for profile simulation testing of defective coatings which were not repaired prior to testing. The panel specimen selected was one employed in past coating evaluations (reference 1) which fit into an existing test facility. The panel test specimen and loading fixture had to fit inside a 1-3/4-inch diameter tube, whose 6-inch long working hot zone permits a uniform temperature in the central 4 inches. The specimen is thus restricted to a 1 by 4 by 0.25 inch size. Figure 3-1 shows the rib stiffened panel configuration and dimensions. Ten panels of each alloy (Cb-752 and C-129Y) were fabricated. After detail parts preparation and chemical cleaning, the ribs were joined to the skins by blind electron beam welding through the skin. Finally, the loading plates were electron beam welded to each end of the ribs and the edges of the panel were rediused.

The Cb-752 alloy panel specimens were R-512E coated by Sylvania. The dimensional change thickness of the skin was 2.3 mils per surface and that of the two ribs was 2.2 and 2.4 mils per surface. The C-129Y alloy panel specimens were VH-109 coated by VAC-HYD. The dimensional change thicknesses were approximately twice those requested, being an average of 4.2 mils per surface on the skin and 3.6 and 3.7 mils per surface on the ribs.

3.3 RIB STIFFENED PANEI SPECIMENS (3 by 12 INCHES) - Rib stiffened panels, 3 by 12 inches, were required to perform structural evaluations of field repair coating systems. The panel specimen is shown in figure 3-2. It was designed to be representative of a full-size rib stiffened panel in all respects except the overall dimensions, which were selected to fit into a load fixture used in conjunction with a 7-inch diameter tube furnace. Two groups of 3 by 12-inch panels were fabricated, with the second group required to eliminate a skin distortion condition present in the first group.

The fabrication of the 3 by 12-inch panel specimens shown in figure 3-1 was accomplished using two columbium alloys, Cb-752 and C-129Y. The required sheet material was chemically milled or chemically cleaned to indicated gauges within 0.001 inch. Detail parts were sheared and the ribs were machined to final dimensions to insure parallel edges. The tool for electron beam welding was designed to align the welding beam with the center of one rib and the rib was then blind welded through the skin. Subsequent ribs were joined to the skin by moving the initial rib to an adjacent locating slot without changing the location of the tool with respect to the welding beam. The second rib was then secured in the identical tooling position as the first rib, and then welded to the skin. Subsequent ribs

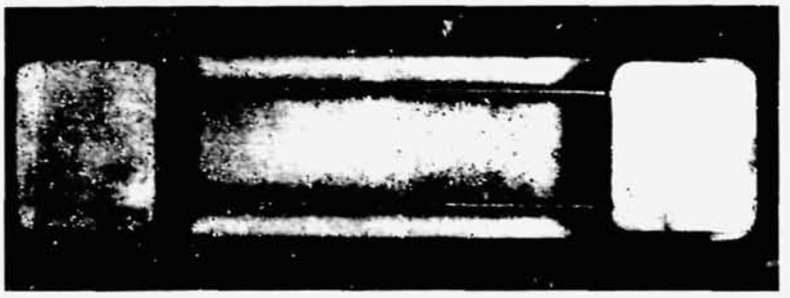

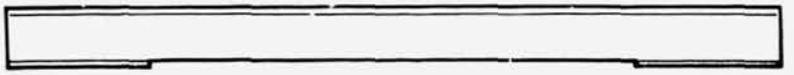

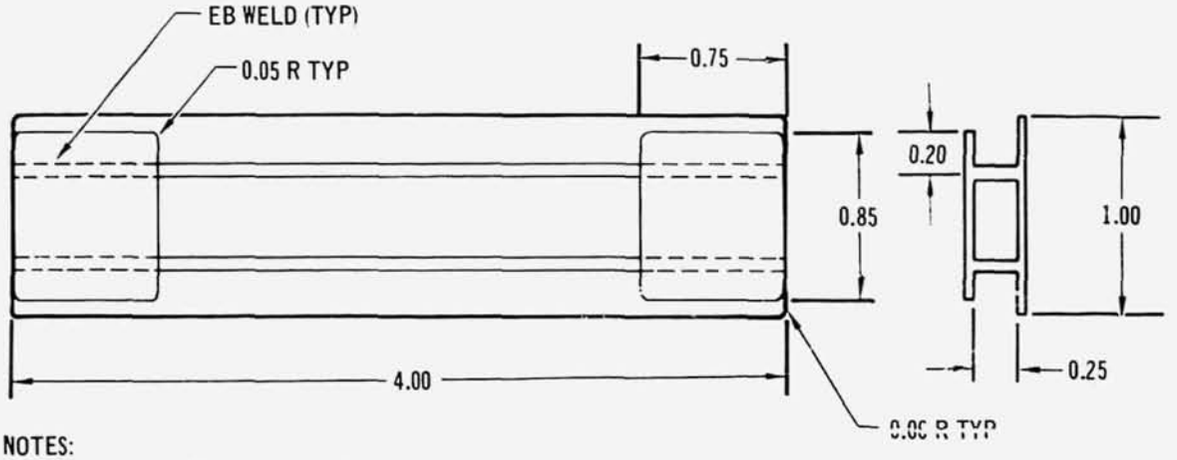

NOTES:
(1) PANEL SKIN 0.008" AFTER COATING
(2) PANEL RIBS 0.016" AFTER COATING
(3) ALL DIMENSIONS ARE IN INCHES.

RIB STIFFENED PANEL SPECIMEN

457-1154

Figure 3-1

were then added to the panel assembly in a similar fashion. After the ribs had been joined to the skin, the straps on the reverse side of the ribs were electron beam welded in place. The final step was to radius the edges to insure good coating quality.

The fusion welding of the skin to the ribs caused a noticeable amount of distortion. Typical examples of this distortion are shown in figure 3-3. The longitudinal bowing of the panels produced a nominal deflection of 0.07 inch in the center of the span and a series of ripples, or buckling of the skin, between the ribs. The maximum depth of the buckles, 0.08 inch occurred in the center of the panel and the buckling of the skin was not noticeable on the unsupported edges.

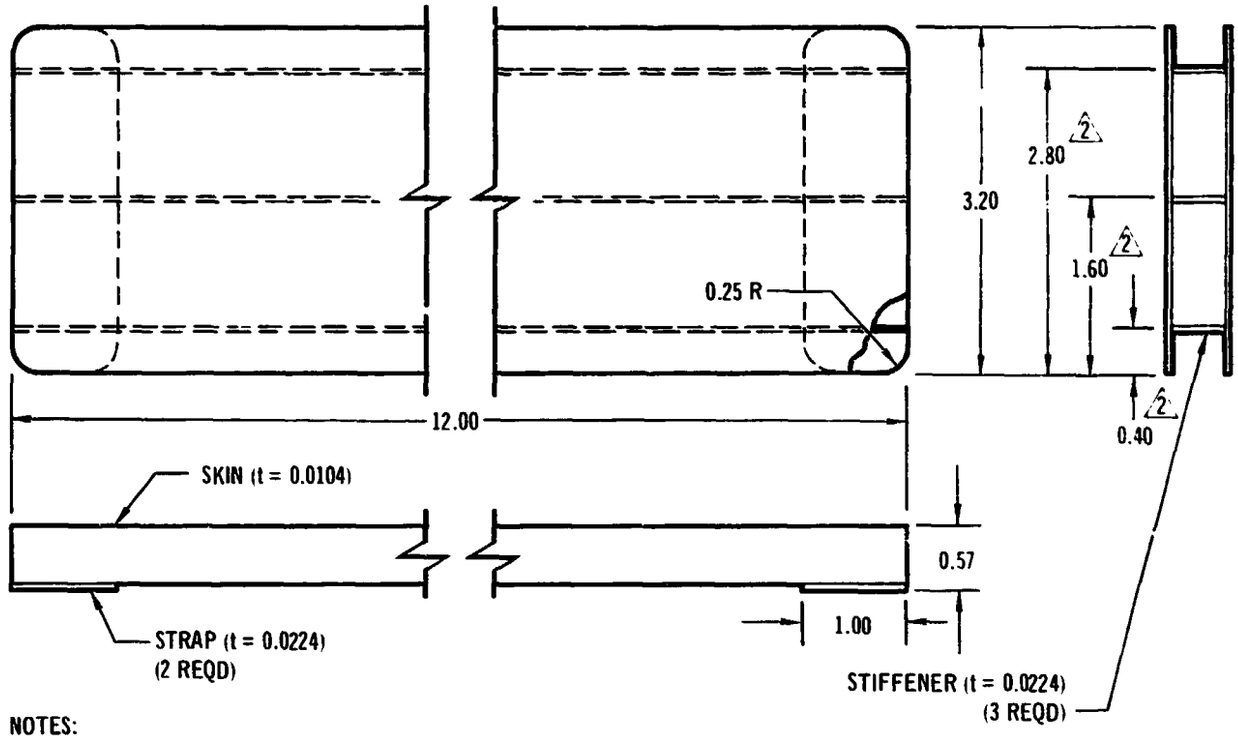

NOTES:
1 – EB WELD STIFFENERS TO SKIN AND STRAPS
2 – DIMENSIONS LOCATE ℄ OF STIFFENERS
3 – DIMENSIONS ARE IN INCHES

457-1709

RIB STIFFENED COLUMBIUM PANEL SPECIMEN

Figure 3-2

It was considered unlikely that the waviness, or skin buckling, could be removed during a stress relief cycle. Since the panels would be thermally stabilized for testing during the coating process, a special stress relief cycle was not employed. While the appearance of the panels was less than desirable, the panels were considered structurally acceptable and it was decided to proceed with the profile testing of the panels as described in section 12. Because the acoustic boost simulation portion of the evaluation showed the skin distortion buckles to be dynamically unstable, fabrication of a second group of panels was initiated.

The undesirable skin distortion was caused by shrinkage of the electron beam fusion weld which joined the ribs to the skin. The rib thickness was 0.022 inch and the skin was 0.012 inch thick. Because the 0.012-inch skin was not of sufficient strength and stiffness, it buckled between the ribs. The problem of producing distortion-free rib stiffened panels was attacked using two simultaneous approaches. The first approach was to prevent distortion during welding by altering the welding

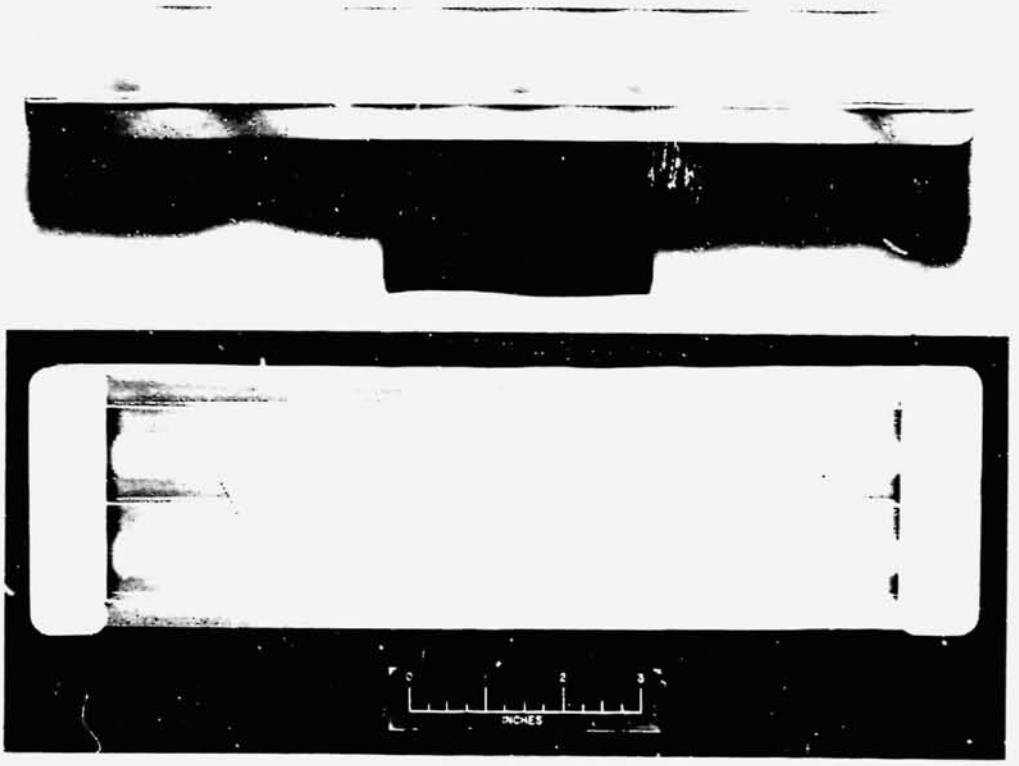

457-1693

Showing Skin Distortion

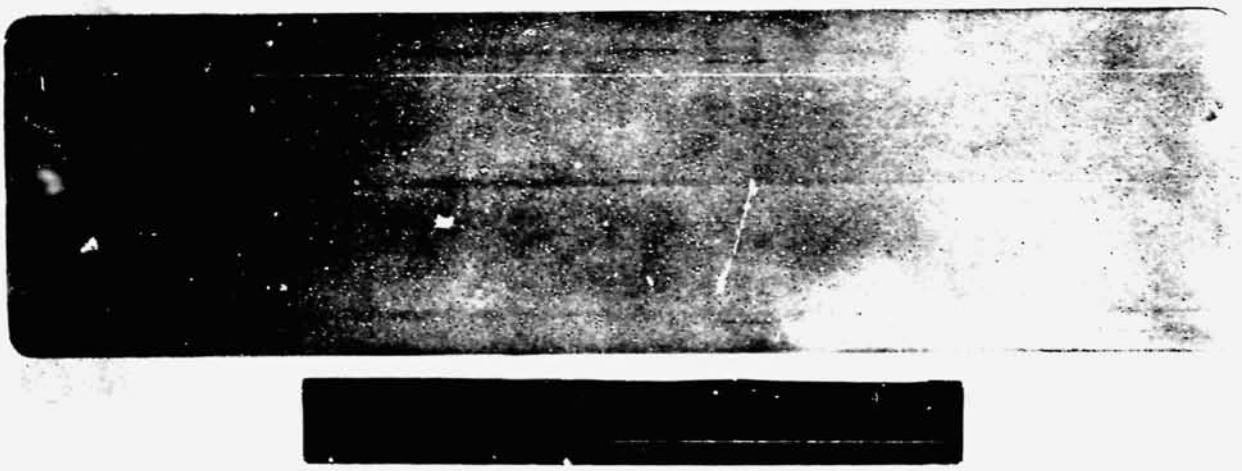

457-2887

After Distortion Removal by Creep Straightening

RIB STIFFENED PANEL SPECIMEN

Figure 3-3

parameters to reduce the heat input and weld shrinkage or to increase the gauge of the skin to resist distortion. The second approach was to allow the distortion to occur during welding and then to remove it by creep forming. The creep forming would require that the ribs be straightened to remove the bow, thus allowing the skin to remain flat.

A welding parameter study was conducted in which the total heat input was minimized. The only constraint on weld nugget size was that the total thickness of the rib had to be joined to the skin so that no crack or faying surface occurred. Several voltage and amperage combinations were tried for three welding speeds ranging up to 200 inches per minute. A measurable but insufficient reduction of skin distortion for the 0.012-inch skin to 0.022-inch rib combination was achieved. Welding parameters were then established for a rib stiffened configuration of 0.020-inch skin and 0.022-inch ribs. Test panels of this gauge combination were successfully welded and the skin distortion was completely eliminated. The increased skin thickness produced a 30-percent weight increase for the panel (an increase of 1.35 lb/ft^2 for 0.012-inch skin to 1.77 lb/ft^2 for the 0.020-inch skin). Since design studies conducted in the beginning of the program had established that only 0.008-inch load bearing skins, after coating, were required to carry the necessary loads, it was decided that the less weight-efficient design employing the 0.020-inch skin would be used only as a last resort.

The second approach, creep forming the rib stiffened panels after welding, was investigated. Experiments were conducted in which rib stiffened skins were straightened by placing machined molybdenum bars between the ribs to provide dead weight loading while the part was heated in a vacuum. Results from the first experiments were good and it was established that 1 hour at 2700°F with a normal pressure of 0.6 lb/in^2 was sufficient to remove the bow in the ribs and the waviness of the skin. A tool (shown in figure 3-4) of sufficient size to creep straighten a 20 by 20-inch rib stiffened panel was constructed of TZM alloy molybdenum. The tool was used to straighten eight 3 by 12-inch panels and four 4 by 10-inch panels. All of these panels were successfully straightened without cracks or other damaging effects and were flat and distortion free. Figure 3-5 shows a full size panel before creep straightening, and figures 3-3, 3-7 and 3-8 show panels after creep straightening.

The rib stiffened panels were fused slurry silicide coated and the R-512E coating was applied to the Cb-752 alloy panels. The first group of panels had a dimensional change coating thickness of 1.6 mils per surface on both the skin and

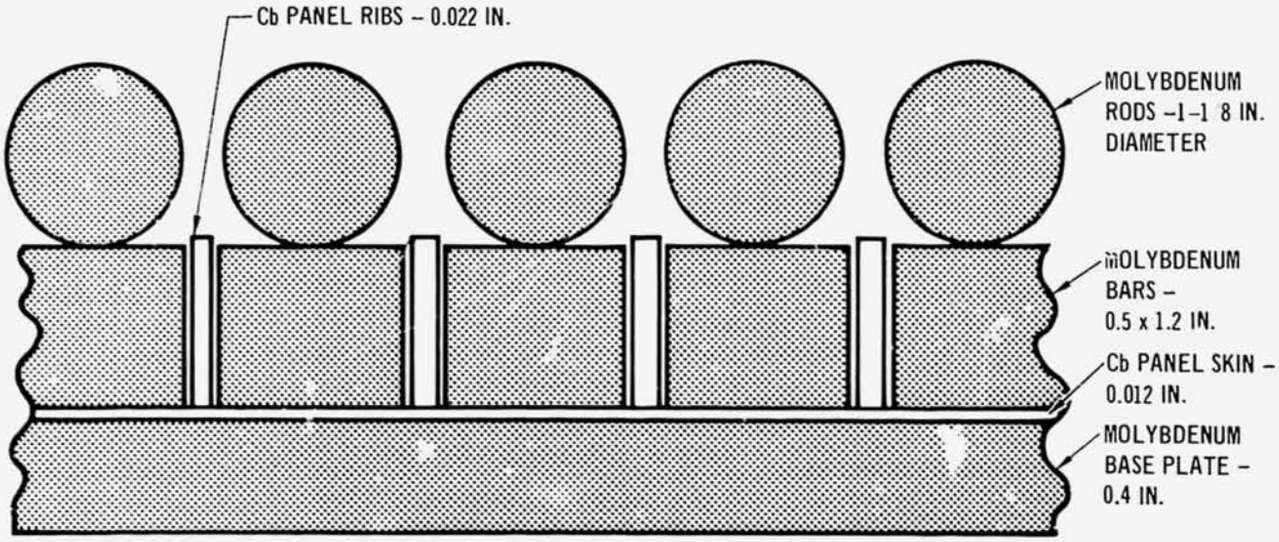

457-2863 RIB STIFFENED PANEL IN MOLYBDENUM CREEP STRAIGHTENING TOOL Figure 3–4

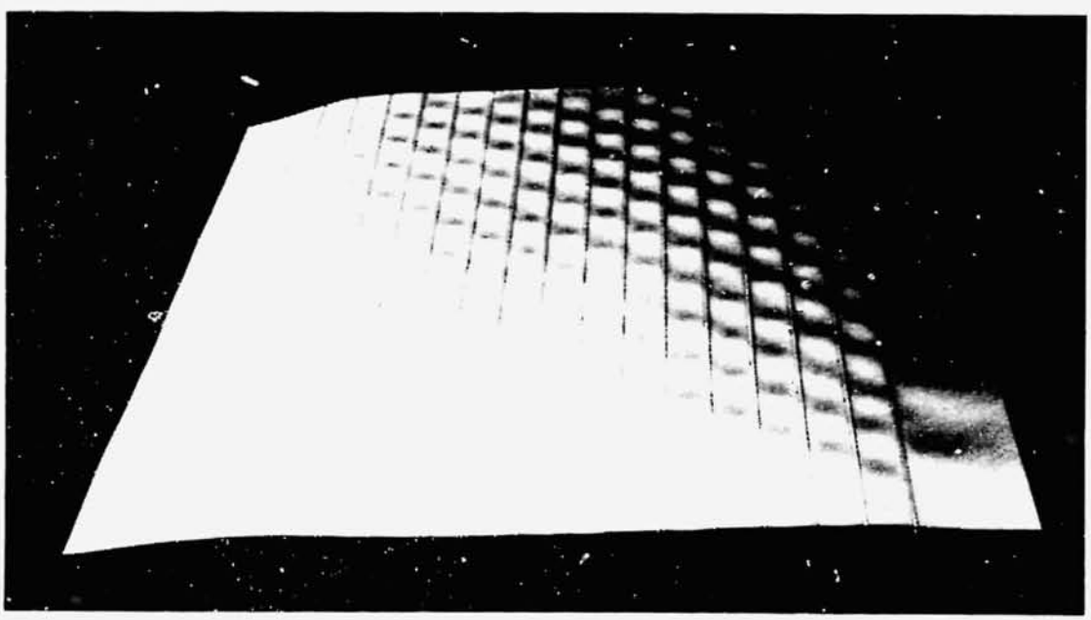

457-2886 20 x 20 INCH PANEL PRIOR TO CREEP STRAIGHTENING

Figure 3–5

ribs and the second group of Cb-752 alloy panels had an average R-512E coating dimensional change thickness of 1.9 mils per surface on both the skins and on the ribs. The first group of C-129Y panels was VH-109 coated to a dimensional change thickness of 1.4 mils per surface on the ribs and 3.3 mils per surface on the skins. The second group of C-129Y panels had a dimensional change coating thickness of 1.8 mils per surface on the ribs and 2.7 mils per surface on the skins.

3.4 SINGLE FACED CORRUGATED PANELS - Initial development and testing of field repair coating procedures was conducted on coupons. A necessary subsequent step was to demonstrate that the repair methods developed were applicable to representative hardware, and that the thin skins being employed were not permanently distorted or otherwise damaged during the repair procedure. The primary hardware design being employed to evaluate repair coatings was the rib stiffened design. Initial attempts at fabricating 3 by 12-inch rib stiffened panels having a 1.2-inch rib spacing produced skin waviness between the ribs, a distortion which would make accurate and meaningful skin distortion measurements difficult. It was decided to employ a single faced vee corrugated panel since a flat, smooth skin could be produced without the delay that would occur while the skin waviness problem was being solved for the rib stiffened design. The single faced vee corrugated panels were of the same skin thickness (0.012 inch before coating) and stiffener spacing (1.2 inches between centers) as those of the rib stiffened panels. The overall panel size was 7.2 inches square so that the center of the panel would not be affected by edge considerations.

The skin and corrugation were joined by the FUDJ (forged upset diffusion joining) welding method, a process which does not require a fusion weldment to be formed, thus avoiding the skin distortion associated with weld shrinkage. Detail parts were fabricated from Cb-752 and C-129Y columbium alloy sheet. After the parts were chemically cleaned, they were put through a roll seam welding machine with one flat wheel for the skin side of the panel and a vee profile wheel (0.03-inch edge radius) matching the shape of the vee corrugation. The operating parameters were selected to produce less than sufficient heat to form a cast nugget and enough pressure to forge the two surfaces into intimate contact. The product at this point was only superficially joined. A vacuum diffusion treatment, in which the joint became diffusion bonded, was conducted at 3000°F for 1 hour. Figure 3-6 shows the skin and corrugation surfaces of a typical panel prior to coating. Although the skins were flat and smooth, a minor problem was experienced with unbonded areas. The unbonded areas were reprocessed through the roll seam welder and diffusion cycle to repair the unbonded areas. The panels were then fused slurry silicide coated to a nominal total coating thickness of 3 mils per surface.

3.5 RIB STIFFENED PANELS (20 by 20-INCHES) - Two full-size rib stiffened panels, one of Cb-752 and one C-129Y alloy, were required to demonstrate the final repair developed on the program. These panels were delivered to NASA for final evaluation testing of the field repair coatings. Panel fabrication was performed using the same tools and procedures employed with the second group of 3 by 12-inch

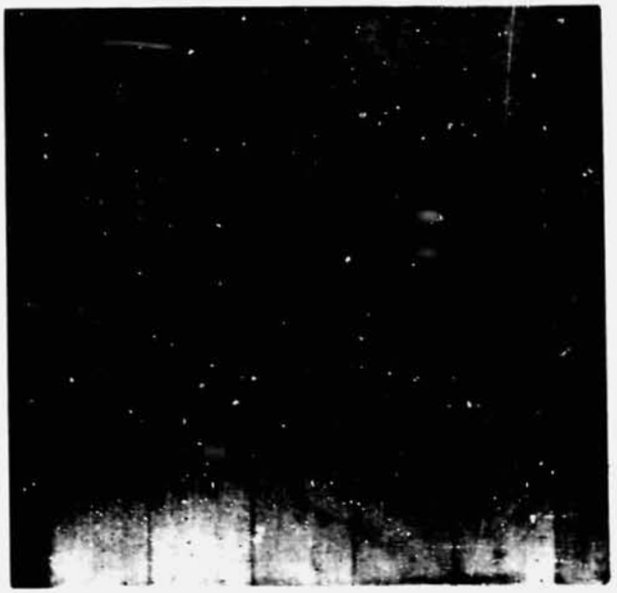

Skin Surface

Vee Corrugation Surface

457-2822

FUDJ WELDED Cb-752 PANELS FOR VERIFYING FIELD REPAIR APPLICABILITY TO REPRESENTATIVE HARDWARE

Figure 3-6

rib stiffened panel reported in section 3.3. After creep straightening, the skins were flat and distortion free. Both panels were fused slurry silicide coated to a nominal total coating thickness of 3.0 mils per surface. The Cb-752 panel was coated with the R-512E and the C-129Y alloy panel with the VH-109 coating. Figures 3-7 and 3-8 show the panels after coating application.

SKIN SURFACE

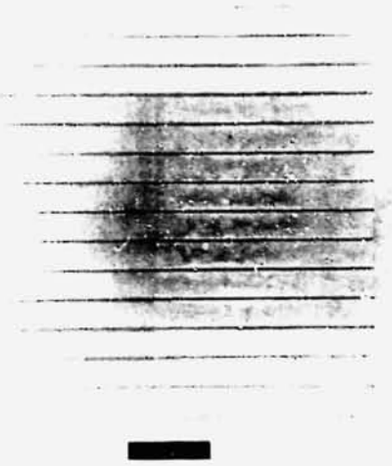

RIB SIDE

C-129Y ALLOY RIB STIFFENED PANELS (20 BY 20-INCH) WITH VH-109 PROTECTIVE COATING

Figure 3-7

SKIN SURFACE

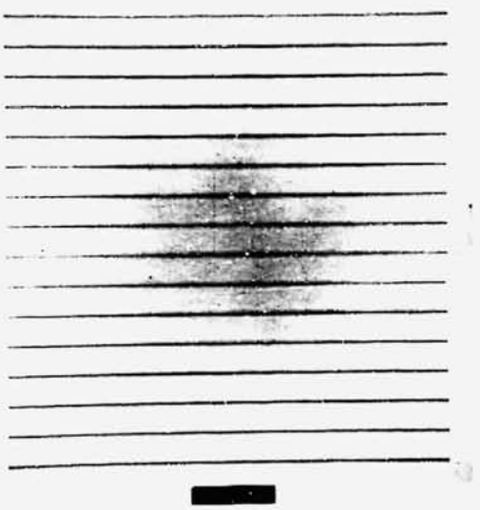

RIB SIDE

Cb-752 ALLOY RIB STIFFENED PANELS (20 BY 20-INCH) WITH R-512E PROTECTIVE COATING

Figure 3-8

4. TEST CONDITIONS

The evaluation of developed field repairs and the profile simulation testing of panel specimens required the selection of a set of test conditions. These test conditions were selected to be representative of a Space Shuttle operational system. Instead of selecting a particular trajectory and point on a specific vehicle, the necessary parameters of time, temperature, pressure, and stress were studied separately. An attempt was made to insure that the full effect of each parameter would be imposed upon the test specimen in a realistic manner. The test conditions had to be representative of the general environmental conditions of the several Shuttle vehicles and missions under consideration, as well as of probable future vehicles. Each of the test parameters will be discussed separately and the rationale for its definition described. The initial test conditions selected are shown in figure 4-1. The flight simulation testing of 3 by 12-inch rib stiffened panel required the use of a 7-inch diameter tube furnace. This furnace would not cool at the required rate and the profile was extended to 1 hour elapsed time. The same temperature pressure, and stress relationships were maintained throughout and are described in section 12.

4.1 TEST TIME - The major influence on test duration was the selection of either a low or high cross range mission. A high cross range time of 2700 seconds was chosen. This is longer then the majority of vehicles surveyed; however, the longer time is a conservative approach which also makes the test results applicable to a wider range of reentry vehicle systems.

4.2 TEST TEMPERATURE - A great many factors were considered in selecting the test temperature profile. Figure 4-2 illustrates some of the parameters surveyed and factors considered (reference 2) The double peak condition illustrated in figure 4-2 was selected as the most severe condition since it represents the greatest time at elevated temperature and also the greatest total heat input for equivalent maximum temperature of a single peak condition. Figure 4-3 shows the temperature as a function of time for the high cross range orbiter used as a guide in selecting the test profile. A maximum temperature of 2400°F was selected, since it is equal to, or higher than, most temperatures surveyed. The selected temperature profile shown in figure 4-1 employed a procedure of comparing the time at or above 2,000, 2,200 and 2,400°F for several possible temperature profiles to insure that the selected conditions were broadly representative. The position of the peak and the cooling rate reflect the capabilities of the testing facility.

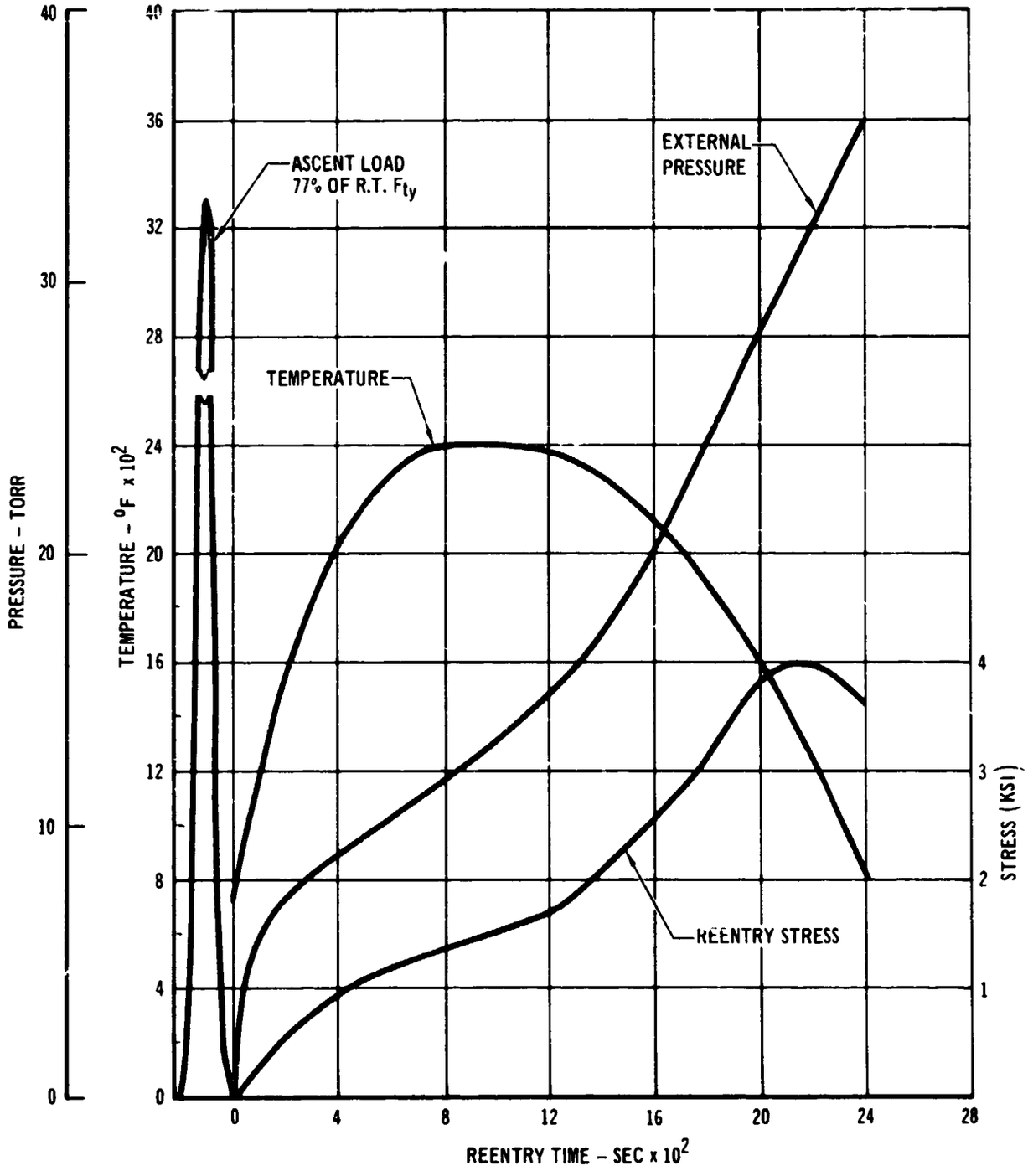

REENTRY PROFILE TEST CONDITIONS

457-1157

Figure 4-1

	PHASE A		PRE-PHASE B (ORBITER "B" MOD 1)			PHASE B (DEVELOPED BY MDAC AS OF 8/1/70)		
	LOW CROSS RANGE MSC–ILRV	HIGH CROSS RANGE (SAMSO)	LOW CROSS RANGE *	MEDIUM CROSS RANGE *	HIGH CROSS RANGE *	HIGH CROSS RANGE MARK I SHAPED - 2000°F INCLUDES [illegible]GINS	[illegible] RANGE [illegible]WBRIDGE LOW ALTITUDE DISPERSED INCLUDES DESIGN MARGINS	LOW CROSS RANGE LOW ALTITUDE DISPERSED 60° BANK NO DESIGN MARGINS
CROSS RANGE (NMI)	231	2,000	350	1,260	1,700	1,500	2,180	140
DOWN RANGE (NMI)	2,000	9,800	2,800	5,400	6,500	6,300	6,500	2,100
$W/C_L S$ (W/S)	(30)	(53)	73	108	156	118	216	60
L/D	0.54	2.2	0.7	1.45	1.75	1.75	2.0	0.52
VEHICLE LENGTH (FT)		160	170	170	170	156	148	148
ENTRY ANGLE (DEG)	–1.6	–1.5	–1.6	–1.6	–1.6	–1.6	–1.6	–1.6
ENTRY TIME (SEC)	1,260	3,100	1,138	2,079	2,523	2,590	2,755	720
ANGLE OF ATTACK (DEG)	60	43–20	53	31	23	14–20	18	60
MAXIMUM DYNAMIC PRESSURE (LBF/FT^2)	35–40		75	125	182	112	272	56
MAXIMUM SURFACE TEMPERATURE (°F)	2,200	2,200	2,100	2,100	2,100	2,000	2,200	2,200
TOTAL HEAT (A) (BTU/FT^2)	7,600	44,400	-	–	–	15,989	22,275	5,[illegible]45
TOTAL HEAT (B) (BTU/FT^2)	–	–	–	–	–	17,623	31,950	5,315
TOTAL HEAT (C) (BTU/FT^2)	–	–	6,116	14,699	16,994	15,055	18,305	4,892
TIME AT MAXIMUM TEMPERATURE (±20°) (A) (SEC)	60	60	–	–	–	140	100	75
TIME AT MAXIMUM TEMPERATURE (±20°) (B) (SEC)	–	–	–	–	–	250	230	100
TIME AT MAXIMUM TEMPERATURE (±20°) (C) (SEC)	–	–	20	250	70	50	60	35

$^*\frac{X}{L}$ = 0.25 WITH X = 42.5 FT AND L = DISTANCE FROM THE NOSE ALONG THE BOTTOM ℄

HEAT PULSE SHAPE
(A) EARLY TEMPERATURE PEAK
(B) DOUBLE TEMPERATURE PEAK
(C) LATE TEMPERATURE PEAK

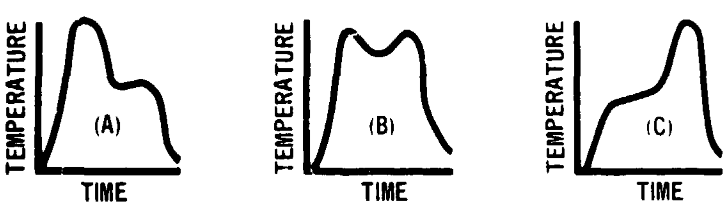

457–1158

SHUTTLE ENTRY TRAJECTORY PARAMETERS

Figure 4–2

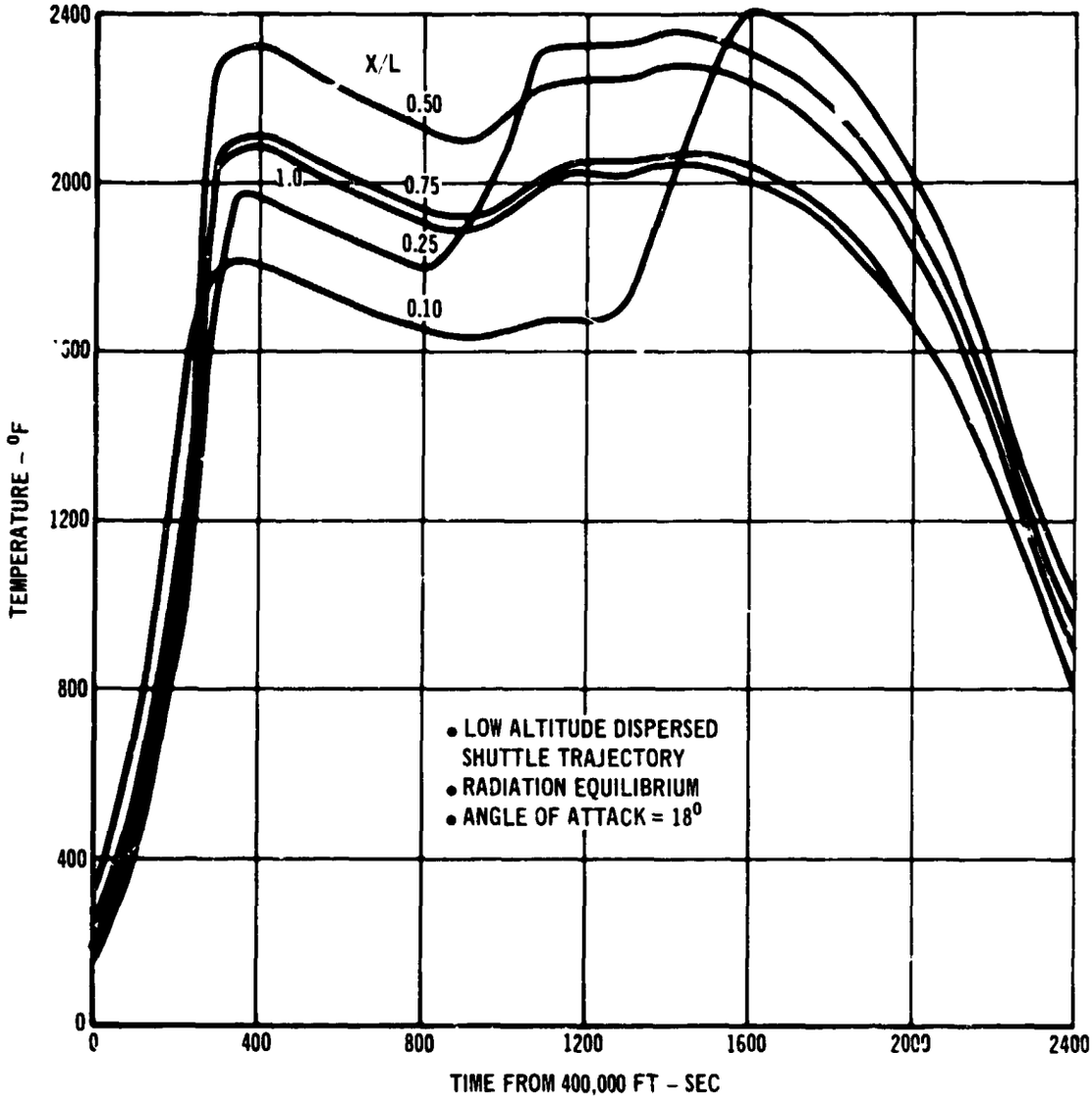

457-1160

TEMPERATURE ON LOWER SURFACE OF HIGH CROSS RANGE ORBITER

Figure 4-3

4.3 EXTERNAL PRESSURE - The air pressure to be employed is an important testing parameter. Since this program is concerned with field applied repairs, the pressure is necessarily restricted to the exterior surface. Figure 4-4 shows the pressure of the lower surface of a high cross range orbiter. It was found that the external pressure variations for various vehicles and reentry conditions were subtle compared with coating performance. The coating and substrate oxidation mechanisms were the same over the range of possible representative pressures that could be selected. The design trajectory for the forward ramp was selected, since it was

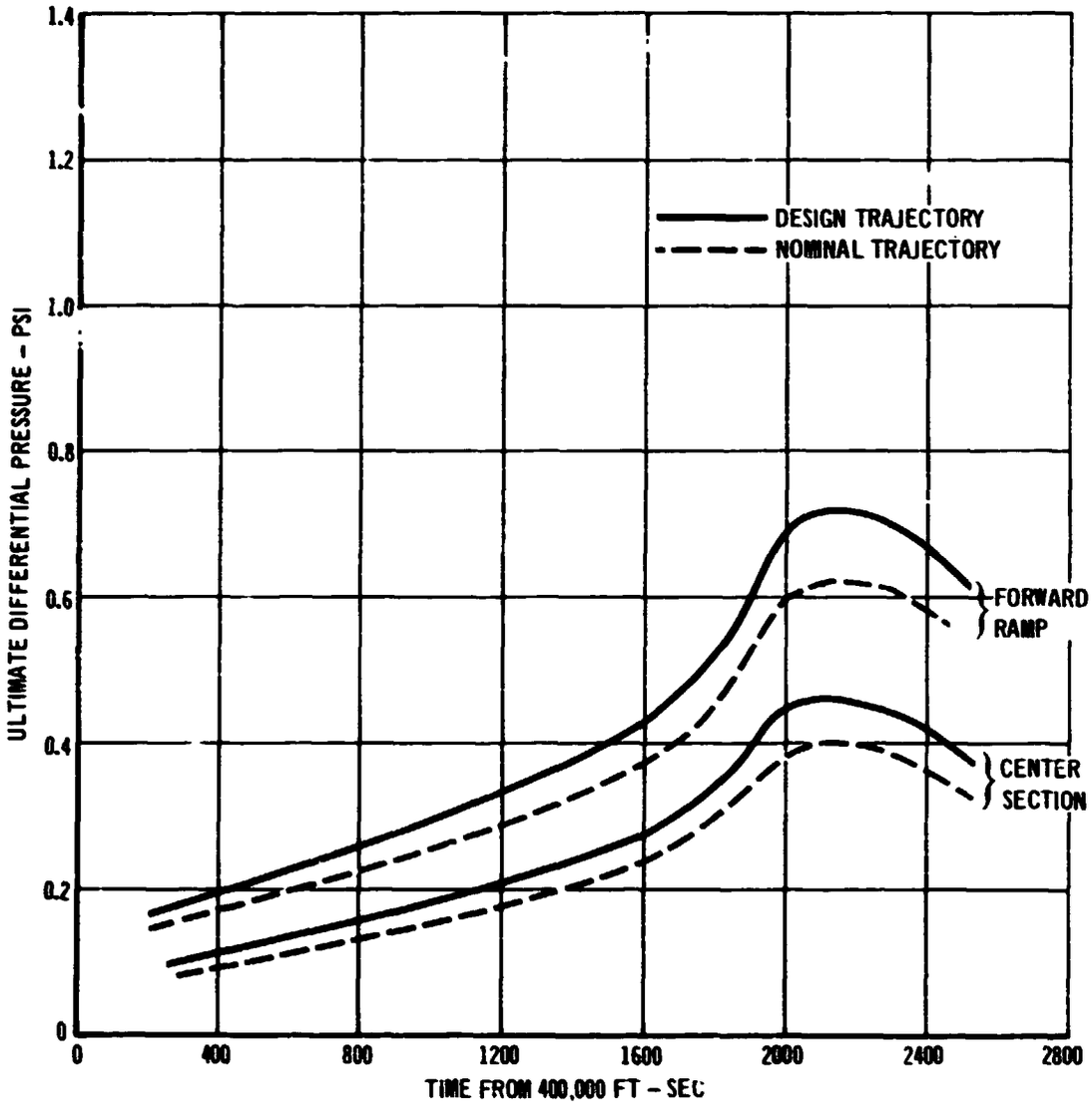

457-1161

SPACE SHUTTLE
HIGH CROSS RANGE ORBITER
BOTTOM CENTERLINE ULTIMATE PRESSURES

Figure 4-4

predicted to be the most severe test for substrate oxidation.

4.4 DESIGN OPTIMIZATION AND STRESS PROFILE CONDITIONS - The proper stress or load to be applied to the panels is a very important environmental test condition because the stressing of columbium substrate affects the protectiveness of the coating. The criterion for failure in the rib stiffened panel specimens was defined as the inability to carry the required loads. The design to be tested had to be defined before the critical member and the appropriate stress level could be determined.

The 1 by 4-inch specimens shown in figure 3-1 were designed to fit into a 1.75-inch testing furnace. Rib depth and rib spacing were not optimized for a full

size panel. It was considered advantageous to optimize the rib stiffened design for a full size panel to determine the proper rib stress to employ. Fabrication of the 3 by 12-inch and 20 by 20-inch rib stiffened pannels for testing in the later stages required this design optimization study; therefore, the study was accomplished before a stress profile for the test conditions was made final.

4.4.1 Rib Stiffened Panel Optimization Study - A strength optimization study was conducted for rib stiffened columbium thermal protection system panels applicable to the Space Shuttle. Panel geometry is shown in figure 4-5. Rib gage (w), skin gage (t), rib spacing (b) and rib height (h) were all varied to obtain minimum weight panels.

Figure 4-5 is an example of the working curves generated in the study. All data on figure 4-5 are for a constant effective thickness (or weight) and a constant skin thickness. The upper curves show ultimate allowable positive bending strengths (causing compression in the skin) and the lower curves represent ultimate allowable negative bending strengths. A plastic bending analysis was used to determine ultimate positive bending strengths. Compression cap strength was based on crippling strength of the flat skin and of a portion of the rib above the neutral axis. The tension cap was assumed to operate at its ultimate tensile stress. Limit negative bending strength (causing compression in the rib) was based on an elastic analysis in which the allowable compressive stress in the rib was based on the rib buckling strength. Ultimate negative bending strength, shown in figure 4-5, was obtained by multiplying limit strength by the safety factor of 1.4.

Constraints were established for the maximum b/t ratio and minimum negative bending strength. Based on previous experience with similar structures, a maximum b/t ratio of 150 was selected to minimize response to acoustic loading. A minimum allowable negative bending strength of 70 in-lb/in was selected, which is based on 1.4 lb/in^2 ultimate pressure acting over a 20-inch span. The negative bending cutoff line, shown in figure 4-5, was used to identify panel cross-sectional properties which meet the negative bending strength requirements. The optimum design moment for this weight is the maximum moment within the b/t cutoff constraint, and the negative moment cutoff line, as shown.

Figure 4-6 is made up from optimum moments determined from curves of the type shown in figure 4-5 which have other effective thicknesses and skin thicknesses of 0.008, 0.012, and 0.016 inch. For any required moment allowable, the 0.008-inch skin thickness (minimum gage) yields the lowest weight design.

The resulting rib stiffened panel design curves are shown in figure 4-7. These

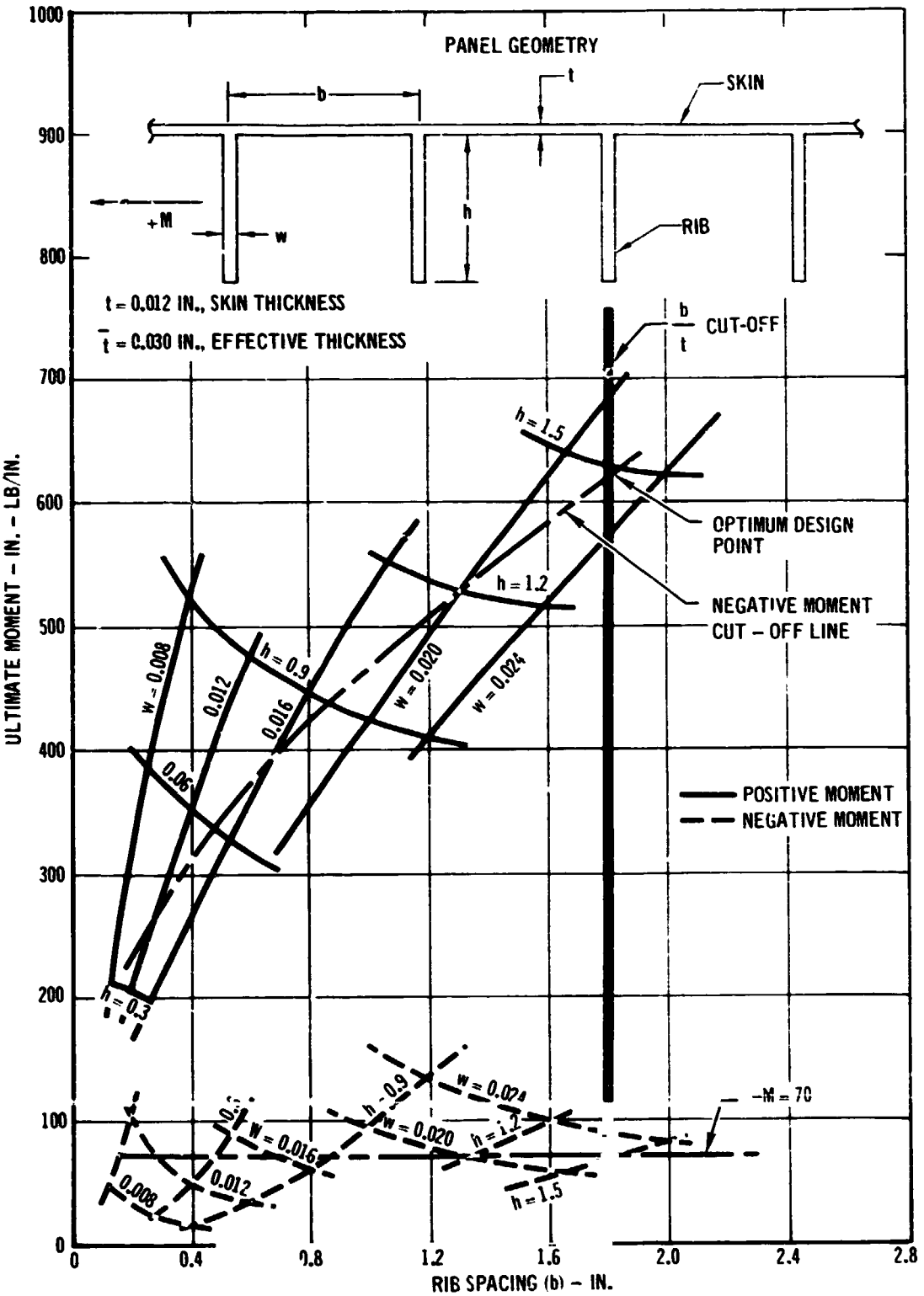

BENDING STRENGTH OF RIB-STIFFENED PANEL
COLUMBIUM FS-85

457-3320

Figure 4-5

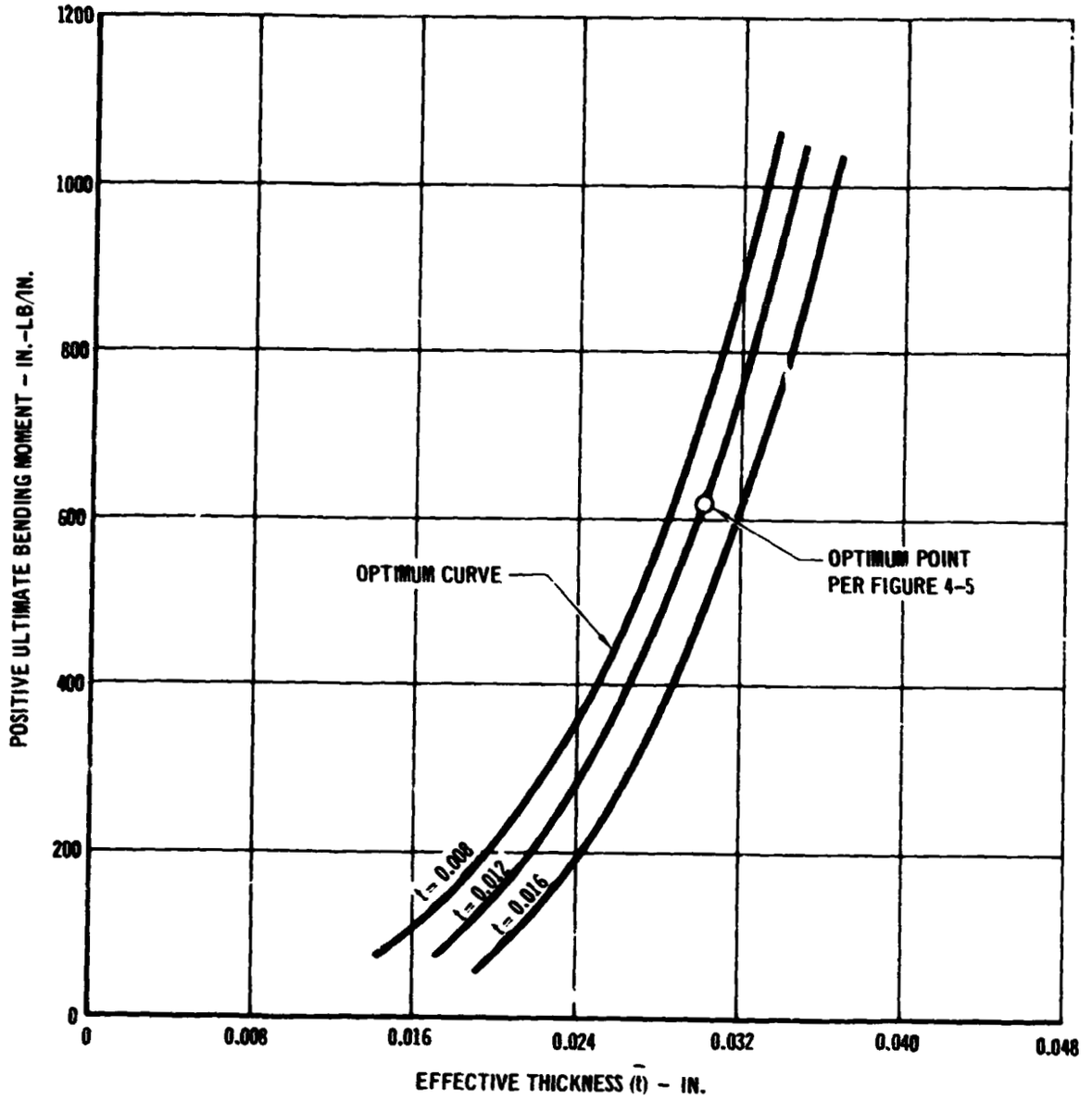

457-1164

MINIMUM GAGE SKIN IS OPTIMUM FOR THE RIB-STIFFENED CONCEPT Figure 4-6

curves can be used to determine h, w, and panel weight as a function of ultimate positive bending moment for columbium FS-85 panels at room temperature. Each design has an ultimate negative bending strength of 70 in-lb/in.

4.4.2 Preliminary Stress Profile Considerations - The results of the rib stiffened panel design optimization study were combined with the Shuttle strength requirements and the effects of different alloys, Cb-752 and C-129Y, were considered.

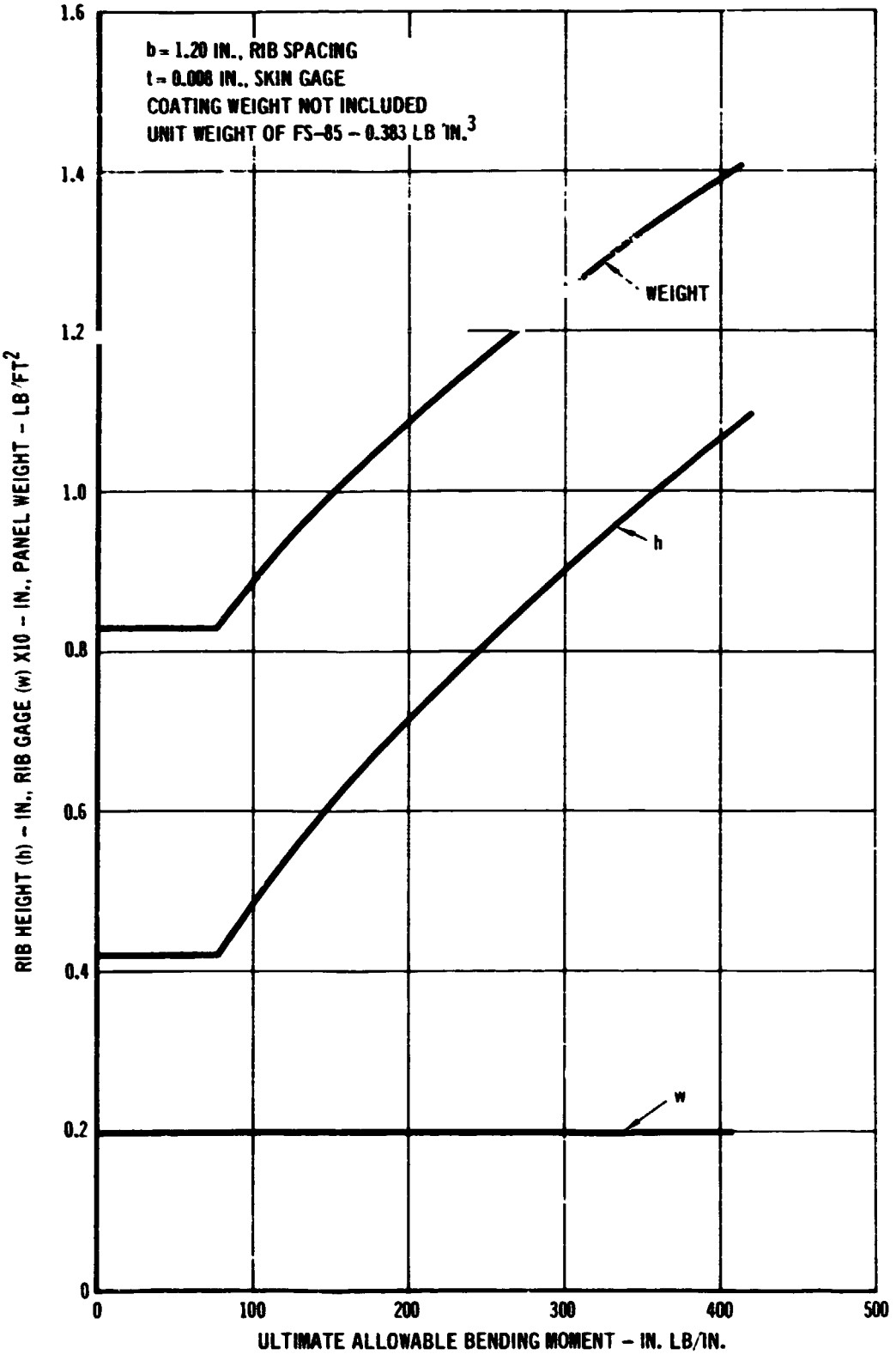

COLUMBIUM FS-85
RIB STIFFENED PANEL DESIGN CURVES

457-1165

Figure 4-7

Ascent - Pressure variations along the high cross range orbiter lower fuselage centerline during ascent are illustrated in figure 4-8. These pressures peak about 66 seconds after liftoff, and are highest in the interaction region between the orbiter and booster. Curves are shown for both the nominal and design trajectories. The design trajectory is obtained by superimposing the effects of winds on the nominal trajectory. Design trajectory loads are used to size panels, whereas loads based on the nominal trajectory are employed in the reuse analysis of panels. Since a venting system has not been defined, and ambient pressure is subject to relatively rapid change during ascent, a 1-lb/in^2 limit burst pressure was assumed to act on all panels. Although a small amount of aerodynamic heating occurs, room temperature material properties were used in designing for these pressure conditions.

Entry - Differential pressures on the bottom centerline of the high cross-range orbiter occurring during entry are shown in figure 4-4 for both nominal and design trajectories. The entry design trajectory was obtained by reducing the

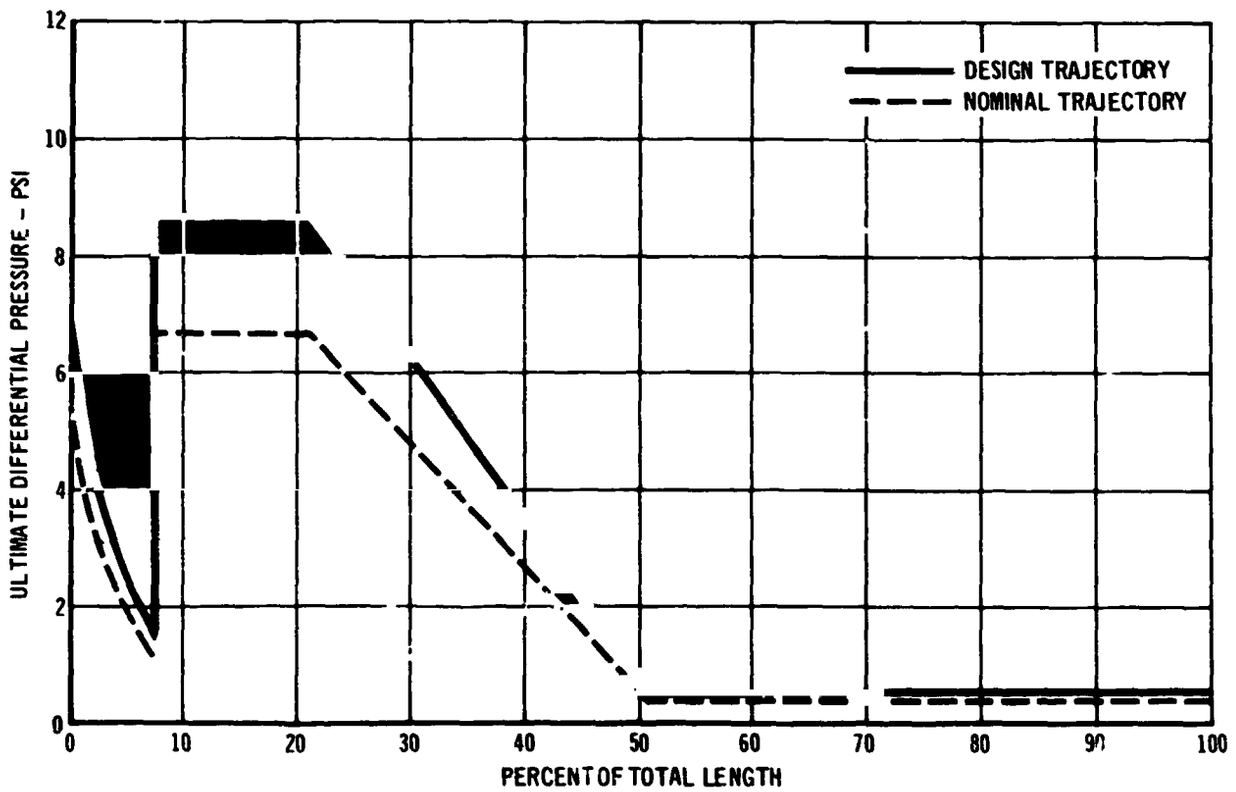

HIGH CROSS RANGE ORBITER
BOTTOM CENTERLINE ULTIMATE PRESSURE DURING ASCENT

457-1166

Figure 4-8

altitude of the nominal trajectory by 2,500 feet at all velocities during entry. The temperature-time profiles during entry for the bottom centerline of this vehicle are given in figure 4-3.

Cruise - Following entry and transition to airplane-type cruise operation, the Shuttle will be subjected to airloads typical of large aircraft. Pressure differentials across the fuselage panels may be as high as 1.75 lb/in^2 ultimate. During this phase of the mission, panel temperatures remain relatively low.

Preliminary Design of Full Size Columbium Panels - Three locations on the orbiter bottom centerline were selected for detailed analysis. The three locations are shown in figure 4-9.

Panel A (at X/L = 0.10) represents a region where all panels would be designed for ascent pressures. Highest ascent pressures (8.7 lb/in^2 ultimate) occur in this area (as indicated in figure 4-9). The resulting columbium rib stiffened panel cross section, along with a curve showing panel strength as a function of temperature, is shown in figure 4-10. The ascent and entry pressure temperature envelopes are also presented in figure 4-10, showing that panel A, which was designed for the ascent condition, is not critical during entry.

Panel B (at X/L = 0.43) represents a panel subjected to the average ascent pressure. The design pressure for panel B (2.54 lb/in^2 ultimate) resulted in the panel cross section shown in figure 4-10. Ascent and entry envelopes shown in figure 4-10 indicate again that the panel was not critical for entry.

Panel C (at X/L = 0.75) is located in a region where pressures are lowest during ascent (0.5 lb/in^2 ultimate). This panel was actually designed for the negative pressure condition of 1.4 lb/in^2 ultimate. The resulting cross section is shown in figure 4-10. A margin of safety exists for both ascent and entry positive pressures.

Prior to the consideration of creep deflection in panel design, panel B was selected as being the most representative panel. (Panel A, which was designed for the highest ascent pressure, would not be subjected to high stresses during entry, and panel C was designed for a burst pressure condition which would not occur on all flights.) Test stress levels for panel B had not only to be based on the nominal trajectory, but had also to correspond to limit rather than ultimate loads. To illustrate this, the ascent test stress level is explained as follows:

(1) The nominal ultimate pressure (1.96 lb/in^2) corresponding to the design ultimate pressure (2.54 lb/in^2) was obtained from figure 4-8;

(2) Dividing 1.96 by 1.4, the factor of safety, the nominal limit pressure

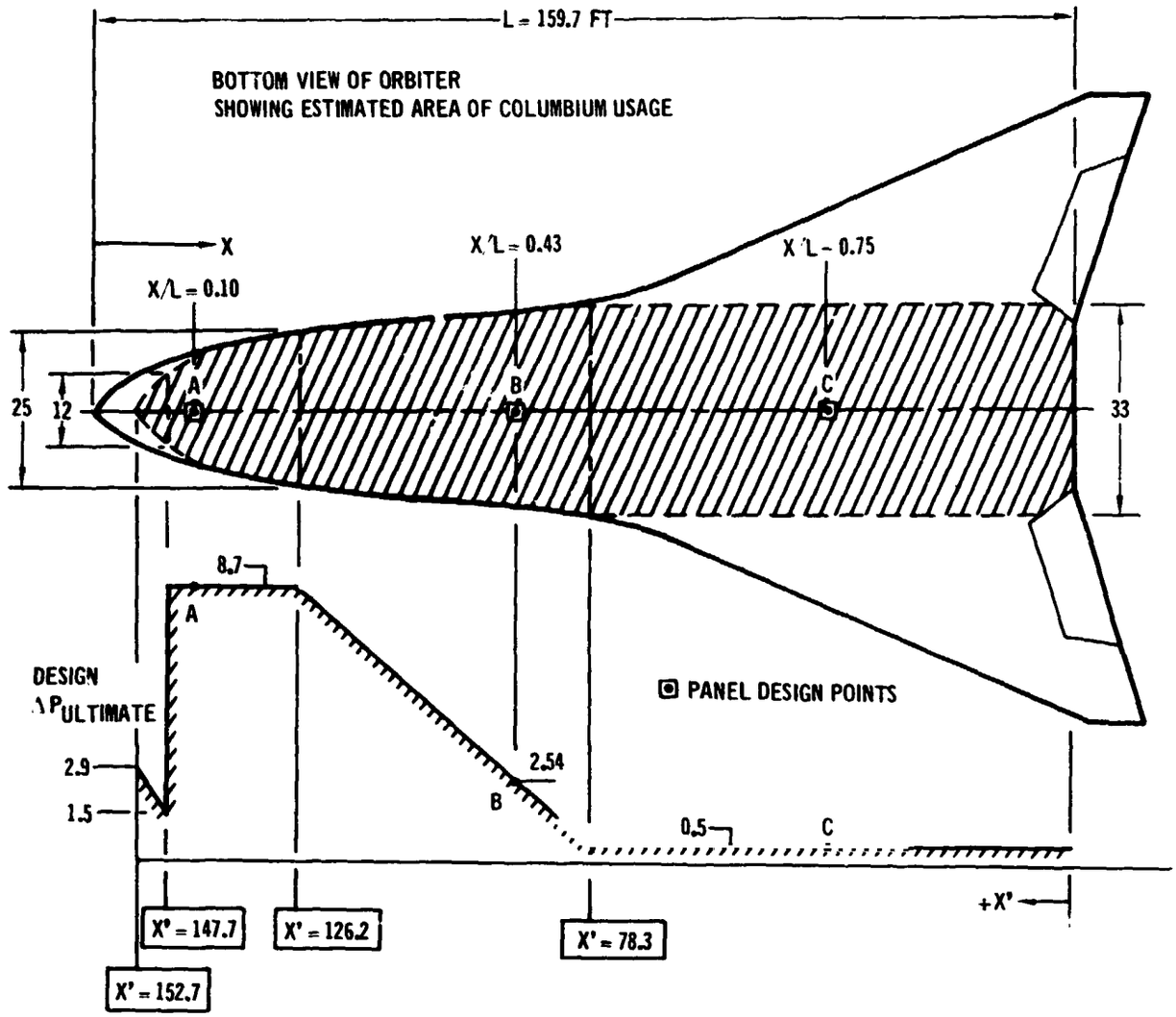

457-1167

ASCENT DIFFERENTIAL PRESSURE DISTRIBUTION AND LOCATION OF PANEL DESIGN POINTS

Figure 4-9

(1.40 lb/in^2) was obtained;

(3) Using the section properties of panel B, the rib outer fiber stress (51,000 lb/in^2) for a 1.40 lb/in^2 panel loading was calculated.

Following the same procedure while using nominal limit, the appropriate pressure stresses were calculated for the entry and cruise conditions. These results, illustrated in figure 4-10, produced the stress-time profile originally selected for flight simulation tests. The temperature-time profile selected for testing (figure 4-1) had temperatures higher than those used in this preliminary work which, as stated previously, caused us to initiate redesign work based on panel creep deflection. Both ascent and entry stress levels for testing were

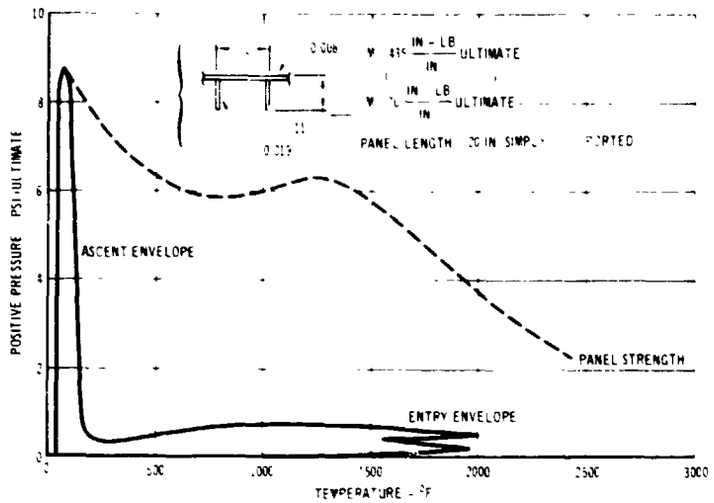

457-1168

X/L = 0.10

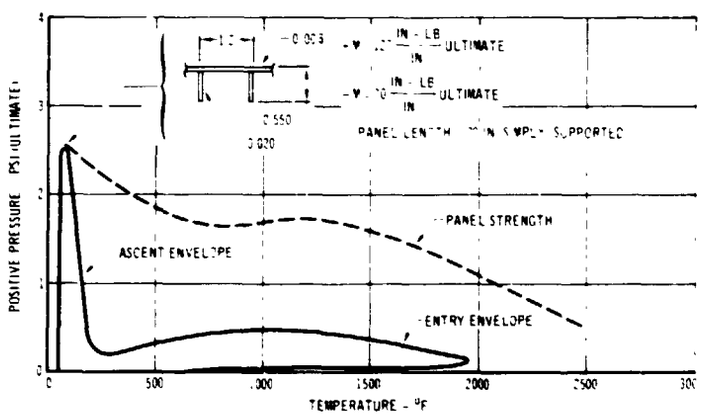

457-1169

X/L = 0.43

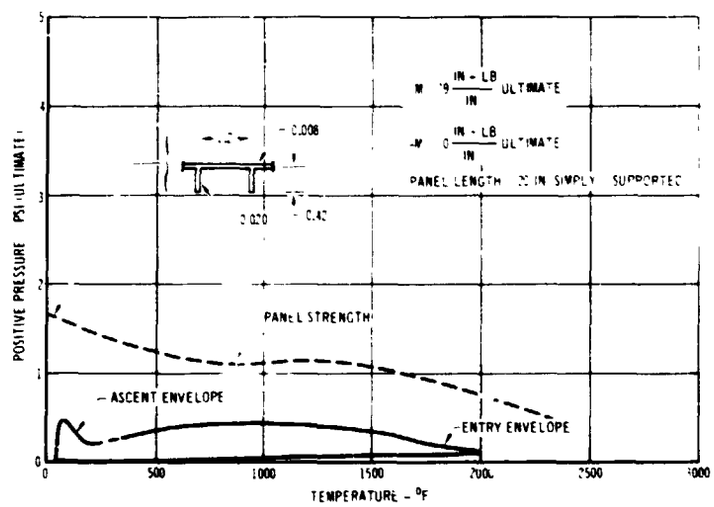

457-1170

X/L = 0.75

PANEL STRENGTH AND FLIGHT ENVELOPE

Figure 4-10

revised as described below.

4.4.3 Final Selection of Test Stress Levels

Ascent - During ascent, the nominal limit stress in the rib outer fiber of panel B was 51,000 lb/in^2. This value is approximately 77 percent of the room temperature yield strength of FS-85. Applying this same percentage to the yield strengths of Cb-752 and C-129Y gives the values 43 and 55 ksi, respectively. Thus, to simulate nominal conditions on panels designed for ascent, each alloy requires a different stress level.

Entry - Analysis using currently available creep properties of the Cb-752 and C-129Y alloys at the maximum test temperature (2400°F) showed that the maximum entry stresses in full size panels of these alloys would have to be limited to about 4000 lb/in^2. This was based on the criterion that total permanent panel deflection (for a 20 by 20-inch panel) after 100 flight cycles must be limited to 0.5 inch. With this creep criterion, excessive creep deflections if full size panels (FS-85, Cb-752 and C-219Y) will not result until a stress of 4000 lb/in^2 is exceeded.

5. DAMAGE CAUSES AND DAMAGE TOLERANCE OF COATED COLUMBIUM

The successful reuse of coated columbium thermal protection panels on a hypersonic reentry vehicle depends upon an accurate appreciation of the causes and effects of local coating damage. While it is true that complete coverage of the columbium substrate is required to maintain substrate mechanical properties, it is also true that coatings have an inherent level of damage tolerance and that not all visual effects of apparent damage to the coating actually impair the effectiveness of the coating. The purpose of the study of damage causes and damage tolerance testing can be summarized as follows:

a) to identify the probable causes of damage to an operational reentry vehicle
b) to illustrate, by example, apparent damage which can be readily detected but does not significantly impair the function of the protective coating
c) to illustrate, by example, damage which will significantly impair the protectiveness of the coating
d) to establish visual criteria for assessing damage repair requirements
e) to identify the types of physical damage which must be located and evaluated by appropriate inspection techniques
f) to determine levels of force required to sustain damage to the protective coatings.

5.1 PROCEDURE - The procedure employed was to consider the following types of damage:

ballistic impact	scratches
edge impact	abrasion
distortion	coating flaws

Each type of damage was considered from the initial viewpoint of experience obtained with past flight hardware programs which employed coated columbium. The applicability of past experience to projected future requirements was analyzed and new or unique requirements were identified. This information was employed to establish a testing method for each type of damage and then damage tolerance testing on coupons was performed.

This study sought to establish coating tolerances to two levels of damage:
(1) damage which would not significantly affect the coating life, and
(2) damage which would cause rapid failure of the protective coating.

An oxidation test of 25 hours at 2400°F in a one atmosphere furnace was used to establish the effect of the damage on the coating. In each type of testing the materials used were Cb-752 alloy with the Sylvania R-512E coating and C-129Y alloy with the VAC-HYD VH-109 coating.

5.2 BALLISTIC IMPACT DAMAGE - Ballistic impact damage usually is caused by an object striking the coated surface. The primary cause is small-mass projectiles, such as hail or micrometeoroids, which strike at relatively high velocities. Ballistic damage also includes handling damage which occurs when objects such as tools strike the surface. This low velocity handling damage to surfaces is discussed in the distortion section of paragraph 5.4.

5.2.1 Past Experience - Past experience with ballistic impact is limited. Two MDC flight vehicles, ASSET and BGRV, which employed coated columbium were single flight designs in which ballistic impact was of minor importance. Ballistic impact considerations were oriented toward preventing impact, as opposed to designing or testing for impact.

Ballistic impact tests at elevated temperature have been conducted by Sylvania on coated columbium intended as a jet engine turbine blade material (reference 3). Ductility of coatings and substrate improves with increasing temperature. The ballistic impact temperature of interest for an operational Shuttle will be approximately room temperature or below and the material will be substantially thinner than turbine blade gauges. Sylvania's experience was employed in this program as test techniques and equipment.

5.2.2 Approach to Ballistic Impact - The approach to the study of ballistic impact in this program will be to determine the energy required to cause coating damage by an average size projectile. In actual practice ballistic impact could cause three distinct types of damage:

a) the projectile could pass through the panel or fracture the substrate
b) the projectile could dent or deform the substrate, thus damaging the coating without necessarily damaging the underlying substrate
c) the projectile could damage the coating without deforming the substrate.

The case of the projectile passing through or fracturing the panel was not considered in this coupon damage and evaluation study, since the primary question concerns the structural integrity of the panel after the coating has been locally destroyed. However, the case was considered in the repair coating application portions, in which the columbium was protected and the hole aerodynamically

repaired.

The case in which the substrate is dented but not fractured requires two important considerations. The coating on the impact surface will encounter compressive loading both from the impact and from being on the compressive (concave) side of the bend. Damage will occur as the compressive strength of the coating is exceeded or shear components interact with normal cracks within the coating. On the reverse side of the impact, the coatings are loaded in tension. Since the coatings are usually already tension cracked, these cracks were expected to open wider without actual loss of coating. The widening of cracks can allow air to penetrate the coating and cause oxidation. This case was also to be considered in evaluating coupons for distortion damage.

The case in which the substrate is not damaged or deformed at impact is obviously a case in which the coating condition is the only consideration. If the gauges of the skin were heavy, or there was underlying support structure to back up the skin, the kinetic energy at impact could be large without deforming or penetrating the substrate. It was anticipated that the primary damage would be sustained on the impact side, with possible crushing and spallation of the coating. This case was investigated by backing up the coated coupon prior to ballistic impact.

5.2.3 Ballistic Impact Testing and Results - The ballistic impacting of the coated columbium coupons was conducted at Sylvania Laboratories, using a calibrated Crossman air pistol. All impacting was performed with a 0.177-caliber, 0.75-gram steel projectile. Velocities of 50 to 210 ft/sec producing kinetic energies at impact of 0.19 to 1.6 lb-ft were investigated. It was determined that a velocity of 210 ft/sec was sufficient to dent severely and to fracture a coated columbium substrate of .020-inch thickness. The majority of the testing was conducted in the range of 50 to 150 ft/sec.

A summary of the testing is presented in table 5-1, and figure 5-1 shows examples of coupons damaged at approximately 200 ft/sec impact velocity. Obviously the coating was damaged to the extent that oxidation testing was not necessary. Figures 5-2 and 5-3 show examples of ballistic sites before and after oxidation testing. Neither the Sylvania R-512E coated Cb-752 nor the VAC-HYD VH-109 was damaged significantly at an impact of 70 ft/sec or less. Figures 5-4 and 5-5 show the effect of backing up the 0.02-inch thick coupons to prevent the metal from yielding. In this case impact velocities as high as 145 ft/sec were required to cause significant loss of coating protectiveness, emphasizing that the damage

Table 5-1

SUMMARY OF BALLISTIC IMPACT TEST RESULTS

SPEC NO.	ALLOY AND COATING	SPECIMEN SUPPORT	IMPACT VELOCITY (FT/SEC)	OXIDATION ONE HOUR CYCLES TO COATING FAILURE AT 2400°F
25-1	Cb-752 R-512E	IMPACT AREA NOT BACKED UP	184	COATING SEVERELY DAMAGED AND NOT TESTED. SEE FIGURE 5-1 FOR VISUAL APPEARANCE
25-2			222	
35-1	C-129Y VH-109		184	
-2			135	
73-1	Cb-752 R-512E	IMPACT AREA NOT BACKED UP	70	25 NF
-2			70	10
-3			70	25 NF
-4			70	17
74-1			55	25 NF
-2			90	1
-3			80	15
-4			70	NF
39-1		SOLID BACK-UP	105	25 NF
-2			145	25 NF
-3			120	25 NF
-4			120	25 NF
96-1	C-129Y VH-109	IMPACT AREA NOT BACKED UP	80	13
-2			80	13
-3			90	1
-4			90	15
915-1			55	25 NF
-2			90	1
-3			80	1
-4			70	25 NF
935-1		SOLID BACK-UP	145	2
-2			145	1
-3			145	24
-4			145	24

457-1172

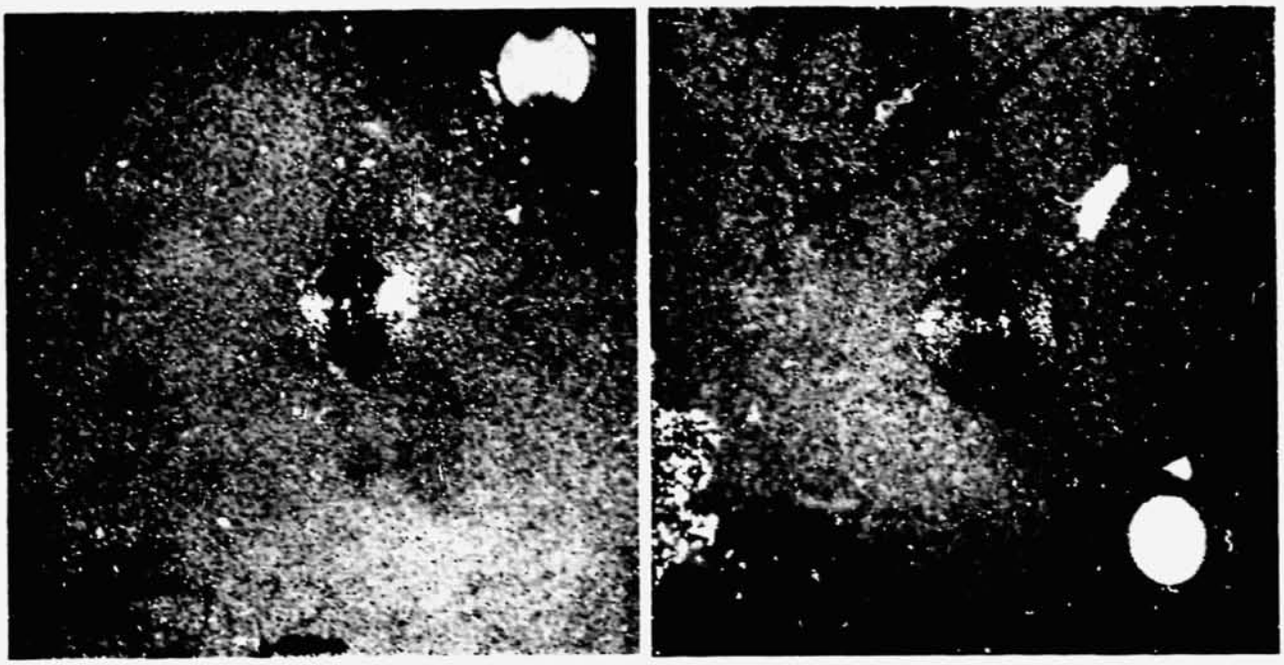

2X

SYLVANIA R-512E COATING AFTER 222 FT SEC IMPACT

4X

VAC-HYD VH-109 COATING AFTER 184 FT SEC IMPACT

457-1175

COATING DAMAGE FROM BALLISTIC PROJECTILES

Figure 5-1

to the coating is closely related to the stability of the underlying substrate. In ballistic impact, a thin skinned heat shield panel would be expected to be less tolerant than a heavier gauge leading edge and such tolerance would probably be proportional to substrate thickness. In thin gauges (0.020 inch or less) yielding of the substrate below the coating would be the limiting factor, because the intermetallic coating does not have sufficient ductility to yield with the substrate upon fracturing.

5.3 EDGE IMPACE - Edge impact damage covers chipping of coated edges, one of the most common types of damage. Chipping differs from surface impact damage in appearance, significance, and the coating tolerance of such damage.

5.3.1 Coated Refractory Metal Experience - Past experience has shown that the most common cause of coating damage is impact on edges. Edges are more susceptible than surfaces to collision damage during handling and installation. The susceptibility of an edge to impact damage is related to the quality of the coating at the edge as well as to the angle of impact and the kinetic energy at impact. Figure 5-6 shows a poorly coated edge and figure 5-7 shows an adequately coated edge.

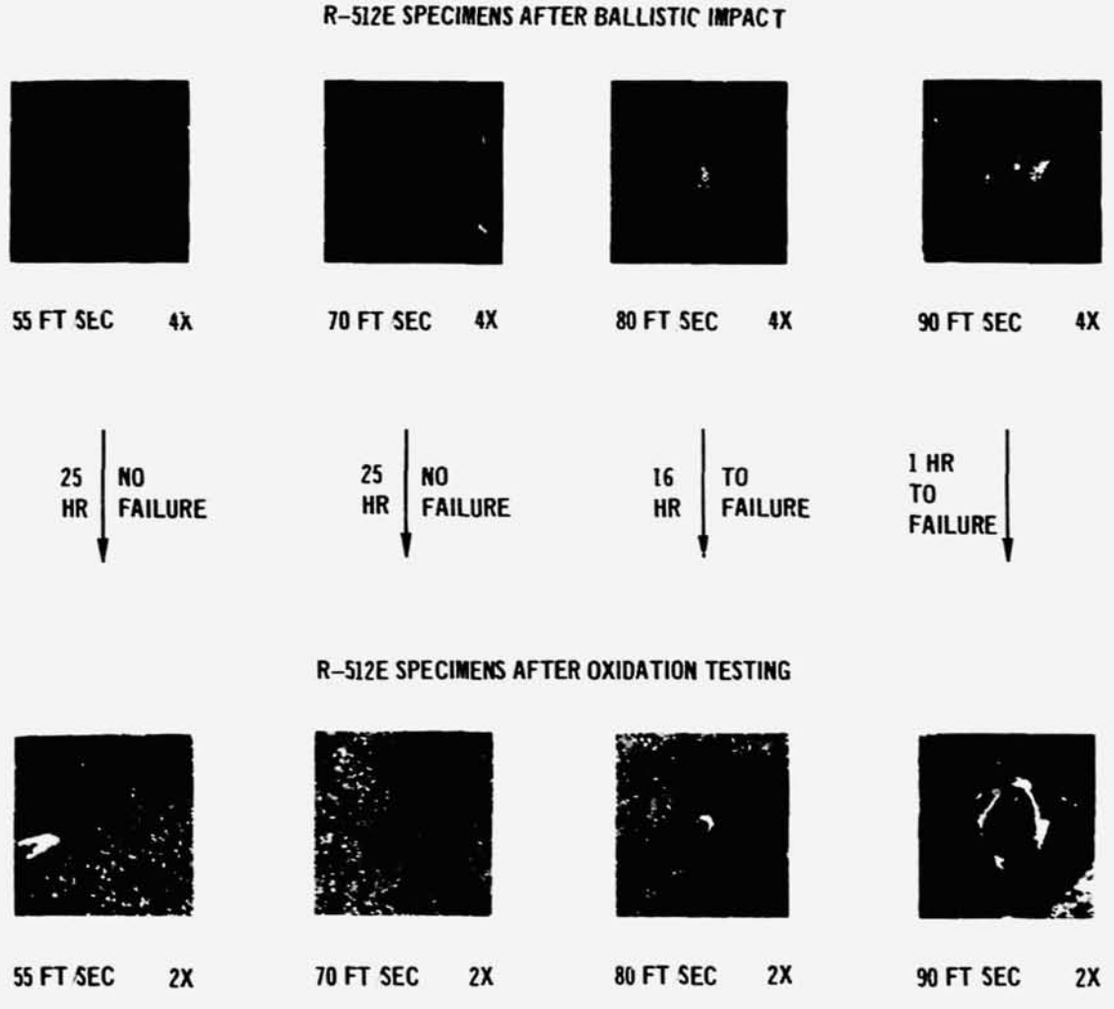

457-1176

SYLVANIA R-512E COATING AFTER BALLISTIC IMPACT AND OXIDATION TESTING 2400°F

Figure 5-2

Past experience has shown that the type of intermetallic compound formed at the interface of the substrate influences the resistance to edge chipping and influences the extent of coating damage. Since shear stresses at the interface of the coating and the substrate can be substantial, it is desirable to have a system which fails within the coating in brittle fracture. This is better than failing in interfacial shear, which allows larger areas to be damaged and the total thickness of the coating to be lost. Figure 5-1 shows these two types of failure in ballistic impact. The R-512E specimens show brittle fracture and the VH-109 specimens show shear at the interface and a larger affected area. Reference 4 describes edge impact testing and coating process studies related to edge damage.

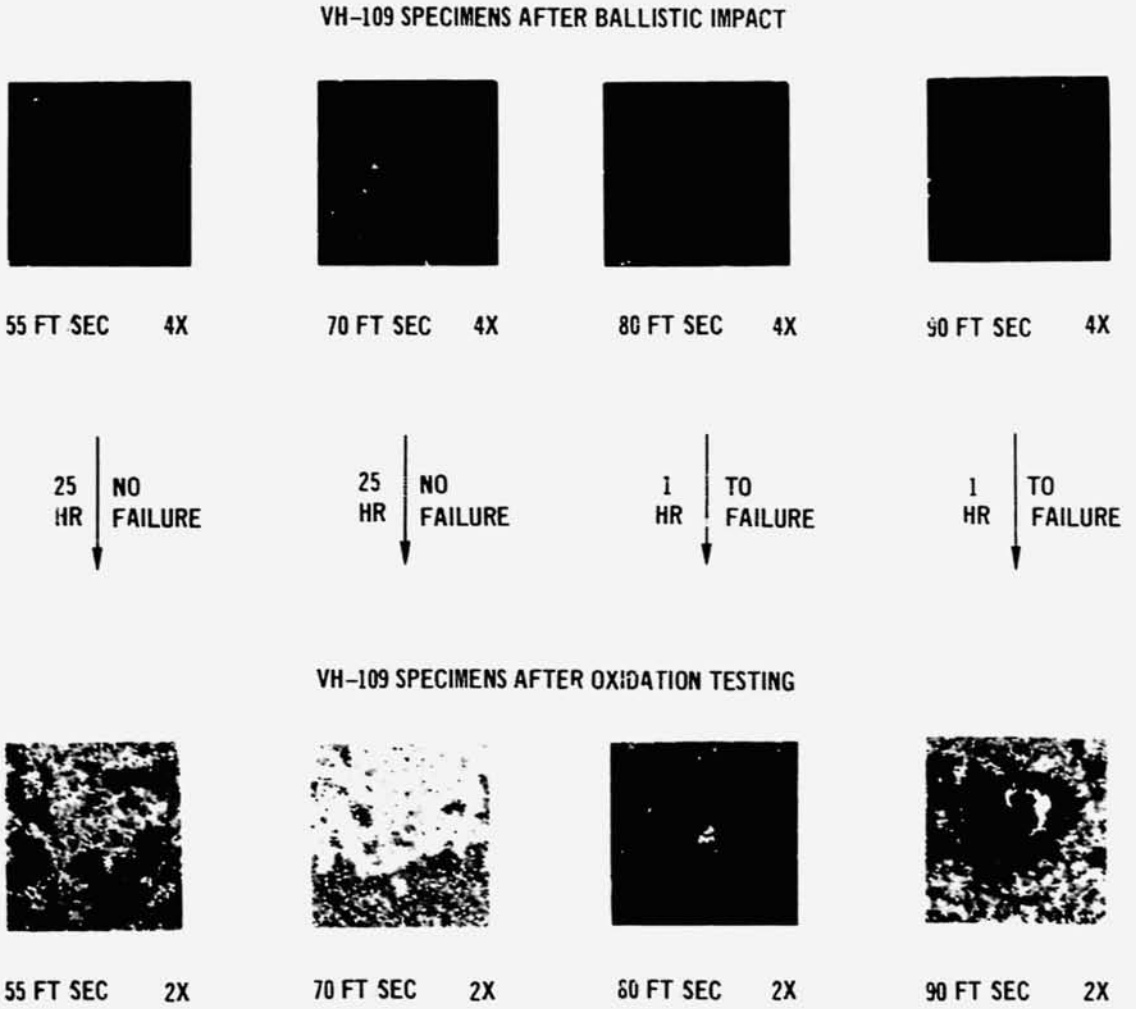

457-1177

VAC-HYD VH-109 COATING AFTER BALLISTIC IMPACT AND OXIDATION TESTING AT 2400°F

Figure 5-3

5.3.2 Program Considerations - It is anticipated that Shuttle edge impact damage considerations will be related primarily to impacts incurred during handling and installations. Although edge impact could occur in flight operations, the probability of surface impact is much greater since the edges are less vulnerable after installation. Edge impact during handling and installation is virtually impossible to quantify, because impact collision could occur with many different objects.

5.3.3 Edge Impact Testing and Results - Simulated edge impact was accomplished with a simple pendulum apparatus in which the pendulum arm was raised to the desired height by rotating and allowed to strike the edge of a test coupon

120 FT SEC

145 FT SEC

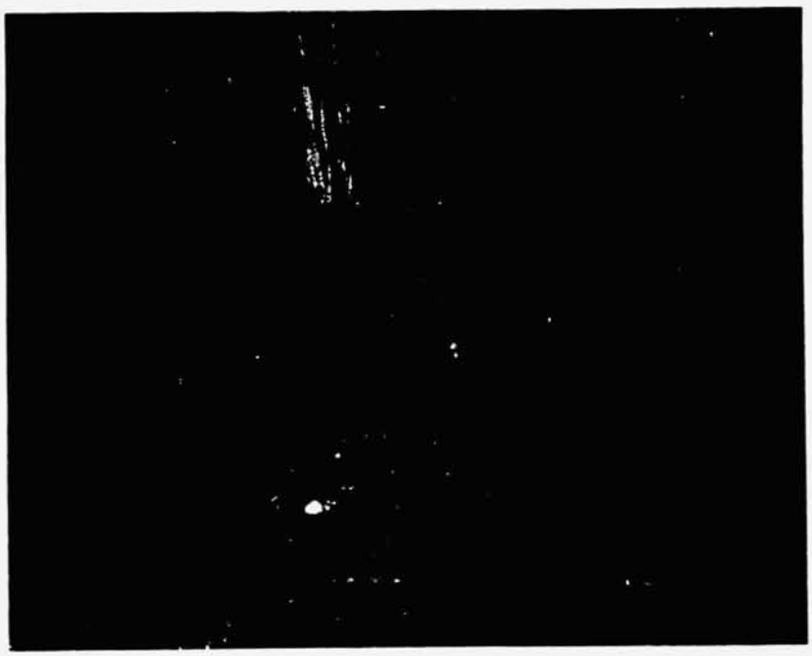

AFTER IMPACT

2.5X

120 FT SEC

105 F. SEC

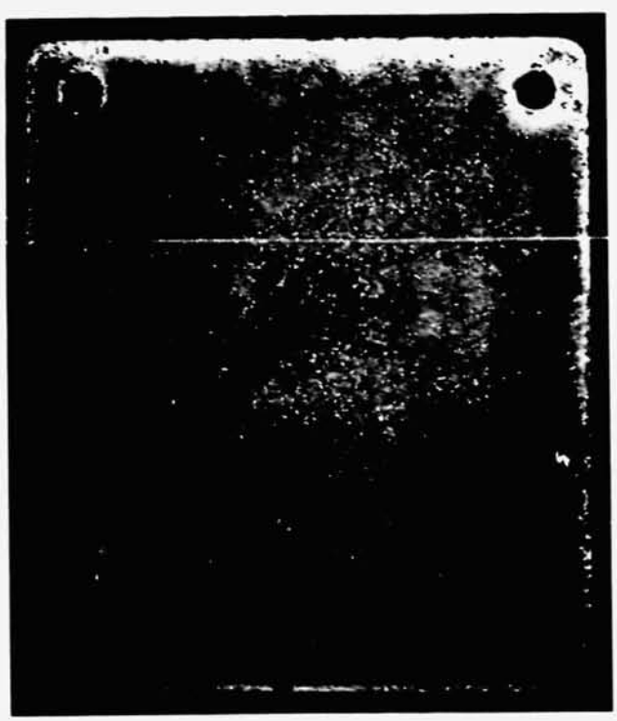

AFTER
OXIDATION

1.6X

SYLVANIA R–512E AFTER BACKED UP BALLISTIC IMPACT AND OXIDATION TESTING AT 2400°F

457–1178

Figure 5–4

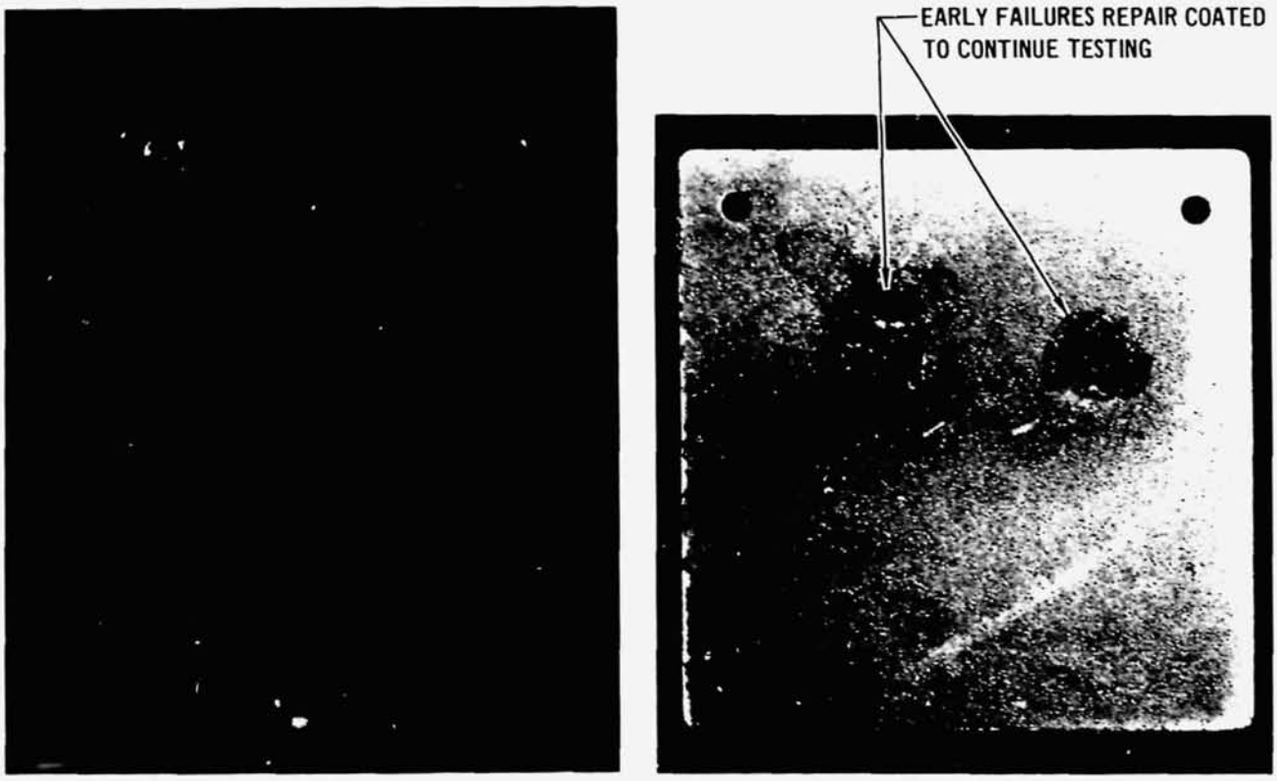

457-1179

VAC-HYD VH-109 AFTER BACKED UP BALLISTIC IMPACT AND OXIDATION TESTING AT 2400°F

Figure 5-5

clamped to hold the edge perpendicular to the free fall patch of the pendulum arm. The impact energy was taken to be the product of the weight of the pendulum arm and the change in height of the center of gravity of the arm during the impact swing. Coupons of R-512E coated Cb-752 and VH-109 coated C-129Y were damaged at various levels and oxidation tested for 25 hours at 2400°F or until failure occurred. Table 5-2 presents the edge impact data and oxidation test results. Examples of edge impact specimens are shown in figures 5-8 and 5-9.

5.4 DISTORTION - Distortion occurs when a metal structure assumes another shape under the influence of a load. Distortion can cause damage to the coating because of the limited ductility of the coating at low or intermediate temperatures. Coatings are generally considered to accept elastic strain of the substrate with no effect upon life. The amount of plastic strain that coatings can tolerate required more research.

5.4.1 Past Coated Columbium Experience - Coating damage due to substrate

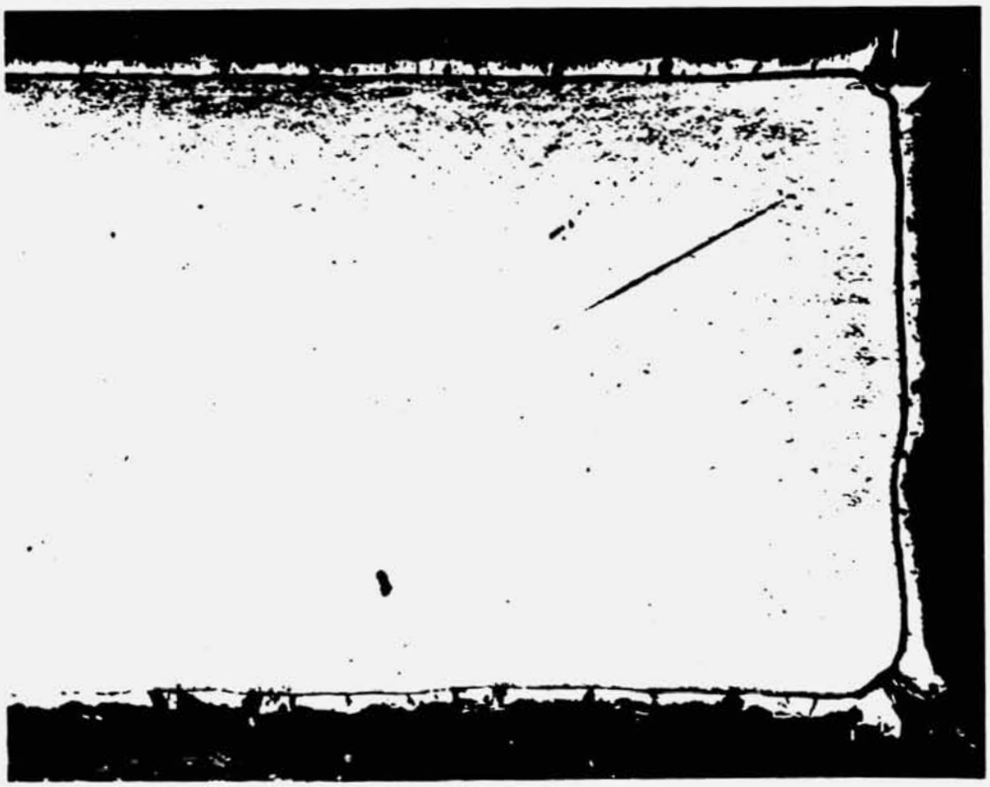

(SILICIDE COATING
ON Mo)
100X

457-1180

EXAMPLE OF POOR QUALITY EDGE COATING

FIGURE 5-6

(VH-109 COATING
ON C-129Y)
100X

457-1181

EXAMPLE OF GOOD QUALITY EDGE COATING

Figure 5-7

Table 5-2

EDGE IMPACT TEST RESULTS

SPECIMEN NO. AND IMPACT SITE	VAC-HYD NO. AND IMPACT SITE	IMPACT ENERGY IN.-LB	OXIDATION LIFE AT 2400°F (HOUR FAILURE OCCURRED)	
			R-512E	VH-109
88-1	68-1	0.03	25 NF	25 NF
2	2	0.06	25 NF	25 NF
3	3	0.06	25 NF	25 NF
4	4	0.09	25 NF	25 NF
5	5	0.12	1	25 NF
6	6	0.15	1	25 NF
7	7	0.18	1	7
8	8	0.20	1	6
51-1	913-1	0.03	25 NF	25 NF
2	2	0.06	25 NF	25 NF
3	3	0.26	1	1
4	4	0.67	1	1
5	5	1.1	1	1
6	6	1.6	1	1
7	7	2.3	1	1
8	8	3.1	1	1

NOTE: NF DESIGNATES THAT THE SPECIMEN DID NOT FAIL.

457-1173

distortion on past flight vehicles has occurred in the use of threaded fasteners. The first area involved the high-torque recesses of a relatively weak columbium alloy (Cb-5Zr). The screw heads were a minimum size and the torqueing of the fasteners caused one side of the tool recess to yield, causing an eyebrow, or burr, of metal to be pushed up. The coating could not deform without fracture and field repair was required to prevent oxidation in severe cases. A second problem involved threaded fasteners in the self-locking mechanism which depend on distortion of part of the nut to effect the locking. This case was a combination of substrate deformation, which tends to weaken the coating, and the natural tendency of the coating to be prone to defects on the edges of the sharp, small radius threads. In both cases, however, the coating sustained damage due to deformation in local areas where elastic strains were high or actual plastic strain occurred. Although it might be argued that the problems were of design rather than of materials behavior, design choices cannot always avoid all material limitations.

The BGRV vehicle successfully employed coated columbium seals for the flair

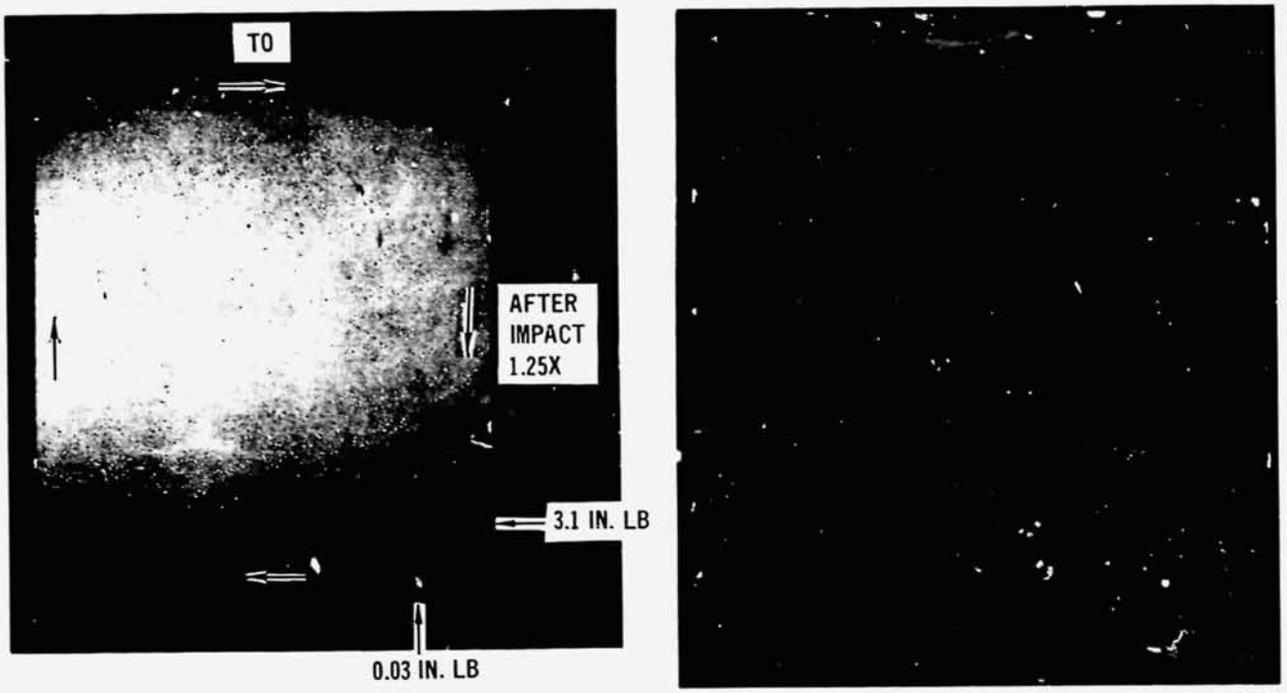

457-1182

SYLVANIA R-512E EDGE IMPACT SPECIMENS

Figure 5-8

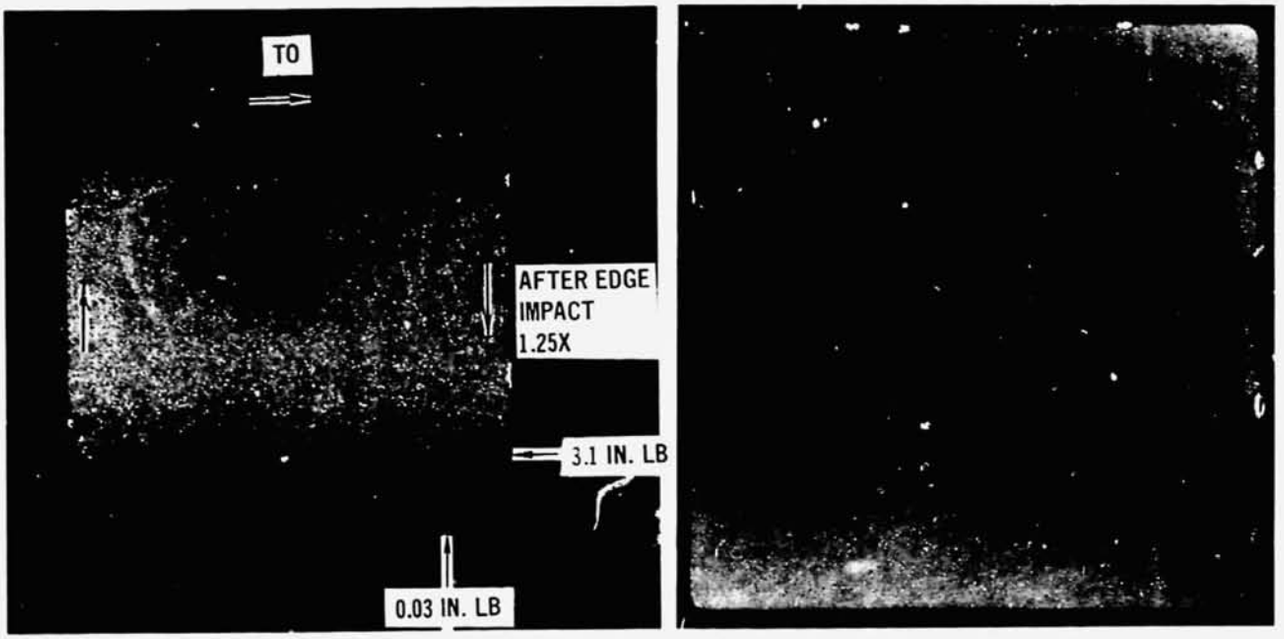

457-1183

VAC-HYD VH-109 EDGE IMPACT SPECIMENS

Figure 5-9

assembly. In this case, the strain magnitudes could be reduced by distributing the bending over a sufficient length to accommodate the desired displacement. Spring clips also have been employed satisfactorily in an expansion joint between coated molybdenum panels and graphite leading edges. Spring clips of both columbium and molybdenum have been used extensively to secure thermocouple sheaths and insulations.

In summary, good design practice does not load coated columbium structures to produce plastic strain. In those cases in which considerable elastic strains have been experienced, the coatings have performed well. In some cases insufficient design latitude has caused plastic strain, and resultant problems in local areas have occurred. Accidental damage can occur in handling and installation, as previously discussed under edge impact. Handling damage can bend a corner of a panel, a clip, or a doubler on the back side of the panel. In such events, the magnitude of the load and the bend radius cannot readily be predicted.

5.4.2 Program Considerations - The primary consideration for a hypersonic reentry vehicle will be handling and installation damage which bends or deforms the substrate and damages the coating. Design areas of possible concern will be the use of columbium spring seals (i.e. around landing gear door) and threaded fasteners. The design and development of these items has not progressed to a point where specific testing criteria can be formulated.

5.4.3 Approach to Deformation - The principal approach to studying coating damage caused by deformation will be to employ bend tests. These tests will yield accurate data concerning the bend angle required for a given bend radius to cause coating damage sufficient to affect coating life. Such data should be applicable to a wide variety of design criteria deformation, as well as to analysis of handling damage.

5.4.4 Distortion Testing and Results - Distortion testing was accomplished with an MAB-216M bend test fixture. Coupons of R-512E-coated Cb-752 and VH-109-coated C-129Y were bent at 2, 10, and 20 T (T = material thickness). Typical examples of these bends are shown in figures 5-10 and 5-11. For each bend radius and coating combination, distortion was induced first to an extent that the life of the coating would not be significantly affected, and secondly, to a point where coating failure would occur rapidly. The specimens used were the 0.020-inch coupons described in section 3. The oxidation testing was conducted at 2400°F at one atmosphere air pressure with the testing terminated after 25 1-hour cycles if failure had not occurred.

TYPICAL SYLVANIA R-512E/Cb-752 BEND SPECIMENS Figure 5-10

The distortion test results are presented in table 5-3 and typical bends for both coatings are shown in figures 5-10 and 5-11. The bend testing produced three types of coating defects. Spalling of the coating on the compression surface and chipping of the edges occurred first as illustrated in figure 5-12. The third and least detrimental type of defect was cracking of the coating on the tension side, illustrated in figure 5-13. Coating damage on the compression surface was found to be the most detrimental with the R-512E and VH-109 coatings showing early failure when bent at 10 T to more than 18 and 9 degrees, respectively. It was found that the compression spallation posed a serious problem when the coating sheared at the substrate, thus producing a total loss of coating in the damaged area (figure 5-12). The tension cracking proved to be much less critical, and repair coatings had to be applied to compression surface damage areas to test the tension cracking condition. The VH-109 coating was bent to a 66-degree permanent set at 2 T and to a 98-degree permanent set at 20 T. Seven hours were required to

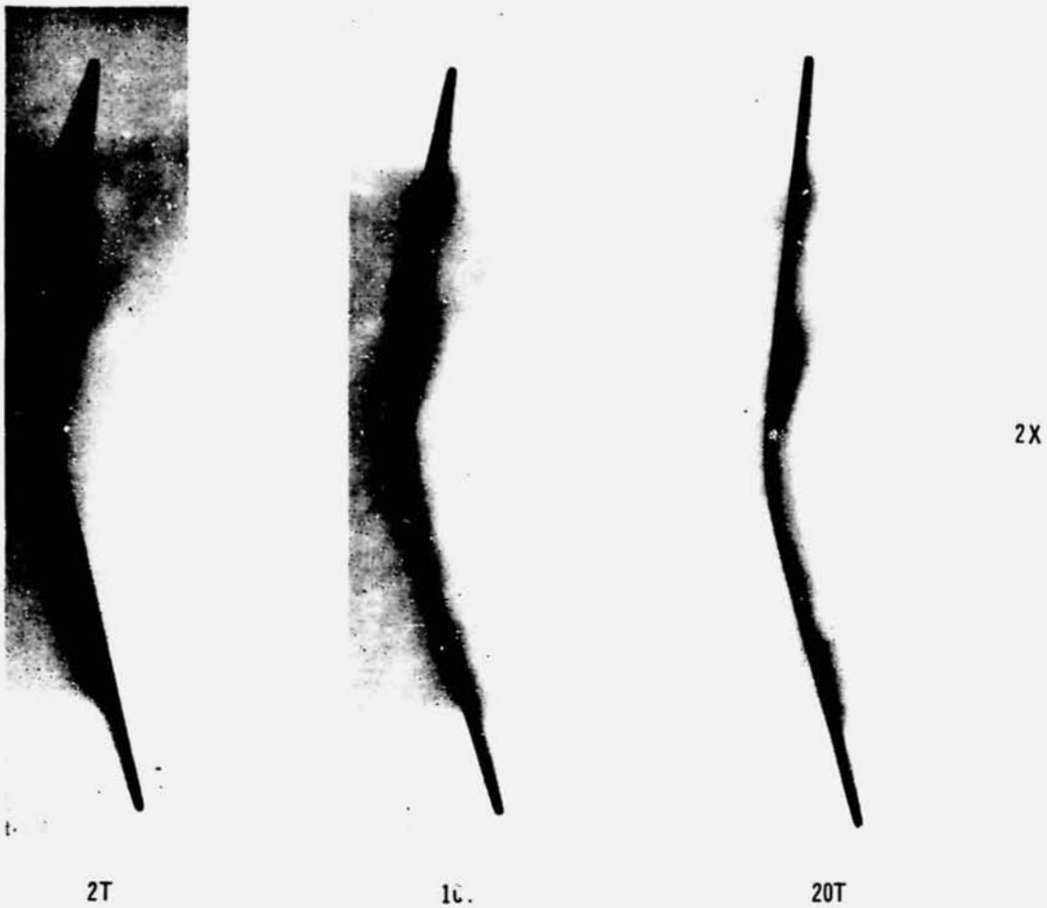

TYPICAL VAC-HYD VH-109/C-129Y BEND SPECIMENS

Figure 5-11

initiate oxidation failure on the tension side. The R-51E coating was bent to a 50-degree permanent set at 2 T and to a 90-degree set at 20 T; it did not fail even after 25 hours at 2400°F. The difference in type of damage sustained on the compression and tension side is shown in cross section in figure 5-14. The coating on the compression surface was sheared at the substrate, leaving a substantial area of unprotected columbium. On the tension surface, the tension crack simply opened up and the coating remained in place. The small area exposed, and the proximity of coating (producing an oxide and closing up the crack), accounts for the great difference in oxidation performance between the surfaces. Figure 5-15 shows typical examples of the oxidation failures which were experienced.

5.5 SCRATCHING

5.5.1 Past Experience - Marks made by softer materials transferred onto the coating are often mistakenly called scratches. Although coatings vary considerably in the texture and physical nature of the surface, most coatings readily show evi-

Table 5-3

BENDING DISTORTION TEST RESULTS

SPECIMEN NO. AND DESIGNATION	BEND RADIUS	ANGLE OF PERMANENT SET - DEG	REPAIRED AREA	OXIDATION LIFE AT 2400°F HOURS	FAILURE LOCATION
SYL-24		17	NONE	1	COMPRESSION AND EDGE
SYL-46		31	NONE	1	COMPRESSION AND EDGE
SYL-91		24	COMPRESSION AND EDGE	25 NF	
SYL-90	2T	50	COMPRESSION AND EDGE	25 NF	
VAC-94		18	NONE	1	COMPRESSION AND EDGE
VAC-910		17	NONE	1	COMPRESSION AND EDGE
VAC-928		25	COMPRESSION AND EDGE	25 NF	
VAC-912		66	COMPRESSION AND EDGE	7	TENSION CRACKS
SYL-47		43	NONE	1	COMPRESSION AND EDGE
SYL-48		39	NONE	1	COMPRESSION AND EDGE
SYL-89	10T	18	NONE	25 NF	
VAC-916		16	NONE	1	COMPRESSION AND EDGE
VAC-922		30	NONE	1	COMPRESSION AND EDGE
VAC-919		9	NONE	25 NF	
VAC-917		98	COMPRESSION AND EDGE	6	TENSION CRACKS
SYL-49		90	NONE	25 NF	
VAC-924	20T	30	NONE	1	COMPRESSION AND EDGE
VAC-937		21	NONE	7	EDGE

457-1174

dence of hard objects being moved acorss the surface with sufficient force to produce a line resembling a scratch. In most occurrences. the object interacting with the coating is not as hard as the intermetallic or oxide compounds present on the surface and the interaction is not strong enough to deform the substrate or fracture the coating. The mark remaining on the surface of the coating either is the softer object which has been abraded away and deposited on the surface of the coating, or is a superficial fracture of the outer layer of the coating. Recall that the color and general physical appearance of the intermetallic compounds that compose most of the coating do not correspond to the gray (often dark and matted) appearance of the coating surface. Because this exterior layer is too thin to be observed in a photomicrographic cross section, knowledge about it is limited, but it is believed to consist of oxides and byproducts of the coating process which are deposited on the surface. In some cases, it can be shown that a scratch has

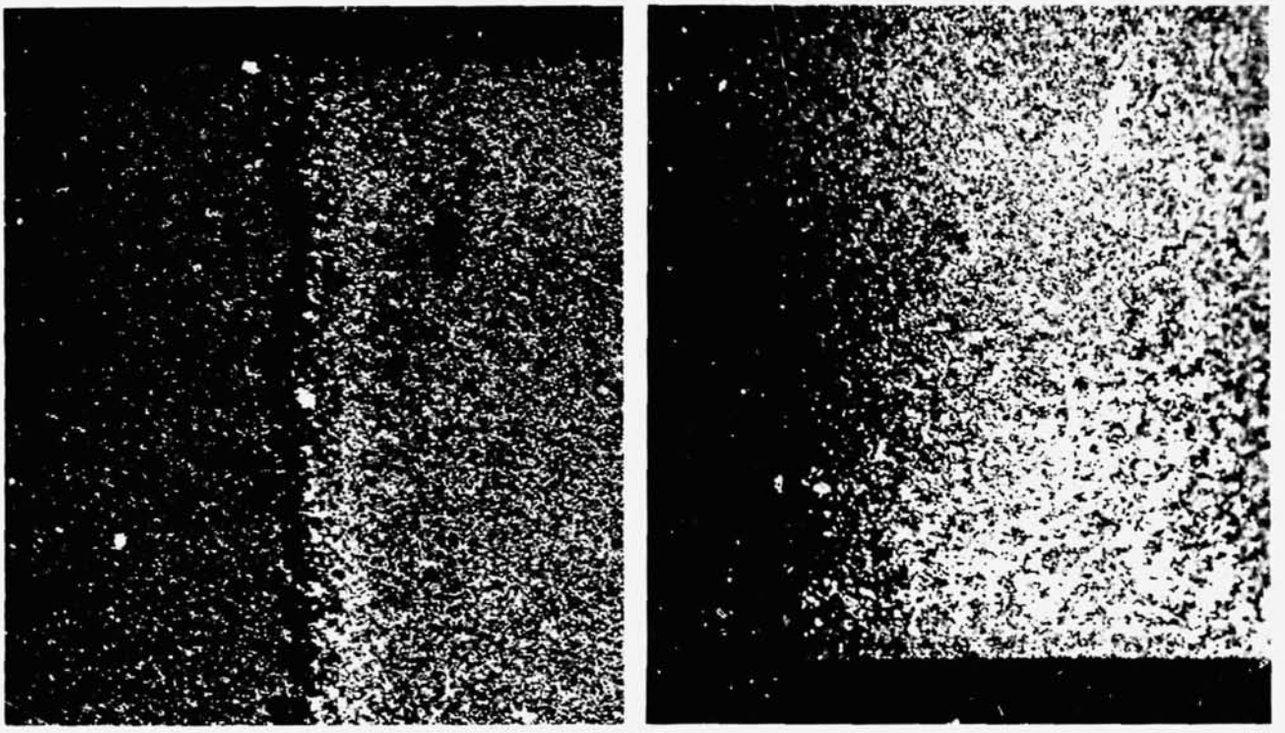

9X

FAILURE WILL OCCUR IN 1 HOUR

FAILURE WILL NOT OCCUR IN 25 HOURS

457-1186

EXAMPLES OF COMPRESSION SURFACE DAMAGE

Figure 5-12

penetrated this layer, exposing the color and physical appearance associated with the actual intermetallic coating.

In the past, scratches and marks on the surface have been examined with low power magnification (i.e., 10X), sometimes with the aid of simple tools. For example, lightly sanding a portion of a scratch will quickly reveal if a superficial layer of the coating has been removed to expose the basic underlying coating compounds. Such sanding is acceptable since the superficial layer of the coating can easily be sanded away with no compromise to the life of the coating. In summary, scratching or marking of the coatings has been a continuing problem requiring inspection and interpretation by people knowledgeable about coating behavior. Almost universally, the conclusion has been that the coating has been marked by another object or that the superficial surface layer has been disturbed with no detrimental effect.

An interesting sidelight to the scratching experience is the inspection to verify the presence of coating. If the process or geometry is such that uncoated areas can occur, the metal can take on the appearance of the coated surface without being coated. In such cases a sharp, hardened scribe has been used to scratch

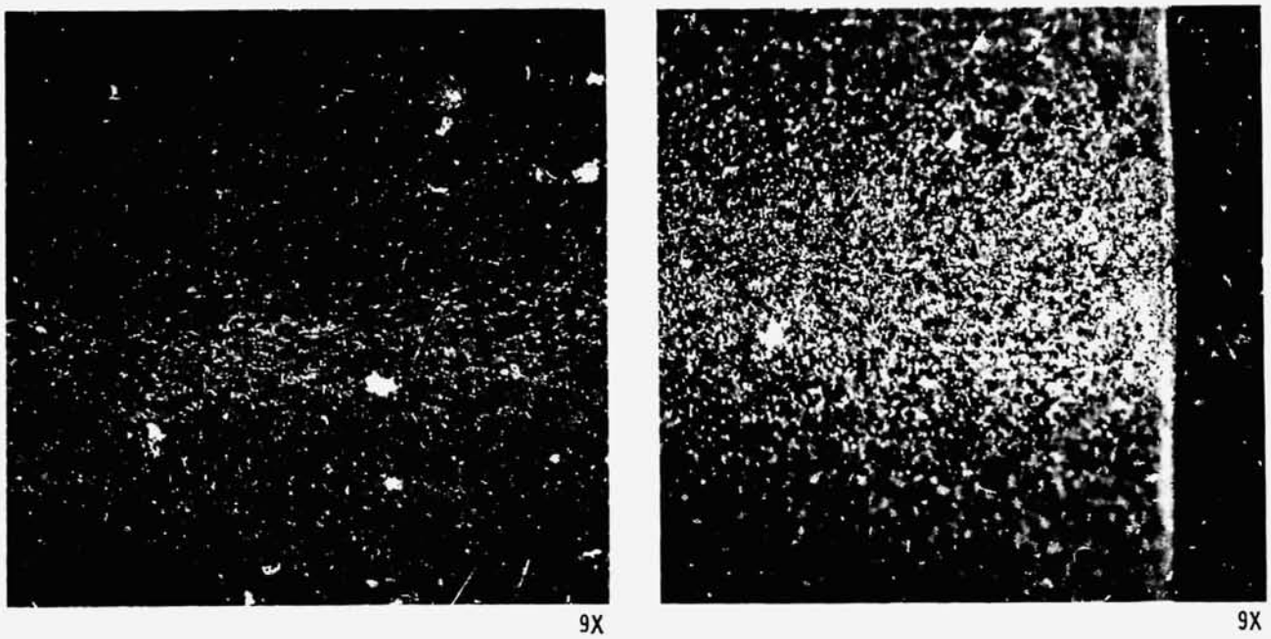

9X

FAILURE WILL OCCUR IN 7 HOURS

9X

NO FAILURE IN 25 HOURS

457-1187

EXAMPLES OF TENSION SURFACE CRACKING

Figure 5-13

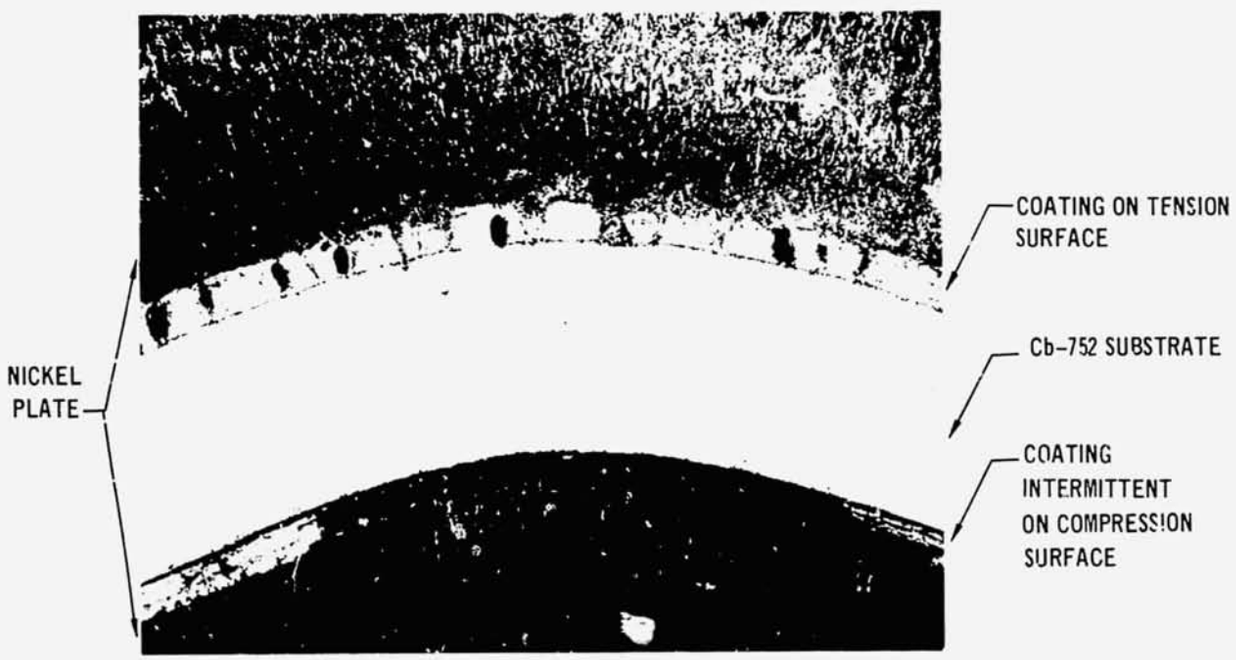

457-1188

R-512E BEND SPECIMEN-- 150X

Figure 5-14

9X

HOUR FAILURE IN COMPRESSION DAMAGE

9X

7 HOUR FAILURE IN TENSION DAMAGE

EXAMPLES OF TYPICAL OXIDATION FAILURES EXPERIENCED IN BEND SPECIMENS

457 1189

Figure 5–15

lightly the questionable area. The vast difference in hardness and ductility between the coating and the substrate is quickly determined.

The limited experience with coating damage due to scratching does not mean that the problem does not require serious consideration. There is some evidence that the more current and presently attactive coating systems may be more susceptible to scratching. It is also known that the hardness and sharpness of the scratching tool are very important in determining the magnitude of force required to damage the coating, as well as the extent and nature of the damage.

5.5.2 Program Considerations - The primary consideration in scratching will be coating damage which may result from handling or installing coated panels. As was the case for edge impact, there are no design criteria which can anticipate the wide variety of objects and conditions which may cause scratching or related damage.

5.5.3 Scratching Damage Testing and Results - For this study, a scratch was defined as damage to the coating caused by a hard, sharp object penetrating and cutting the coating to a measurable depth. Line deposits from softer objects or superficial disturbances of the surface were not considered. The scratches were cut into the coatings with a 60-degree tungsten carbide tool mounted in a milling machine. The specimen surface was located perpendicular to, and just touching, the tool over the desired length of stroke. The tool then was pushed into the coating to the desired depth and the machine table driven to produce the desired depth of cut. In an initial set of specimens scratch defected, the Sylvania R-512E coating was cut to a depth of 1/2, 1, 1-1/2, and 2 mils (figure 5-16) and the VAC-HYD VH-109 coating was cut to a depth of 1/2, 1, 1-1/2, 2, and 3 mils (figure 5-17). After oxidation testing at 2400°F for 25 1-hour cycles at one atmosphere, the scratches had produced no oxidation failure in either coating (see figures 5-16 and 5-17).

A second set of coupons was similarly prepared, with scratch depths of 2, 4, 6, and 8 mils (milling machine tool depth measurements). Since the milling machine measurements used the highest points of the coating surface as a zero reference and local variations in coating thickness or coupon waviness could cause the true average scratch depth to be less than the milling machine readings, other measurement techniques were applied. An optical scratch depth device employed

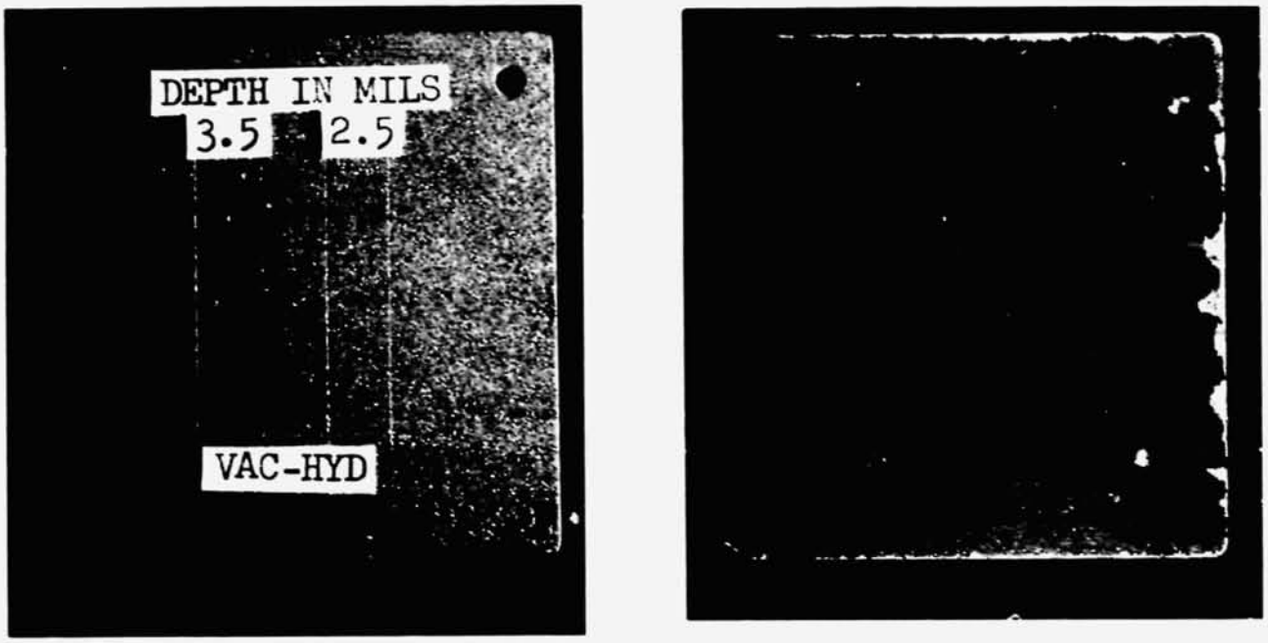

BEFORE OXIDATION TESTING 1.4X

AFTER OXIDATION TESTING 25 HOURS – 2400°F 1.4X

VAC–HYD VH–109 SCRATCH TESTS BEFORE AND AFTER OXIDATION TESTING

Figure 5–16

457–1191

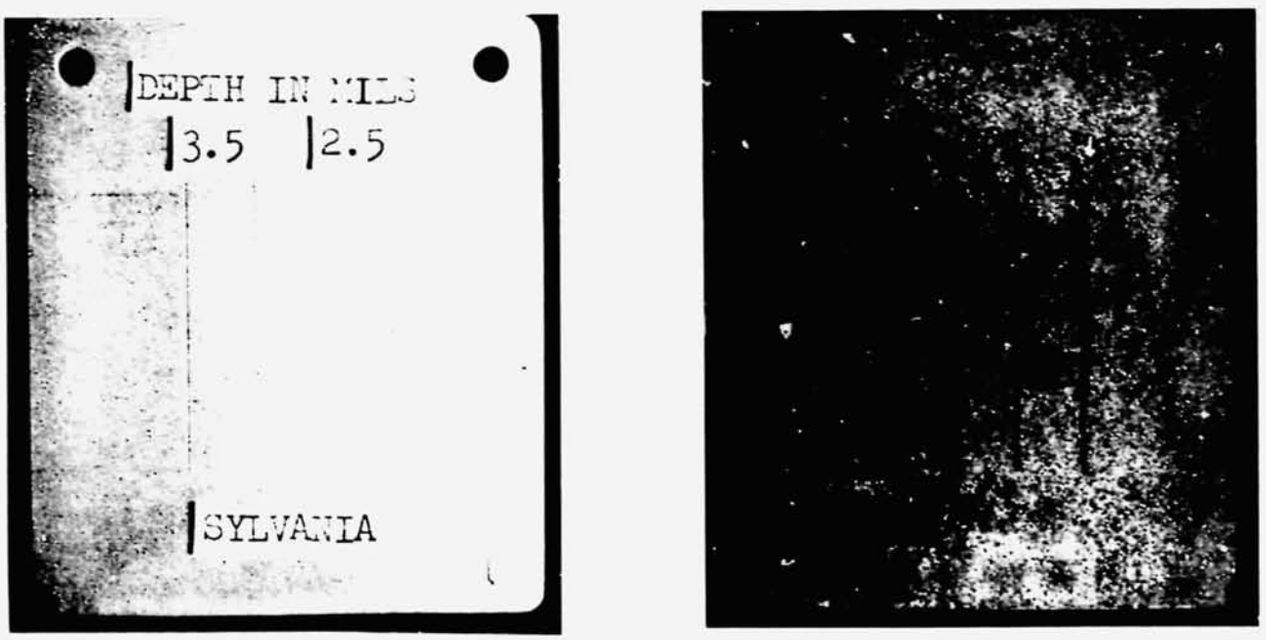

BEFORE OXIDATION TESTING 1.4X

AFTER OXIDATION TESTING 25 HOURS AT 2400°F 1.4X

SYLVANIA R–512E SCRATCH TESTS BEFORE AND AFTER OXIDATION TESTING

457–1190

Figure 5–17

on the second set of test specimens indicated an average scratch depth of 1.5 to 2 mils less than the milling machine readings. These depths were confirmed by metallographic examination which also revealed that the carbide tool in the milling machine was deforming the metal slightly, accounting for the difference in depth measurements (see figure 5-20). Thus, the scratch depths for the second R-512E series of 2, 4, 6, and 8 mils were corrected to 0.6, 1.9, 4.2, and 5.8 mils, respectively, and those for the second VH-109 series of 2, 4, 6, and 8 mils were corrected to 0.6, 2.2, 4.3, and 5.9 mils, respectively. After oxidation testing conducted at 2400°F, the 6 and 8-mil cuts in both coatings failed in the first hour at 2500°F, but the 2 and 4-mil scratches did not fail after 25 hours. Figures 5-18 and 5-19 show these specimens before and after oxidation testing, and figure 5-20 shows a metallographic section through scratches of 4 mils in depth (2 mils by optical measurement device). Note that the coating is cracked and broken in the scratch area, indicating that a clean cut was not being made. In actual practice, it is unlikely that a material of sufficient hardness will contact the coating to cut or scratch without physically damaging the remaining coating.

5.6 ABRASION DAMAGE - Abrasion, which occurs when two surfaces in contact are caused to move with respect to each other, may adversely affect a surface by wearing away or by galling.

5.6.1 Coated Refractory Metal Experience - MDAC has considerable experience with abrasion in the production of the ASSET and BGRV flight systems. Abrasion has occurred in low cycle/low load applications, such as thread interaction in fasteners, spring clips, panel seals, etc. Although abrasion was considered carefully, it has never been a problem. The BGRV program employed coated columbium in a flare seal application and in a special monoball bearing. In these applications the LB-2 aluminide coating was applied to Cb-752 columbium alloy, which proved to be very satisfactory. Figure 5-21 shows a sliding seal test specimen after 6,000 cycles of 8 lb/in loading, with a 1-inch stroke length and a frequency of 47 cycles per minute. A photomicrograph through the area of highest wear is shown in figure 5-21.

A detailed test program was conducted to select and qualify coated columbium as the bearing material to be used at 2500°F. (The final bearing configuration is shown in figure 5-22.) Candidate materials, including LB-2-coated Cb-752, were fabricated into simple radial bearings and tested under BGRV reentry conditions.

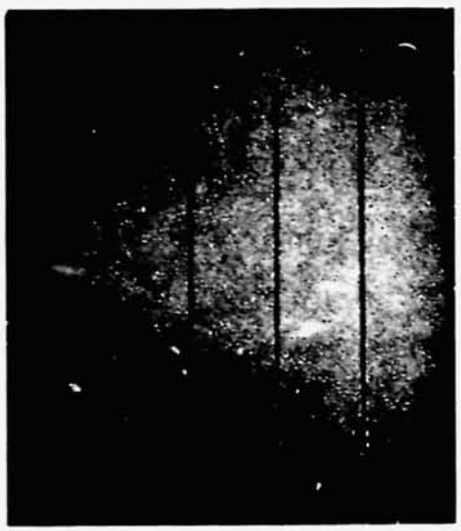

1.2X

BEFORE OXIDATION TESTING

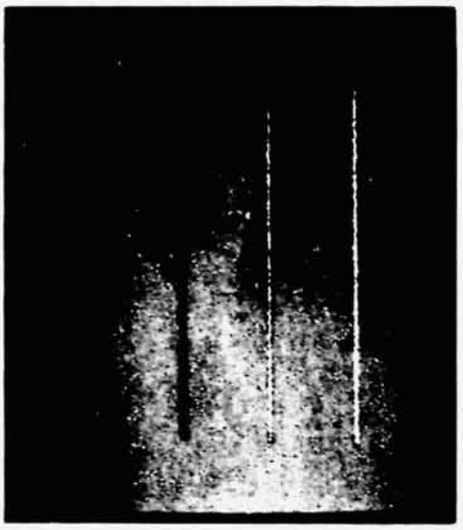

1.2X

AFTER OXIDATION TESTING AT 2400°F FOR 25 HOURS

SYLVANIA R-512E SCRATCH TEST SPECIMENS

457-1192

Figure 5-18

1.2X

BEFORE OXIDATION TESTING

1.2X

AFTER OXIDATION TESTING AT 2400°F FOR 25 HOURS

457-1193

VAC-HYD VH-109 SCRATCH TEST SPECIMENS

Figure 5-19

BEFORE OXIDATION TESTING

AFTER 5 HOURS AT 2400°F

SCRATCH DEPTHS OF 2 MILS BEFORE AND AFTER OXIDATION TESTING

Figure 5-20

457-1216

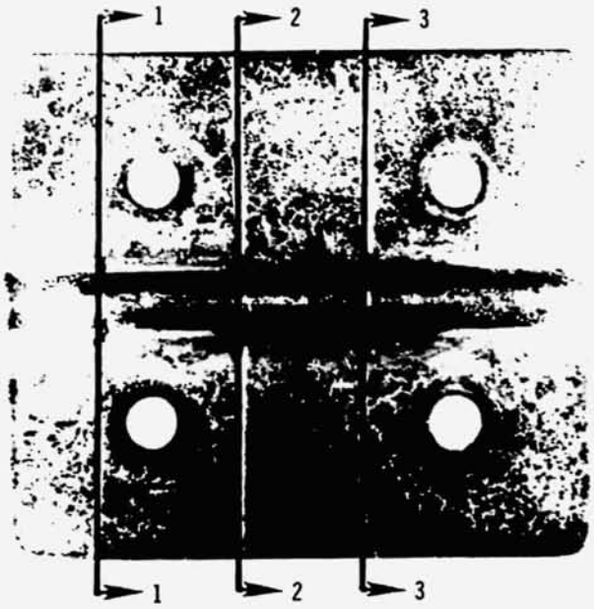

SLIDING SEAL SPECIMEN

PHOTOMICROGRAPH OF COATING IN WEAR AREA
250X

RESULTS OF BGRV SLIDING SEAL TEST

Figure 5–21

457–1194

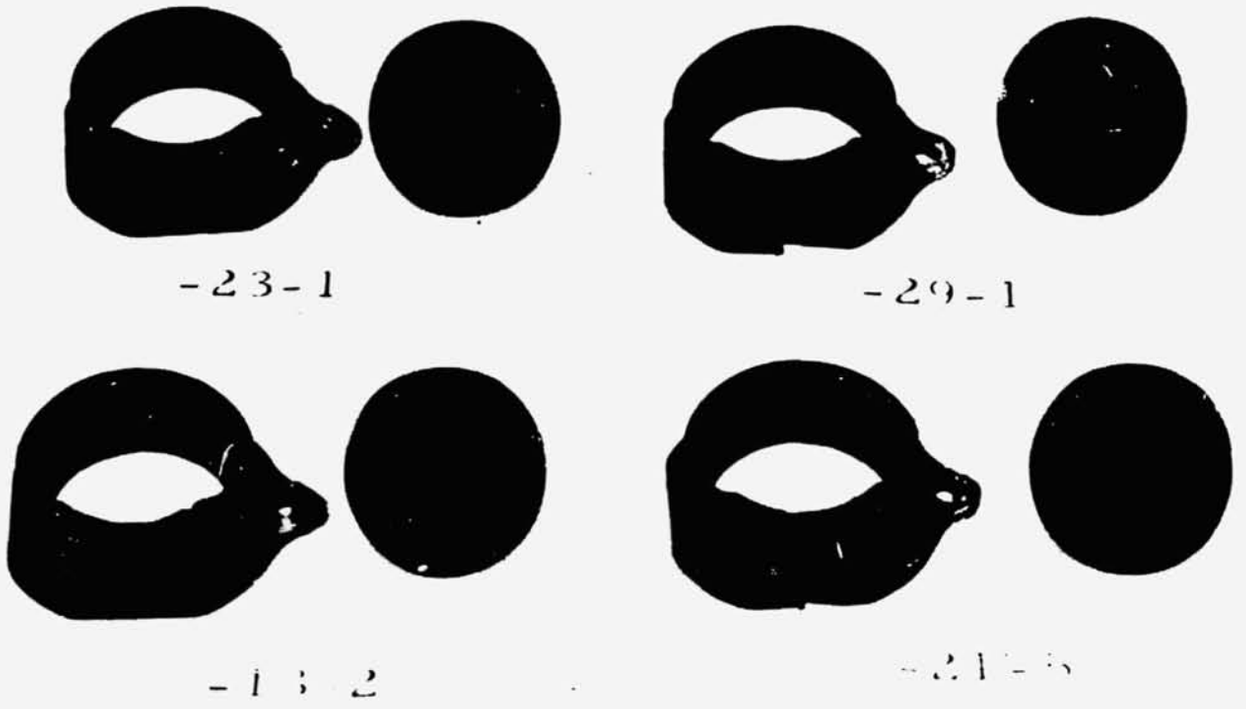

BGRV COATED COLUMBIUM BEARINGS Figure 5-22

Since coated columbium proved to be the material with the lowest coefficient of kinetic friction and best withstood wear under the required loads, this material was selected. The bearings qualified and were used successfully on the flight hardware. Generally, no major problems have been encountered in our comprehensive experience in abrading applications of coated columbium.

5.6.2 Program Considerations - The several possibilities for which abrasion will need to be considered include thread interaction in fasteners, spring clips for insulation or instrumentation, door seals, and panel expansion joints. Specific applications for which specific test parameters could be defined were not identified.

5.6.3 Abrasion Testing and Results - An abrasion test apparatus, set up and available in the Materials Laboratory, was employed. Since specific design conditions and parameters were not defined, a broad-interest abrasion test was sought. The apparatus reciprocated a loaded specimen holder against solidly mounted coupons, by means of a hydraulic ram coupled to the specimen holder through a strain measurement link. The internal details of the test apparatus are shown in

figure 5-23. A square inch of each coated alloy was epoxy bonded to the wear pads and the common coated material was positioned on the carrier bar with mechanical fasteners. The apparatus was assembled and the stroke length adjusted to 0 22 inch, a normal force of 875 lb/in^2 of bearing area was applied, and a ram force of 2,000 lb was required to sustain the motion. One set of specimens was tested for 1139 cycles (2278 strokes) and when the strain indicator showed a major change in the surfaces of the coatings, cycling was terminated. A second set of specimens was tested for one-half the number of cycles (631) as the first set. The following table gives the normal loading for each combination of specimens tested:

SPEC. NO.	NUMBER OF CYCLES	WEAR AREA (IN^2)	NORMAL STRESS (LB/IN^2)
VAC-925		0.91	961
VAC-934	1139	0.88	994
SYL-6		0.96	910
SYL-7		0.94	931
VAC-936		0.87	1006
VAC-92	631	0.90	972
SYL-9		0.74	1182
SYL-10		0.67	1306

The specimens after testing are shown in figure 5-24. Oxidation testing was not conducted, since the specimens would have failed immediately in the areas in which galling had occurred and the underlying substrate had been disturbed.

5.7 COATING DEFECTS - Coating defects are chemical or physical anomalies which occur in the coating and lead to premature oxidation failure.

5.7.1 Past Experience - Although documented cases of chemical anomalies or defects in coated columbium hardware exist, these are usually associated with coatings in which sufficient reliability has not been demonstrated. Quality assurance testing on a regular basis can be expected to identify such cases. The presence of physical anomalies is much more common and represents the area of greatest concern. Intermetallic or diffusion coatings generally reproduce the physical surface of the columbium accurately, therefore, physical defects in the coating are commonly associated with disturbance of the columbium surface being coated. Edges and corners represent disturbances in the surface being coated and have proven to be the most probable area of early coating failures.

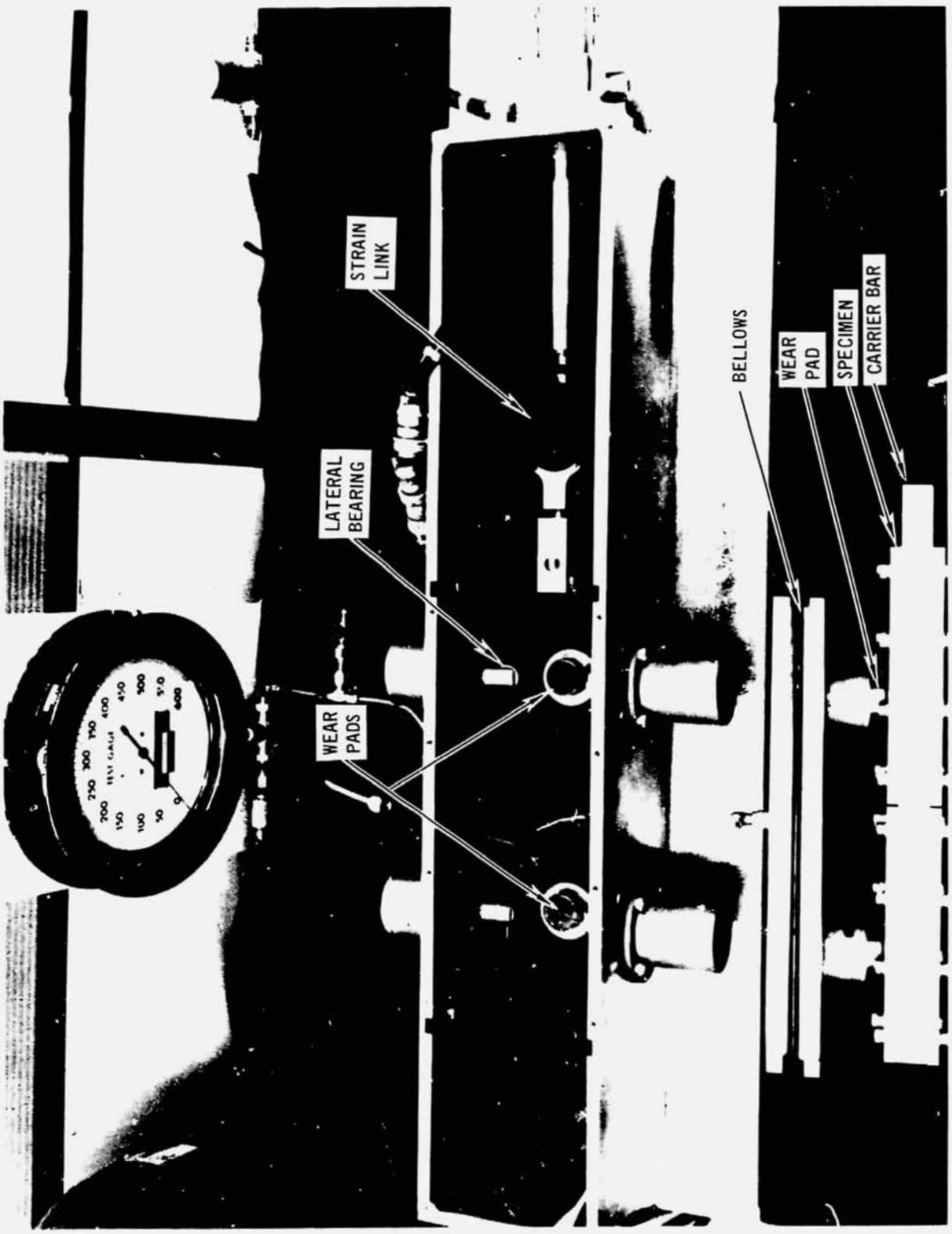

INTERNAL PARTS OF ABRASION TEST APPARATUS

457-1196

Figure 5-23

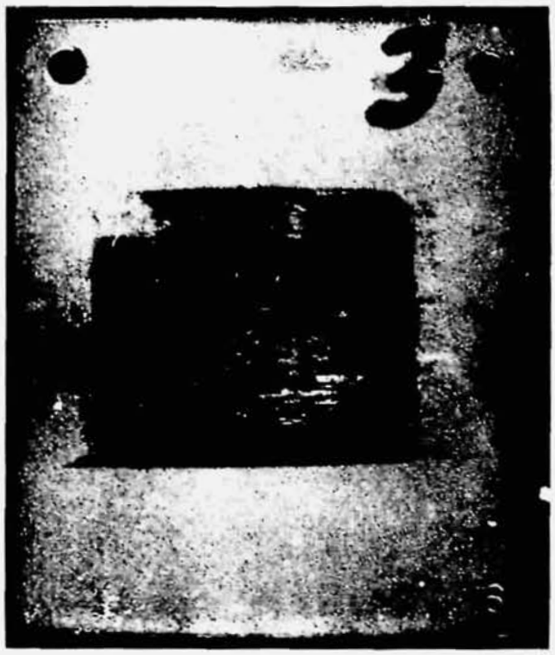

1.5X

R-512E

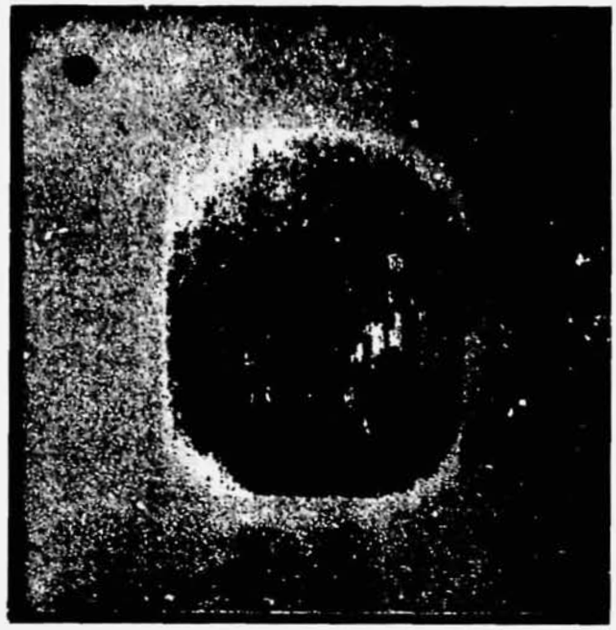

1.6X

VH-109

457-1197

TYPICAL RESULTS OF ABRASION TESTING

Figure 5-24

While coatings vary in their ability to protect sharp edges, it has become standard practice to radius all edges and corners, and the more generous the radii, the better the performance of sheet metal parts. MDAC has paid particular attention, on all refractory metal programs, to edge preparation to limit coating defects on edges.

5.7.2 Edge Defect Testing - A series of edge defect test specimens was prepared to study the effects of sharp edges. Standard 2 by 2-inch coupons, described in paragraph 3, were prepared from 0.020-inch columbium alloy sheet. To increase the length of linear edge distance, four 1/2-inch diameter holes were drilled in each coupon. The burrs were removed from the edges but they were not radiused, and the coupons were coated with the request that the edge preparation not be improved.

The dimensional change coating thickness was determined to be 2.2 mils per surface for the Sylvania R-512E and 2.6 mils per surface for the VAC-HYD VH-109. A careful examination for edge cracking revealed very little edge cracking in the R-512E and a moderate amount in the VH-109, with the differences noted attributable to differences in coating thickness. The specimens were tested for 25 hours at 2400°F. The VH-109 specimens did not show any oxidation failures in the 25-hour test. One of the holes in the R-512E series showed an oxidation failure after 20

hours at 2400°F. Figures 5-25 and 5-26 show these specimens before and after oxidation testing.

Judging from the quality of the edges after coating, it was not surprising that these specimens performed reasonably well in oxidation. However, edge cracking is clearly a potential point for early coating failures and should be avoided. It is believed that the fused slurry silicide process has a tendency to produce better edge quality than coatings available in the past. Assuming there is adequate slurry present on the edges, the chemical reactions at the coating temperatures are so aggressive that areas such as sharp edges are consumed at an increased rate by the slurry. This smooths out the edges, reducing the tendency of the coating to crack on the edges. Coating thickness is an important factor in edge quality, and must be closely controlled to yield optimum edge coating quality.

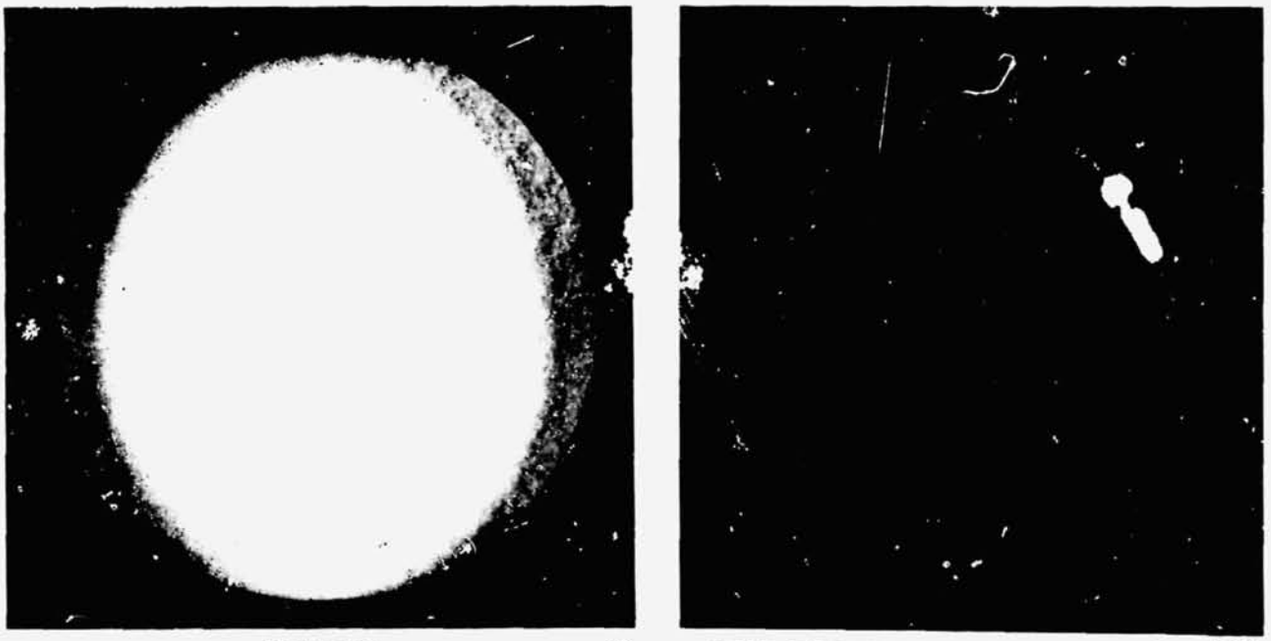

AS COATED 6X

AFTER OXIDATION TESTING 20 HOURS – 2400°F 4.2X

TYPICAL SYLVANIA R-512E COATING ON EDGE TEST COUPONS

Figure 5-25

457-1198

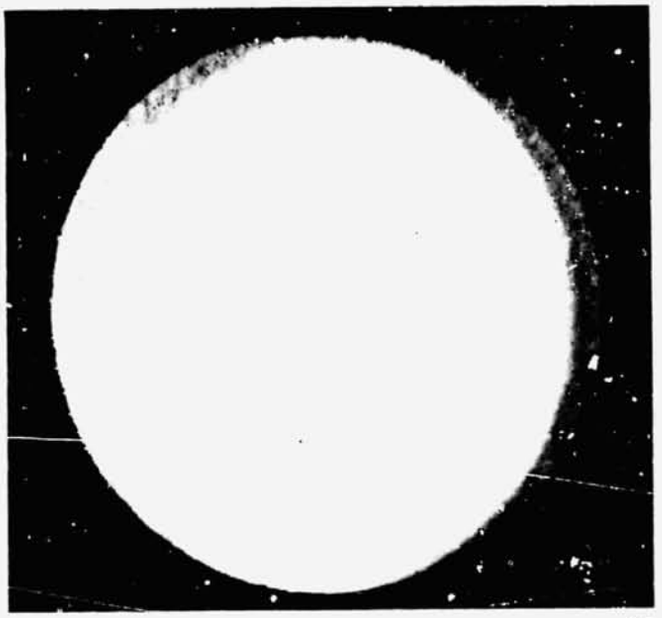

AS COATED 6X

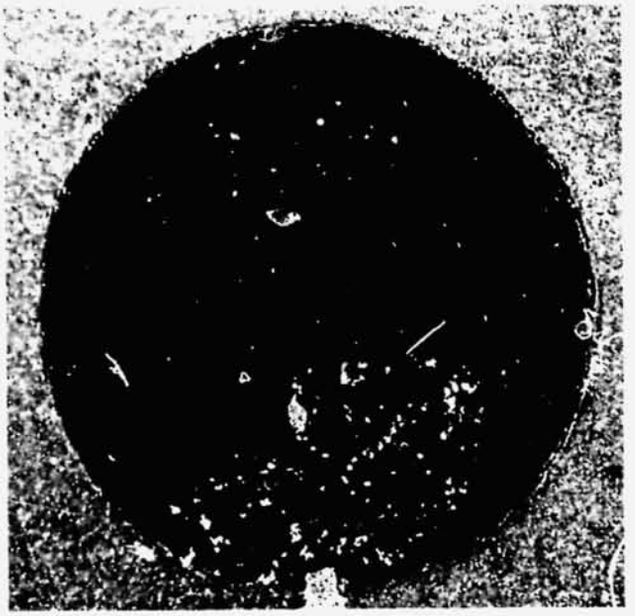

AFTER OXIDATION TESTING 25 HOURS – 2400°F 6X

TYPICAL VAC–HYD VH–109 COATING ON EDGE TEST COUPONS

Figure 5–26

6. STRUCTURAL INTEGRITY TESTING OF PANELS WITH UNREPAIRED COATING DAMAGE

A series of rib stiffened panel specimens was flight simulation tested in an intentionally damaged and unrepaired condition to define the necessity for field repairing local damage to coated columbium thermal protection panels. The specimens employed were 1 by 4-inches, which was the largest that could be tested with existing facilities. Subsequent testing of repair-coated panels was accomplished in a new flight simulation apparatus described in section 12. The 1 by 4-inch specimens were quite acceptable for obtaining the qualitive results desired to demonstrate field repair requirements. The general procedure involved the alternate exposure of the panels to reentry simulation under load and boost acoustic fatigue loading.

6.1 SPECIMEN PREPARATION - The rib stiffened panel specimens described in paragraph 3 were intentionally damaged after protective coating. All defects were located on the exterior skin side of the panels to simulate damage which would be repairable in the field. Two sizes of defects were employed, 0.12 and 0.06 inch in diameter. The coating was completely removed to the columbium substrate by gritblasting. A Porta-blast gritblaster was used to remove the coating from the 0.12-inch diameter defects and a Micro-blaster was employed to produce the 0.06-inch diameter defects. The defects were placed in the center of the panels (2 inches from each end) to match the center of the maximum bending moment area on the specimen. Two defect locations were investigated - on the skin over the rib and on the skin midway between the ribs. Defects on the edges of the skin were not tested because previous testing has shown that the edges are the least critical area (reference 1). Figure 6-4 illustrates the defected specimens prior to testing.

6.2 PROFILE TESTING - The profile simulation testing was conducted in the profile simulator shown in figure 6-1 and employed the profile shown in figure 4-1. The load was applied to the panel specimens using a four point loading fixture fabricated from FS-85 alloy columbium and protected with the R-512E coating. The loading fixture and the bending moment distribution it produced are shown in figure 6-2. The loading fixture containing the specimen was then positioned in the furnace and secured to the loading drive mechanism. The boost load was applied and released, and the facility then automatically followed the time, temperature, pressure, and stress profile. After returning to approximately

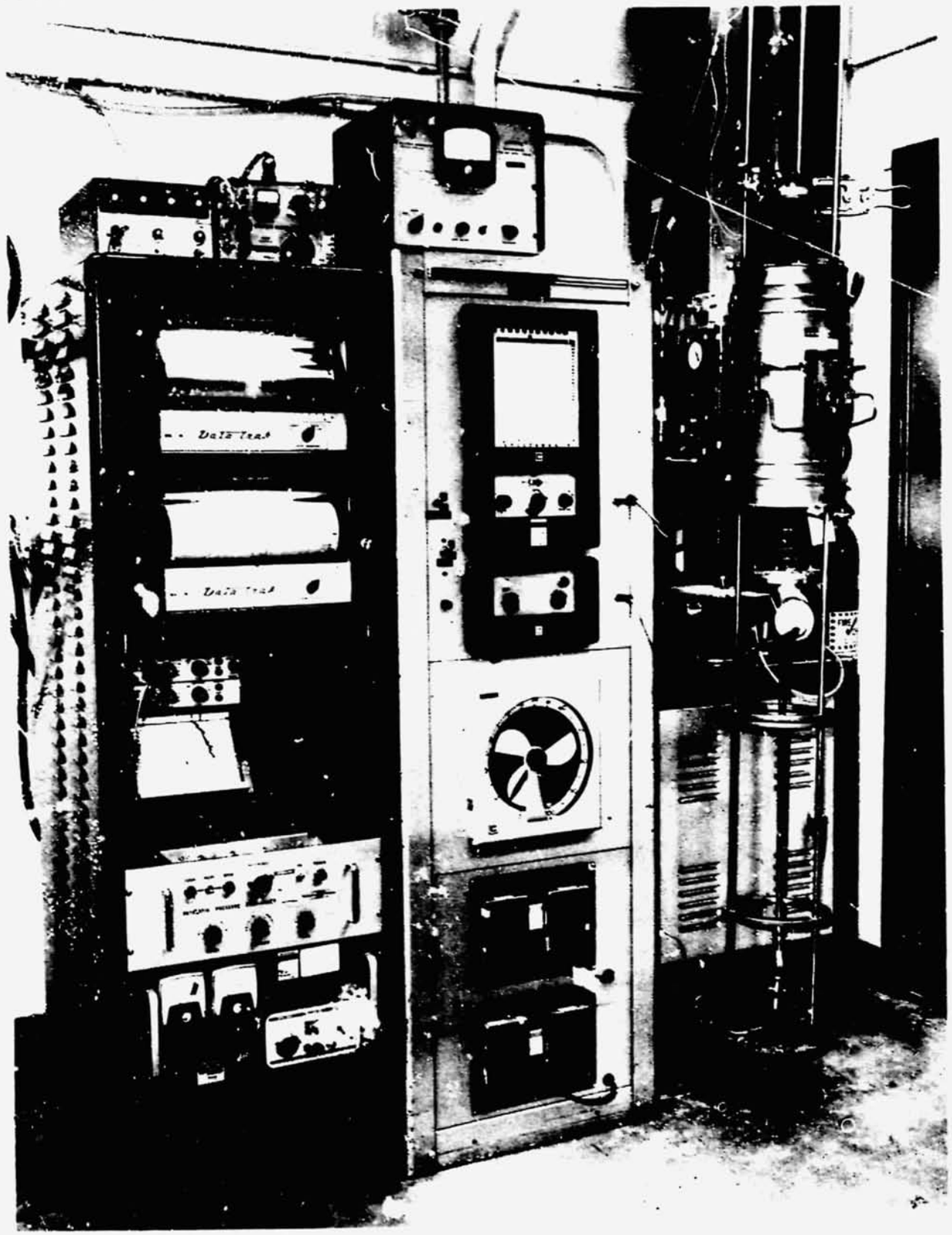

457-1201

PROFILE TEST SIMULATION TEST FACILITY

Figure 6-1

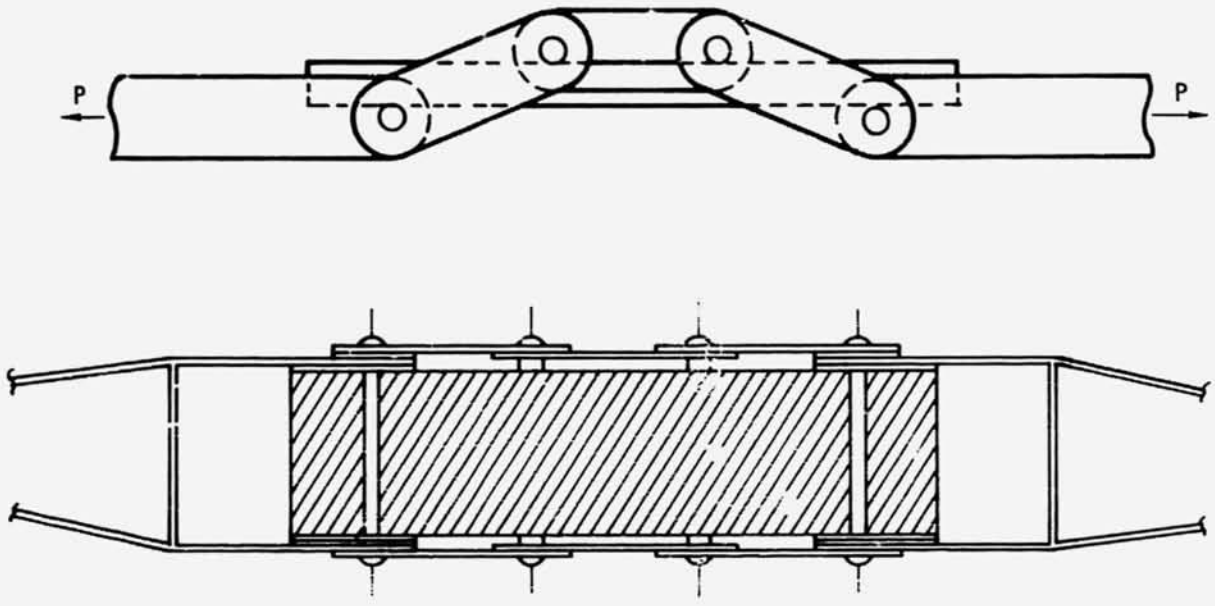

457-1155

Four Point Loading Fixture

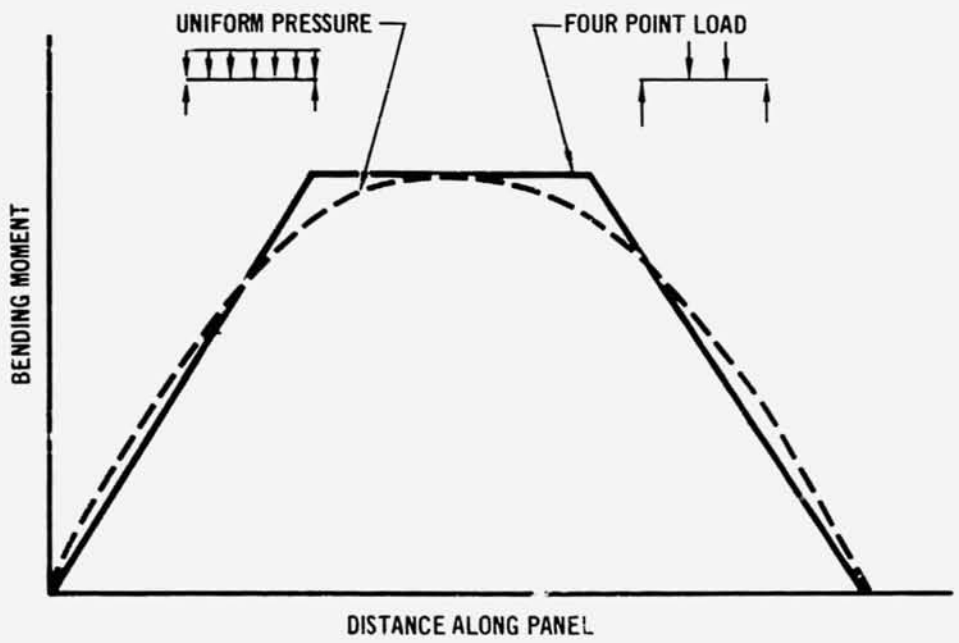

Panel Bending Moment Distribution

457-1156

Figure 6-2

room temperature, the boost load was reapplied and the entire procedure repeated. After each 10 cycles, the panel was removed and visually examined to determine the extent of oxidation within the defect area, and to check for crack initiation. Deflection measurements were made after each 10 profile cycles in a nondefected area. Prior to starting the second series of 10 profile cycles, the panels were vibration tested to simulate boost acoustic loading.

6.3 ACOUSTIC SIMULATION TESTING - The initial step was to fabricate and calibrate a fixture for the acoustic simulation testing. Initial attempts were made to use a random acoustic driver; however, at the maximum output of 173 db, it would not produce the desired stress level in the skin. A new fixture was fabricated and mounted to an electrodynamic exciter system.

A special vibration fixture was fabricated to support the rib stiffened panel specimen in a simply supported configuration. The fixture consisted of two U-shaped clamps mounted on each end of an aluminum plate. The panel was installed within the clamps of the fixture to obtain a pin-ended clamp condition on each end of the specimen. A machined aluminum block was positioned in each end of the panel specimen to prevent the panel's ribs from buckling when a preload was applied to the panel by the clamp assemblies. The panel/fixture assembly was installed on a 6,000 pound-force electrodynamic exciter unit. A single piezoelectric type accelerometer was mounted on the vibration fixture to control the input acceleration levels to the test specimen. Figure 6-3 shows the panel and vibration fixture assembly.

The calibration panel had a 3-element strain rosette attached to the skin in the center of the panel. The panel was initially excited sinusoidally from 500 to 3,000 Hz at an input acceleration level of approximately 17.7 g_{rms}. Sinusoidal excitation was used to identify the panel's predominant bending frequencies. During sinusoidal excitation, on-line frequency response plots were made to determine the frequencies of peak response. The frequency response plots were obtained by plotting the ratio of the strain response amplitude to the input acceleration amplitude as a function of frequency. The bending mode of interest was determined to be in the frequency range of 1500 to 1900 Hz. The panel was then subjected to random excitation at an input overall acceleration level of approximately 79 g_{rms}. This acceleration level was the highest random acceleration level attainable with the exciter system. The exciter/equalizer system was fully attenuated below 1500 and above 1900 Hz, using bandpass filters to provide the maximum acceleration to the test specimen in the frequency band of 1500 to 1900 Hz. The rms stress

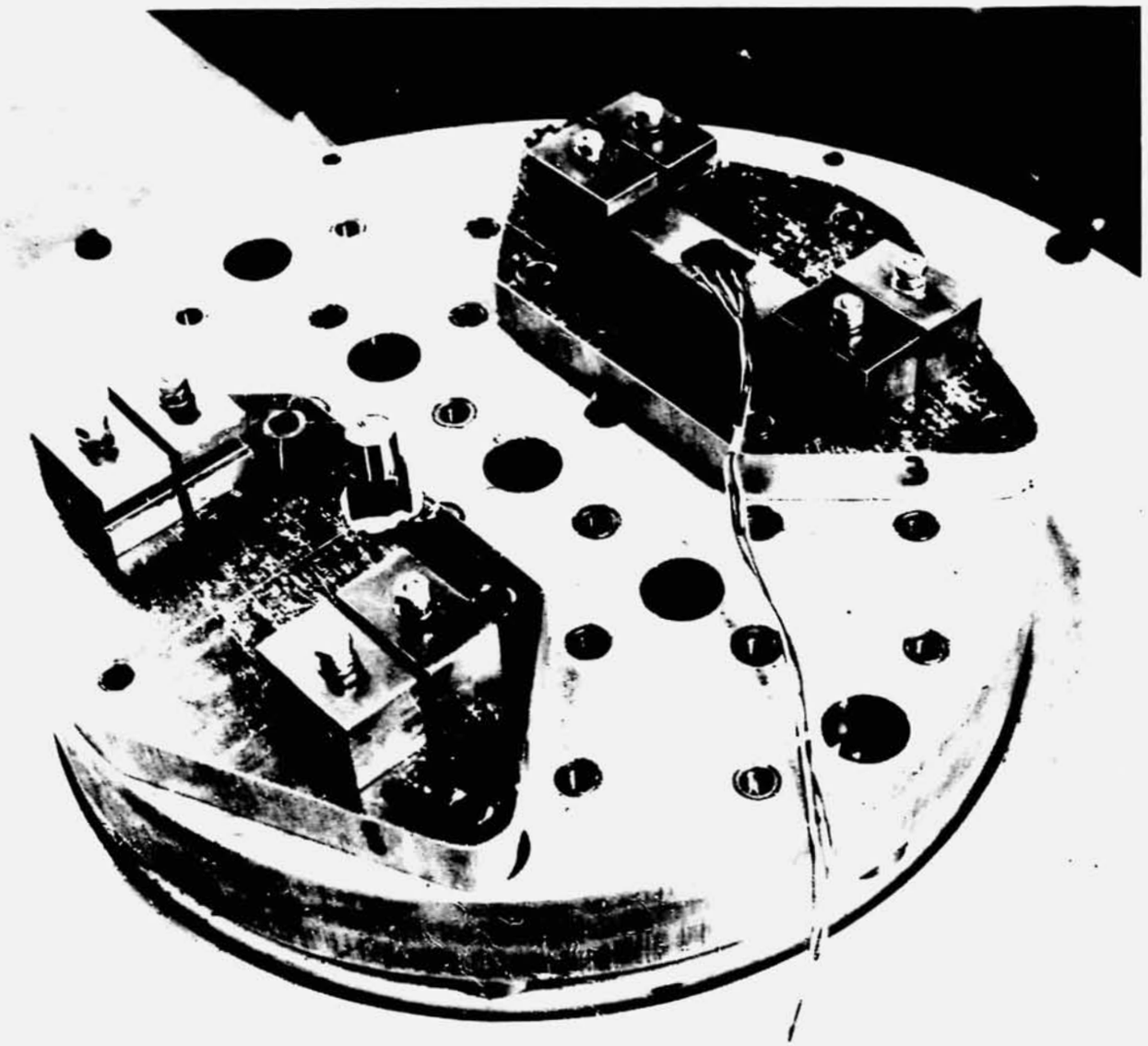

457-1202

RIB STIFFENED PANEL SPECIMEN IN VIBRATION SETUP

Figure 6-3

level measured from the output of the strain gage installed on the panel during the random vibration test was 3810 lb/in^2 and was considered to be a sufficient stress level for testing the rib stiffened panels with unrepaired damage. The test panels were subsequently subjected to the same random vibration environment used for the calibration panel. The unrepaired specimens were alternately subjected to profile cycling and vibration testing after every 10 cycles until structural failure occurred.

6.4 UNREPAIRED DAMAGE TEST RESULTS - A total of eight rib stiffened panel specimens were tested, four Sylvania R-512E coated Cb-752 and four VAC-HYD VH-109

coated C-129Y alloy. The initial set of four specimens (two coated alloy combinations and two defect locations) had 0.12-inch diameter defects. The second set of four specimens had 0.060-inch diameter defects placed at the same defect locations. Table 6-1 summarizes the profile and boost acoustic simulation tests.

The initial set of 4 specimens was given 10 profile cycles. In the case of both the Cb-752 and C-129Y panels, a hole was oxidized through the skin. The holes associated with the defects located between the ribs were equal in diameter to the 0.12-inch diameter coating defect. In the case of the defects located in the skin over the ribs, the additional volume of columbium restricted the oxidation hole area to one small hole through the skin on each side of the rib (see figure 6-5).

The acoustic simulation testing of the initial set of four rib stiffened panel specimens was conducted after the tenth profile cycle in accordance with paragraph

Table 6-1

RIB STIFFENED PANEL SPECIMEN TEST RESULTS

PANEL NUMBER	ALLOY AND COATING	DEFECT SIZE (IN DIA) & LOCATION	TOTAL PROFILE CYCLES	BOOST VIBRATION EXPOSURES-TIME (SECS)	RESULTS OF TESTING
VH-12	C-129Y-VH-109	0.12 - OVER RIBS	21	2-427	OVERLOADED ACCIDENTALLY AND CRACKED BOTH RIBS
VH-14	C-129Y-VH-109	0.12 - BETWEEN RIBS	10	1-400	RIBS CRACKED ADJACENT TO LOAD PAD
SYL-5	Cb-752-R-512E	0.12 - OVER RIBS	10	1-400	RIBS CRACKED ADJACENT TO LOAD PAD; SKIN CRACKED FROM DEFECT AREA
SYL-6	Cb-752-R-512E	0.12 - BETWEEN RIBS	10	1-400	RIBS CRACKED ADJACENT TO LOAD PAD
VH-16	C-129Y-VH-109	0.06 - OVER RIBS	50	5-135	NO STRUCTURAL FAILURE
VH-15	C-129Y-VH-109	0.06 - BETWEEN RIBS	50	5-135	NO STRUCTURAL FAILURE
SYL-3	Cb-752-R-512E	0.06 - OVER RIBS	50	5-135	NO STRUCTURAL FAILURE
SYL-2	Cb-752-R-512E	0.06 - BETWEEN RIBS	31	2-54	OVERLOADED ACIDENTALLY; BROKE IN TWO

457-1199

RIB STIFFENED PANEL SPECIMENS

6.3. The time selected was 900 seconds, equivalent to ten 90-second boost duration periods. Cracks were observed in two specimens at approximately 270 seconds, and testing was terminated at 400 seconds, with three of the four specimens having experienced cracking. Typical failures are shown in figure 6-6 with the crack initiating from the inside edge of the load pad and progressing into the rib. Of the eight possible ribs in the initial series, five ribs cracked in a similar manner. One panel, C-129Y panel number 12, did not show any cracking after the 400-second test. These failures were not associated with the damage spots intentionally put into the coating. There was, however, one crack in Cb-752 panel number 5 which initiated in the coating damage area and progressed parallel to the rib, through the electron beam weldment on both sides of the damage site area. This failure is shown in figure 6-5.

An analysis of these fatigue failures was conducted prior to performing additional panel acoustic loading tests. The original stress levels and predicted number of cycles had been compared with C-129Y alloy fatigue strength data (reference 5) and it was concluded that the selected conditions would not fail the unaffected C-129Y alloy. With the random cycle energy input test procedure being employed, the early failure made the use of this data suspect. It was further concluded that the point of crack initiation had experienced a stress level of approximately 11,000 lb/in^2 due to the fact that the back of the rib was farther from the panel neutral bending axis and a local stress concentration area (estimated concentration factor of 3) was caused by the termination of the load pad (see figure 6-6). The point of failure initiation was estimated to have experienced 11,000 lb/in^2_{rms} for 460,000 cycles. This condition was compared with a probable fatigue strength curve for Cb-752 which employed simple tension-tension loading data corrected for compression-tension load and random loading effects. According to this adjusted data, the rib failure was predicated at 300,000 cycles, which compares favorably with the 460,000 cycles experienced; thus, the rib was shown to be the critical member and it was decided to adjust the test time (number of cycles) to preclude rib fatigue failure in an undefected area for the remaining panels to be tested. A test time of 27 seconds was selected, which was expected to yield fatigue failure initiation in the rib after 60 cycles.

The second series of 4 rib stiffened panel specimens containing the 0.06-inch diameter defects were profile tested for 10 profile cycles and a 27-second vibration test without initiating a structural failure. The oxidation of the skin for either alloy or damage location did not quite produce a hole through the skin.

DEFECTS IN SKIN OVER RIBS

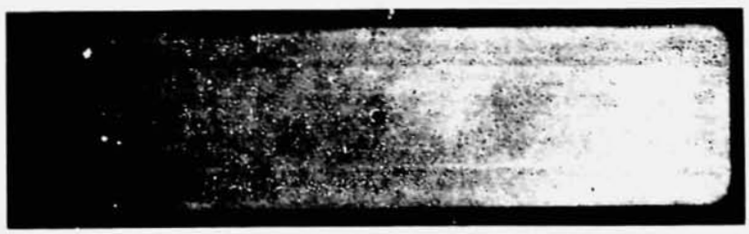

DEFECT IN SKIN BETWEEN RIBS

DEFECTS IN COATED RIB STIFFENED PANEL SPECIMENS PRIOR TO TESTING

457-1200

Figure 6-4

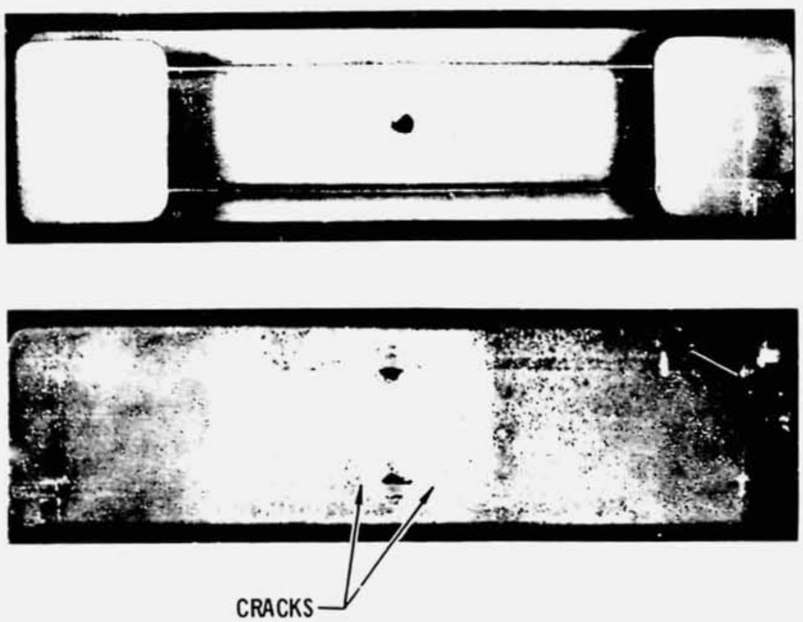

TYPICAL RIB STIFFENED PANEL SPECIMENS WITH
.12 INCH DEFECTS AFTER 10 PROFILE CYCLES

457-1204

Figure 6-5

457-1205

FATIGUE CRACK INITIATING AT TERMINATION OF LOAD PAD

Figure 6-6

The only change in the 4 panels after the second sequence of 10 profile cycles and a 27-second vibration was that a hole had been oxidized through the skin at each defect site. The average diameter of the hole in the free skin was 0.07 inch in diameter. Oxidation failures in the area of clamping for the vibration tests were ignored, since they were in a low stress area and not close to the coating damage sites.

Between the twentieth and thirtieth profile cycles, Cb-752 panel number 2 was overloaded and broken in two. A failing load was not obtainable. Interestingly, the panel did not fail through the hole located at the damage site. The contamination zone around the defect area was determined metallographically to be 0.067 inch in diameter greater than the perimeter of the oxidation hole. Since the failure occurred 0.15 inch from the perimeter of the defect oxidation hole, the failure occurred in the unaffected Cb-752 alloy. Apparently the increase in oxygen content strengthened the Cb-752 sufficiently to compensate for the loss of load bearing cross section in the defect. Figure 6-7 shows the broken panel and figure 6-8 shows a cross section of the skin through the defect oxidation area.

The remaining three panels, 2 C-129Y alloy and 1 Cb-752, progressed through 50 profile cycles and the associated vibration cycles without structural failure. The only evident change was in the diameter of the oxidation hole located in the defect area. The average hole diameter was 0.2 inch in the skin. Figure 6-9 shows the panels after the 50 profile and acoustic cycles. The testing was terminated at this point because the holes had become so large that the condition would not be tolerable in an operational flight panel.

Creep deflection during the testing was negligible. The same specimen configuration, test conditions, and equipment were employed on another program in which the panels were not defected. The creep deflections compared favorably with

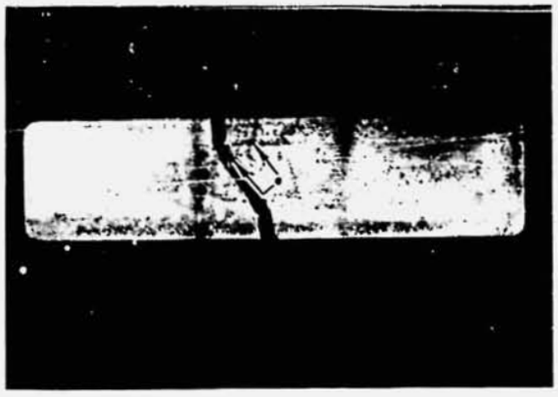

457-1206

PANEL SPECIMEN FAILED FROM ACCIDENTAL OVERLOADING –
FAILURE NOT THROUGH DEFECT

Figure 6-7

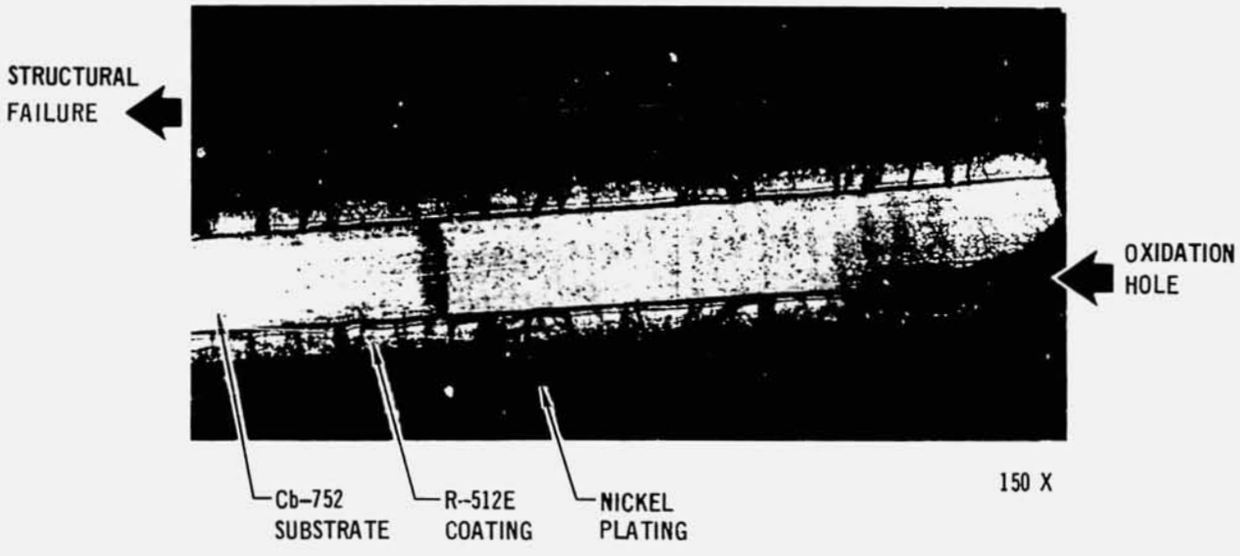

457-1207

PANEL SHOWN IN FIGURE 6-6 IN DEFECT AREA –
NOTE FAILURE IN OUTSIDE CONTAMINATION AREA

Figure 6-8

those predicted during the test profile selection (reference 6). This verified that the test method meets the desired conditions and indicated that lack of deflection was attributable to a strengthening of the columbium due to oxygen migration into the substrate from the defect area.

6.5 COMMENTS AND OBSERVATIONS - The following comments and observations are pertinent to the testing of the rib stiffened panel specimens having unrepaired coating defects:

(a) Local coating damage sites in the skins of columbium panels require

PANEL SYL – 3

PANEL VH –15

PANEL VH – 16

RIB STIFFENED PANEL SPECIMENS AFTER 50 PROFILE CYCLES
(END FAILURES DUE TO CLAMPING IN VIBRATION FIXTURE)

Figure 6–9

457-1208

repair coating to prevent holes from being oxidized through the skin. Holes would be undesirable because they would permit boundary layer gasses to enter the vehicle. The structural integrity of rib stiffened panels was not impaired by holes in the skin up to 0.2 inch in diameter.

(b) The panel specimen employed was not designed for an adequate evaluation of the fatigue effects associated with the skin defects under evaluation. However, the testing performed indicates that grossly deleterious fatigue strength effects are not associated with the local loss of coating protectiveness.

7. CERAMIC FIELD REPAIR DEVELOPMENT

The most common type of field repair coating employed in the past has been ceramic cements. Ceramic repairs have the advantage of being easy to apply in the field, since they require little, if any, special equipment. MDAC has successfully used these types of repairs on coated refractory metals for glide reentry vehicles which did not require long lives or high reuse capabilities. Reference 7 describes the use of a commercially available cement (Sauereisen No. 63) as a field repair material for the ASSET vehicle. Subsequent studies (references 8 and 1) indicated that longer life compositions were available while maintaining the advantage of easy application.

The chief disadvantage of the ceramic cements is that the life was found to be much less than that of the fused slurry silicides. Also, the ceramic cements were found to allow oxygen to penetrate to the columbium substrate, causing contamination due to oxygen solution. The passage or leakage of oxygen was always higher during the initial heating to elevated use temperatures, at which point the high temperature bonding mechanism of the cement was realized and the cement became sealed. Further oxygen contamination typically occurs at a lower rate, causing the contaminated area to increase slowly. Thus, past experience had shown that an improvement in ceramic cements could be achieved by increasing their lives and reducing or eliminating the contaminated and embrittled area in the columbium substrate below the ceramic repair.

7.1 BASIC APPROACH AND PROCEDURES - The ceramic cement compositions of interest were evaluated on the two columbium alloy and coating systems used on this program, namely the Sylvania R-512E coating on Cb-752 and the VAC-HYD VH-109 coating on C-129Y. Both coatings are fused slurry silicides though differing in composition. The initial evaluation was conducted by oxidation testing at 1 atmosphere in 1 hour cycles up to 25 hours at 2400°F. This was arbitrarily selected as a screening test to yield an oxidizing potential similar to 100 reentry profile cycles under external surface conditions. Repair compositions which passed the 1 atmosphere screening test were evaluated under the reentry profile conditions of time, temperature, and air pressure shown in figure 4-1.

The ceramic field repair development was conducted over a period of several months and was divided into the following general phases:

a) identify ceramic compositions employed in the past and evaluate promising repairs on coatings of current interest
b) perform compatibility testing of candidate repair materials in contact with both fused slurry silicide coatings
c) develop ceramic repair compositions to meet specific requirements of this program
d) develop an alternate low temperature vehicle system with improved physical characteristics and performance.

The final evaluation of all developed repairs, including the ceramics, was accomplished with 3 by 12-inch rib stiffened panels. These repaired panels were tested under simulated reentry flight conditions as described in section 12.

7.2 INITIAL CERAMIC REPAIR DEVELOPMENT EFFORT - A review of past development effort indicated that three basic compositions should be evaluated on the Sylvania R-512E and VAC-HYD VH-109 coatings. Coated coupons 2 by 2-1/4 inches were prepared with intentional defects 1/4-inch in diameter. A standard defect was selected to enable comparison of repair compositions. Defects were produced by gritblasting the coating from the desired area down to the columbium substrate. The initial compositions (see appendix A for complete composition) evaluated were:

a) pyrex frit, aluminum oxide, and boron in a lacquer binder (with and without Al_2O_3 flame spray undercoat)
b) pyrex frit, columbium disilicide, and silicon carbide in a colloidal silica binder
c) pyrex frit, Sauereisen no. 8 cement, columbium disilicide, and aluminum oxide in a colloidal silica binder.

The repair coating thicknesses and test results are presented in table 7-1. The composition A was effective in protecting the columbium substrates for 25 hours at 2400°F. In both alloys there was an adverse reaction between the repair and the fused slurry silicide coating on the periphery of the ceramic for those repairs in which the precoating with flame-sprayed aluminum oxide was not present. The reaction with the VH-109 coating was severe and general coating failures occurred in a discolored area around the repairs. A series of experiments (numbers 1 through 4 in table 7-1) were conducted in which the thickness and diameter of the aluminum oxide flame-sprayed undercoating was verified. It was determined that a larger diameter and thickness of aluminum oxide improved the compatibility (reduced

Table 7-1

INITIAL EXPERIMENTS
SPECIMEN DESCRIPTION AND TEST RESULTS OF CERAMIC FIELD REPAIR DEVELOPMENT

EXP NO.	SPECIMEN NO.	REPAIR COMPOSITION	FLAME SPRAY Al_2O_3 THICKNESS (MILS)	REPAIR THICKNESS (MILS)	OXIDATION CHECK TEST		GENERAL COMMENTS ON REPAIRED AREA, AFTER OXIDATION CHECK TEST
					PROFILE CYCLES	AIR ATMOSPHERE 1-HR CYCLES AT 2400°F	
1	S-1E	A	1.2	14 5		25 NF	DULL BLACK SURFACE
	S-1F	A	1.3	12.6		25 NF	DULL BLACK SURFACE
	S-1G	A		19.7		15 F	FAILED IN DEFECT AREA
	S-1H	A		16.9		25 NF	DULL BLACK SURFACE
	V-1A	A	1.3	15.5		25 NF	MANY SMALL REPAIR COAT REACTION
	V-1B	A		18.0		25 NF	FAILURES OTHER THAN REPAIRED AREAS, AT 9 HR
	V-1C	A	1.5	16.4		25 NF	
	V-1D	A		15.0		25 NF	
2	S-2E	B		40.2		1 F	FAILED IN DEFECT AREA
	S-2F	B		35.7		1 F	FAILED IN DEFECT AREA
	S-2G	C		14.8		25 NF	WHITE SURFACE
	S-2H	C		12.0		9 F	FAILED IN DEFECT AREA
	V-2A	B		26.4		1 F	FAILED IN DEFECT AREA
	V-2B	B		23.9		1 F	FAILED IN DEFECT AREA
	V-2C	C		13.1		25 F	WHITE REPAIR SURFACE
	V-2D	C		10.5		2 F	FAILED IN DEFECT AREA
3	S-3E	D	3.2	17.8		25 NF	LIGHT GRAY SURFACE
	S-3F	A	4.0	10.0		25 NF	LIGHT GRAY SURFACE
	S-3G	D	1.5	16.8		25 NF	LIGHT GRAY SURFACE
	S-3H	A	2.0	8.0		25 NF	LIGHT GRAY SURFACE
	V-3A	D	3.0	16.0		25 NF	DULL BLACK TO LIGHT GRAY
	V-3B	C	3.7	15.9		25 NF	DARK GRAY TO LIGHT GRAY
	V-3C	D	1.5	19.1		25 NF	DULL BLACK TO MEDIUM GRAY
	V-3D	C	1.4	16.7		15 F	FAILED IN DEFECT AREA
4	S-4A	A	4.8	13.8	10 NF		TEST TERMINATED – SECTIONED FOR PHOTO-MICROGRAPHS OF INTERNAL STRUCTURE
	S-4B	D	4.1	23.9	10 NF		
	S-76A	A	4.8	16.5	20 NF		TEST TERMINATED – SECTIONED FOR PHOTO-MICROGRAPHS OF INTERNAL STRUCTURE
	S-76B	A		20.0	20 NF		
	S-77A	A	3.3	18.7	80 NF		TEST TERMINATED – SECTIONED FOR PHOTO-MICROGRAPHS OF INTERNAL STRUCTURE
	S-77B	A		22.5	80 NF		
	V-5A	A	5.0	12.9	20 NF		SHRINK CRACKS IN REPAIR COAT
	V-5B	A		16.3	10 F		FAILED IN REPAIRED AREA
	V-7A	A	4.9	12.5	30 NF		SHRINK CRACKS IN REPAIR COAT
	V-7B	A		14.5	20 F		FAILED (COATING REACTION)
5	S-85A	E		22.0		1 F	COATING REACTION
	V-33A	E		19.7		1 F	COATING REACTION
6	S-86A	F		16.9		1 F	FAILED IN DEFECT AREA
	V-36A	F		17.3		1 F	COATING REACTION – DEFECT AREA, FAILED
7	S-92A	G		14.1		1 F	COATING REACTION
	V-62A	G		15.1		1 F	COATING REACTION

F – FAILURE
NF – NO FAILURE

NOTE:
CERAMIC COMPOSITIONS WERE APPLIED IN ACCORDANCE WITH APPENDIX C.

457-3321

Table 7-1

INITIAL EXPERIMENTS
SPECIMEN DESCRIPTION AND TEST RESULTS OF CERAMIC FIELD REPAIR DEVELOPMENT (Continued)

EXP NO.	SPECIMEN NO.	REPAIR COMPOSITION	FLAME SPRAY Al_2O_3 THICKNESS (MILS)	REPAIR THICKNESS (MILS)	OXIDATION CHECK TEST		GENERAL COMMENTS ON REPAIRED AREA, AFTER OXIDATION CHECK TEST
					PROFILE CYCLES	AIR ATMOSPHERE 1-HR CYCLES AT 2400°F	
8	S-94A	H		15.3		1 F	FAILED IN DEFECT AREA
	V-33B	H		14.6		1 F	COATING REACTION & DEFECT AREA. FAILED
9	S-85B	I		12.4		1 F	FAILED IN DEFECT AREA
	V-36B	I		13.0		1 F	COATING REACTION & DEFECT AREA. FAILED
10	S-86B	J		16.2		1 F	COATING REACTION
	V-62B	J		15.4		1 F	COATING REACTION
11	S-92B	K	22.0	7.6		1 F	FAILED IN DEFECT AREA
	V-33C	K	20.1	7.0		1 F	COATING REACTION & DEFECT AREA. FAILED
12	S-94B	L		18.5		1 F	NO GREEN STRENGTH - SPALLED
	V-36C	L		17.0		1 F	DEFECT AREA FAILURE - COATING SPALLED
13	S-85C	M		13.7		1 F	HEAVY COATING REACTION
	V-62C	M		12.5		1 F	COATING REACTION
14	S-86C	N		17.9		1 F	COATING REACTION
	V-33D	N		16.7		1 F	COATING REACTION
15	S-92C	O		15.5		1 F	HEAVY COATING REACTION
	V-62D	O		15.1		1 F	COATING REACTION & DEFECT AREA. FAILED
16	S-94C	P		12.6		1 F	FAILED IN DEFECT AREA
	V-36D	P		13.0		1 F	COATING REACTION & DEFECT AREA FAILED
17	S-94D	R		5.6		1 F	POOR ADHESION - POWDERED OFF
	V-33E	R		4.9		1 F	POOR ADHESION - POWDERED OFF

F - FAILURE
NF - NO FAILURE

NOTE:
CERAMIC COMPOSITIONS WERE APPLIED IN ACCORDANCE WITH APPENDIX C.

457-3322

reaction between ceramic and coating), but higher levels of contamination of the columbium substrate occurred. Reduced pressure profile tests were conducted on both coatings (R-512E and VH-109) repaired with the repair composition A, with and without the flame-sprayed aluminum oxide undercoating.

The experiments indicated that for R-512E composition A was acceptable without the flame-sprayed aluminum oxide for up to 80 reentry pr file cycles. Figure 7-1 shows the results of 1 atmosphere and Figure 7-2 shows the effects of aluminum oxide flame spray in the low pressure reentry profile testing.

The repair of the VH-109 with the ceramic composition A required a flame-sprayed alumina undercoating of 3 mils to eliminate oxidation failure of the VH-109, adjacent to the repair caused by incompatibility. Figure 7-3 is a photomicrograph of a repair incorporating the flame spray after 25 hours at 2400°F. There was minimal oxidation contamination of the columbium below the repair. However, the reduced pressure profile test caused failures in 10 to 30 cycles. Figure 7-4 shows an example of the extensive substrate contamination present when the aluminum oxide was used. In the case in which the aluminum oxide was not included (figure 7-4), the oxygen contamination was minimal, but oxidation failures occurred in the VH-109 adjacent to the repairs. The aluminum oxide flame spray undercoating was not satisfactory for VH-109 since it permitted substrate contamination. At the same time, the pyrex frit, aluminum oxide, and boron repair composition A was chemically incompatible with the VH-109 coating. Thus, it was concluded that a new repair composition for the VH-109 coating had to be developed.

A number of other candidate repair materials which were either used in the past, found in the literature, or newly identified were evaluated for both the R-512E and VH-109 coatings. The results are described in table 7-1 under experiments 5 through 17. Coating compositions E through R were employed and the exact compositions are presented in appendix A. All of the compositions failed quickly and were therefore not pursued. Observations on particular materials, however, were used in subsequent experiments for correction of the compatibility problem noted with the VH-109 coating.

7.3 COMPATIBILITY TESTING - As an initial step in developing a new composition for the VH-109 coating, a series of compatibility tests was performed. A total of 26 materials, representing potential ceramic binders, fillers, modifiers, and vehicle systems were mixed and placed on the coating in a small spot. Coupons were prepared for both the VH-109 and R-512E coating, as it was very little

457-1717

NOTE: REPAIR WITHOUT FLAME SPRAYED Al_2O_3

150X

REPAIR OF R-512E COATED Cb-752 WITH COMPOSITION A AFTER 25 HOURS AT 2400°F

Figure 7-1

NOTE: REPAIR INCLUDING FLAME SPRAYED Al_2O_3

150X

457-1722

REPAIR OF VH-109 COATED C-129Y WITH COMPOSITION A AFTER 25 HOURS AT 2400°F

Figure 7-3

150X

WITH AL_2O_3 FLAME SPRAY

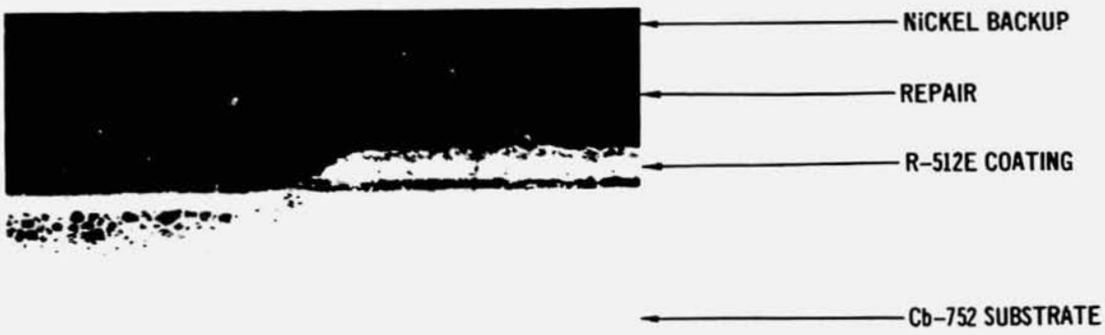

75X

WITHOUT AL_2O_3 FLAME SPRAY

REPAIR COMPOSITION A ON R-512E SILICIDE COATING AFTER 80 REENTRY PROFILE CYCLES

457-1720

Figure 7-2

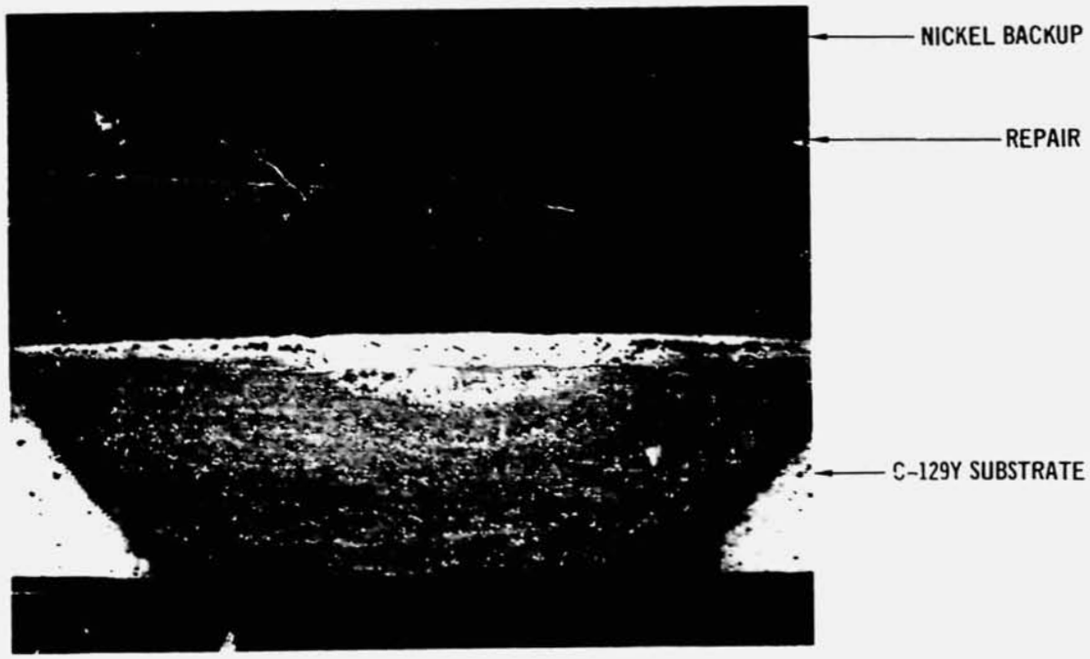

GROSS CONTAMINATION ASSOCIATED WITH
FLAME SPRAYED AL_2O_3 UNDERCOATING

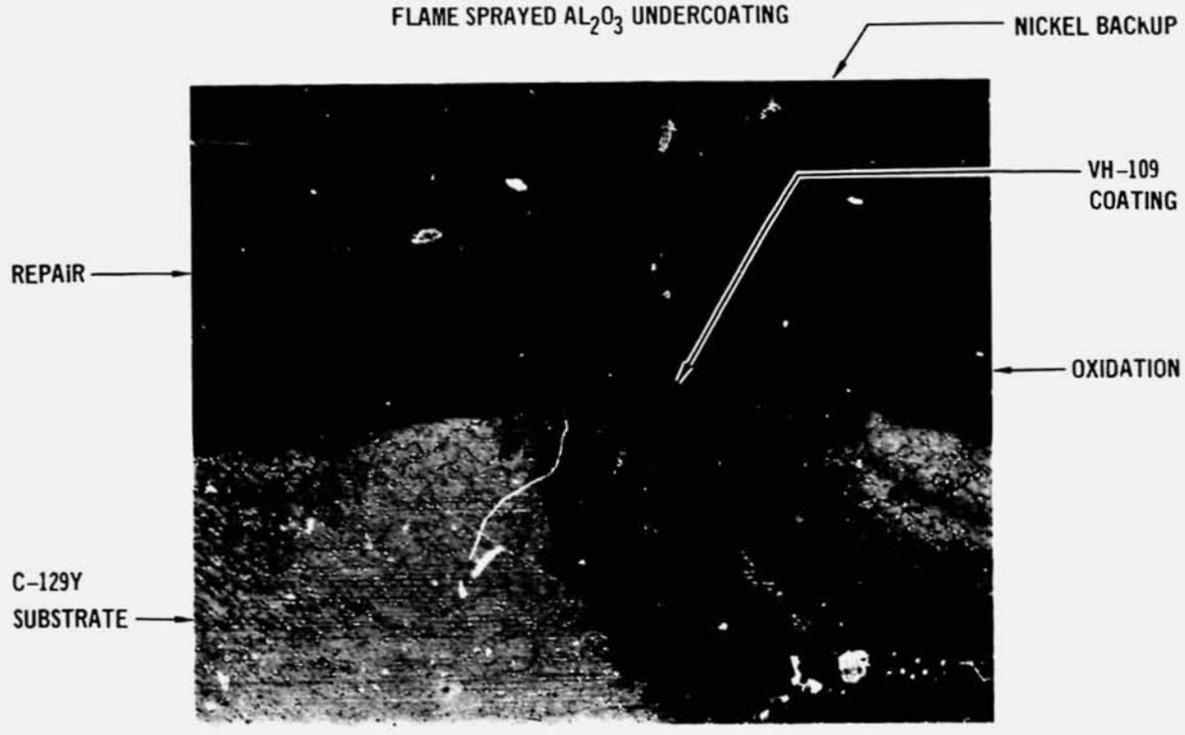

OXIDATION FAILURE OF VH-109 COATING ADJACENT TO REPAIR
WITHOUT AL_2O_3 FLAME SPRAYED UNDERCOATING

REPAIR COMPOSITION A ON VH-109 COATING AFTER 30 PROFILE CYCLES

457-1727

Figure 7-4

additional effort to test a second coating system. After applying the candidate materials, the coupons were exposed to 2400°F in air at 1 atmosphere for 1 hour. The results of these compatibility tests are presented in table 7-2. Figure 7-5 shows typical coupons before and after thermal exposure.

The information gained from these tests was used to select ceramic repair ingredients for developing a repair for both the VH-109 and R-512E coatings. In selecting ingredients for repair, a controlled amount of chemical reactivity is desirable to achieve chemical bonding and ensure good adhesion. The results of these tests gave a first approximation of the better repair materials, and the relative amounts of them that should be used.

7.4 CERAMIC DEVELOPMENT EMPHASIZING REPAIR OF VH-109 - The results of the compatibility testing described in paragraph 7.3 provided a group of materials which were potential ingredients for a compatible VH-109 repair. The following set of criteria was employed based upon the initial experiments:

a) the composition must provide adequate protection of the uncoated columbium substrate in the defect area

b) the composition must be compatible with VH-109 coating in the overlap area, while having sufficient reactivity with the VH-109 to ensure good chemical bonding

c) the repair must not cause failure of the VH-109 coating at the periphery of the ceramic repair.

An Edisonian experimental approach was employed in which a substantial number of compositions were produced and evaluated against the above ceiteria. Table 7-3 presents the compositions studied, the repair coating thicknesses used, and the oxidation results achieved in experiments 18 through 30. The product of this investigation was four compositions which passed the 25-hour oxidation screening test at 2400°F in 1 atmosphere air. These compositions are:

a) H-1 composition (columbium disilicide, a Si-Cr-Fe alloy powder, pyrex frit, and boron powder in a lacquer vehicle)

b) P-1 (columbium disilicide, pyrex frit, and boron in a lacquer vehicle)

c) T-1 (columbium disilicide, pyrex frit, iron, and boron in a lacquer vehicle)

d) U-1 (pyrex frit and boron in a lacquer vehicle).

(See appendix A for exact compositions.)

Table 7-2

SPECIMEN DESCRIPTION AND TEST RESULTS ON COMPATIBILITY STUDIES ON SYLVANIA R-512E AND VAC-HYD VH-109 HIGH TEMPERATURE PROTECTIVE SILICIDE COATINGS

NO.	REPAIR MATERIALS USED	REACTION RESULTS AFTER 1-HOUR AT 2400°F (AIR ATMOSPHERE)	
		SYLVANIA	VAC-HYD
1	POSITIVE SOL (PS-7) AL_2O_3 STABILIZED COLLOIDAL SILICA	H	EH
2	SAUEREISEN NO. 8 + DISTILLED WATER	S	S
3	PYREX FRIT NO. 7740 + CENILAC	MH	EH
4	CENILAC (6 PARTS CELLULOSE NITRATE LACQUER TO 5 PARTS TTT226 LACQUER THINNER)	NONE	NONE
5	COLUMBIUM SILICIDE + CENILAC	VS	VS
6	COLUMBIUM SILICIDE + PS-7	EH	EH
7	60% Si - 20% Cr - 20% Fe (ALLOY) + CENILAC	S	VS
8	60% Si - 20% Cr - 20% Fe (ALLOY) + PS-7	H	H
9	AL_2O_3 (-270 MESH) + CENILAC	VS(FUSED)	VS(FUSED)
10	AL_2O_3 (-270 MESH) + PS-7	H	H
11	TUNGSTEN METAL POWDER, PURIFIED + CENILAC	M	H
12	TUNGSTEN METAL POWDER, PURIFIED + PS-7	H	H
13	TANTALUM (-325 MESH + CENILAC	VS	NONE
14	TANTALUM (-325 MESH) + PS-7	MH	MH
15	HAFNIUM (8 MICRONS) + CENILAC	MH	VS
16	HAFNIUM (8 MICRONS) + PS-7	MH	EH
17	Na_2SiO_3	EH	EH
18	AL_2O_3 (-270 MESH) + SYTON	S	VS
19	SYTON (NH_4^+ STABILIZED COLLOIDAL SILICA)	NONE	NONE
20	AL_2O_3 + Na_2SiO_3	EH	M
21	AL_2O_3 + 1:1 DISTILLED WATER AND PS-7	M	S
22	AL_2O_3 + 1:1 DISTILLED WATER AND Na_2SiO_3	MH	S
23	60% Si - 20% Cr - 20% Fe (ALLOY) + SYTON	S	NONE
24	60% Si - 20% Cr - 20% Fe (ALLOY) + Na_2SiO_3	M	EH
25	SAUEREISEN NO. 8 + COLUMBIUM SILICIDE (4:1) + DISTILLED WATER	M	NONE
26	60% Si - 20% Cr - 20% Fe (ALLOY) + COLUMBIUM SILICIDE (1 1) + CENILAC	VS	NONE

VERY SLIGHT - VS
SLIGHT - S
MEDIUM - M
MEDIUM HEAVY - MH
HEAVY - H
EXTREMELY HEAVY - EH

457-1722

BEFORE

AFTER

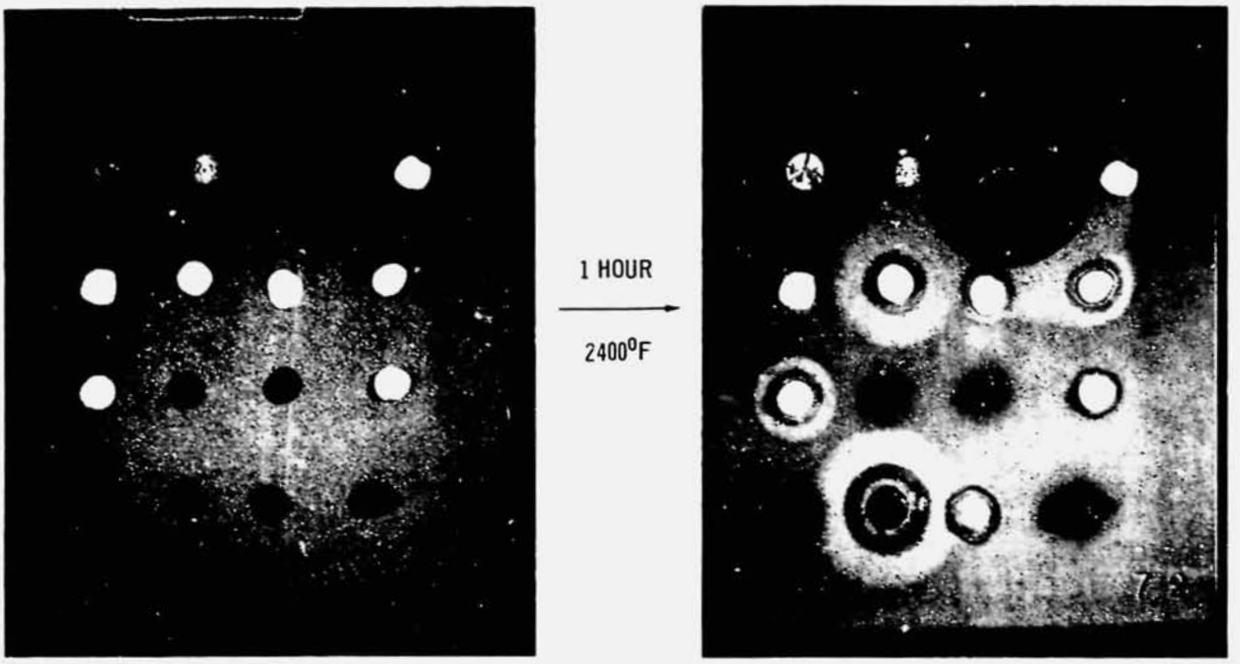

R-512E Coating

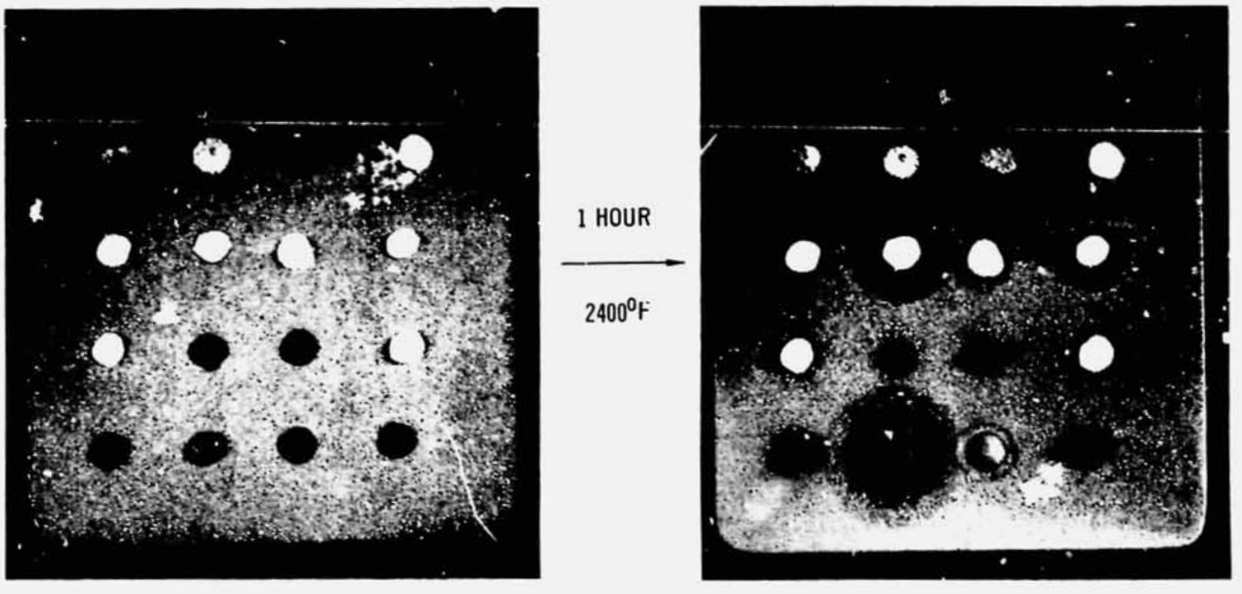

VH-109 Coating

COMPATIBILITY TESTING OF REPAIR MATERIALS AND FUSED SLURRY SILICIDE COATINGS
(See Table 7-2)

457-3323

Figure 7-5

Table 7-3

VH-109 COATING REPAIR STUDIES
SPECIMEN DESCRIPTION AND TEST RESULTS

EXP NO.	SPECIMEN NO.	REPAIR COMPOSITION	FLAME SPRAY Al_2O_3 THICKNESS (MILS)	REPAIR THICKNESS (MILS)	OXIDATION CHECK TEST		GENERAL COMMENTS ON REPAIRED AREA, AFTER OXIDATION CHECK TEST
					PROFILE CYCLES	AIR ATMOSPHERE 1 HR CYCLES AT 2400°F	
18	V-19A	S		18.0		1 F	FAILED – POWDERY, POOR ADHERENCE
19	V-19B	T		22.0		1 NF	CRACKS THROUGHOUT REPAIR COAT – OVERALL PINK DISCOLORATION, SLIGHT REACTION
20	V-40A	U		15.0		1 F	FAILED IN DEFECT AREA
	V-40B	V		9.0		1 F	FAILED IN DEFECT AREA
	V-40C	W		16.0		1 F	FAILED IN DEFECT AREA
	V-40D	X		14.0		1 F	FAILED IN DEFECT AREA
21	V-19C	Y		11.0		9 F	ONE SMALL FAILURE ON EDGE OF DEFECT; MEDIUM COATING REACTION
	V-19D	Z		20.0		7 F	GROSS FAILURE IN DEFECT – MAY HAVE STARTED ON 1ST CYCLE – COMPATIBLE
22	V-4A	V-1		10.0		6 F	3 DARK GREEN AREAS IN DEFECT AFTER 1ST CYCLE – TOTAL DEFECT FAILURE AT 6 HR
	V-4B	B-1		23.0		1 F	GROSS IN DEFECT AREA
	V-4C	V-1		19.0		6 F	2 VERY SMALL FAILURES IN DEFEAT
	V-4D	[illegible]		17.0		1 F	GROSS IN DEFECT AREA

F – FAILURE
NF – NO FAILURE

NOTE:
CERAMIC COMPOSITIONS WERE APPLIED IN ACCORDANCE WITH APPENDIX C.

457-0324

Table 7–3

VH–109 COATING REPAIR STUDIES
SPECIMEN DESCRIPTION AND TEST RESULTS
(Continued)

EXP NO.	SPECIMEN NO.	REPAIR COMPOSITION	FLAME SPRAY Al_2O_3 THICKNESS (MILS)	REPAIR THICKNESS (MILS)	OXIDATION CHECK TEST		GENERAL COMMENTS ON REPAIRED AREA. AFTER OXIDATION CHECK TEST
					PROFILE CYCLES	AIR ATMOSPHERE 1-HR CYCLES AT 2400°F	
23	V–25A	W–1		10.0		2 F	GREEN ERUPTIONS – YELLOW OXIDE BENEATH IN DEFECT AREA
	V–25B	D–1		11.0		2 F	GREEN ERUPTIONS – YELLOW OXIDE BENEATH IN DEFECT AREA
	V–25C	E–1		9.0		2 F	GREEN ERUPTIONS – YELLOW OXIDE BENEATH IN DEFECT AREA
	V–25D	F–1		12.0		1 F	GROSS IN DEFECT AREA
24	V–43A	G–1		9.0		2 F	FAILED IN DEFECT AREA
	V–43B	H–1		3.0		25 NF	LITTLE TO NO REACTION–VERY GOOD APPEARANCE
	V–43C	I–1		12.0		1 F	GREEN WHITE SPOTS ON DEFECT AREA. YELLOW OXIDE AFTER 3 HR
	V–43D	J–1		12.0		1 F	FAILED IN DEFECT AREA
25	V–24A	K–1		3.0		1 F	GROSS IN DEFECT – BLACK & GLASSY ELSEWHERE
	V–24B	L–1		8.0		2 F	GROSS IN DEFECT – ATTACK ON BASE METAL ACCELERATED
	V–24C	M–1		15.0		2 F	GROSS IN DEFECT – BLACK & GLASSY ELSEWHERE – SLIGHT COATING REACTION
	V–24D	N–1		17.0		2 F	GROSS IN DEFECT – MEDIUM TO HEAVY COATING REACTION
26	V–10A	H–1		15.0		14 NF	DISCONTINUED – NO FAILURES TO THIS POINT
	V–10B	H–1		6.0		13 F	FAILED IN DEFECT AREAS WHERE ERUPTIONS IN REPAIR COAT FROM INITIAL FUSSION OCCURRED
	V–10C	H–1		10.0		13 F	
	V–10D	H–1		9.0		14 F	DISCONTINUED – NO FAILURES TO THIS POINT
27	V–8A	O–1		19.0		25 NF	3/8 IN. PINK STAIN RING AROUND DEFECT – COMPATIBLE
	V–8B	H–1		7.0		1 F	ONE SMALL SPOT ON DEFECT EDGE – VERY SLIGHT REACTION
	V–8C	H–1		10.0		25 NF	LIGHT YELLOW DISCOLORATION AROUND DEFECT
	V–8D	H–1		16.0		25 NF	LIGHT YELLOW DISCOLORATION AROUND DEFECT
28	V–71A	O–1		23.0		25 NF	VERY LIGHT BROWN RING AROUND DEFECT – COMPATIBLE
	V–71B	H–1		5.0		1 F	4 SMALL FAILURES IN DEFECT
	V–71C	H–1		10.0		25 NF	COMPATIBLE
	V–71D	H–1		17.0		25 NF	COMPATIBLE
29	V–18A	H–1		14.0	50 NF		SLIGHT SPALL ON ONE EDGE. SECTIONED FOR PHOTOMICROGRAPHS
	V–17A	H–1		14.0	50 NF		IN PROCESS. (HOLD FOR FURTHER TESTING)

F – FAILURE
NF – NO FAILURE

NOTE:
CERAMIC COMPOSITIONS WERE APPLIED IN ACCORDANCE WITH APPENDIX C.

457-3325

Table 7-3

VH-109 COATING REPAIR STUDIES
SPECIMEN DESCRIPTION AND TEST RESULTS
(Continued)

EXP NO.	SPECIMEN NO.	REPAIR COMPOSITION	FLAME SPRAY Al_2O_3 THICKNESS (MILS)	REPAIR THICKNESS (MILS)	OXIDATION CHECK TEST		GENERAL COMMENTS ON REPAIRED AREA, AFTER OXIDATION CHECK TEST
					PROFILE CYCLES	AIR ATMOSPHERE 1-HR CYCLES AT 2400°F	
30	V-6A	P-1	13.8			25 NF	REPAIR COATING APPROXIMATE THAT OF THE COATING IN APPEARANCE
	V-6B	R-1	14.6			3 F	REPAIR SPALLED ON 2ND CYCLE - ONE VERY SMALL FAILURE IN CENTER OF DEFECT
	V-6C	S-1	10.0			20 F	ONE VERY SMALL FAILURE IN CENTER OF DEFECT - DULL BROWN
	V-6D	T-1	10.5			25 NF	DULL BLACK
	V-6E	U-1	10.3			25 NF	GROSS BLACK OVER DEFECT - GRAY AREA 1/4 IN. AROUND REPAIR
	S-41A	A-1	9.7			25 NF	TEST TERMINATED FOR METALLOGRAPHIC EXAMINATION
31	S-42A	H-1	10.8			25 NF	TEST TERMINATED FOR METALLOGRAPHIC EXAMINATION
32	S-43A	P-1	10.9			25 NF	TEST TERMINATED FOR METALLOGRAPHIC EXAMINATION
33	S-44A	S-1	10.8			21 F	FAILED AT PERIMETER OF REPAIR
34	S-45A	T-1	10.8			25 NF	TEST TERMINATED FOR METALLOGRAPHIC EXAMINATION
35	S-46A	U-1	10.5			25 NF	TEST TERMINATED FOR METALLOGRAPHIC EXAMINATION

F - FAILURE
NF - NO FAILURE

NOTE:
CERAMIC COMPOSITIONS WERE APPLIED IN ACCORDANCE WITH APPENDIX C.

457-3326

A metallographic examination was performed to determine the degree of contamination associated with each of the repairs which passed the one atmosphere screening test. Typical results are shown in figure 7-6. In the case of each of the compositions, with the exception of T-1, the degree of contamination was minimal, and the compositions were considered to have passed the air atmosphere screening test and to be ready for reentry profile evaluation.

The three compositions specifically developed for the VH-109 coating, which passed the air atmosphere screening test, were applied to R-512E-coated Cb-752 coupons. The results of this experiment are shown in table 7-3 under experiments 18 through 22. The 25-hour screening oxidation test was conducted at 2400°F at 1 atmosphere air. Each of the compositions (H-1, P-1, and U-1), passed the screening test without oxidation. The coupons were checked metallographically, and the internal contamination of the Cb-752 substrate was minimal. It was concluded that these compositions should be profile tested since they appeared to be equal to, or better than, the A-1 composition which had already been developed and shown to be satisfactory for R-512E coated Cb-752. Figure 7-7 illustrates typical results obtained with these compositions.

A series of reentry profile tests was performed on the ceramic repair compositions which satisfactorily passed the 25-hour screening test at 2400°F in 1 atmosphere air. The test conditions were the time, temperature, and air pressure reentry profiles shown in figure 4-1. The ceramic repair compositions H-1, P-1, and U-1 were applied to defected coupons of both R-512E-coated Cb-752 and VH-109-coated C-129Y. The composition A-1, previously reentry profile tested, was included with the R-512E-coated Cb-752 group for comparison. Two repairs were included on each coupon tested. In cases in which one of the two repair areas failed, the repair was replaced to provide for the continuation of the testing of the unfailed repair site. The testing was terminated after 100 profile cycles, or when both repair areas had failed. Upon completion of the profile oxidation testing, metallographic examinations were used to determine the extent of substrate contamination.

Profile oxidation testing results are presented in table 7-3. The A-1 composition repair on the R-512E coating proved to be effective in preventing oxidation and allowing minimal oxygen contamination below the repair in 100 simulated reentries. The H-1 composition showed 1 failure after 80 profile cycles, and the second H-1 repair passed a 100-cycle exposure without oxidation. Metallographic examination of the 100-cycle H-1 repair site showed more depth of contamination

150X

457-1725

Composition P-1

150X

Composition U-1

CERAMIC REPAIR COMPOSITIONS FOR VH-109 COATING
AFTER 25 HOURS AT 2400°F

457-1726

Figure 7-6

COMPOSITION U-1

COMPOSITION P-1

CERAMIC REPAIR COMPOSITIONS ON R-512E COATING AFTER 25 HOURS AT 2400°F IN AIR

457-1724

Figure 7-7

than either A-1 or U-1 compositions, but this depth was not considered excessive. The U-1 repaired coupons before and after testing are shown in figure 7-8 with a metallographic cross-section. The U-1 repair proved to be a dense uniform material which allowed minimal oxygen to pass into the Cb-752 substrate. The P-1 repairs were the least effective, permitting oxidation failures to occur in the repair area within 30 to 60 profile cycles.

The repair of the VAC-HYD VH-109 coating was not as successful as the repair of the R-512E, but showed satisfactory results with the H-1 and U-1 repairs. The H-1 repair showed very little surface porosity and a good exterior appearance. The depth of oxygen penetration (average 6 mils) was slightly lower than for the same H-1 repair on Cb-752, and the results were considered satisfactory. The U-1 repair of the VH-109 coating showed the lowest amount of contamination of the systems tested, an average of 2.5 mils into the C-129Y substrate. Some surface porosity associated with the U-1 is believed responsible for the early failure of specimen 55A. The coupon before and after 100 simulated profile cycles is shown in figure 7-9 with a photomicrograph of the repair area. As was the case with the Cb-752, the P-1 repairs on the VH-109-coated C-129Y were the least effective. One of the specimens showed oxidation failure after 80 simulated reentry cycles, and the second after 100 cycles.

It was concluded from this series of profile tests that the compositions H-1 and U-1 show promise as repair methods for VH-109 coated C-129Y and should be structurally evaluated on panels. The same compositions, plus the A-1 repair, appear satisfactory for the R-512E coating on Cb-752. In each case, the chemical compatibility was excellent. The physical characteristics of the repairs were not as consistent as desirable. Both surface and internal porosity needed further study, since we believe that early failures are related to porosity within the repairs.

7.5 IMPROVEMENT OF CERAMIC REPAIR LOW TEMPERATURE VEHICLE SYSTEM - Previous evaluations of ceramic composition repairs have shown a multimission reentry capability of 100 cycles. There were a few random early failures and some variations in the extent of substrate contamination below the ceramic repairs, conditions which have been attributed to porosity in the ceramic repair systems. The cause of this porosity was ascribed to the low temperature cellulose nitrate lacquer vehicle system. At room temperature, the lacquer forms a tightly bonded repair which does not permit the uniform outward diffusion of gaseous decomposition products during heating to the ceramic fusion temperature. Since the ceramic

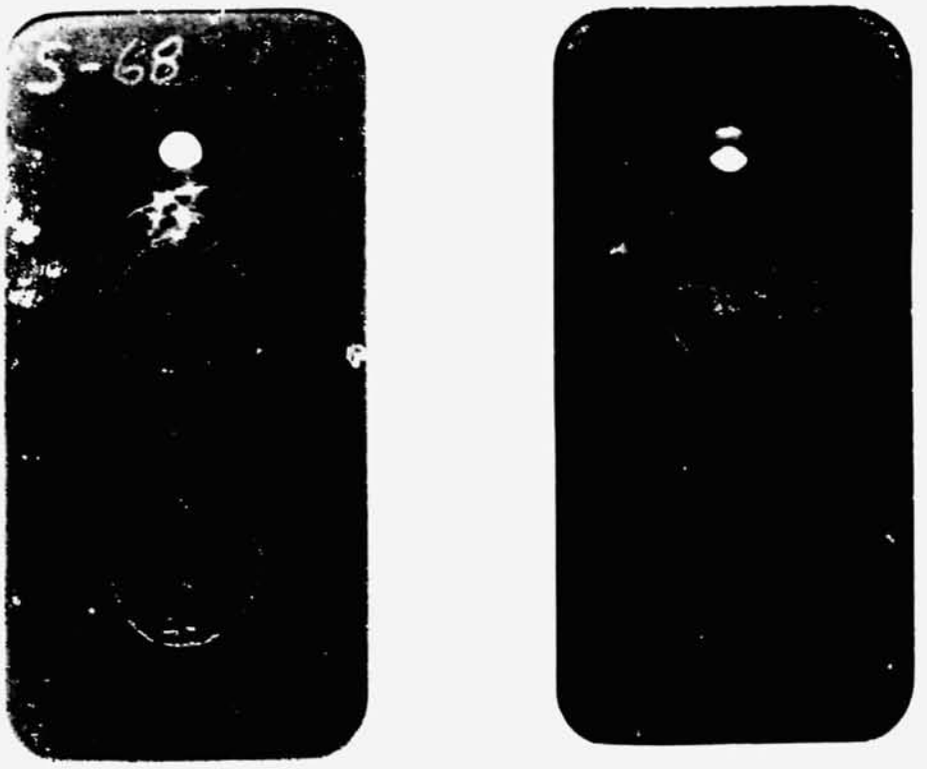

AS REPAIRED 2X

AFTER 100 CYCLES 2X

457-2816

U-1 REPAIR OF R-512E COATING

150X

457-2817

CROSS SECTION OF U-1 REPAIR OF R-512E COATING AFTER 100 SIMULATED REENTRY CYCLES

Figure 7-8

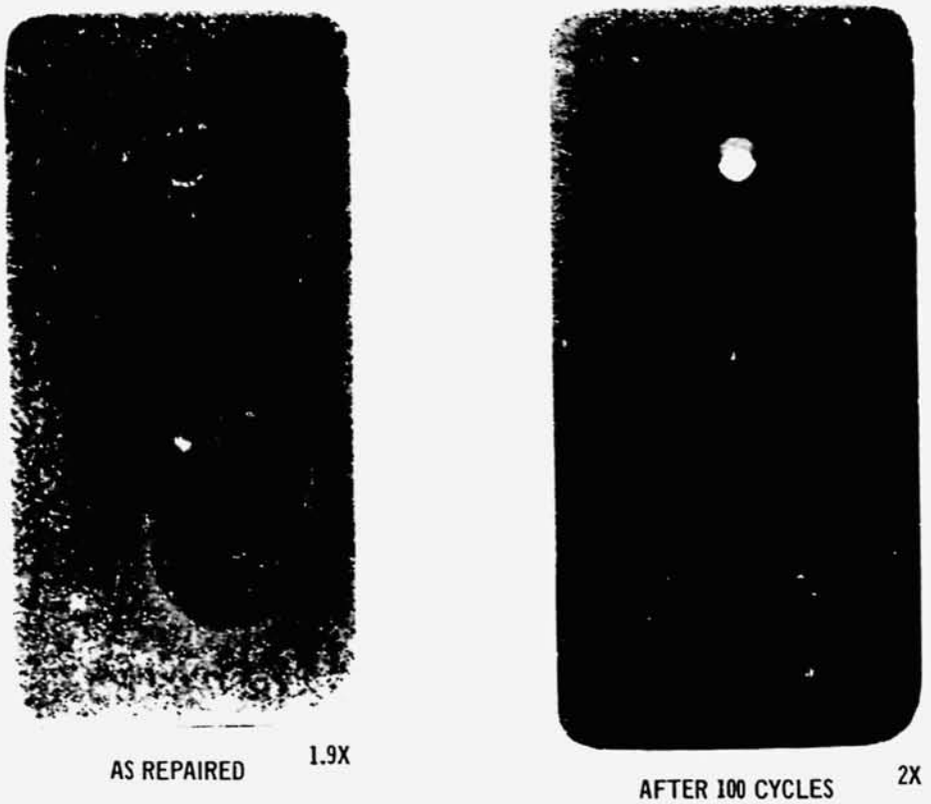

AS REPAIRED 1.9X

AFTER 100 CYCLES 2X

457-2811

U-1 REPAIR OF VH-109 COATING

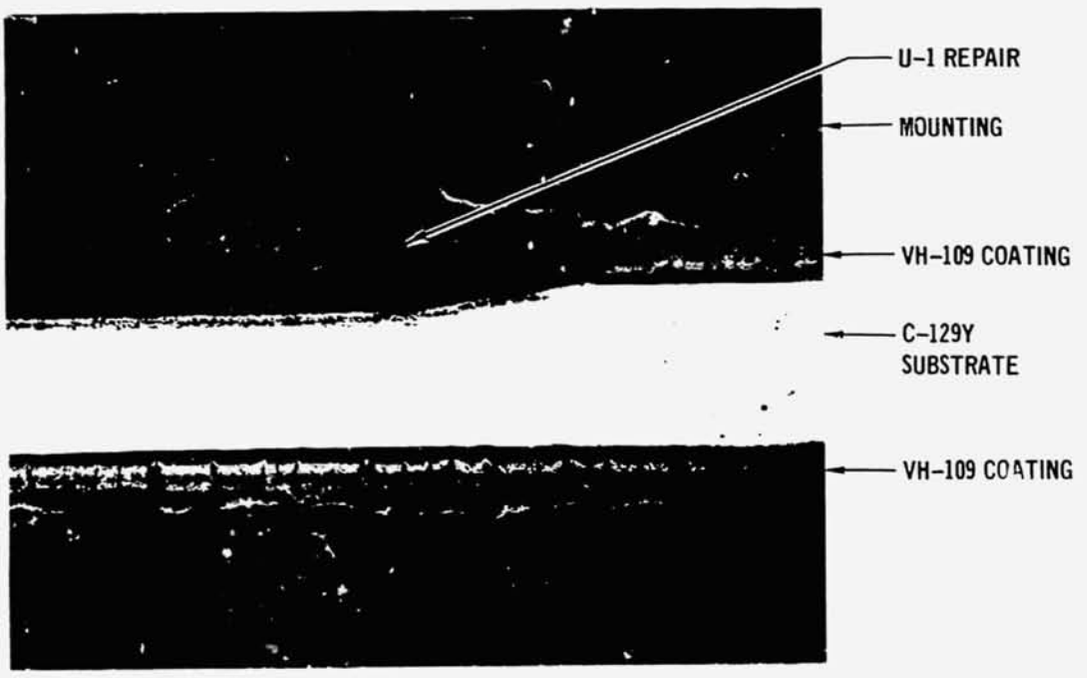

50X

CROSS SECTION OF U-1 REPAIR OF VH-109 COATING AFTER
100 SIMULATED REENTRY CYCLES

457-2812

Figure 7-9

constituents performed effectively, a criterion of the study was established in which only the low temperature vehicle system would be altered so that desirable elevated temperature properties could be maintained.

The first approach to eliminating the surface porosity was to increase the time to achieve the ceramic fusion temperature. While this technique appeared to reduce the surface porosity, it was not an improvement sufficient to meet the objectives. The second approach was to replace the lacquer with another organic vehicle. Coupons of R-512E coated Cb-752 and VH-109 coated C-129Y were defected by grit blasting with fused aluminum oxide (220 mesh) to produce 1/4-inch diameter defects. A total of 22 different experiments involving 36 ceramic compositions was conducted. The experimental and test results are presented in table 7-4. The systems which showed the best oxidation performance and the least porosity were repair compositions which had been previously developed, but in which the low temperature vehicle system was changed to an ethyl alcohol base. The ethyl alcohol was saturated with a commercial corn starch (Eastman Organic Chemical Company's Technical Grade Zein) which functions as a suspension agent.

Oxidation test evaluations conducted at both 1 atmosphere pressure and under reentry profile test conditions proved the new compositions to be equal or superior to the previous compositions. We emphasize that the high temperature components remain unchanged. The following list shows the current composition designations and the previous compositions from which they were derived:

COMPOSITION DERIVATIVES
FOR IMPROVED CERAMIC REPAIRS

Original Composition Designation	Improved Derivative Composition Designation
U-1	J-2 (for R-512E)
U-1	E-2 (for VH-109)
H-1	O-2 (for VH-109)
A-1	N-2 (for R-512E)

The improved versions of the ceramic compositions have in common a substantially improved surface texture and physical appearance. Figure 7-10 shows the final improved composition having no significant surface porosity after 110 reentry profile cycles. The physical microstructure has been substantially improved, as shown in figure 7-11. Improved ceramic repair compositions were ready for evaluation on 3 by 12-inch rib stiffened panels under reentry flight simulation in order to prove adequacy of the repairs under structural strains and acoustics.

Table 7–4

DEVELOPMENT OF IMPROVED VEHICLES SYSTEM SPECIMEN DESCRIPTION AND TEST RESULTS

EXP NO.	SPECIMEN NO.	REPAIR COMPOSITION	REPAIR THICKNESS (MILS)	OXIDATION CHECK TEST		GENERAL COMMENTS ON REPAIRED AREA, AFTER OXIDATION CHECK TEST
				PROFILE CYCLES	AIR ATMOSPHERE 1-HR CYCLES AT 2400°F	
36	S–75A	X–1	7.0		3 F	REPAIR SPALLED
	S–75B	Y–1	11.4		25 NF	ROUGH TEXTURE WITH POROSITY
	S–19A	Z–1	11.4		10 F	INTERREACTION WITH R–512E
37	V–60A	Z–1	11.0		25 NF	MEDIUM POROSITY
38	S–81A	A–2	11.4		25 NF	MEDIUM ROUGHNESS & POROSITY
	S–81B	B–2	7.1		25 NF	BLACK, GLASSY & SMOOTH
39	S–82A	C–2	6.5		1 F	SPALLED
	S–82B	D–2	5.1		17 F	OXIDATION FAILURE IN DEFECT
40	S–47A	E–2	11.8		25 NF	BLACK, GLASSY & SMOOTH
41	V–17A	E–2	9.9		25 NF	BLACK, GLASSY, SMOOTH & SLIGHT REACTION WITH VH–109
42	V–37B	E–2	20.8	110 NF		GLASSY, SMOOTH & SLIGHT REACTION WITH VH–109
	V–37B	E–2	18.0	110 NF		GLASSY, SMOOTH & SLIGHT REACTION WITH VH–109
43	S–61A	F–2	13.1		5 NF	ROUGHNESS & POROSITY
	V–17B	F–2	14.2		1 F	DEFECT EDGE FAILURE
44	S–61B	G–2	7.1		1 F	ROUGHNESS, POROSITY & OXIDATION
	V–17C	G–2	9.1		1 F	EDGE FAILURE
45	S–36A	H–2	10.6		2 F	SPALLED
	S–36B	I–2	11.0		2 F	SPALLED

F – FAILURE
NF – NO FAILURE

NOTE:
CERAMIC COMPOSITIONS WERE APPLIED IN ACCORDANCE WITH APPENDIX C.

Table 7-4

VH-109 COATING REPAIR STUDIES
SPECIMEN DESCRIPTION AND TEST RESULTS
(Continued)

EXP NO.	SPECIMEN NO.	REPAIR COMPOSITION	FLAME SPRAY Al_2O_3 THICKNESS (MILS)	REPAIR THICKNESS (MILS)	OXIDATION CHECK TEST		GENERAL COMMENTS ON REPAIRED AREA, AFTER OXIDATION CHECK TEST
					PROFILE CYCLES	AIR ATMOSPHERE 1-HR CYCLES AT 2400°F	
46	S-50A	J-2		9.5		25 NF	SEMI-GLASSY – SMOOTH
	V-15A	J-2		10.1		25 NF	SEMI-GLASSY – SMOOTH, MEDIUM REACTIVITY WITH VH-109
47	S-A7A	J-2		15.5	110 NF		GLASSY WITH SLIGHT ROUGHNESS
	S-A7B	J-2		13.5	110 NF		GLASSY WITH SLIGHT ROUGHNESS
48	S-20A	K-2		11.6		5 NF	ROUGHNESS & POROSITY
	S-20B	L-2		10.4		5 NF	HEAVY ROUGHNESS & POROSITY
	S-20C	M-2		9.7		5 NF	MEDIUM ROUGHNESS & POROSITY
49	S-53A	N-2		15.0		25 NF	SLIGHT ROUGHNESS
	V-38A	N-2		14.6		20 NF	COUPON FAILURE – NOT REPAIR RELATED
50	S-A12A	N-2		14.5	110 NF		NON-GLASSY – SLIGHT ROUGHNESS
	S-A12B	N-2		11.2	110 NF		NON-GLASSY – SLIGHT ROUGHNESS
51	S-52A	O-2		12.1		25 NF	NON-GLASSY – SLIGHT ROUGHNESS
	V-22A	O-2		12.3		25 NF	NON-GLASSY – SLIGHT ROUGHNESS
	S-13A-A	O-2		15.5	110 NF		NON-GLASSY – SLIGHT ROUGHNESS
	S-13A-B	O-2		14.0	110 NF		NON-GLASSY – SLIGHT ROUGHNESS
52	V-26A	P-2		9.8		5 NF	MEDIUM ROUGHNESS – POROSITY
	V-26B	R-2		11.3		5 NF	MEDIUM ROUGHNESS – POROSITY
53	S-18A	S-2		10.5		1 F	SPALLED
	S-18B	T-2		11.0		2 F	SPALLED
	S-18C	U-2		10.1		5 NF	SHRINKAGE CRACKS – MEDIUM ROUGHNESS
	S-18D	V-2		9.6		5 NF	SHRINKAGE CRACKS – HEAVY ROUGHNESS
54	S-14A	W-2		12.3		25 NF	SMOOTH & GLASSY
	S-14B	X-2		10.5		25 NF	SMOOTH & GLASSY WITH SLIGHT REACTION WITH R-512E
	S-14C	Y-2		11.2		5 NF	GLASSY – MEDIUM ROUGHNESS
55	S-17A	Z-2		9.9		25 NF	SMOOTH & GLASSY
	S-17B	A-3		10.3		5 NF	GLASSY WITH SLIGHT ROUGHNESS
56	V-39A	H-1		13.4	110 NF		NON-GLASSY – MEDIUM ROUGHNESS
	V-39B	H-1		12.8	110 NF		NON-GLASSY – MEDIUM ROUGHNESS
57	V-52A	H-1		11.1	110 NF		NON-GLASSY – MEDIUM ROUGHNESS
	V-53A	P-1		10.3	110 NF		NON-GLASSY – MEDIUM ROUGHNESS
	V-55A	U-1		10.9	110 NF		GLASSY – MEDIUM ROUGHNESS
58	S-65A	A-1		10.7	110 NF		GLASSY – MEDIUM ROUGHNESS
	S-66A	H-1		12.2	110 NF		NON-GLASSY – MEDIUM ROUGHNESS
	S-67A	P-1		10.3	60 F		FAILED ON EDGE OF DEFECT
	S-68A	U-1		11.3	110 NF		GLASSY – SLIGHT ROUGHNESS

F – FAILURE
NF – NO FAILURE

NOTE:
CERAMIC COMPOSITIONS WERE APPLIED IN ACCORDANCE WITH APPENDIX C.

457-3328

SYLVANIA R-512E COATED Cb-752 COUPONS

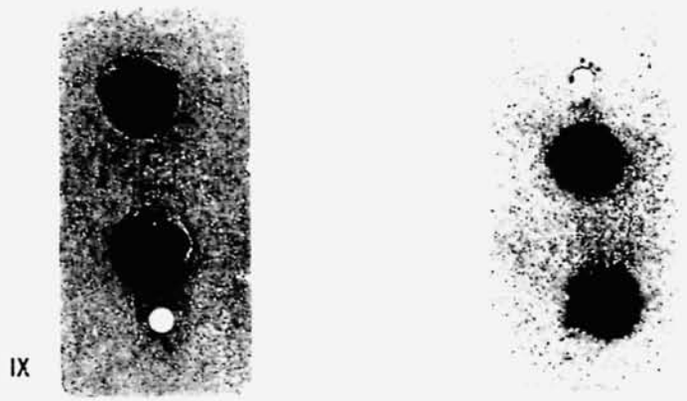

VAC-HYD VH-109 COATED C-129Y COUPONS

457-2855

CERAMIC COMPOSITION REPAIRS WITH IMPROVED VEHICLE SYSTEM AFTER 110 REENTRY PROFILE CYCLES

Figure 7 – 10

250X

N–2 COMPOSITION AFTER 25 HOURS AT 2400°

457–2879

250X

O–2 COMPOSITION AFTER 25 HOURS AT 2400°F

PHOTOMICROGRAPHS OF CERAMIC REPAIR SHOWING DENSE STRUCTURE ASSOCIATED WITH IMPROVED VEHICLE SYSTEM

457–2882

Figure 7–11

8. DIFFUSION BARRIER STUDIES

Ceramic composition repairs are attractive because they can be applied quickly and easily in the field. Although these repairs effectively prevent oxidation of columbium by eliminating formation of the bulky, nonprotective Cb_2O_5, they do permit some oxygen to reach and dissolve in the columbium substrate. This oxygen solution contamination occurs in two stages: (a) initially, in the outer 2 to 5 mils of the substrate in the repair area during the first heating to 2000°F, at which time fusion occurs and seals the repair; and (b) during subsequent service cycles (up to 100 reentries), in which additional contamination occurs which brings the total depth to 4 to 8 mils. While this minor oxygen contamination in a local defect area has not been shown to impair the structural integrity of heat-shield panel skins, it is believed that ceramic repairs would be more universally utilized if such an oxygen solution zone could be eliminated.

The diffusion barrier concept would eliminate the oxygen solution zone by interposing a barrier between the ceramic repair and the substrate which would stop oxygen diffusion before it reached the columbium. The initial approach to such a diffusion barrier was to brush plate one of the noble metals from the group of rhodium, rhenium, and iridium. The primary criterion for selection of these metals was their predicted compatibility with the fused slurry silicide coatings and their oxidation resistance. The brush plating process was selected as the application technique because it could be readily accomplished in the field. The initial experiments were conducted with rhodium because it was the easiest metal to brush plate.

8.1 DEVELOPMENT AND EVALUATION OF DIFFUSION BARRIERS - The first task in development of the diffusion barrier concept was to determine the parameters for obtaining an adherent plating of the two columbium alloys of interest. The Meta Chemical Division of SIFCO Company, Cleveland, determined that preparatory cleaning by light alumina gritblasting was sufficient to provide an adherent plating. The light alumina gritblasting was used with the ceramic repairs and was considered a functional cleaning method for brush plating. The cleaning and processing derived for the uncoated alloys were applied to coated coupons having a 1/4-inch defect. It was found that the rhodium plated satisfactorily on the defected coupons (as shown in figure 8-1) in which 0.2 mil of rhodium is applied to a defected R-512E coated Cb-752 coupon. Brush plated rhodium diffusion barriers of 2 and 4 mils were

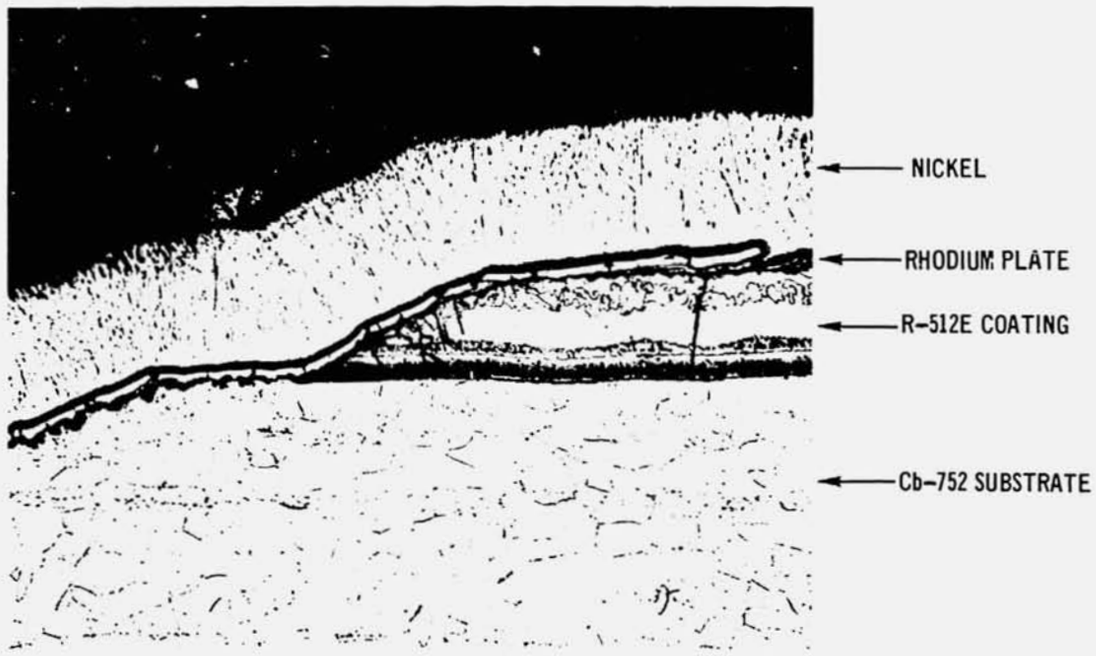

457-2810

0.2 MIL RHODIUM BRUSH PLATE ON R-512E COATED Cb-752

Figure 8-1

evaluated in a 1-atmosphere screening test at 2400°F. In cases in which oxidation tests were conducted on rhodium as the only means of protecting the defect area, failure occurred within one 15-minute cycle at 2400°F. The rhodium was spalled from the defect area by the formation of columbium oxide below the rhodium plate. A series of specimens was prepared in which defective R-512E-coated Cb-752 coupons were brush plated with 0.4 mil of rhodium. The plated defect areas were ceramic repair coated with the A-1, U-1, and H-1 compositions. Each specimen was given an oxidation exposure in air at 2400°F for 30 minutes. After this short exposure, a metallographic examination was performed to determine the effectiveness of the rhodium barrier during the critical initial ceramic fusion period. The rhodium was found to be ineffective in preventing oxygen contamination of the substrate for each of the three ceramic compositions. The U-1 composition is shown in figure 8-2. Although the rhodium was the desired thickness (over 0.4 mil) and physically satisfactory, oxygen diffused through the rhodium, causing substrate contamination. The A-1 repair was found to be less compatible with the rhodium than the U-1 composition. The rhodium was partially destroyed, causing an uneven barrier coverage with oxygen contamination of the Cb-752 substrate. The H-1 repair composition was found to be totally incompatible with the brush plated rhodium. We concluded that the diffusion of oxygen through the rhodium is so great that rhodium is not a good diffusion barrier within the practical limits of rhodium plate thicknesses.

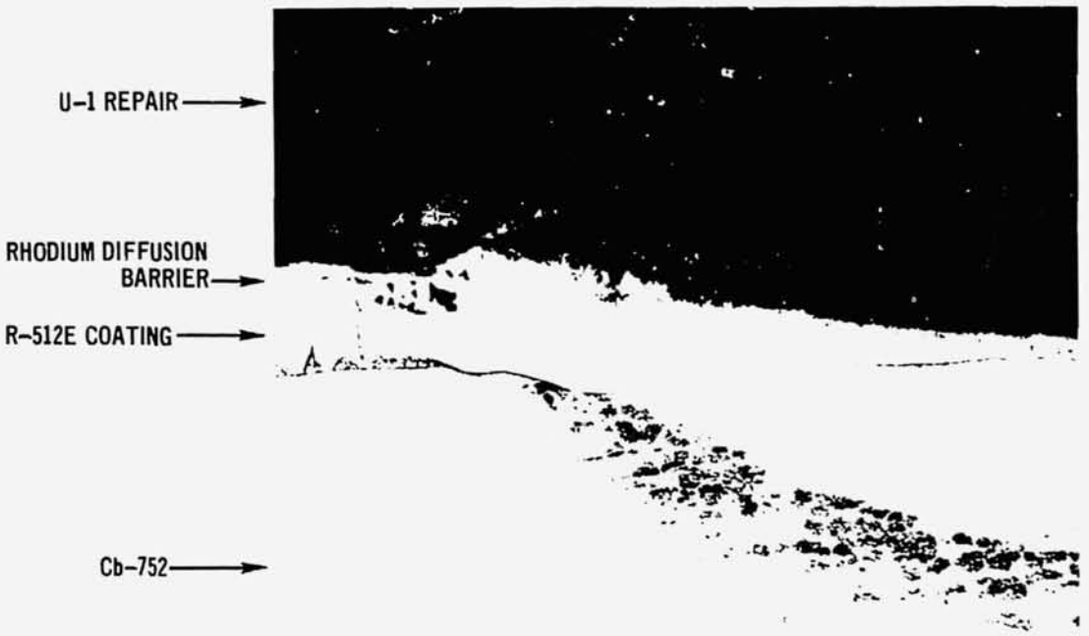

U-1 CERAMIC REPAIR COMPOSITION WITH RHODIUM DIFFUSION BARRIER AFTER 10 MINUTES AT 2400°F AND ONE ATMOSPHERE PRESSURE

457-2806

Figure 8-2

Attempts were made to brush plate rhenium. The rhenium adhesion was satisfactory but the rate of deposition was too slow to be practical. At the rates achieved, it would require 4 hours to brush plate 0.4 mil of rhenium, an impractical time for field repair procedure. Iridium was considered to be more difficult to plate than rhenium and was, therefore, eliminated from consideration.

Other metals and intermetallics were considered as diffusion barriers. Molybdenum and tungsten were candidates because of their compatibility with the repairs and with the fused slurry silicides, their low oxygen solubility, and their low oxygen diffusion rates. Attempts to formulate plating solutions in conjunction with iron or chromium provided useless. A second approach pursued was to use a metal which would form an intermetallic compound upon reaction with the columbium substrate. Chromium was successfully plated but proved to be incompatible with the ceramic repair, and oxidation failures occurred rapidly. Aluminum was used by applying foil to defect areas in coupon specimens using overlapping tack spot welds. As was the case with the chromium, incompatibility with the ceramics destroyed the aluminum before a columbium aluminide could be formed. While the concept of the diffusion barrier is sound, a satisfactory combination of materials has not been identified.

9. PLASMA NEEDLE REPAIRS

The plasma needle is a low amperage welding machine designed for joining thin gauge materials. It employs an argon stabilized plasma flame with the electrical arc struck within the torch, or between the torch and work place. Since the flame is relatively small, quick local heating with adequate temperature control was expected. The object was to develop a repair method in which the fused slurry silicide coating could be replaced in a defective area by techniques similar to torch brazing.

The plasma needle used was a Linde model with Torch No. PT-12. The machine was operated in the transferred and nontransferred arc modes. Initial experiments were conducted with uncoated and coated C-752 coupons with gritblasted defects. The processing cycles were performed in air with the torch mounted in an adjustable micrometer holder over the coupon. The coupons were instrumented on the back with a thermocouple. The following observations were made:

a) The target temperature, 2700°F, could be achieved only with difficulty. Overheating could burn holes through the coupons and the torch had to be located directly over the thermocouple to stabilize at 2700°F. After stabilizing, a lateral torch displacement of 0.050 inch produced a temperature drop of 200 to 400°F.

b) Attempts to effect reformation of the fused slurry silicide coating produced varying results. Although some encouraging melting and apparent reaction occurred, consistent results could not be obtained. Nonuniform wetting of the defect area occurred with evidence of slurry oxidation.

c) Equipment problems caused by reradiation from the coupon tended to overheat the torch.

An experiment was conducted in an argon welding chamber to isolate the cause of the inconsistent results. Wetting and flow of the R-512E slurry occurred, but sufficient time and temperature could not be obtained to produce the desired coating structure. Figure 9-1 shows a repair attempt in argon in which melting occurred but the reaction of the slurry with the columbium was not achieved. The repairs show evidence of oxidation presumed to be coming from minute amounts of water leaking from the water cooled torch. A clean weld bead could be run on titanium sheet in the argon chamber with a heliarc torch. However, discoloration of the titanium occurred when weld beads were run with the plasma needle torch. This confirmed that the plasma needle flame was not free of oxidizing gas.

457-2805

UNSUCCESSFUL PLASMA NEEDLE REPAIR ATTEMPT

Figure 9-1

It was concluded that the plasma needle torch was not a practical method for repair of the fused slurry silicide coating for the following reasons:

a) The flame from the plasma torch heated an area which was too small to be used effectively in a handheld repair method. (A more diffused flame torch might help.)

b) The flame was not sufficiently clean to allow uniform wetting of the slurry or coating formation.

c) The equipment was difficult to use and to control.

10. PLASMA SPRAYED REPAIRS

The field repair of coated columbium panels by plasma spraying was investigated because of the ease and practicality of plasma spraying. The following advantages were identified:

a) Portable equipment can be readily used in the field

b) Repairs can be made quickly

c) The repair is fully protective as applied.

Plasma deposited coatings have been evaluated for the protection of refractory metals with limited success. The development of new plasma spraying techniques and the availability of smaller particle size spray materials have permitted the deposition of improved coatings. The density and uniformity of the current plasma sprayed coatings would make them high potential candidates as field repair coatings.

10.1 OXIDATION EVALUATION OF PLASMA DEPOSITED REPAIRS - The plasma spraying was accomplished by METCO Incorporated of Westbury, New York. Of primary interest were intermetallic compounds, which have been shown to be the most successful materials for protecting the refractory metals. In addition to the intermetallics, other candidate materials were evaluated for repairs.

Cb-752 coupons with the R-512E coating were intentionally defected by grit-blasting the coating from a 1/4-inch diameter spot with 220 mesh alumium oxide. After METCO plasma deposited various repairs to an area 1/4-inch in diameter, the coupons were returned to MDAC for evaluation. The standard screening oxidation test of twenty-five 1-hour cycles in air at 2400°F was conducted on each type of repair. In addition, each repair material was profile tested to the conditions shown in figure 4-1. The exposures were conducted in sets of 10 profile cycles until repair failure occurred, or until a total of 100 cycles was run. Metallographic specimens of the promising repairs were examined after the screening and profile oxidation exposures.

A summary of results for the evaluation of the plasma sprayed repairs is presented in table 10-1. The first series of plasma sprayed repairs includes the oxide specimens 1 through 12 of table 10-1. These repairs were aluminum oxide and aluminum oxide-titanium oxide composites. The powders and spraying procedures were developed by METCO to produce high density coatings. Figure 10-1 shows the type of early failures experienced, in which spalling of the repair occurred upon cooling after the first cycle. It is believed that a combination of chemical

Table 10-1

EVALUATION OF PLASMA DEPOSITED FIELD REPAIR COATINGS

SPEC NO.	METCO REPAIR DESIGNATION	REPAIR TYPE	REPAIR THICKNESS (MILS)	TEST CONDITIONS		TEST RESULTS
				ONE ATMOSPHERE OXIDATION CYCLES AT 2400°F	REDUCED PRESSURE PROFILE CYCLES	
1	130	ALUMINUM OXIDE – TITANIUM OXIDE COMPOSITE	10.6	1	–	FAILED – REPAIR SPALLED
2			7.0	–	10	FAILED – REPAIR SPALLED
10	131 V.F.	ALUMINUM OXIDE – TITANIUM OXIDE COMPOSITE	5.8	1		FAILED – REPAIR SPALLED
12			9.9		10	FAILED – REPAIR PERIPHERY
5	105 S.F.	ALUMINUM OXIDE	10.6	1	–	FAILED – REPAIR SPALLED
6			6.6	–	10	FAILED – REPAIR SPALLED
14	443	ALUMINUM NICKLE – CHROMIUM COMPOSITE	9.3	11	–	FAILED – OXIDE GROWTH LIFTED REPAIR
16			6.2	–	10	SMALL FAILURE – REPAIR PERIPHERY
18	XP 1137	CHROMIUM SILICIDE	10.4	22	–	FAILED – REPAIR CENTER
20			6.6	–	30	FAILED – REPAIR SPALLED
21	XP 1133	MOLYBDENUM DISILICIDE	6.3	25		NO FAILURES – GOOD APPEARANCE
24			6.5		100	NO FAILURES – GOOD APPEARANCE
26	ZrB_2	ZIRCONIUM DIBORIDE	8.2	22		FAILED – REACTION AT REPAIR PERIPHERY
28			9.9		10	FAILED – REACTION AT REPAIR PERIPHERY
29	T S R-1097-5	GLASS-CERAMIC	9.3	4	–	FAILED – REPAIR SPALLED
31			9.9	–	10	FAILED – REACTION WITH SILICIDE
33 (1)	T S R-1033-2	GLASS CERMET	8.9	25	–	NO FAILURE
35			7.0	–	10	FAILURE – REPAIR SPALLED
36			7.5	1	–	FAILED – REPAIR SPALLED
37	T S R-1033-7	GLASS CERMET	7.7	1	–	FAILED – REPAIR SPALLED
39			10.1	–	10	FAILED – REPAIR SPALLED
40			10.1	13	–	FAILED – OXIDATION REPAIR CENTER

(1) SPECIMEN 33 HAD A CERAMIC REPAIR APPLIED OVER PLASMA SPRAY TO DETERMINE IF INSUFFICIENT OXIDATION RESISTANCE CAUSED FAILURE.

457-2843

incompatibility and thermal expansion mismatch contributed to the failure. The R-512E fused slurry silicide coating beneath the oxide repair in the overlap area spalled off with the oxide repair down to the Cb-752 substrate. Profile exposures resulted in the same type of failures for the sprayed oxides.

The second type of material evaluated as a plasma deposited repair was METCO 443. This is an exothermic aluminum/nickel-chromium alloy composite. The air

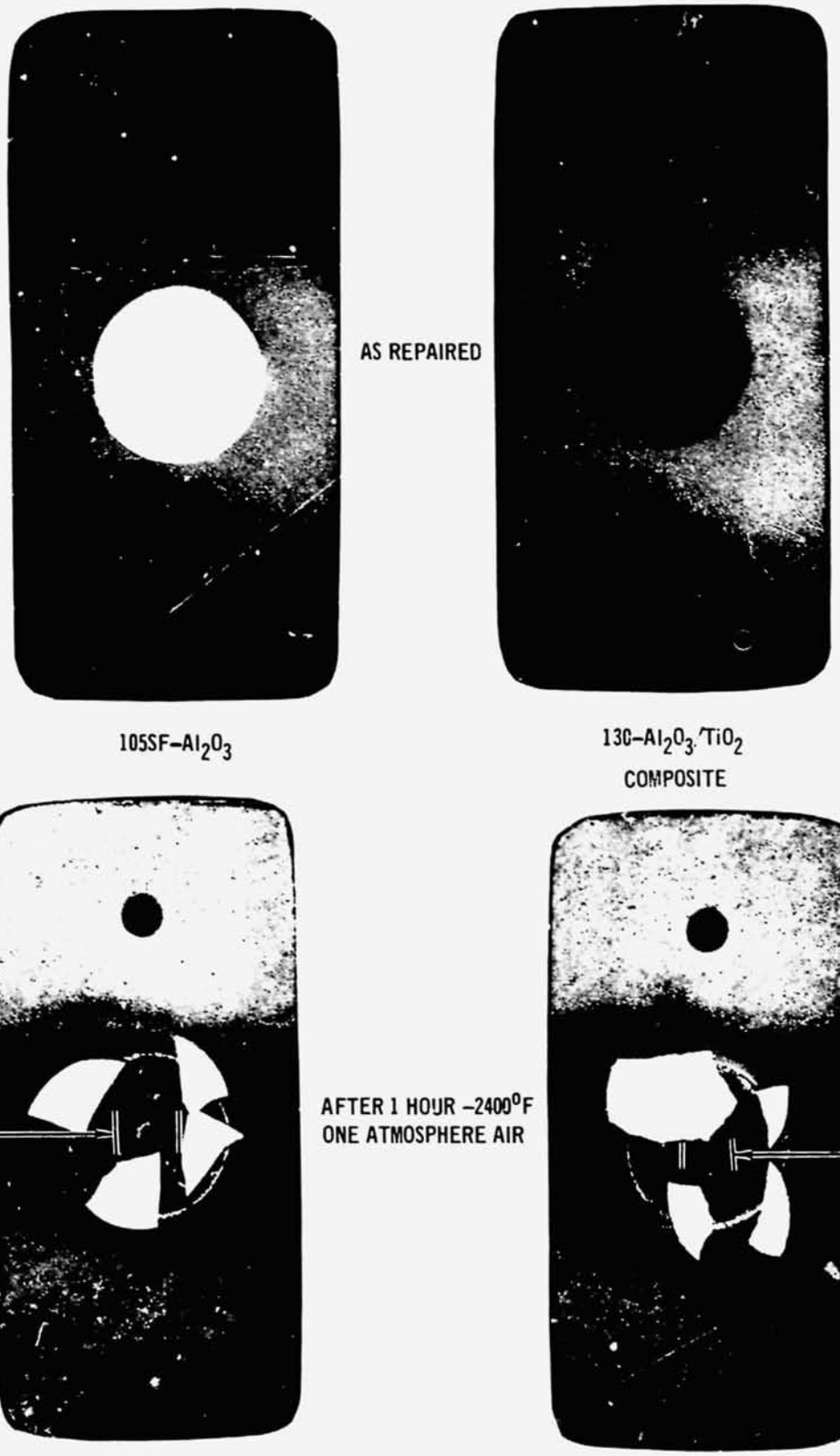

PLASMA SPRAYED OXIDE REPAIRS SHOWING SPALLING TYPE FAILURE
(Photographs 2X)

457–2802

Figure 10–1

atmosphere oxidation specimen failed after 11 cycles, with a considerable volume of columbium oxide growing beneath and lifting off the repair. The profile exposure specimen had a small oxidation failure after 10 cycles. It was concluded that the METCO 443 did not provide sufficient oxidation resistance. A series of glass bonded ceramics and cermets under the METCO designation T/S R-1097-5, TS-4-1033-2, and T/S R-1033-7 were evaluated. These materials failed in oxidation tests, both screening and profile, at relatively short times but with some scatter. One specimen, number 33, had a ceramic repair of the U-1 composition applied over the plasma deposit. This specimen survived twenty-five 1-hour cycles at 2400°F, thus establishing that the glass bonded ceramics and cermets offered insufficient oxidation protection.

A series of intermetallic plasma sprayed repairs were evaluated which showed promise as reliable repairs. The first intermetallic material evaluated was zirconium diboride. The 1 atmosphere screening test coupon failed at 22 hours at 2400°F by a small oxidation spot on the periphery of the repair area. The sample which was profile tested experienced the same conditions at 10 profile cycles. In both cases it was concluded that a subtle compatibility problem was present since the oxidation failures were in the overlap area of the R-512E coating. Figure 10-2 shows a cross section of the zirconium diboride repair area after 22 hours at 2400°F. The amount of contamination of the columbium substrate below the repair was minimal. The porosity of the plasma sprayed coating appears to be the greatest of the three intermetallic materials sprayed.

The second intermetallic material evaluated was chromium silicide. Table 10-1 summarizes the results of the evaluation. The air atmosphere oxidation test produced oxidation failures within the repair area after 22 hours at 2400°F. Part of the repair thickness spalled off by failing cohesively after thirteen 1-hour cycles, reducing the remaining coating thickness to approximately 2.5 mils. The profile test specimen similarly spalled a portion of the repair thickness at 20 cycles and general oxidation failures occurred after 30 profile cycles (see figure 10-3). A metallographic examination of the air atmosphere test specimen revealed that the contamination below the repair was minimal, as shown in figure 10-3. It was concluded that a repair thickness of 6.6 mils was too thick to prevent cohesive spalling of the exterior of the repair. Oxidation testing indicated that a lesser thickness (approximately 4 mils) would be sufficient for oxidation resistance.

The third intermetallic material evaluated as a plasma sprayed repair was molybdenum disilicide. The repair passed the screening oxidation test at 2400°F

150X

457-2801

PHOTOMICROGRAPH OF PLASMA SPRAYED ZIRCONIUM DIBORIDE REPAIR AFTER 22 HOURS AT 2400°F

Figure 10-2

150X

PHOTOMICROGRAPH OF CHROMIUM SILICIDE REPAIR AFTER 22 HOURS AT 2400°F

457-2800

Figure 10-3

in 1 atmosphere for 25 hours without oxidation failure (see figure 10-4). The metallographic examination showed that very little substrate contamination had occurred. The profile tests were conducted and no oxidation failures or adverse reactions were observed through 100 profile cycles. The metallographic examination revealed that the repair was dense and compatible; the contamination zone in the substrate was limited to about 8 mils, as shown in figure 10-4. It was concluded that the molybdenum disilicide showed a high potential for being a high quality practical repair. Further testing of the molybdenum disilicide repair was undertaken and other intermetallics, zirconium diboride and chromium silicide, which had a lower potential as repairs were dropped from consideration.

The oxidation resistance of the molybdenum disilicide plasma sprayed repair was adequately demonstrated. However, prior to the repair of panels for structural evaluation, it was necessary to establish that the plasma spraying did not cause distortion of the thin (10-mil) columbium skins being used. A single faced corrugated panel (as shown in figure 3-6) with the R-512E fused slurry silicide coating was used to evaluate the distortion effects of plasma spraying. A series of defects, both 1/8-inch and 1/4-inch diameter, were gritblasted on the skins at locations over the welds and between the welds. Molybdenum disilicide was plasma sprayed over each defect, overlapping the repair of the R-512E coating by approximately 1/8-inch. A mask of 1/8-inch thick steel was employed to protect the surrounding area from overspray and to act as a heat sink to minimize the heat input to the thin skin. This technique proved highly successful and the panel was repaired in six locations with no measurable distortion. Figure 10-5 shows this panel after plasma spray repair.

The plasma sprayed repair using molybdenum disilicide was considered to be a highly practical and effective repair fully qualified for flight simulation profile testing on 3 by 12-inch rib stiffened panels.

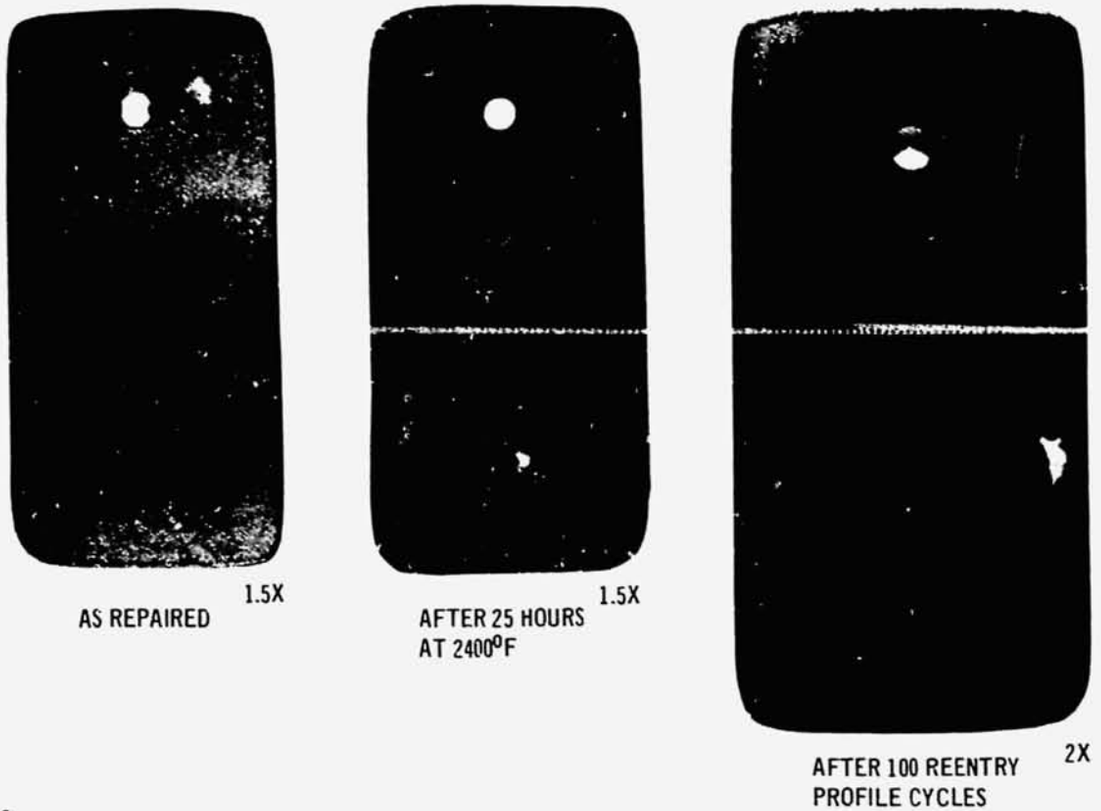

1.5X
AS REPAIRED

1.5X
AFTER 25 HOURS
AT 2400°F

2X
AFTER 100 REENTRY
PROFILE CYCLES

457-2835

MOLYBDENUM DISILICIDE PLASMA SPRAYED REPAIRS OF R-512E OF Cb-752

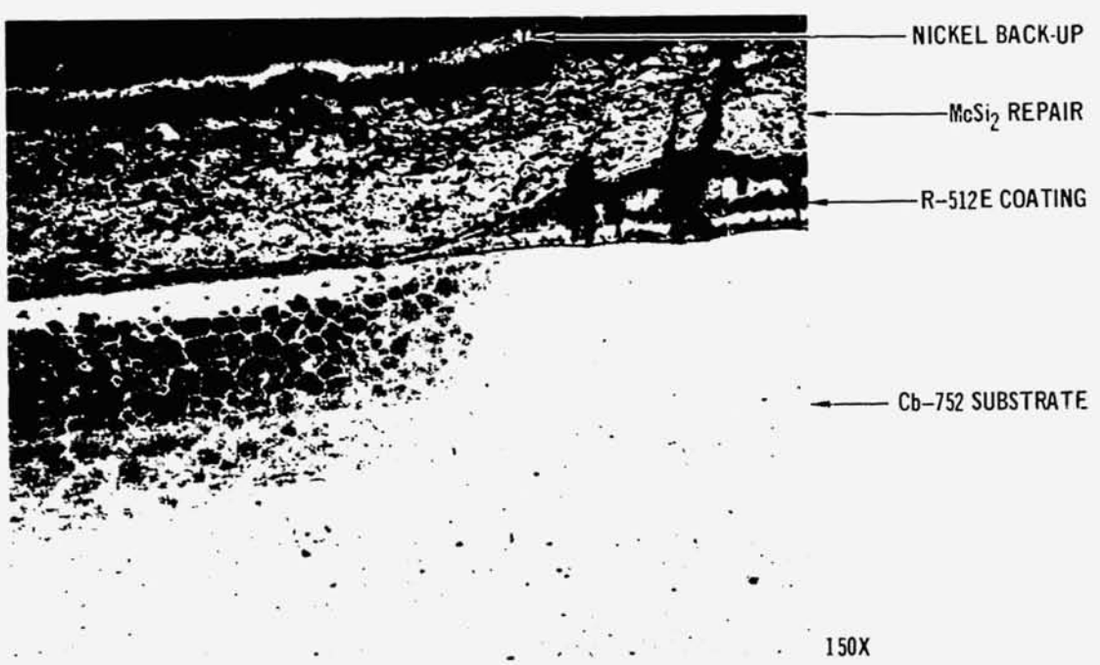

150X

CROSS SECTION OF MOLYBDENUM DISILICIDE REPAIR AFTER
100 REENTRY PROFILE CYCLES

457-2836

Figure 10-4

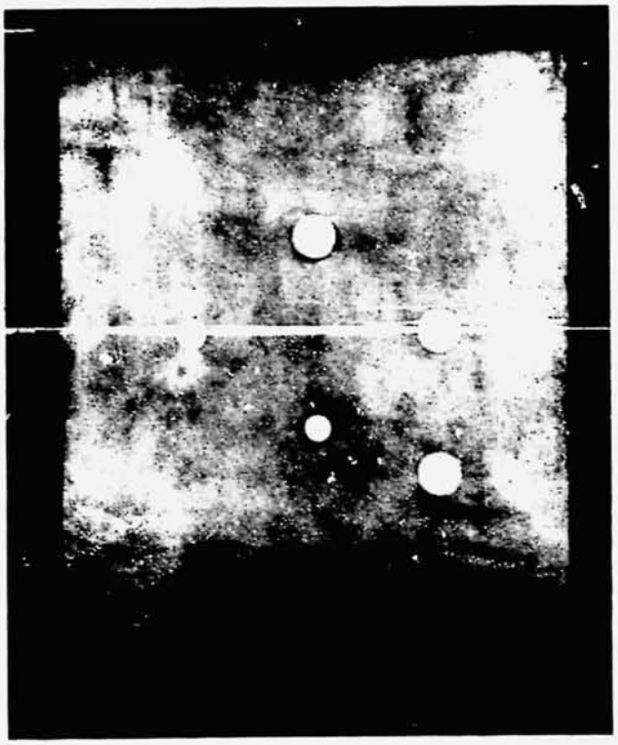

PLASMA SPRAYED MOLYBDENUM DISILICIDE FIELD REPAIR OF CORRUGATED PANEL SHOWING LACK OF DISTORTION OF 10 MIL SKIN

Figure 10–5

457–3329

11. FIELD REPAIR BY REAPPLICATION OF THE FUSED SLURRY SILICIDE COATING

The fused slurry silicide coatings have demonstrated the longest and most reliable protective lives for columbium base alloys. It would, therefore, follow that a field repair coating, based upon the fused slurry silicide coating would be the longest life repair that could be expected with the current status of coating technology. The replacement of the coating in a local defect area has the disadvantage that it is not as easy and practical to accomplish in the field as other types of field repairs. The main purpose of this study was to develop a repair method which was simple and easy to accomplish while maintaining the advantage of long and reliable protective life.

Sylvania High Temperature Composites Laboratory conducted the study of field repairs methods for replacing the fused slurry silicide coating in a local defect area. The technical effort was divided into two parts. Initially, a new and practical repair method was developed; then, the limitations of the method and the applicability to thin skinned hardware were determined.

11.1 BACKGROUND AND TECHNICAL APPROACH - The reapplication of intermetallic coatings under field repair conditions has been accomplished several times in the past. The repair of LB-2 coated columbium assemblies by two different field repair methods was accomplished on the ASSET program and is described in reference 7. The first method employed the induction heating of the repair area with the required protective atmosphere provided by constructing an argon tent around the repair area. The second method successfully employed a ceramic retort, or shell, molded over the repair with heat supplied by a large oxyacetylene torch. The repair of a fused slurry silicide coated columbium heat shield panel by Sylvania is described in reference 8. The method involved using a portable induction furnace. A vacuum retort is sealed to the panel to be repaired through an O-ring seal, and the temperature supplied by induction heating. In each of these cases the repair method sought to duplicate the processing conditions which were employed in originally forming the coating (see figure 11-1).

Past success in reapplying protective coatings to columbium under field conditions clearly demonstrated the feasibility of the general method. Two disadvantages were obvious in the past efforts. First, each of the methods was specialized for a particular area to be repaired, and, in the case of the three examples cited, the methods could not be interchanged if they were still to

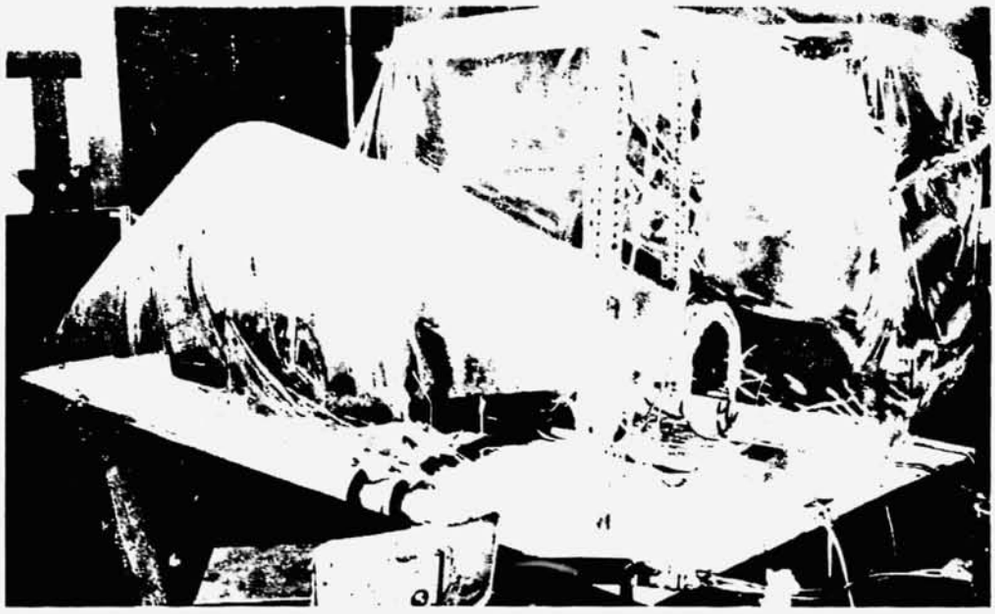

457-1732

Local Coating Repair of ASSET Upper Body Using Induction Heating in an Argon Tent

457-1730

Torch/Ceramic Shell Repair of ASSET Upper Body

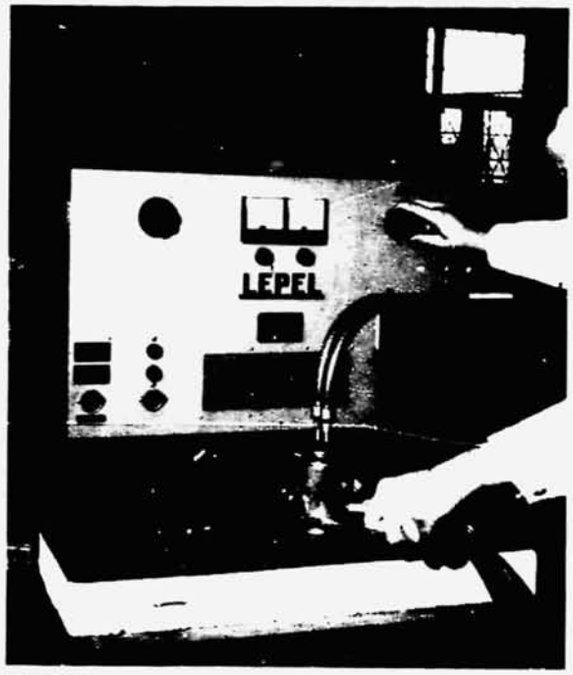

457-1731

Sylvania Portable Induction Heated Coating Repair Furnace

REPAIR METHODS USED IN THE PAST TO REPLACE ORIGINAL INTERMETALLIC COATING

Figure 11-1

maintain their effectiveness. Thus, each repair job was unique and specialized, with associated high costs. A practical field repair method must be able to cover a wide range of hardware locations and conditions without requiring specialized techniques or equipment. The second disadvantage was in approximating the typical processing time at high temperature of 1 hour. One hour, or even one-half hour, at 1900 to 2500°F may be difficult to maintain without overheating backup structures or onboard equipment. Also, the maintenance of an inert atmosphere becomes more critical and difficult with increasing processing time. To eliminate or minimize these disadvantages, the object of the development study was to minimize processing time and atmosphere requirements, while maintaining the advantage of a long-life repair associated with replacing the fused slurry silicide coating.

The technical approach was to investigate the possibility of forming the coating rapidly while maintaining the same coating structure and oxidation resistance. A second step was to investigate potential heating sources which would reproduce the rapid process conditions identified with practical equipment. Minimum atmosphere requirements were studied to further improve the practicality of the method.

11.2 INITIAL DEVELOPMENT OF REPAIR METHOD - The initial experiment was to determine if the processing time for the fused slurry silicide coating could be reduced to 1 to 5 minutes without sacrificing the protectiveness of the coating.

Coupons of Cb-752 alloy were prepared and R-512E slurry was applied to a nominal mass of 20 mg/cm^2. The coupons were processed in a Brew Vacuum Furnace in which the heating and cooling time could be minimized. Figure 11-2 shows the heating cycle employed for this study. The processing temperatures investigated were 2600, 2700, 2800, and 2900°F, and holding times of 1 and 5 minutes were employed for each temperature condition.

Each of the eight processing conditions was examined metallographically to determine if the coating was structurally the same as that formed during a standard processing cycle (1 hour at 2580°F). Figures 11-3 and 11-4 show the microstructures observed. The microstructures for the 1-minute processing show normal coating structures at 2700 and 2800°F. Incomplete reaction is indicated at 2600°F with excessive reaction and coarse columnar structure at 2900°F. The 5-minute processing specimens show a normal coating structure at 2600 and 2700°F, with excessive reaction indicated at 2800° and 2900°F. Triplicate coupons were oxidation tested to the reentry time-temperature-pressure conditions shown in figure 4-1, and the results are presented in figure 11-5. It can be seen that the 1-minute processing at 2600, 2700 and 2800°F produced a coating with a cyclic profile life

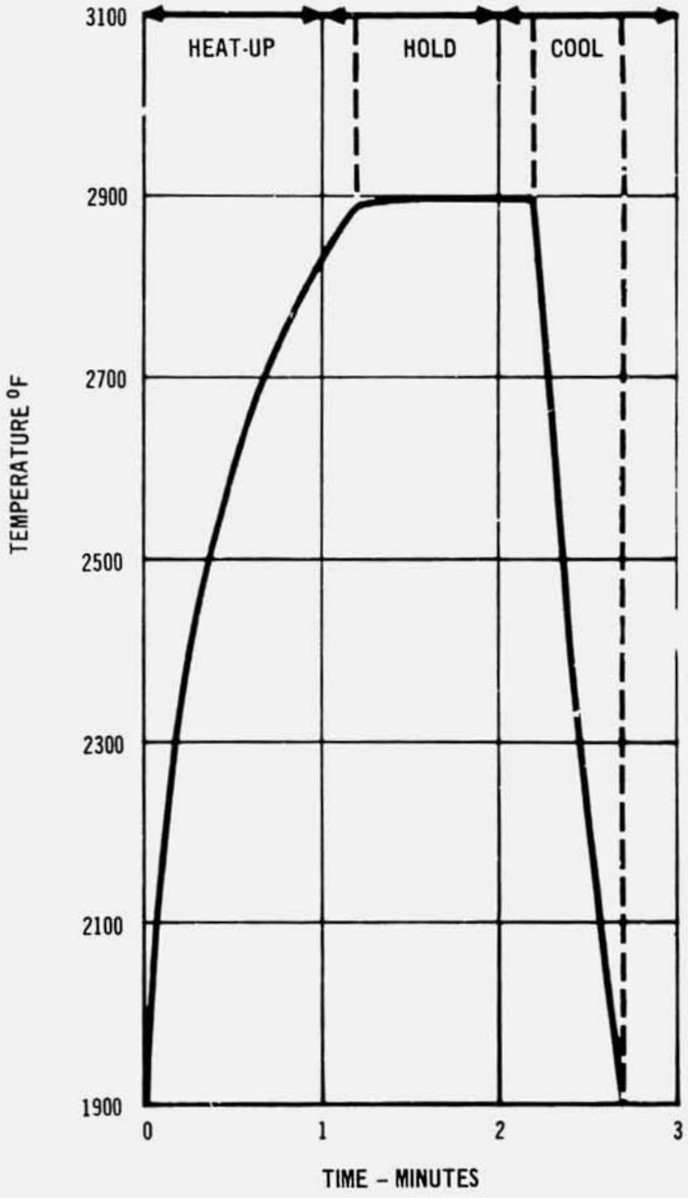

457-1710

HEATING CYCLE FOR RAPID COATING FORMATION STUDIES

Figure 11-2

of 200 or more cycles. The 5-minute processing gave an optimum life at 2700°F, which is in excess of 200 reentry profile cycles. It was concluded that processing at 2700°F would produce a coating of satisfactory quality, with temperature variations of 100°F not being of significant concern. A processing time of 1 minute was shown to be sufficient, with up to 5 minutes being satisfactory at 2700°F. These results were considered very encouraging as the potential appeared good for developing a rapid coating repair method with wide processing tolerances and broad

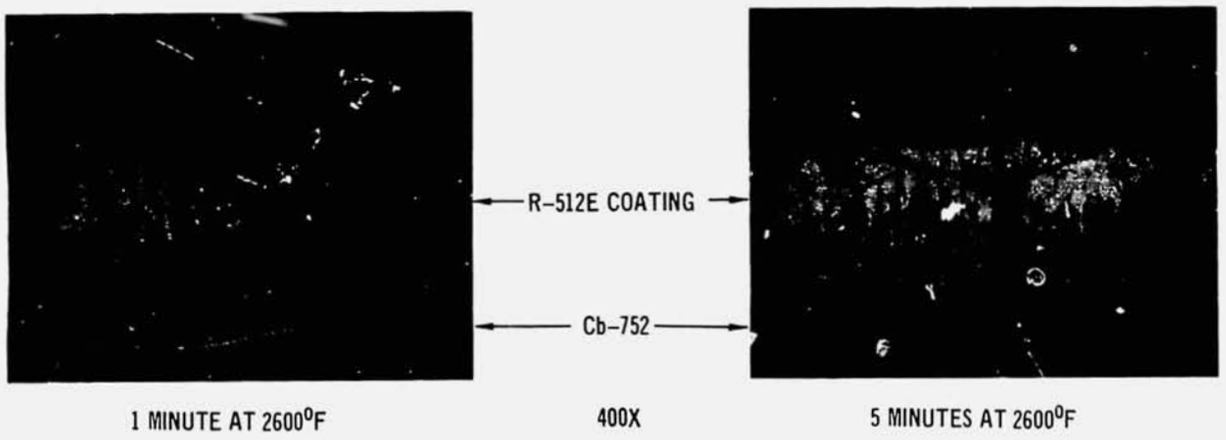

457-1711

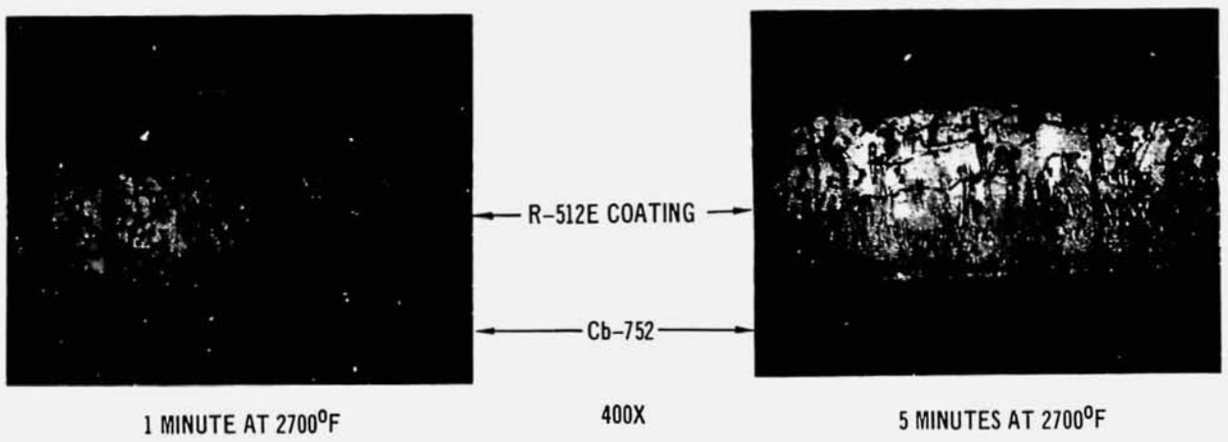

457-1712

PHOTOMICROGRAPHS OF RAPID COATING FORMATION STUDY

Figure 11-3

applicability.

Several heating sources were reviewed for applicability to a practical field repair method. A focused radiant lamp manufactured by Research Incorporated, designated model number 40-85, in which the focal point of the radiant energy was 1/8 inch below the shield, was selected, and an argon gas supply was connected to cool the lamp and provide an inert atmosphere for the repair area (see figure 11-6). The initial experiments were designed to determine the maximum temperature attainable with the lamp spot heater, and its heating and cooling characteristics. Instrumented coated columbium samples were readily heated to 2900°F (lamp operated at 150 volts), and the heating and cooling rates were found to be more rapid than those experienced in the laboratory vacuum furnace. Therefore, it was decided to

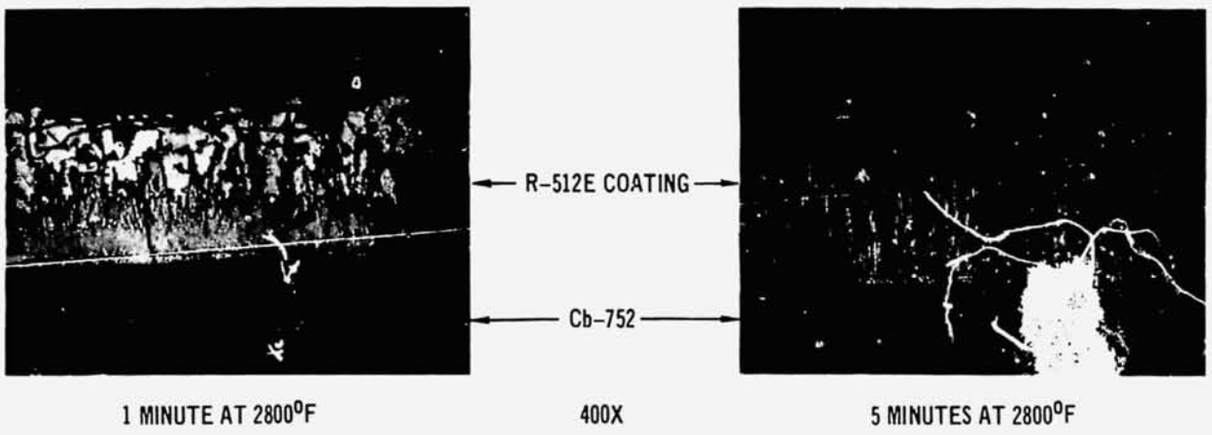

457-1713

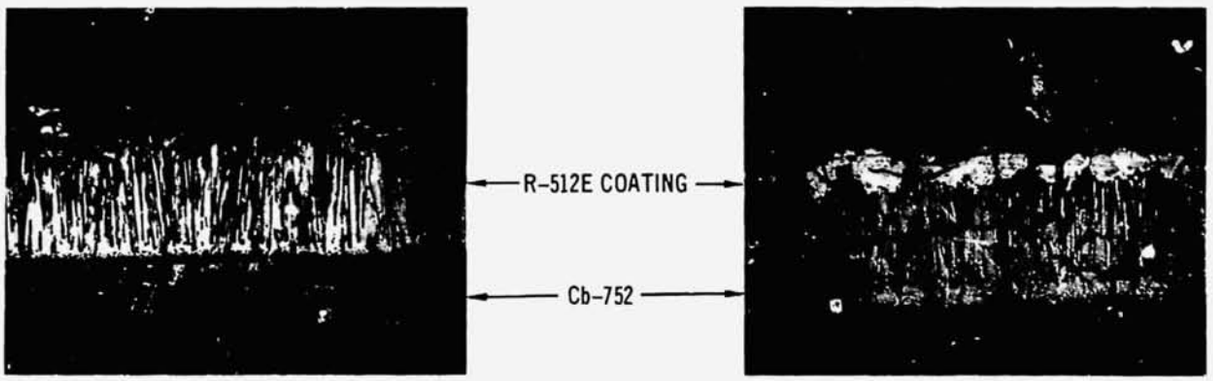

457-1714

PHOTOMICROGRAPHS OF RAPID COATING FORMATION STUDY

Figure 11-4

employ a processing condition of 2 minutes at 2700°F to account for the difference in heating rate between the lamp and the vacuum furnace (figure 11-14 shows the lamp in operation).

Defects were produced in R-512E-coated Cb-752 coupons by grinding a 1/8-inch area through the coating to the substrate. A slurry of 20Cr-20Fe-60Si was applied to the area with an eyedropper, and the radiant spot heater was used to heat the repair area to 2700°F for 2 minutes. Examination of the resulting repair coating metallographically showed the coating structure to be normal for the R-512E; the thickness was considered good (2.5 mils) and no contamination or other deleterious effects to the substrate were noted. The repair was repeated several

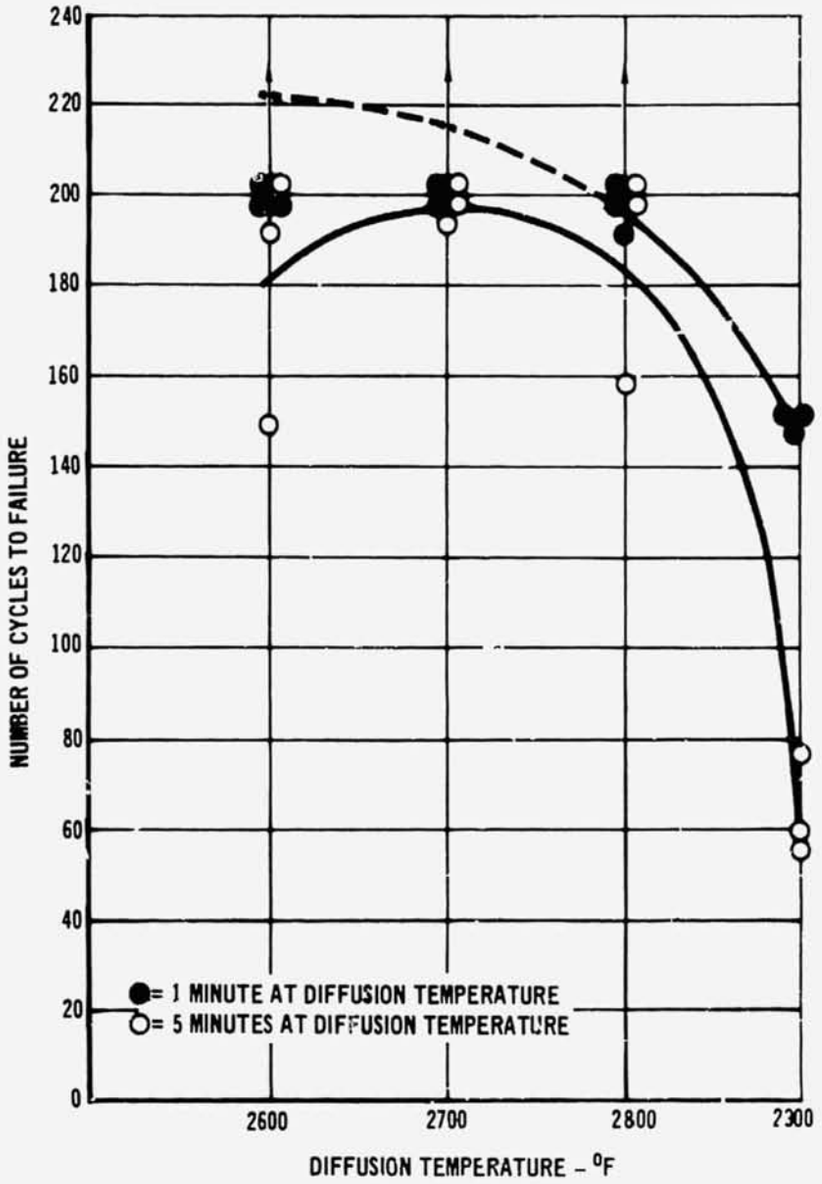

REENTRY PROFILE OXIDATION TEST RESULTS OF R-512E COATINGS PRODUCED IN RAPID COATING FORMATION STUDY

457-3330

Figure 11-5

times with satisfactory results. As a final demonstration of the feasibility of the lamp repair method, five coupons of R-512E-coated Cb-752 were defected and repaired using the radiant lamp method. The coupons were reentry profile tested per the time, temperature, and pressure conditions of figure 4-1. The testing was terminated at 110 cycles and no evidence of coating failure was noted in any of the

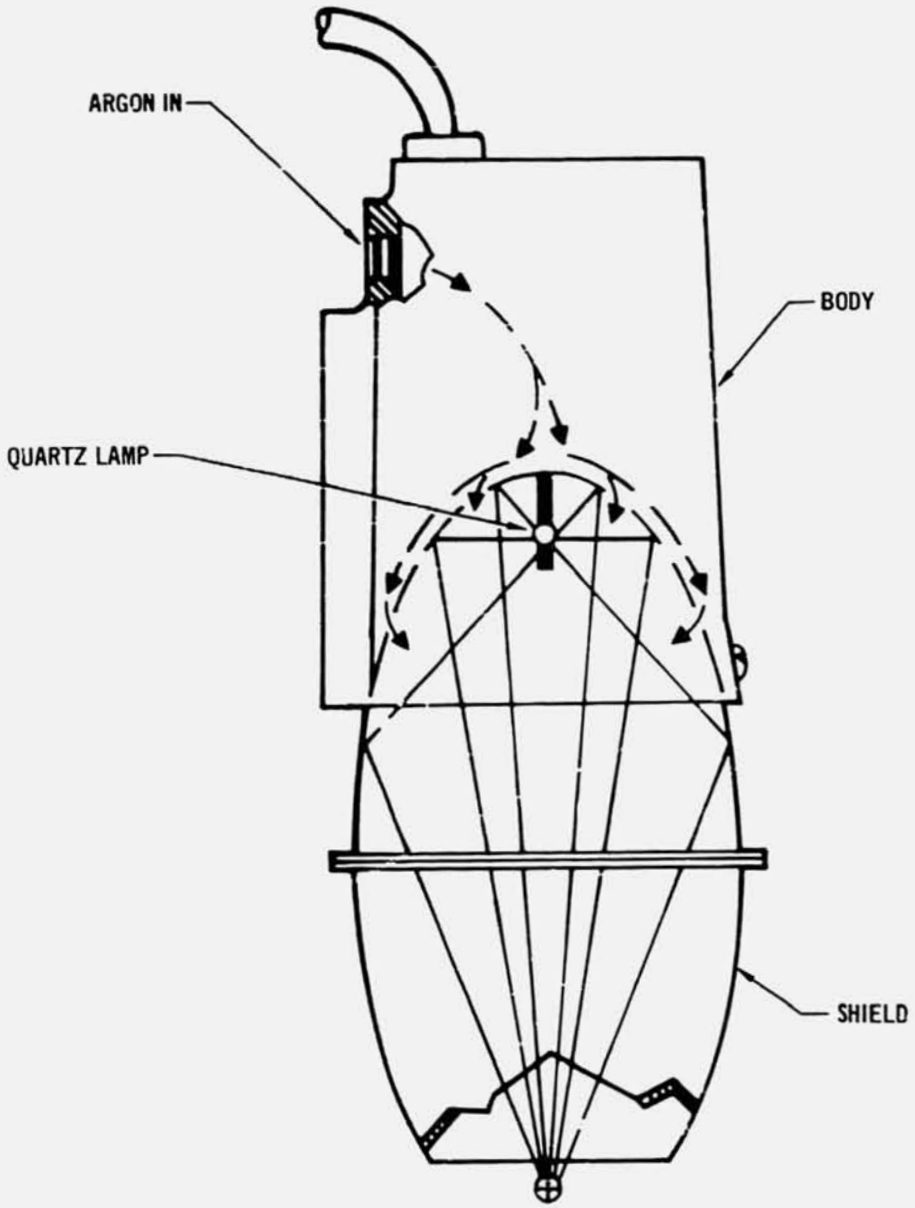

457-1715

PORTABLE RADIANT LAMP HEATER

Figure 11-6

coupons. Metallographic examinations were made of the coupons after oxidation testing, and the condition of the coating and substrate appeared normal in every respect.

It was concluded from this phase of the field repair development program that the radiant lamp method of repair met all the objectives of simplicity and broad practicality as a means of replacing the fused slurry silicide coating. The properties of the repair coating have been shown to be more than adequate.

11.3 LIMITATIONS AND HARDWARE CONSIDERATIONS ASSOCIATED WITH LAMP REPAIR METHOD - The lamp repair method appeared to have a high potential for being a simple procedure for achieving reliable repair of defect sites with broad applicability. A series of experiments was conducted to investigate the limitations of the method and to demonstrate that typical hardware could be safely repaired under field conditions associated with an operational reentry vehicle.

11.3.1 Process Refinement - The initial development effort indicated that control of the repair coating thickness required consideration. This was studied from the standpoint of the mass of slurry applied to the defect site and the wetted area produced. Since it was very difficult to determine the thickness or unit weight of slurry that is sprayed or brushed over a defect site, it was considered advantageous to be able to apply the repair materials as dry preforms of uniform thickness. Preforms were prepared by pouring an acrylic base slurry of the R-512E composition onto a silicone coated paper. After air drying at ambient temperature, the flexible sheet of dried R-512E slurry was removed readily from the paper and was able to withstand punching, shearing, or hand scissor cutting into any desired shape. Figure 11-7 illustrates the preforms cut from such a sheet.

A study was performed to determine the effect of heating rate, final temperature, and heating cycle time on the size of the resulting wetted area and on the structure of the repair coating. These tests were performed on uncoated Cb-752 sheet coupons with R-512E preforms, 1/8 by 1/8 by 0.025 inch in size and having an average unit weight of 50 mg/cm^2. The cycles investigated and the results are listed in table 11-1. The processing sequence designated C was judged superior on the basis of visual and metallographic observations.

In a subsequent series of tests the effect of the heating cycle on the protective efficiency of the repair was studied. The Cb-752 coupons were furnace coated with approximately 30 mg/cm^2 R-512E. Defects, 1/8 by 1/8 inch, were ground through the coating and into the base metal. A 1/8 by 1/8 by 0.025-inch thick (50 mg/cm^2) R-512E preform was placed over the defects in each of the three specimens and fired with the spot heater under three different sets of conditions, as shown in table 11-2. Two of the heating cycles were identical to those employed in the wetting study (designated B and C, in table 11-1) and the third was a

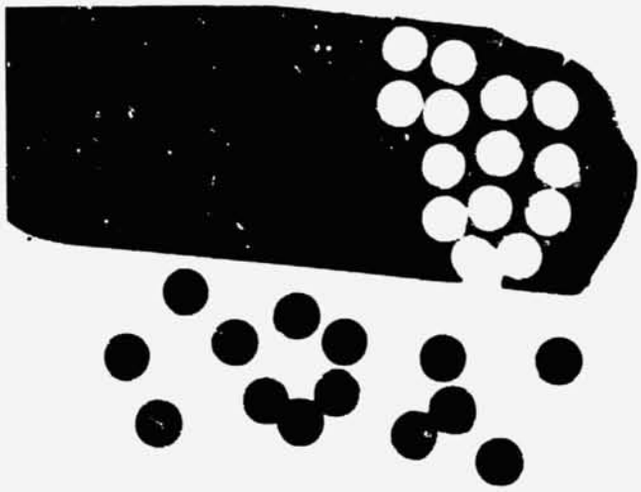

Preforms and Sheet

Preform in Place on Defect

457 -2867

R-512E PREFORMS CUT FROM SLIP CAST SHEET

Figure 11-7

modification of heating cycle C, designated C-2. Heating cycles C and C-2 resulted in better wetting and in generally cleaner surfaces. All three specimens were tested in the 1-atmosphere slow cyclic test. The sample representing heating cycle C was removed for metallographic study after 20 cycles and the other 2 were tested for 31 cycles. No defects were noted in or near the repaired areas. A fourth specimen which was defected similarly, but not repaired, was tested as a control along with these three repaired specimens. It showed obvious signs of base metal oxidation very early and, after 10 cycles, it had developed a hole through the entire sheet thickness.

Metallographic sections through the repair areas of the coupons representing

Table 11-1

EFFECT OF HEATING CYCLE ON WETTING AND STRUCTURE OF REPAIR COATING

SAMPLE NO.	DESIGNATION	HEATING CYCLE		TIME AT MAXIMUM TEMPERATURE	AREA WETTED	COATING STRUCTURE
		RATE	MAXIMUM TEMPERATURE °F			
1201430-1	A	PREHEAT AT 900°F 30 SEC UP TO TEMPERATURE IN 3 SEC	2700	2-1/2 MIN	40X PREFORM AREA	STRUCTURE WELL DEFINED COATING TOO THIN (1 - 1-1/2 MILS)
1201431-2	B	PREHEAT AT 900°F 30 SEC UP TO MELTING POINT IN 3 SEC, POWER OFF	APPROX 2400-2500	3 SEC	9X PREFORM AREA	COATING VERY THICK (5 MILS); STRUCTURE NOT WELL DEFINED
1201431-3	C	PREHEAT AT 900°F UP TO TEMPERATURE IN 1 MIN	2700	1-1/2 MIN	16X PREFORM AREA	STRUCTURE WELL DEFINED THICKNESS GOOD (ABOUT 2 MILS)

Table 11-2

EFFECT OF HEATING CYCLE ON PROTECTIVENESS OF REPAIR

SAMPLE NO.	DESIG-NATION	RATE	MAXIMUM TEMPERATURE	TIME AT MAXIMUM TEMPERATURE	AREA WETTED	SLOW CYCLIC TEST 800-2400°F 40 MIN CYCLES
1201434-2	B	PREHEAT AT 900°F - 30 SEC UP TO MELTING POINT IN 3 SEC, POWER OFF	APPROX 2400-2500°F	3 SEC	4X PREFORM AREA	31*
1201434-1	C	PREHEATED AT 900°F - 30 SEC UP TO TEMPERATURE IN 1 MIN	2700°F	1-1/2 MIN	40X PREFORM AREA	20*
1201434-3	C-i	PREHEAT AT 900°F - 30 SEC UP TO 2500°F IN 1 MIN THEN UP TO MAXIMUM IN 1 MIN	2700°F	1-1/2 MIN	40X PREFORM AREA	31*
1201434-4	-	UNREPAIRED CONTROL	-	-	-	10**

*TEST STOPPED AT INDICATED TIME; NO FAILURES NOTED
**HOLE DEVELOPED THROUGH UNREPAIRED CONTROL SPECIMEN

457-2880

heating cycles C and C-2 were prepared. In each case a well formed coating roughly equivalent to the original coating thickness covered the entire repaired area. There was a slight buildup at the rim of the defect, but by far the major portion of the coating from the preform went into the defect area. Most of the adjacent area wetted was covered by a very thin layer of the repair slurry which blended into the original coating. Microhardness traverses were made which indicated no evidence of substrate contamination, thereby establishing complete effectiveness of the repair procedure.

11.3.2 Repair Size Capability - Tests were performed to determine the maximum size area that could be satisfactorily repaired using the techniques described above employing the modified spot heater.

An R-512E preform, 0.350 inch in diameter, weighing 100 mg, was placed in the center of a 1 by 1-inch Cb-752 uncoated coupon. The preform was then fused with the spot heater using a second modificaton of the heat cycle (C-3), which consisted of preheating for 30 seconds at 900°F, heating to 2500°F within 1 minute, continuing to heat to 2700°F within an additional 15 seconds, and holding at 2700°F for 1-1/2 minutes. The specimen was sectioned through the center and photomicrographs showing the microstructure at the centerline and at a radii of 1/8, 1/4 and 3/8 inch are given in figure 11-8.

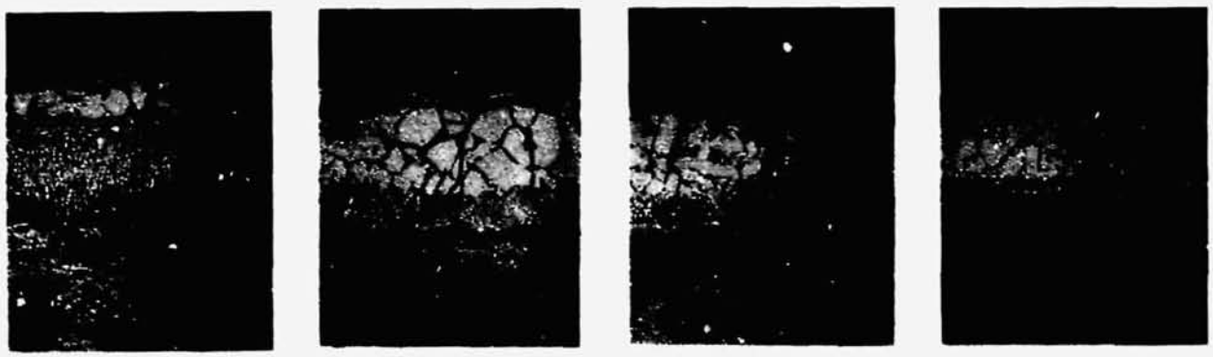

EFFECT OF DISTANCE FROM CENTERLINE OF REPAIR ON R-512E COATING STRUCTURE

Figure 11-8

A group of 10 coupons were R-512E furnace coated to a finished coating unit weight of 18 to 20 mg/cm^2. These coupons were subsequently preoxidized in air for one hour at 2400°F to simulate a used, coated piece of hardware. The coating was then removed completely from large, circular areas by grit blasting with fused aluminum oxide grit at 60 lb/in^2 with rubber masks to protect the remainder of the specimen. Half of the group was stripped of a 3/8-inch diameter area and the remaining group was stripped of a 1/2-inch diameter area. A slightly larger mask (approximately 1/4 inch larger than the defect diameter) was then used for cleaning the annular area surrounding the defect. In this case, steel grit was used at 20 lb/in^2 to remove the oxide film without damaging the coating. A 0.225-inch diameter R-512E preform, weighing 65 mg, was placed at the center of each defected area and fused using the C-2 heat cycle. In every case the preform wet the entire defect plus the cleaned annulus surrounding the defect. The repaired specimens were evaluated by 1-atmosphere slow cyclic testing and by reduced pressure reentry simulation testing. The test conditions and results are given in table 11-3. Photographs illustrating every important step of defecting, repair, and proof testing of these specimens are shown in figure 11-9. Note that not a single coating failure occurred in the repaired area of any of the 10 specimens. Photomicrographs of the repaired coatings after testing, shown in figures 11-10 and 11-11, are generally typical of R-512E coatings that have been similarly exposed. It was

Table 11-3

PROOF TEST RESULTS OF LARGE AREA DEFECT REPAIRED SPECIMENS

SPECIMEN NO.	DEFECT SIZE (DIA IN.)	1 ATM SLOW CYCLIC TEST 800-2400°F (NO. 40 MIN CYC)	SIMULATED EXTERNAL PRESSURE REENTRY PROFILE (NO. 40 MIN CYC)
120014-38-8	1/2	-	114*
-10	1/2	-	114*
-11	1/2	-	114*
-12	1/2	36*	-
-13	1/2	36*	-
-14	3/8	-	114*
-15	3/8	-	114**
-16	3/8	36*	114*
-17	3/8	36**	-

*TOP EDGE FAILURE

457-2861

**TEST STOPPED - NO COATING FAILURE NOTED

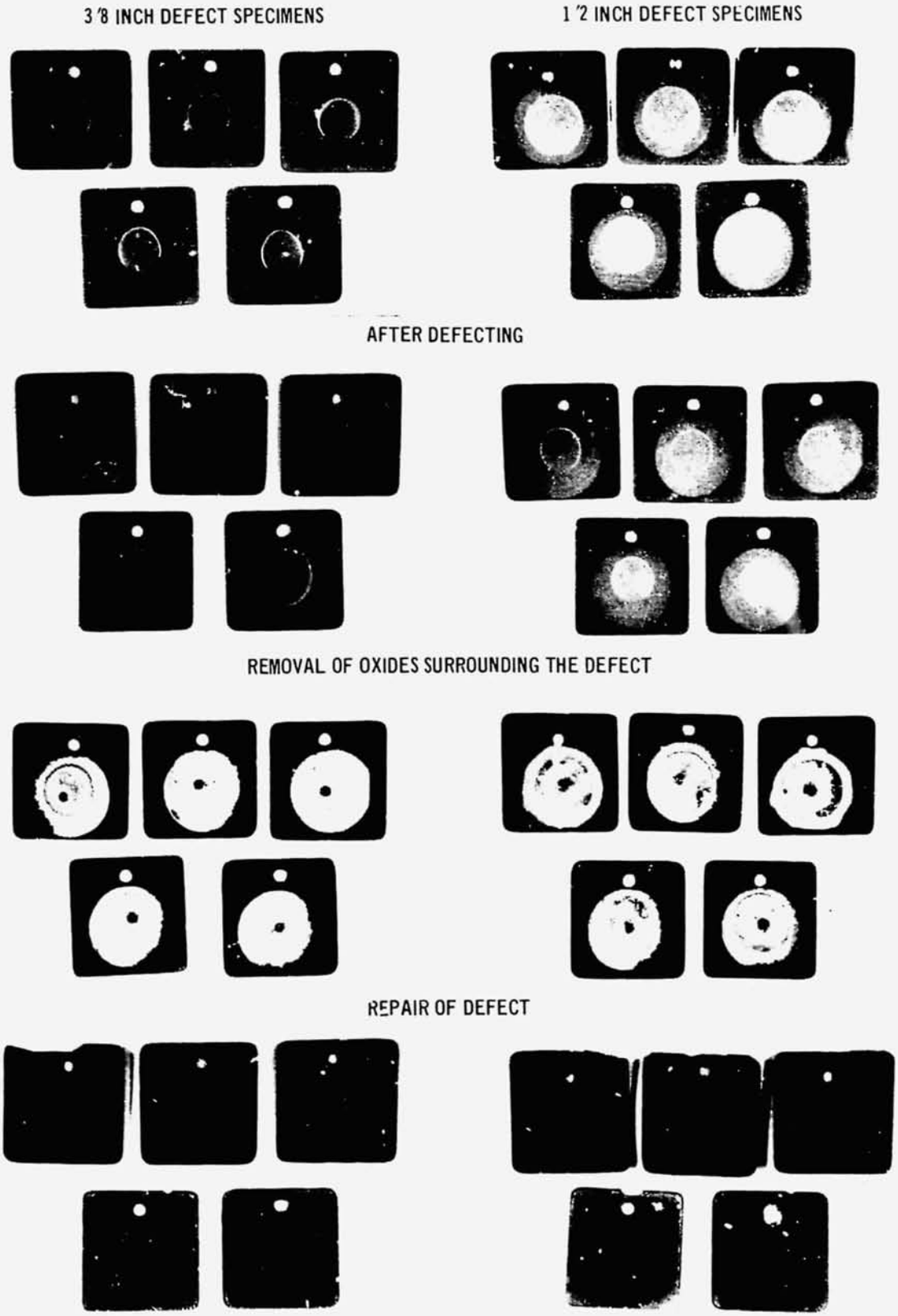

457-2871

RESULTS OF REPAIRING 3/8 AND 1/2 INCH DEFECT AREAS

Figure 11-9

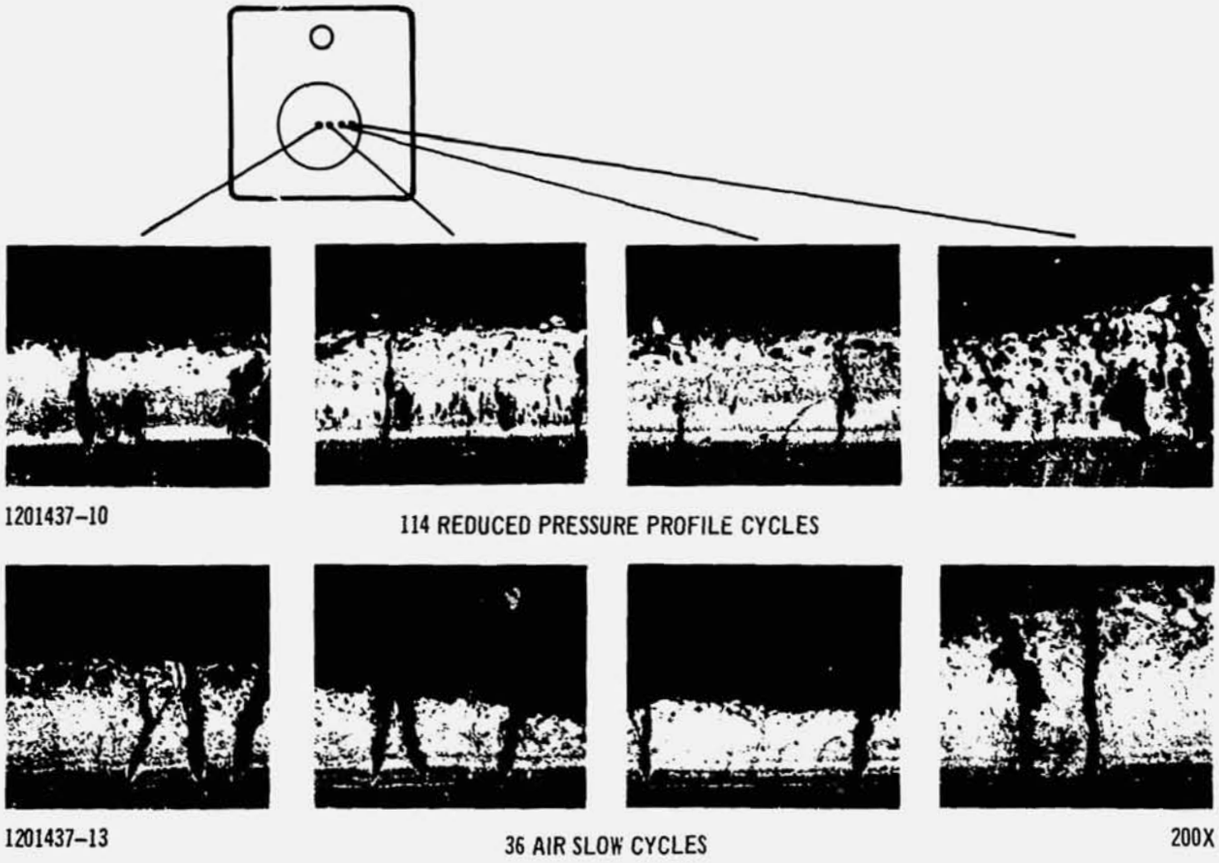

457-2872

PHOTOMICROGRAPHS OF 1/2 INCH DIAMETER DEFECT SPECIMENS AFTER REPAIR AND TEST

Figure 11-10

concluded that defects up to 1/2 inch in diameter could be satisfactorily repaired using the radiant spot heater.

11.3.3 Repair bility Of Contaminated Defects - Since defects may occur or manifest themselves in flight and result in contamination of the underlying substrate, it is necessary to demonstrate that the repair technique can be applied to such defect sites. Two R-512E-coated Cb-752 defected coupons were exposed in an air furnace for 15 minutes at 2400°F, resulting in the formation of a yellowish columbium oxide over the entire defected areas. This treatment also undoubtedly resulted in contamination of the columbium alloy substrate by the solution of oxygen in the substrate. One of these specimens was then remasked to allow grit blasting of the oxidized and contaminated area and a small annulus adjacent to the defect. This was done with steel grit at 20 lb/in^2 in order to permit removal of any additional metal in the defect area or coating in the surrounding area.

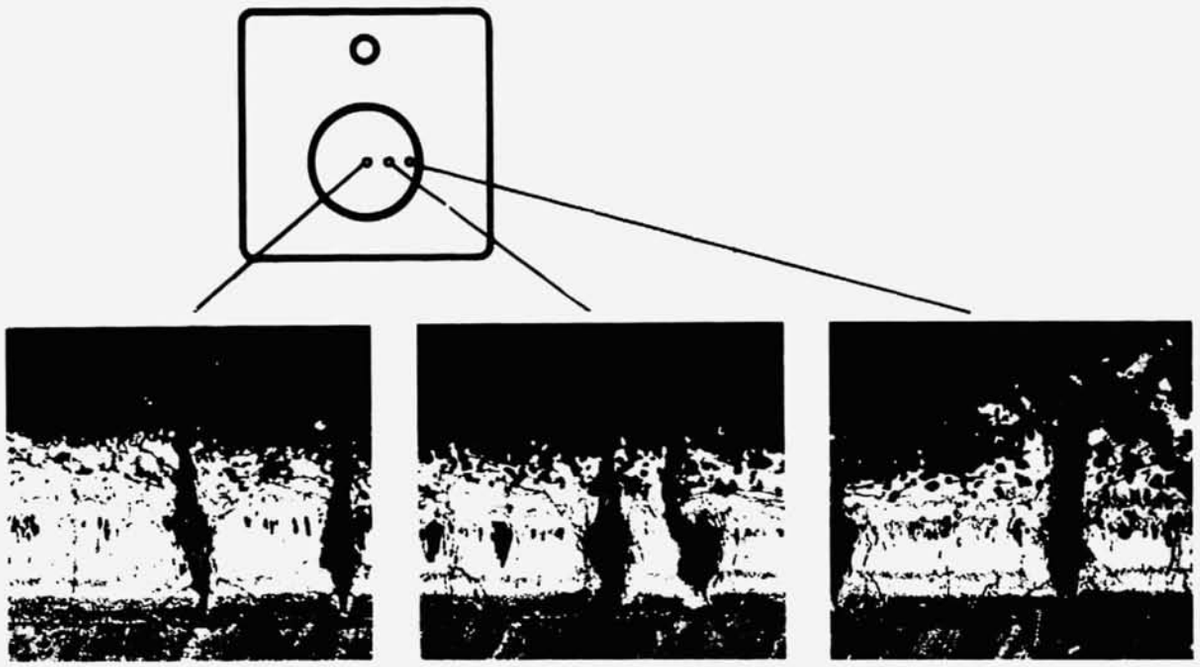

1201437-15

114 REDUCED PRESSURE PROFILE CYCLES

1201437-18

36 AIR SLOW CYCLES

200X

PHOTOMICROGRAPHS OF 3/8 INCH DIAMETER DEFECT SPECIMENS AFTER REPAIR AND TEST

457-2873

Figure 11-11

This specimen was then repaired using an R-512E perform and the C-2 heat cycle. Both specimens were then exposed to 9 atmospheric pressure slow cycles. The repaired specimen evidenced no sign of substrate oxidation as a result of this exposure. The unrepaired control specimen continued to oxidize, resulting in a 1/4-inch diameter hole through the sheet. Metallographic examination of the repaired coupon revealed a normal repair coating thickness and structure.

11.3.4 Repairability Of Hole-Type Defects - An experiment was performed to evaluate the applicability of the developed repair methods to hole-type defects and, if necessary, to modify these techniques so that the lamp method could be

used satisfactorily. The repairs were to be accomplished by recoating hole edges or by some combination of patching and recoating. It was also required that the technique be applicable to the repair of hole defects in the skins of typical panels.

The experimental specimens were 1 by 1 by 0.016-inch Cb-752 coupons coated with R-512E, preoxidized for 1 hour at 2400°F, after a 1/8-inch diameter hole was drilled through the center. The first experiment consisted of grit blasting (steel grit at 20 lb/in^2) a 0.350-inch circular area centered over the drilled hole, placing a 0.350-inch diameter R-512E preform over this cleaned area, and firing the preform through the C-2 heat cycle. The specimen was supported by two 1/8-inch diameter ceramic rails during application of the heat cycle. The coating wet the cleaned area on the face side, but did not wet the opposite side. The specimen was tested in the atmospheric slow cyclic test and showed substrate oxidation at the hole defect after the first cycle. This experiment was repeated with two changes: a washer preform was used in place of a solid disc, and the hot spot placed off center rather than over the hole. Results were identical.

In the next experiment a washer-type R-512E preform was placed over the grit blasted hole area. This assembly was then sandwiched between two pieces of R-512E coated Cb-752 of which the bottom piece had been preoxidized. This whole assembly, sketched in figure 11-12, was then fired through heat cycle C-2. After firing, both the top and bottom coated Cb-752 sheets readily parted. The coating appeared to have completely wet the cleaned area on the front face, the cut hole edge, and some of the backface adjacent to the hole edge. This specimen was slow cycle tested in air for 14 standard test cycles with no evidence of substrate oxidation. Photomicrographs of sections through the repaired hole edge after oxidation testing are included in figure 11-12. Apparently the bottom sheet serves to form a faying surface which helps to draw the fused coating materials around and over the hole edge by capillary action and hold it there long enough for it to react with the base edge and with the oxidized back surface which it normally would not wet. The top sheet acts as a heat transfer agent, capturing the most intensive heat flux over the hole which would otherwise be lost and transferring it to the preform and sample by conduction and reradiation.

Efforts then were directed to adapting this procedure to make it applicable to typical panel configurations. Obviously, in many panel designs, one cannot readily position a backup sheet under a hole defect. The first attempt at repairing a hole in a simulated panel face sheet was performed by placing a defected

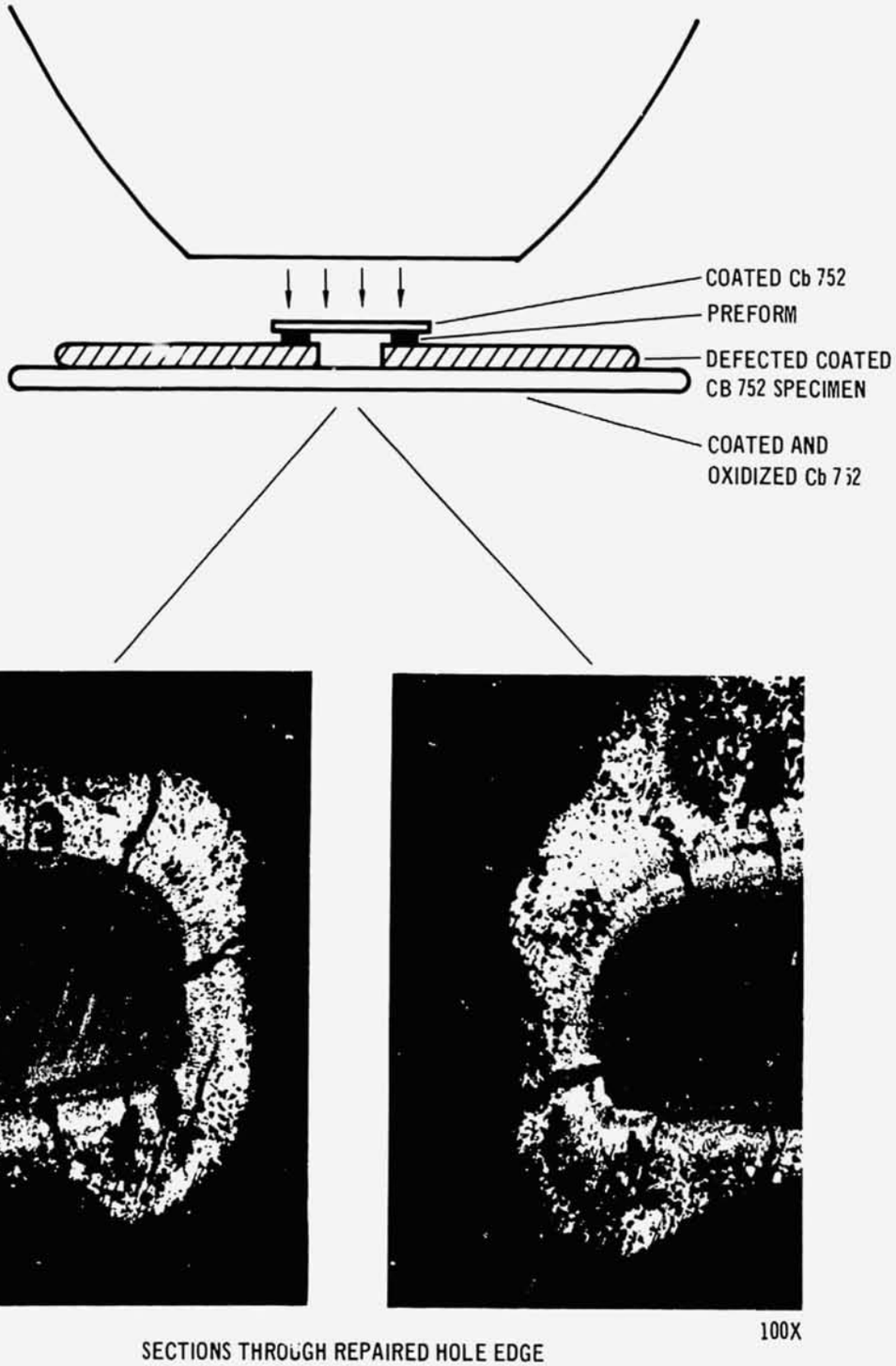

SECTIONS THROUGH REPAIRED HOLE EDGE
AFTER EXPOSURE TO 14 SLOW CYCLES

REPAIR OF DRILLED HOLE EMPLOYING RADIANT LAMP SPOT HEATER

457-2854

Figure 11-12

specimen across the open end of a small folded columbium box, placing a washer-type R-512E preform around the defect, covering the area with a small coated Cb-752 coupon, and firing this assembly through heat cycle C-2. The coating did not wet the hole edge or the back side surfaces adjacent to the defect, and the specimen showed substrate oxidation all around the hole after one slow air cycle. Obviously, the absence of the backing sheet was crucial.

In the next experiment a small, uncoated columbium plug was pressed into the hole, the R-512E preform was put in place and subjected to the C-2 heat cycle with the spot heater. After firing, it appeared that the entire cleaned area of the face side and all the plug surfaces, top and bottom, were wetted and coated, and that the plug had been brazed into the hole. The specimen was exposed to two air slow cycles (with no evidence of substrate oxidation) and subsequently was sectioned for metallographic examination. Figure 11-13 shows the repair apparatus schematically and includes photomicrographs through the patch repaired hole. The hole edges were protected by coating and the plug was well coated. Again, this was a result of capillary action in the crevice between the plug and the hole edge, drawing the coating down over the edge where the normal good wetting properties of the fused silicides on uncoated columbium resulted in complete coating of the plug.

11.3.5 Evaluation Of Panel Distortion - A small 7 by 7-inch R-512E coated single faced, vee-corrugated panel fabricated from 0.012-inch Cb-752 was defected and repaired using the techniques described above. The object was to evaluate the ability of these techniques to accomplish repairs in typical hardware, and to determine the extent of panel distortion caused by this procedure.

The panel was defected by grinding through the coating approximately 3 mils into the substrate. An R-512E preform was placed over the defect and the standard C-2 heat cycle was applied with the spot heater. This procedure is illustrated in figure 11-14. Dial guage readings were taken at numerous points on the panel face before and after the repair procedure, with the panel unrestrained (lightly taped to surface plate). Three separate repair cycles were performed. The first repair caused an average depression between the welds of 5 mils with a maximum displacement of 13 mils. The second repair attempt produced similar, but slightly less, distortion. During the third repair sequence, an average inward displacement of 7 mils occurred with a maximum distortion being 30 mils. In most cases the displacement was below the plane of the skin between the corrugations.

Repairs 1, 2, and 3 to the corrugated panel did not wet as well as previous repairs performed on specimens using the same parameters, probably because of the

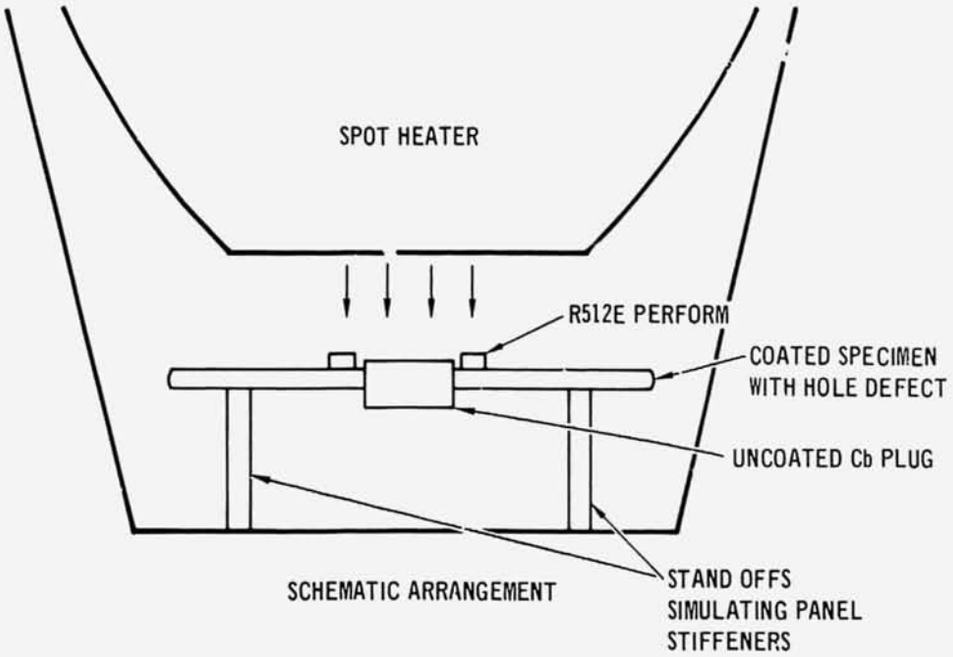

SECTION THROUGH
REPAIRED PLUGGED HOLE

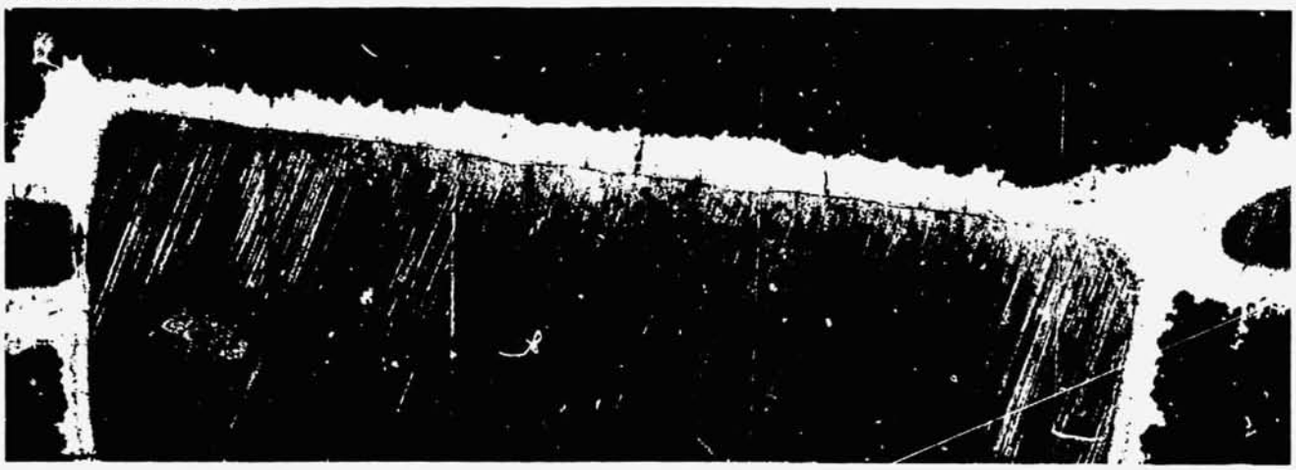

10X

457-2877

REPAIR OF A HOLE IN A SIMULATED PANEL FACE SHEET Figure 11-13

loss of heat from the repair site to the panel and into the metal surface plate. Another repair was made the same way, except that a sheet of Silfrax insulation was placed between the panel and the surface plate and the spot heater was lowered so that its housing contacted the panel. The repair produced by this modified procedure wet an area essentially equivalent to that produced on specimens in the earlier work. Obviously, in practice, some minor variations in procedure and in processing parameters will have to be made to account for variations in panel size

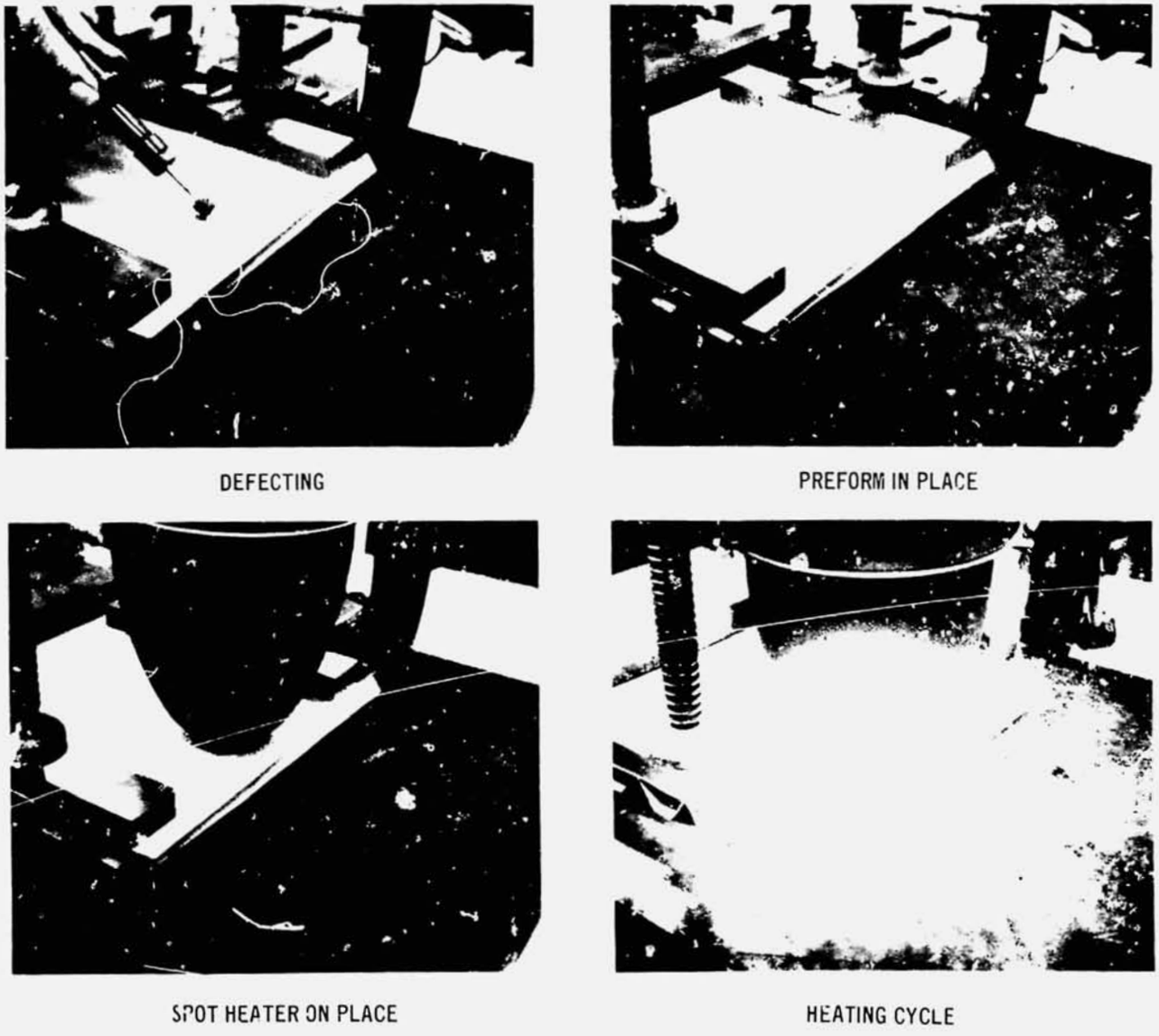

457 2883

PANEL REPAIR SEQUENCE

Figure 11-14

and construction, surface conditions, location of defect and size of defect.

Another 7 by 7-inch single faced, corrugated panel fabricated of C-129Y alloy and coated by VAC-HYD with the VH-109 process was similarly defected, repaired and subsequently evaluated for effectiveness of repair and for the extent of distortion caused by the repair procedure. Two sites were defected by grinding through the coating into the substrate. Surface height measurements were taken along a line parallel to and 1 inch from the repair line with the panel lying unrestrained on a surface plate. The distortion which occurred was similar to that noted for the R-512E coated Cb-752 panel. The distortions were generally down or inward close to the repair sites because the test panel face sheets were generally dimpled down-

ward between the stiffeners. A few isolated sites on each panel were found in which the face sheets were bowed upward and, when simulated repair runs were made at these locations, the distortion in each case was upward. Both repaired 7 by 7-inch panels were given a 1-hour, 2400°F, 1-atmosphere air proof test after repair. The defect sites all appeared to be fully protected by the repair procedures developed in this program.

While the evaluation of potential skin distortion was only qualitative, the results indicate that possible distortion could occur and would have to be considered in actual field repair applications. It is believed that distortion would not be a prohibitive factor in most cases.

11.4 OBSERVATIONS AND CONCLUSIONS - Field repair achieved by replacing the fused slurry silicide in a defect area employing the focused radiant lamp spot heater is considered a successful method ready for structural testing. The repair method meets the original requirements of a simple and reliable field repair procedure. The equipment required is very inexpensive, the repairs are accomplished quickly without special atmosphere or seals, and the repair lives are well in excess of 100 cycles under reentry conditions.

12. FLIGHT SIMULATION TESTING OF FIELD REPAIRS

A major objective of this program was to develop reliable repair methods and procedures which are easy to accomplish in the field. Establishing the performance and reliability of the repairs requires an evaluation procedure which realistically imposes the operational and environmental parameters which the field repairs will experience in service. The test conditions defined in Task I (as reported in section 4) included boost acoustic loading, boost and landing static loads, and simultaneously imposed reentry parameters of temperature, air pressure, and stress as a function of time. Each is an important parameter in evaluating the combined effects of predicted service. The evaluation used a panel of typical hardware design, rib stiffened and of a realistic size, 3 by 12 inches. Since the main function of the field repairs is to protect the columbium panels from oxidation so that the load bearing properties can be maintained, the proper criterion for evaluating repaired panel performance is the ability to carry design loads under simulated flight conditions. The purpose of the evaluation was to demonstrate that the field repairs developed would adequately protect columbium heat shield panels and maintain structural integrity under simulated flight conditions. The repairs which demonstrated this functional protection for more than 100 missions were put on full-size (20 by 20-inch) rib stiffened panels for evaluation by NASA-MSFC.

Two groups of rib stiffened panels with field repairs on the external skin were tested under simulated flight conditions. The first group of panels was used to evaluate ceramic and silicide coating replacement field repair methods at a midpoint in their development. Although the field repairs generally performed well, the panels did not perform to expectations. A second set of rib stiffened panels was fabricated and coated to improve the panel performance and thus make possible better evaluation of the repair coatings. The final repair developments, including ceramic compositions, the lamp repair method and the plasma sprayed repairs, were tested on the second set of panels.

12.1 REENTRY PROFILE TESTING PROCEDURE - The evaluation of the field repair coated panels was accomplished in the apparatus illustrated in figure 12-1. A 7-inch diameter Astro Furnace was modified to provide for a vacuum sealed loading rod to pass through the bottom of the furnace. The four-point loading fixture (described in section 6) was attached to an electric drive motor through a strain

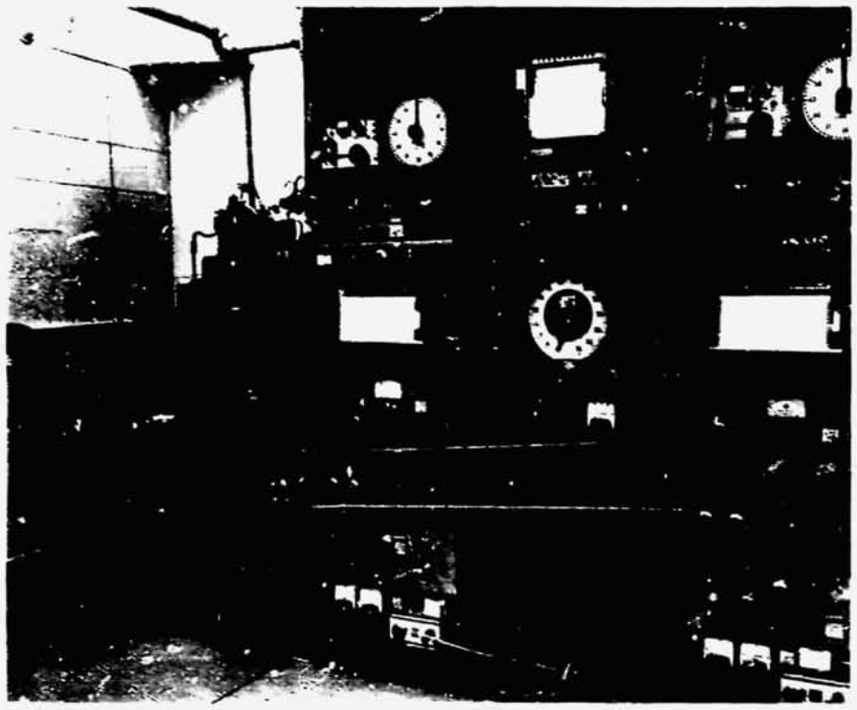

FLIGHT SIMULATION TEST FACILITY USED TO EVALUATE 3 BY 12-INCH RIB STIFFENED PANELS

Figure 12-1

link which was automatically controlled to follow a predetermined bending stress profile. Air pressure and temperature were automatically recorded and controlled to follow their respective profiles.

The test conditions employed were to be the same as those employed with the 1 by 4-inch panels tested in Task I of the program and reported in section 6. Since it was found that the larger Astro Furnace could not be cooled as quickly as the small furnace, a 1-hour cycle was selected to replace the original 45-minute cycle. The same time and temperature relationships were maintained between the two profiles. The total time above 2000°F was 1200 seconds, above 2200°F was 780 seconds, and at 2400°F was 300 seconds. The difference between the profiles occurred in the cooling time below 2000°F. The large furnace cooled to approximately 1100°F at the end of the 1-hour cycle. The ascent load of 77 percent of room temperature rib tensile ultimate yield load was applied before each series of reentry profile cycles. This functioned as a proof load to determine whether the previous cycle had impaired the load bearing capabilities. The stress profile was expanded to a 1-hour cycle by employing the same temperature/stress relationship used in the original test profile. The air pressure profile increased from

10 to 30 torr during the 1-hour cycle. The combined profiles are shown in figure 12-2. After each series of reentry profile cycles, the panel was subjected to an acoustic loading.

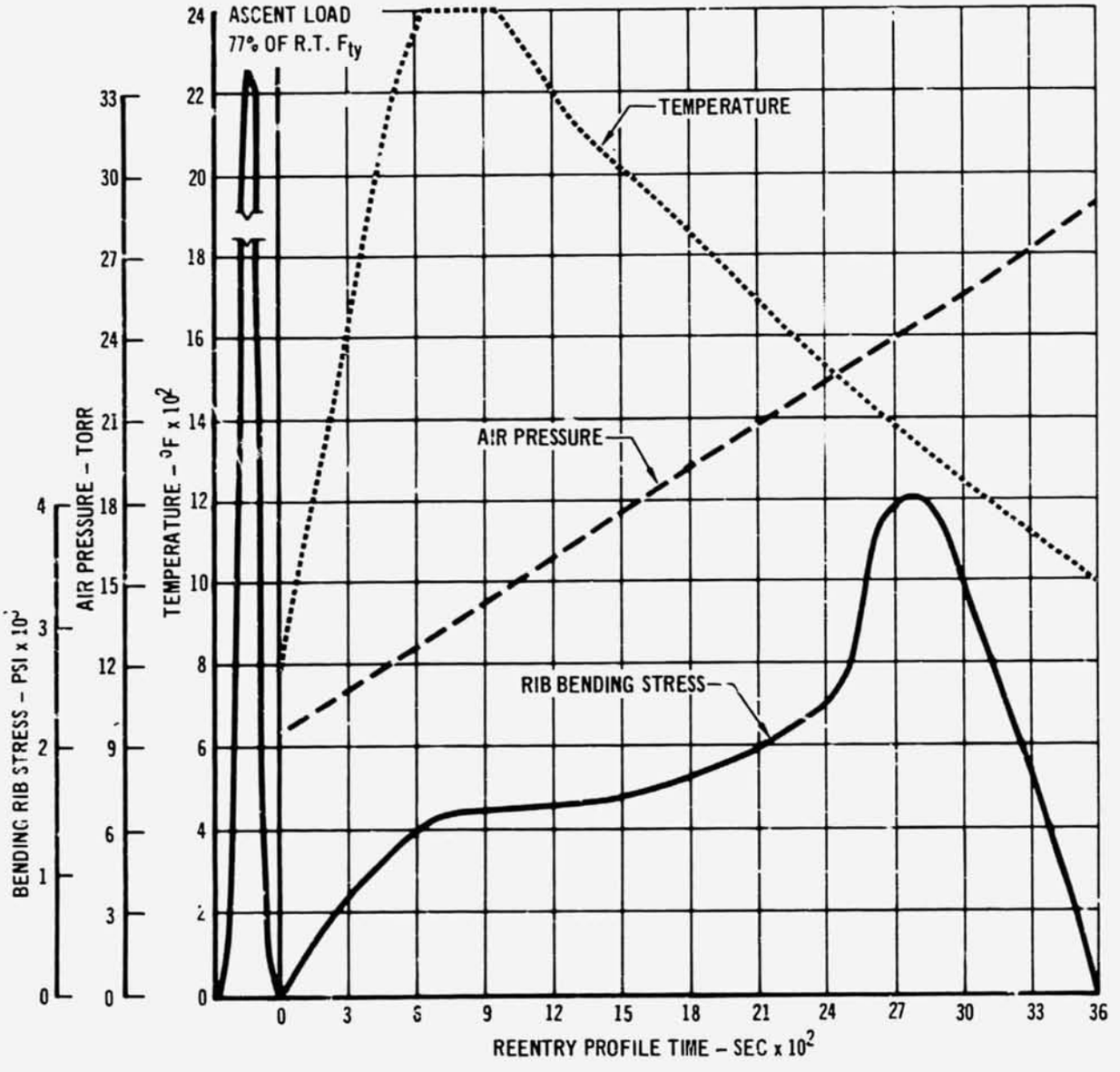

REENTRY PROFILE TEST CONDITIONS

457-2846

Figure 12-2

12.2 BOOST ACOUSTIC TESTING PROCEDURE - The general procedure used for the first group of panel specimens was to determine the frequency and decibel level required to produce 4000 lb/in^2 (rms). Stress level selection was based upon the results obtained in testing the 1 by 4-inch panels described in section 6. The

1 by 4-inch rib stiffened panel specimens which were acoustic fatigue tested indicated that the random loading fatigue limit for the columbium substrate was 10,000 lb/in^2 (rms) for 800,000 cycles. The rib was the critical member in the rib stiffened panel design, with the rib stress being 2.5 times higher than the skin stress. The 4,000 lb/in^2 (rms) skin stress corresponds to the 10,000 lb/in^2 (rms) limit stress of the ribs. After the frequency and decibel level necessary to achieve 4,000 lb/in^2 (rms) skin stress were established, each of the repair coated panels was evaluated at the same conditions for 28.6 seconds for each profile cycle, the time corresponding to 800,000 cycles for 100 panel profile exposures.

The calibration was accomplished using a Cb-752 3 by 12-inch rib stiffened panel identical to the panels which were profile tested, except that the calibration panel did not contain the repair coatings. The panel specimen was instrumented with a strain gage (3-element 45-degree strain rosette) in the center of the load area. A special acoustic fixture was fabricated to support the panels in a simple supported configuration. The fixture consisted of two V-shaped clamps mounted on each end of a steel plate. The panel was installed within the clamps of the fixture to obtain a pin-ended clamp condition on each end of the panel. Machined aluminum blocks were positioned in each end of the panel between the load pads and the skin to prevent the panel webs from buckling when a preload was applied to the panel by the clamp assemblies. A double-walled test chamber of 1 ft^2 cross-sectional area was positioned in front of an acoustic horn. The panel and fixture assembly was then installed in the test chamber. A box constructed of wood and filled with acoustic insulation was attached over the back of the panel to reduce the sound pressure incident upon the backside of the panel. Photographs of the panel and acoustic fixture assembly are presented as figures 12-3 and 12-4.

The calibration panel was initially excited sinusoidally from 50 to 500 Hz at an input acoustic level of 161 db. Sinusoidal excitation was used to identify the panel's predominant bending frequencies. The outputs of the strain rosette and microphone were recorded on FM magnetic tape. The frequency response plots were obtained by using a log ratio computer which plotted the ratio of the recorded response strain amplitude to the recorded input pressure amplitude as a function of frequency. The signals were filtered using a dual-channel tracking filter employing 5 Hz bandwidth filters before obtaining the ratio. The exciter/acoustic system was fully attenuated below 50 Hz and above 500 Hz due to the

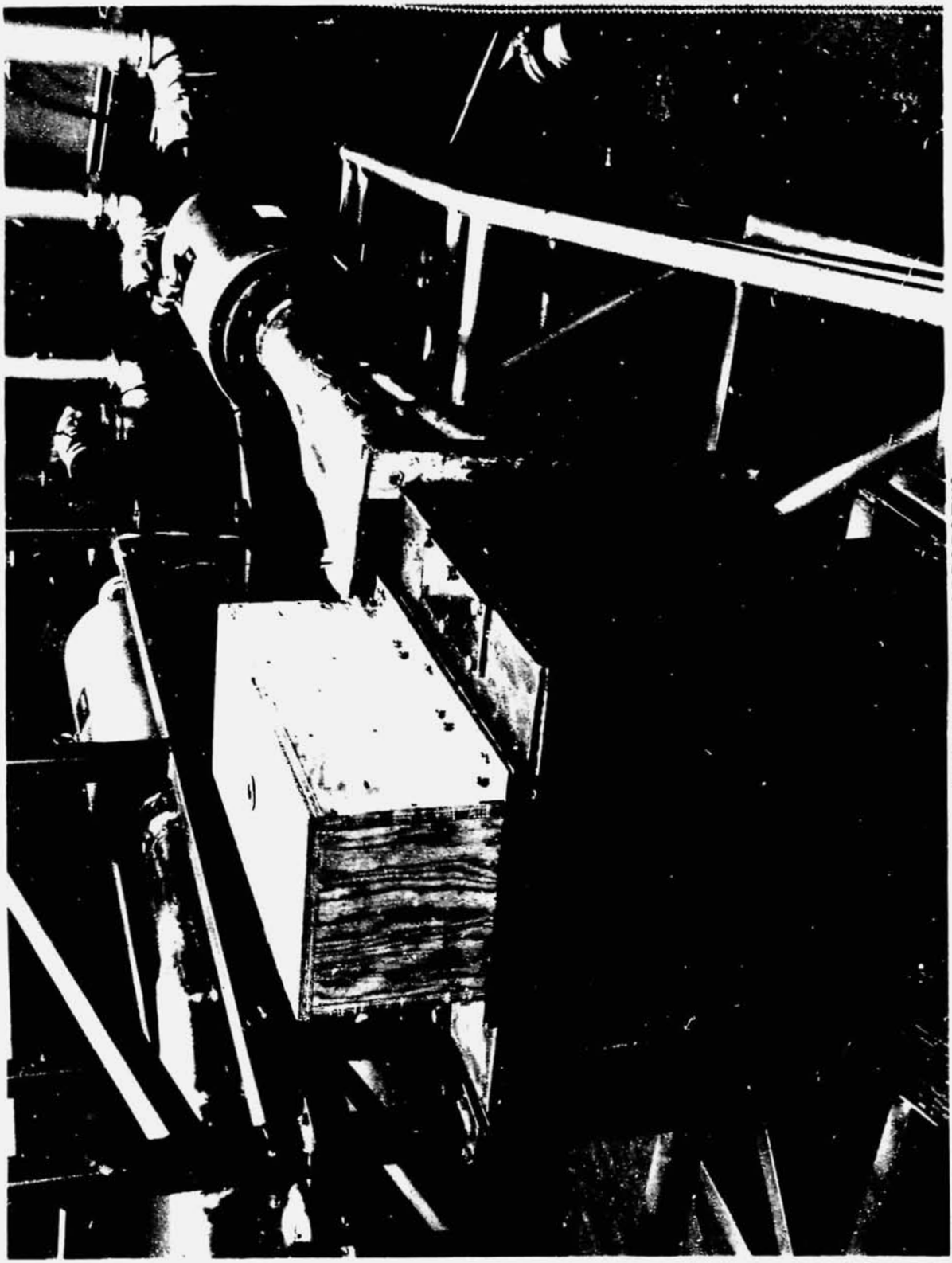

ACOUSTIC TEST APPARATUS

457-2834

Figure 12-3

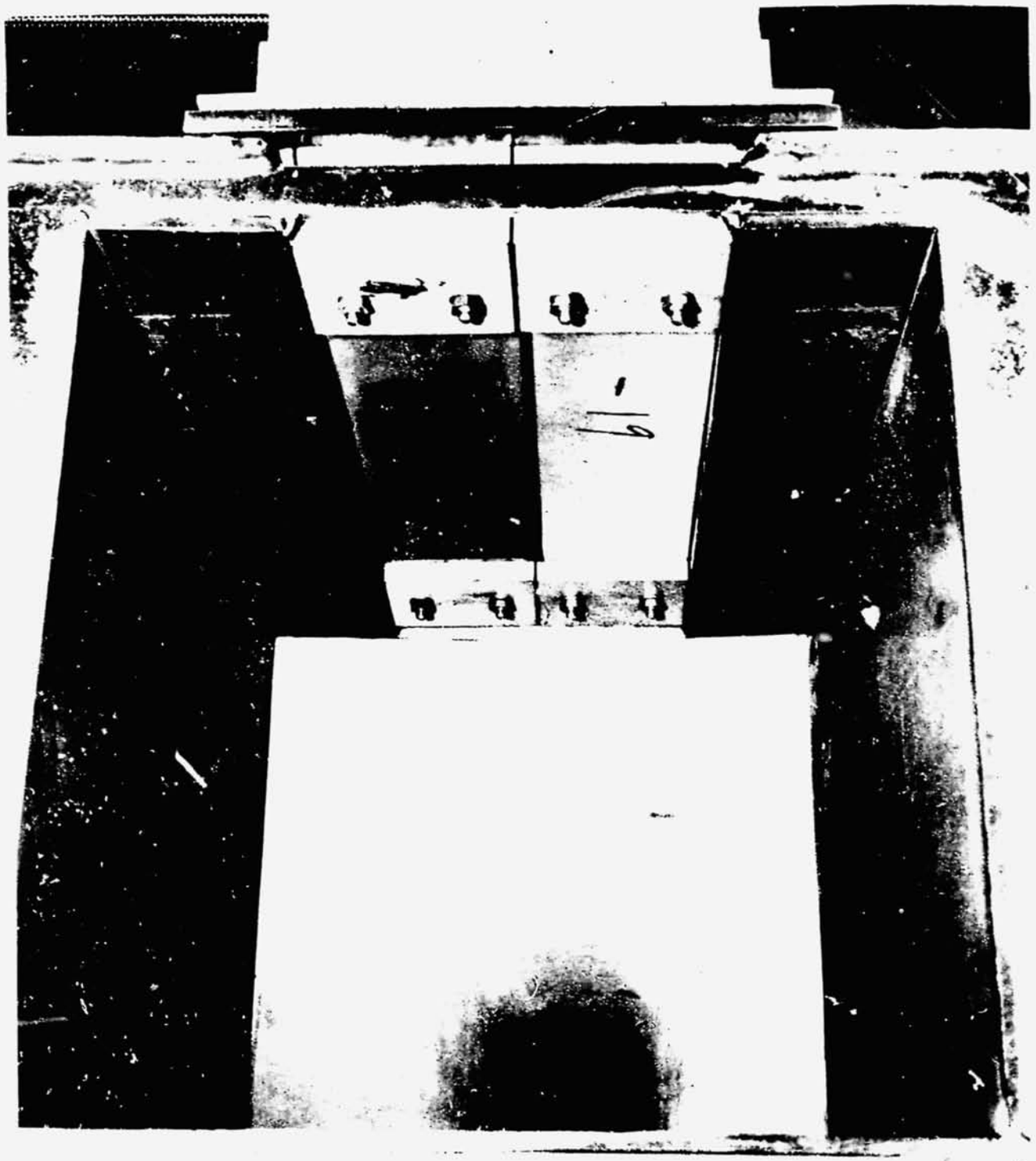

RIB STIFFENED PANEL IN ACOUSTIC FIXTURE

Figure 12-4

characteristics of the system. The acoustic level on the calibration panel was increased until the rms stress level, determined from the output of the strain gage, measured 4000 lb/in^2 (rms). An acoustic level of 167 db was required to obtain 4000 lb/in^2 (rms). All subsequent panels were subjected to the same random acoustic environment as used for the calibration panel. The repair coated rib stiffened panels were alternately tested thermally and acoustically after every 10 cycles until structural failure on the panel occurred.

The testing of the second group of rib stiffened panels was conducted in a similar manner to that of the first group with a few exceptions. The pin-ended support was changed to a floating support to eliminate the possibility of local damage to the coating by repeated preload in the clamp area. This change in support required a recalibration which was conducted as described above. The second change involved the test stress level which established at 3,080-lb/in^2 random mean skin stress. The original 4,000-lb/in^2 rms was selected because it was determined to be the rib failing limit at 800,000 cycles. The evaluation of the first group of panels and other related testing (reference 10) confirmed this (4,000 lb/in^2 rms) as the limit stress. Therefore, a level of 77 percent of the established limit stress was selected as a realistic testing level. The acoustic exposure was conducted after each series of 22 profile cycles for a time of 660 seconds. The number of profile cycles per series was increased from 10 to 22 cycles to accommodate 3-shift testing.

12.3 PANEL EVALUATION - GROUP 1 - The first group of 3 by 12-inch rib stiffened panel specimens was fabricated and coated per section 3.3. The testing was conducted midway in the development of the field repairs and represents preliminary results. The structural performance of the panels prohibited a full evaluation of the repairs which necessitated making the second group of rib stiffened panel specimens.

12.3.1 Panel Specimen Preparation - Prior to applying the field repair coatings to be evaluated, standard defects were gritblasted through the fused slurry silicide coating on the panel skins. Gritblasting was selected as the method of defecting because the size, shape, and depth of the defects could be accurately reproduced. A suction-type gritblaster was used at 40 lb/in^2 air pressure with 220 mesh fused aluminum oxide. A template with a 1/8 or 1/4-inch diameter hole was employed. The change of color between the coating and substrate was used to determine when all of the coating had been removed. Figure 12-5 shows the defect pattern selected. Two defect locations were used for each repair, one

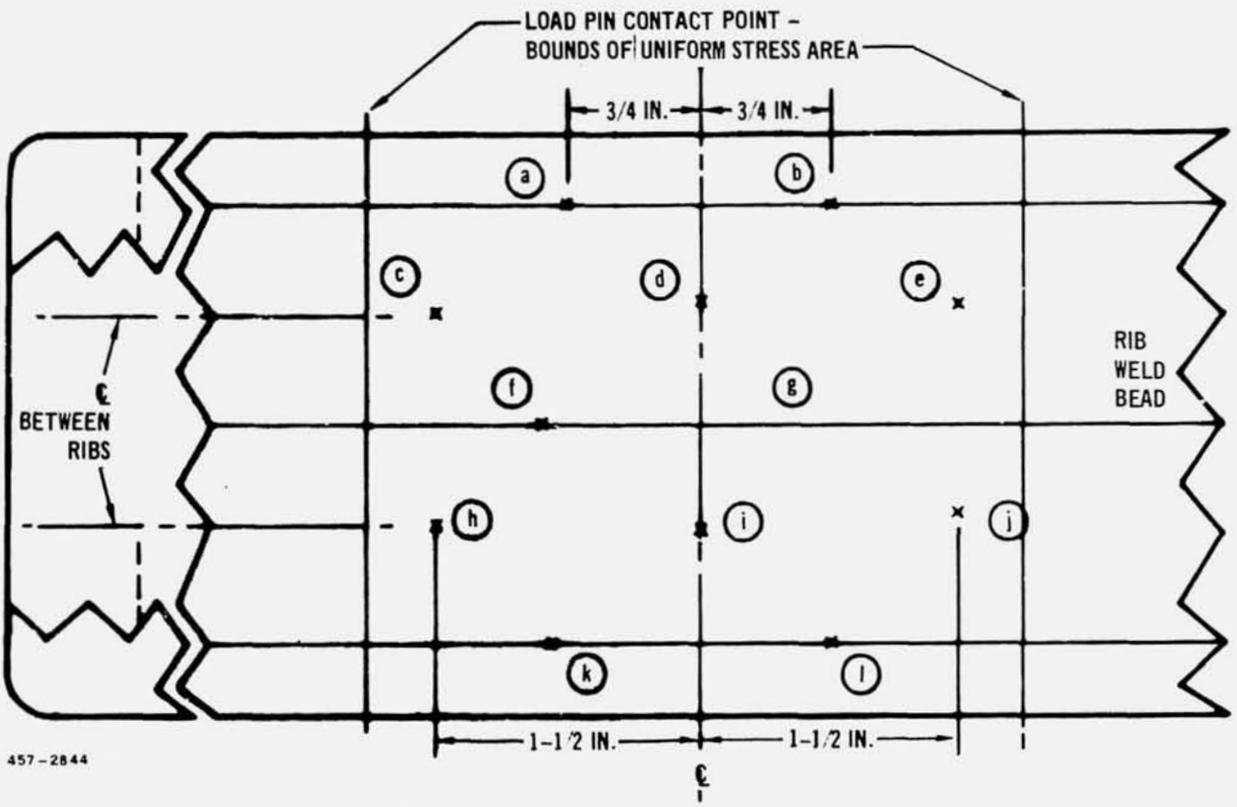

REPAIR SITE LOCATIONS FOR 3 by 12 INCH PANELS

Figure 12-5

directly over a rib and a second halfway between two ribs. Table 12-1 presents the type, size, and location of the repair coatings evaluated.

Each of the four panels had two 1/8-inch diameter defects gritblasted at locations d and e. The panels were then sent to Sylvania for repair coating, employing the method of replacing the fused slurry silicide coating with the focused radiant lamp. At this point, Sylvania was only halfway through the development effort for this method. However, the method had proved satisfactory on coupon specimens, and typical hardware experience and test data would be valuable in guiding further development. Also, a second set of 3 by 12-inch rib stiffened panels would be tested at a later date. Sylvania employed the general procedure described in section 11.2. One drop of R-512E slurry was placed on the defect area, which was then heated to 2700°F and held for 2 minutes. The thickness of the repair areas was believed to be marginal, based upon nondestructive coating thickness evaluations. It was decided to repeat the repair procedure on two of the four panels. Panels SYL 6 and VAC 11 were double repaired and panels SYL 4

Table 12 -1

FIELD REPAIR COATINGS EVALUATED

REPAIR SITE DESIGNATION	DEFECT SIZE (DIAMETER-IN.)	DEFECT LOCATION	REPAIR TYPE	
			Cb-752/R-512E PANELS	C-129Y/VH-109 PANELS
a	1/4	OVER RIB	CERAMIC A-1	CERAMIC H-1
b	NONE	-	-	-
c	1/4	BETWEEN RIBS	CERAMIC A-1	CERAMIC H-1
d	1/8	BETWEEN RIBS	SYL R-512E/LAMP	SYL R-512E/LAMP
e	1/4	BETWEEN RIBS	CERAMIC P-1	OPEN SITE
f	1/8	OVER RIB	SYL R-512E/LAMP	SYL R-512E/LAMP
g	1/4	OVER RIB	CERAMIC U-1	CERAMIC U-1
h	NONE	-	-	-
i	1/4	BETWEEN RIBS	CERAMIC U-1	CERAMIC U-1
j	1/4	BETWEEN RIBS	CERAMIC H-1	CERAMIC P-1
k	1/4	OVER RIB	CERAMIC P-1	OPEN SITE
l	1/4	OVER RIB	CERAMIC H-1	CERAMIC P-1

457-2845

and VAC 10 were left with the single repair cycle. The appearance of the Sylvania lamp repairs before testing is shown in figure 12-6. The physical appearance was considered good. One panel, SYL 6, had a small depression in the coating located 0.2 inch from the defect area and on the outer periphery of the overlap area, as noted in figure 12-6.

After the lamp repairs were completed, the remaining 1/4-inch defects were gritblasted on the panel skins and ceramic repaired. The repairs were applied according to the procedure described in appendix C. The repairs were furnace fused simultaneously at 2050°F for 5 minutes. Table 12-1 gives the designations of the four ceramic compositions applied to the Cb-752/R-512E panels and the three compositions applied to the C-129Y/VH-109. Figure 12-6 shows the ceramic repairs prior to testing.

12.3.2 Results of Profile Test Evaluation - Results of the profile evaluation of the 3 by 12-inch rib stiffened panels are summarized in table 12-2. Most of the field repairs performed well in preventing oxidation of the columbium substrate. The panels did not structurally perform up to expectations because of early acoustic failures or poor coating performance, independent of the repair sites on the panel skins. Results of each of the four panels will be discussed separately.

12.3.2.1 Profile Evaluation Results of Cb-752 Panel SYL-4 - The R-512E coating and repairs previously described were applied to panel SYL-4. It then

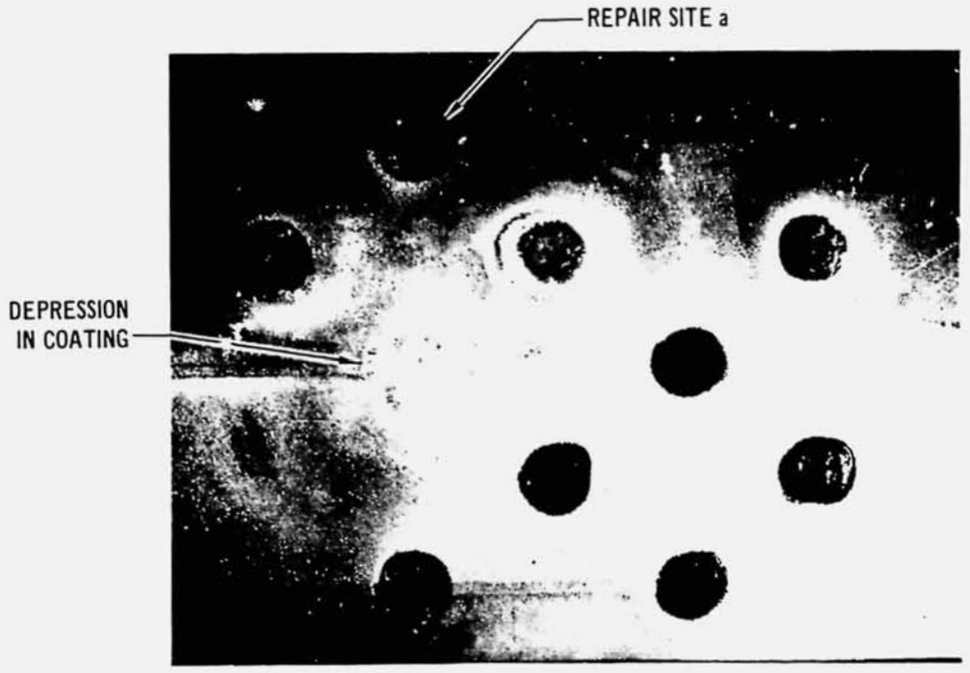

Cb–752 Panel SYL–6 1X

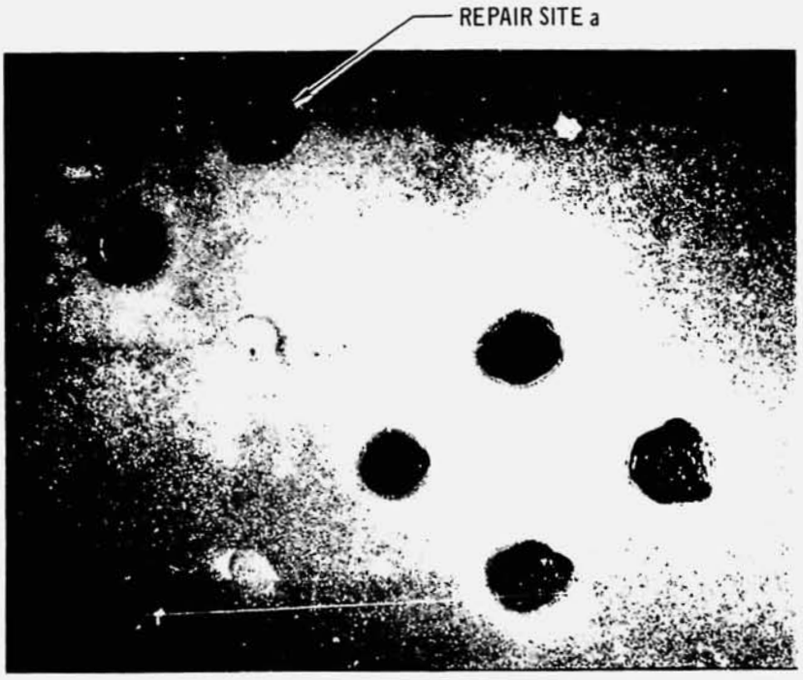

C–129Y Panel VAC–11 1X

TYPICAL APPEARANCE OF FIELD REPAIR COATED PANELS PRIOR TO TESTING

(See Table 12–1 for Repair Designations)

457-2837

Figure 12–6

Table 12-2

OXIDATION TEST RESULTS OF FIELD REPAIR COATING SITES

PANEL SPEC NO.	TYPE AND LOCATION OF REPAIR SITES: CERAMIC FIELD REPAIRS								SYLVANIA R-512E REPLACEMENT REPAIRS		TOTAL OXIDATION CYCLES - REASON FOR TERMINATING TEST
	A-1 R	A-1 BR	P-1 R	P-1 BR	U-1 R	U-1 BR	H-1 R	H-1 BR	LAMP REPAIR R	LAMP REPAIR BR	
SYL-4	20 NF	20 F[2]	20 NF	20 NF	20 NF	20 NF	20 NF	20 NF	20 NF	20 NF	20 - ACOUSTIC PANEL FAILURE
SYL-6	80 NF	80 NF	80 NF	80 NF	40 F[1]	80 NF	70 F	20 F	10 F	20 F	80 - ACOUSTIC PANEL FAILURE
VAC-10	NOT TESTED	NOT TESTED	50 NF	50 NF	50 NF	50 NF	50 NF	50 NF	50 NF	10 F	50 - EXCESSIVE PANEL DEFLECTION
VAC-11	NOT TESTED	NOT TESTED	100 NF	100 NF	100 NF	100 NF	100 NF	30 F	100 NF	100 NF	100 -

[1] REPAIR CHIPPED DURING THIRD ACOUSTIC EXPOSURE

[2] FAILURE CAUSED BY INTERFERENCE WITH LOADIN .XTURE

SYMBOLS:
F - FAILURE
NF - NO FAILURE
R - REPAIR OVER RIB
BR - REPAIR BETWEEN RIBS

457-2847

experienced a total of 20 profile simulations and two 286-second acoustic exposures. The panel failed in acoustic fatigue during the second acoustic exposure, and is shown in figure 12-7. The acoustic failure was judged to be unrelated to the repairs on the skin. One A-1 ceramic repair located at repair site c failed after 20 profile cycles, but it should be noted that this repair was damaged by the fixture load rod during the initial 10 exposure cycles.

After the initial set of 10 profile exposure cycles, numerous incipient coating failures were noted on the reverse side of the panel on the edges of the ribs. This condition had been noted on the ribs of other R-512E coated panels (reference 6) and was assumed to be caused by a thin coating on the rib edges. Therefore, the rib edges were repair coated with the U-1 composition after the initial set of 10 exposure cycles, and further oxidation of the rib edges was eliminated. Metallographic examination of a rib edge confirmed that the R-512E coating was thin. Minimum thickness noted in four different areas sectioned was 0.3 mil.

Panel SYL-4 was metallographically examined to determine the status of the

457-2825

PANEL SYL-4 AFTER ACOUSTIC FATIGUE FAILURE

Figure 12-7

repairs. The ceramic repairs appeared basically as expected. The depth of contamination because of oxygen solution below the repairs was slightly more extensive than that noted in profile exposures of repair coupons where the bending stress was absent. Sylvania's nondestructive inspection results of thin coating were confirmed. Although an oxidation failure was not initiated, the substrate shows oxygen contamination and failure would be expected to occur in less than 100 profile cycles.

12.3.2.2 Profile Evaluation Results of Cb-752 Panel SYL-6 - The second R-512E coated Cb-752 alloy panel was repair coated as previously described and was identical to panel SYL-4. Panel SYL-6 failed in the boost acoustic simulation cycle after 80 reentry profile exposure cycles and 7 intermediate acoustic exposures of 286 cycles each. The failure was similar to the acoustic fatigue failure experienced with panel SYL-4 shown in figure 12-7. The panel and coating performed well through the 80 reentry profile exposure cycles. The edges were assumed to be thin (as previously described) for panel SYL-4, and the U-1 ceramic repair composition was applied to the edges of the ribs prior to testing.

The repair area prior to testing is shown in figure 12-6, while the repair area after 80 flight simulation cycles is shown in figure 12-8. Ceramic repair compositions A-1 and P-1, applied over and between the ribs, did not experience any oxidation failures through the 80 reentry profile cycles. The U-1 ceramic repairs located between the ribs did not fail in oxidation through the 80 profile cycles. The second U-1 site (located over a rib) failed after 40 profile cycles. The failure initiated in a chipped area of the repair, which occurred during the acoustic exposure after 30 profile cycles, and is the only case noted in which a ceramic repair was damaged during acoustic exposure. Each of the oxidation

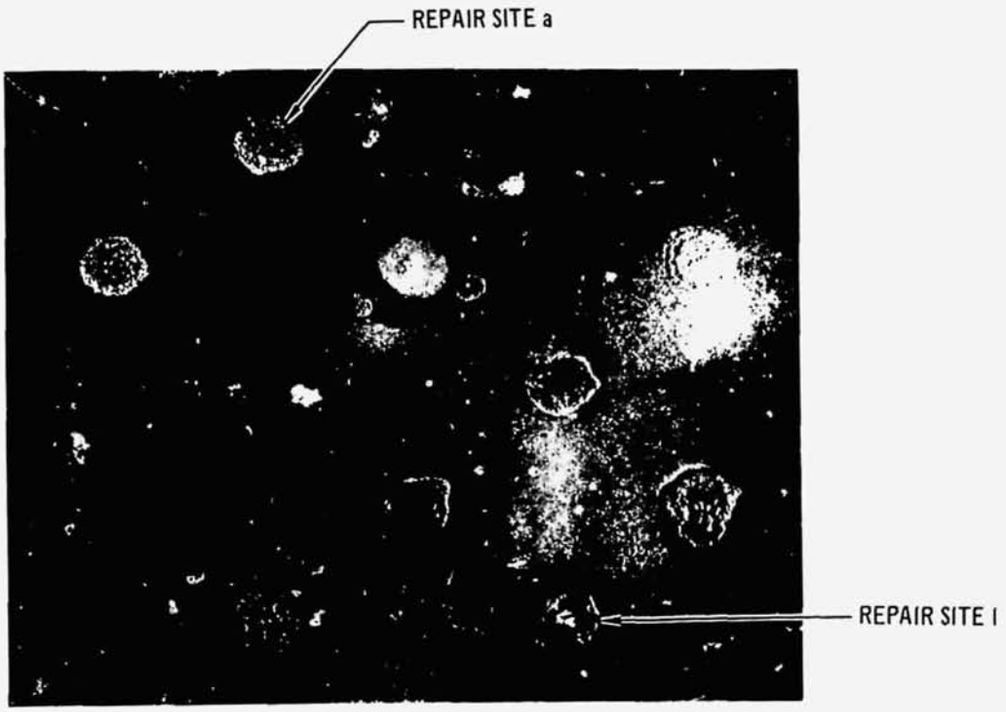

1X

REPAIR AREA OF PANEL SYL-6 AFTER 80 PROFILE REENTRY CYCLES

457-2838

Figure 12-8

failures was repaired with the U-1 ceramic composition to provide oxidation protection during subsequent testing of unfailed repairs. The H-1 ceramic composition proved to be the poorest, with 1 repair site failing after 20 profile reentry cycles, and the second site failing after 70 profile cycles.

The repairs effected by replacing the R-512E coating employing the focused radiant lamp failed after 10 profile cycles in 1 case, and after 20 profile cycles in the second case. Figure 12-9 shows the failure of the lamp repair over the rib at repair site f after 10 reentry profile cycles. The oxidation failure occurred at the periphery of the heat affected zone of the repair area approximately 0.2 inch from the 1/8-inch defect gritblasted in the coating. It can be noted from figure 12-8 that the actual defect areas in which the coating had been removed had not failed after 80 reentry profile cycles, but there was a total of 5 oxidation failure spots on the periphery of the 2 lamp repair sites.

12.3.2.3 Profile Evaluation Results of C-129Y Panel VAC-11 - The initial C-129Y alloy panel was coated with the VH-109 fused slurry silicide coating and was repair coated at eight sites as described above. The panel was exposed to

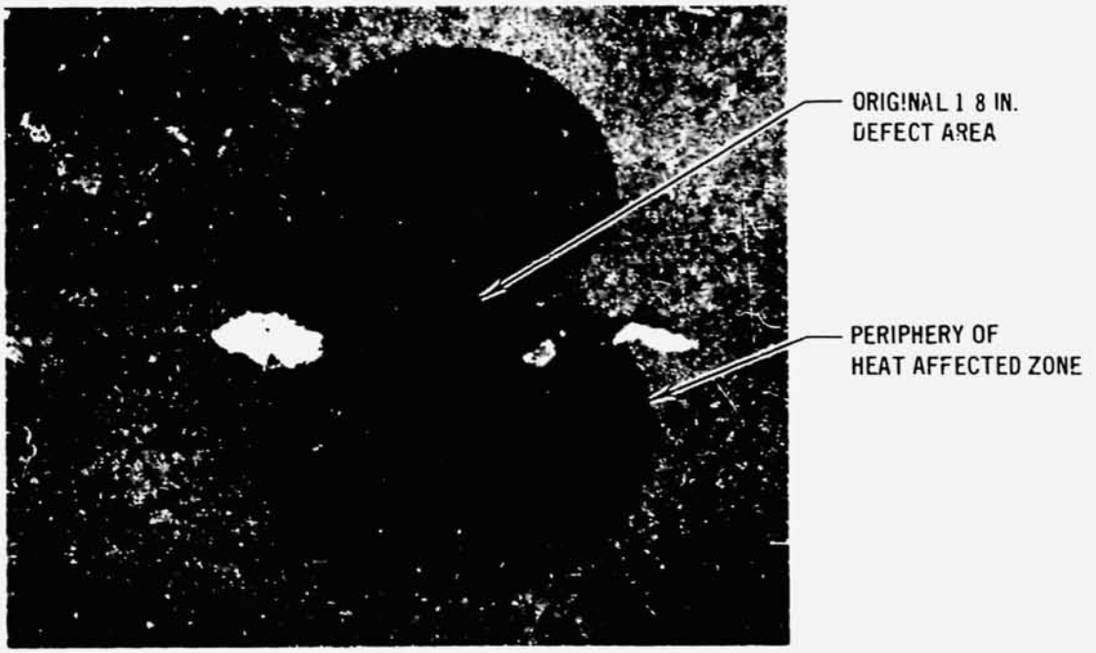

4.8X

Enlarged View of Lamp Repair Site f
Showing Oxidation Failure

463-2797

PANEL SYL-6 AFTER 10 REENTRY PROFILE CYCLES

Figure 12-9

100 reentry pressure oxidation cycles with only 1 repair failing in oxidation. The panel structural performance was severely limited by poor coating performance, and the loading had to be terminated after 20 reentry profile exposure cycles.

The performance of the repair sites was considered very good. Figure 12-10 shows the repair area of panel VAC-11 after 100 cycles. The only repair oxidation failure was a ceramic H-1 composition at repair site i, which failed between exposure cycles 20 and 30. A small hole was oxidized through the skin, following the assumption that the oxidation failure occurred during or shortly after the twentieth cycle. The second H-1 repair site, as well as the U-1 and P-1 ceramic repairs and the two lamp repairs, performed satisfactorily through 100 cycles.

The structural performance of the VAC-11 panel was poor. An excessive amount of deflection and general coating oxidation failure of the ribs were noted after 20 reentry profile exposure cycles. The panel deflection, 0.22 inch in the center of the load span, was considered to constitute a structural failure, and all subsequent dynamic acoustic and static loading was terminated. All profile exposure cycles greater than 30 were conducted using the time, temperature, and air pres-

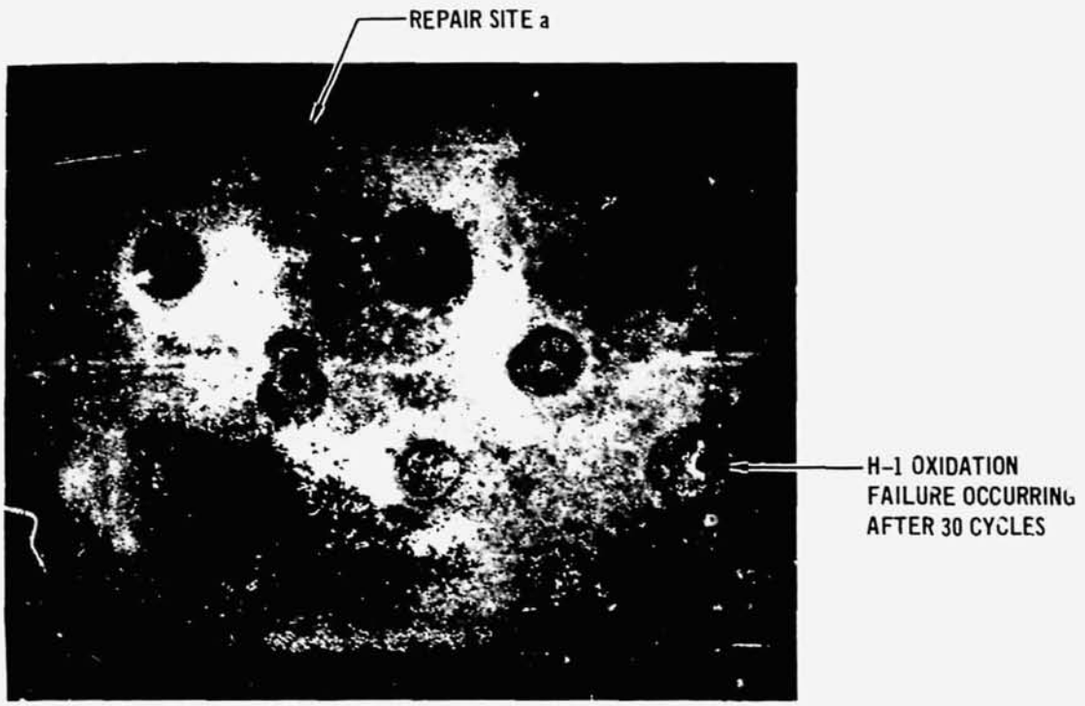

1X

457-2840

PANEL VAC-11 AFTER 100 PROFILE CYCLES SHOWING GOOD REPAIR PERFORMANCE

Figure 12-10

sure of figure 12-2, without employing the stress profile.

The coating was found to be failing in several locations after 20 reentry profile cycles. Extensive and generalized coating failure occurred on the ribs. The extensive area affected and the severity of the oxidation permitted a considerable volume of oxygen to dissolve and react with the rib. This generalized condition is believed to be responsible for the excessive amount of panel deflection. The mechanism of high elongation during profile cycling is believed to be caused by the internal oxidation of the hafnium with concurrent loss of its solid solution strengthening benefits. In addition to the oxidation failures on the ribs, extensive oxidation failures occurred on both ends of the panel in the load pad area. One panel, without repair coating, was sectioned for metallographic examination of the coating structure and of the thickness in the areas found to be failing prematurely. It was discovered that the coating thickness was uneven and thin on one surface of the ribs and in the load pad area. Rib coating thickness was found to be uneven, reaching a minimum of 0.7 mil per surface. The coating thickness in the load pad area was a minimum of 0.4 mil. The coating was 3.5 to

4.5 mils per surface on the exterior of the skin and the coating performed well.

12.3.2.4 Profile Evaluation Results of C-129Y Panel VAC-10 - The second C-129Y panel was coated and repaired in the same manner as that used for the previously described panel VAC-11. Panel VAC-10 experienced the same type of poor structural performance as panel VAC-11. Excessive panel deflection caused termination of the loading after 20 reentry profile cycles. The temperature and air pressure profiles were terminated after 50 cycles, at which time oxidation failures occurred at only 1 of the 8 repair sites.

The three ceramic repair compositions being tested, H-1, U-1 and P-1, each appeared in excellent condition. One of the Sylvania lamp repair areas, site d, had a small coating failure after 10 reentry cycles. This was a repair site which was single-cycle repaired and was suspected to be thin (see paragraph 12.3.1).

Panel VAC-10 experienced a general coating failure in the middle of the center rib. The coating failure on one rib surface caused a bow in the rib due to the unbalanced compressive stresses on the two opposite surfaces of the rib. (Cooling from the coating process causes a compressive stress in metal due to thermal expansion differences.) The coating failure and bow in the rib are shown in figure 12-19. The bow in the center rib caused the tensile stress of the reentry load profile to be carried by the two outside ribs and an excessive deflection (0.16 inch) occurred. On the second series of profile load cycles, the stress was reduced by 33 percent to account for the 1 rib which was not carrying its share of the load. By the end of 20 profile cycles, the remaining 2 ribs were experiencing generalized coating failures, the panel deflection had increased to 0.18 inch, and the application of loads during profile cycling was terminated.

12.3.3 Results of Boost Acoustic Load Exposures - The results of the acoustic exposures for group 1 panels were generally poor. The Cb-752 panels tested, a total of three, showed considerable variation in the number of cycles, or total exposure time, to failure. The C-129Y alloy panels being profile tested received very few acoustic exposure cycles, since excessive panel deflections occurred early in testing and structural loading was terminated. One C-129Y panel without repairs or thermal cycles was exposed to a full 800,000 cycles without failure. The analysis of the acoustic fatigue results was vigorously pursued to insure that the problems experienced in these panels could be rectified prior to testing the second group of rib stiffened panel specimens.

The results of the acoustic testing are summarized in table 12-3. The first panel to fail in acoustic exposure testing was Cb-752 alloy specimen SYL-4. The

Table 12-3

TEST CONDITIONS USED FOR EVALUATING FIELD REPAIR COATED RIB STIFFENED PANELS

PANEL NUMBER	ALLOY AND COATING	CONDITION	ACOUSTIC EXPOSURE TIME (SECONDS)	NUMBER OF CYCLES	RESULTS
SYL-4	Cb-752 AND R-512E	FIELD REPAIRED AND ALTERNATE PROFILE EXPOSURES	570	150,000	SKIN AND RIB FAILURE
SYL-6			2290	605,000	SKIN FAILURE PARALLEL TO RIB
SYL-3		NOT REPAIRED NO THERMAL CYCLES	1140	300,000	SKIN FAILURE PARALLEL TO RIB
VAC-10	C-129Y AND VH-109	FIELD REPAIRED AND ALTERNATE PROFILE EXPOSURES	0	0	RIB BOWING PER PARAGRAPH 7.3.4 PRECLUDED ACOUSTIC TESTING
VAC-11			570	150,000	PANEL DEFLECTION PER PARAGRAPH 7.3.3 TERMINATED ACOUSTIC TESTING WITHOUT FAILURE.
VAC-7		NOT REPAIRED NO THERMAL CYCLES	2850	800,000	NO FAILURE OR DAMAGE.

457-2849

failure occurred after 20 reentry profile cycles and during the second acoustic exposure cycle (570 seconds or 150,000 cycles). The failure was extensive, as shown in figure 12-7, and included fracture of the skin parallel and adjacent to the rib welds and fracture of two ribs in the center of the panel. The original analysis of the panel indicated that the ribs were the most highly stressed and should fail prior to the skins. However, the failure occurred at less than 20 percent of the predicted number of cycles. Because of the extensive damage, it should be noted that after the initial failure, independent of where it occurred, the dynamic response of the panel was significantly changed and was no longer represented by the conditions established by the calibration panel. The following questions were posed by the failure:

a) Was the failure initiated in the rib, leading to excessive amplitude and skin failure?

b) Was the failure initiated in the skin, leading to rib instability and failure?

c) Were the field repairs the cause of, or a contributor to, the failure?

d) Were the skin buckles related to the failure?

e) Were the welds of inferior quality, causing early failure?

f) Was the failure caused by some unique abnormality of the panel or test procedure not considered in the original analysis?

Answers to these questions were sought by examining the failed panel by metallographic and fracture analyses. The fracture surfaces were smeared by the surfaces rubbing together after failure and no conclusions could be made about the failure initiation site or sequence of failures. Metallographic analysis revealed a few other cracks adjacent to the failure sites, but specific conclusions were impossible. Unfortunately, the analyses of the SYL-4 panel were not able to answer any of the above questions or indicate a probable cause of the poor performance.

Two panels which did not have repairs on the skin and had not been thermal cycled were acoustic tested to failure or to 800,000 cycles. The C-129Y panel, VAC-7, survived the test without failure or damage. The Cb-752 panel (SYL-3) failed after 300,000 cycles. The failure occurred in the skin parallel to the ribs in the same manner as that observed with the previous panel, except that the ribs remained intact. Metallographic sections were prepared which showed a significant number of fatigue cracks in the Cb-752 substrate adjacent to the fracture plate. These fatigue cracks were present in both the weldments and in the unwelded sheet. The following conclusions were indicated from the results of this test:

a) the skin failures were not initiated from the ribs failing

b) the field repairs were not a major factor in failure initiation of the skin

c) the failures were a normal acoustic fatigue failure and not an anomaly of the panel or test procedure.

While several questions were resolved, the cause of the skin failures was not yet established.

The final Cb-752 panel, shown in figure 12-11, to fail in acoustic exposure was panel SYL-6 which failed after 605,000 cycles. The panel had experienced 80 reentry profile cycles. This length of time at elevated temperature was sufficient to allow a thin layer of coating oxide to be formed on the panel skin. This oxide layer showed compression spalling in several areas which were 0.4 to 1.0 inch in length and parallel to the rib welds. The spalled areas were coincident with the skin buckles, which were concave below the nominal plane of the skin and were located only on the side of the rib which was a concave buckled surface. Figure 12-12 indicates the location of these spalled areas. It was established that such

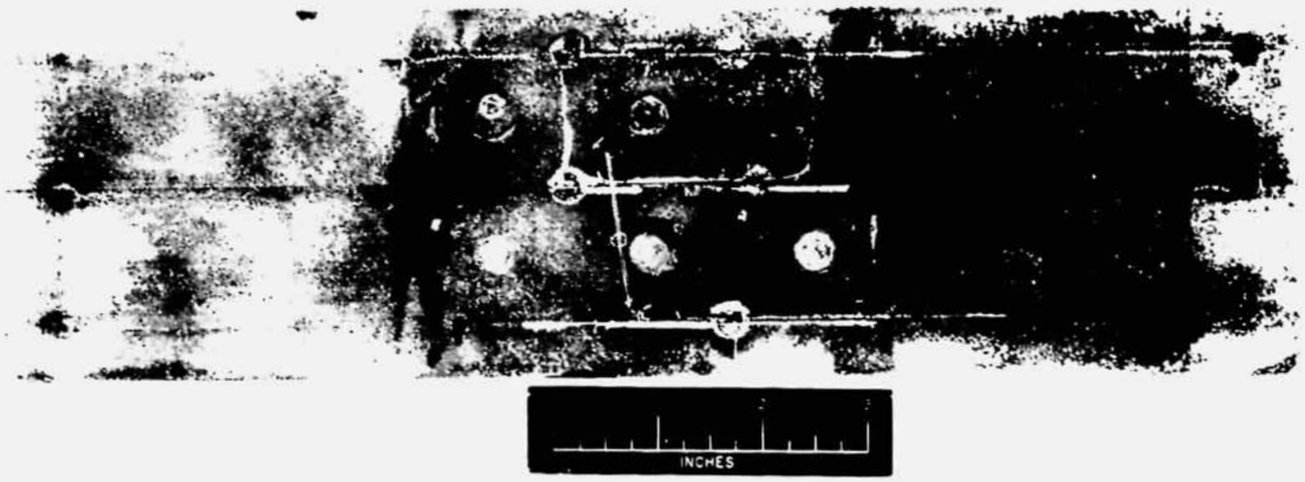

PANEL SYL-6 AFTER 80 REENTRY PROFILE CYCLE SHOWING
AREAS OF ACOUSTIC FATIGUE FAILURES

457-2830

Figure 12-11

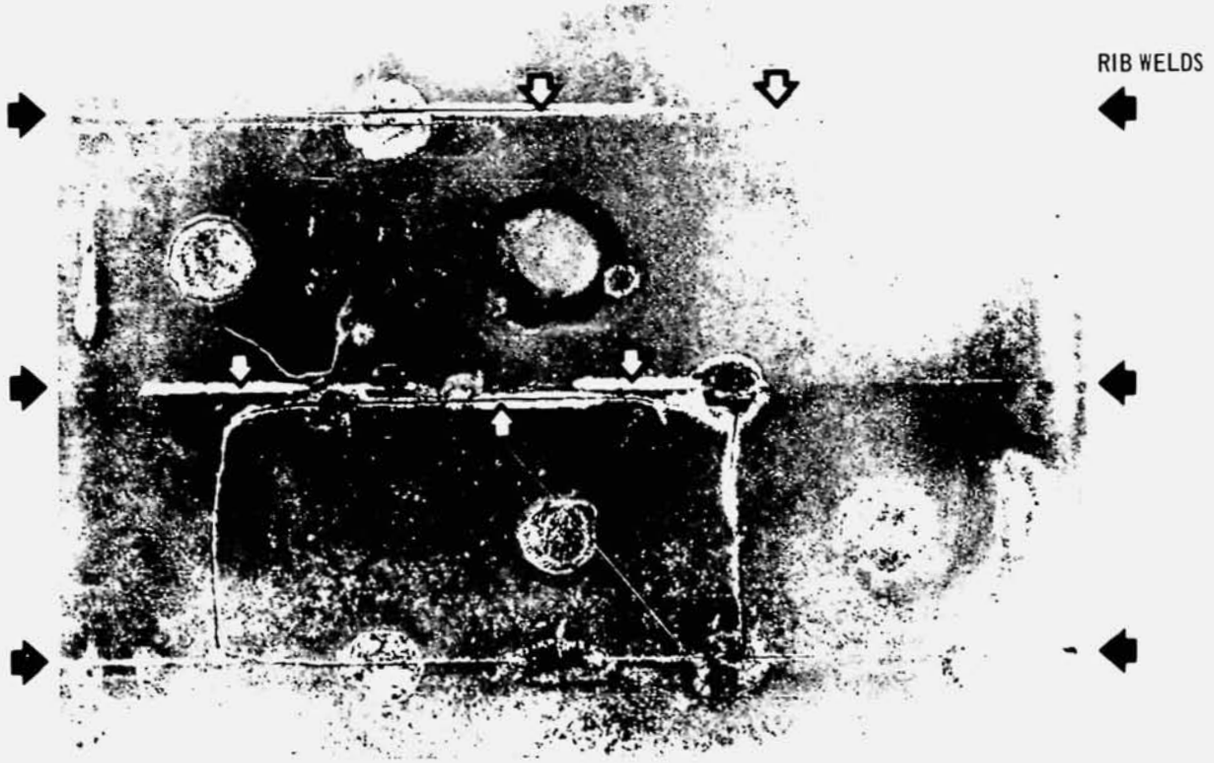

(White Arrows Show Spalled Areas)

FAILED AREA OF PANEL SYL-6 SHOWING COMPRESSION SPALLING OF
COATING OXIDE SURFACE COINCIDENT WITH CONCAVE SKIN BUCKLES

457-2829

Figure 12-12

spalled areas are caused by deflecting the columbium to produce compressive loading. Tension loading produces hairline cracks, as opposed to spalling of the surface of the coating. Thus, it was confirmed that the buckles which were concave below the plane of the skin had dynamically popped to a convex position above the plane of the skin. It is not known that the buckles popped through on every cycle. However, when pop-through did occur, the local stresses in the skin adjacent to the weld would be at, or above, the material yield strength, and would be expected to fail rapidly in a fatigue-type loading.

It was concluded that the skin buckles had to be eliminated, and steps were taken to replace the 3 by 12-inch rib stiffened panels for the second group of reentry profile evaluation of field repairs. It was predicted that this would eliminate the failure of the skins and that the rib would become the critical member as originally predicted.

12.4 PANEL EVALUATION - GROUP 2 - The second group of 3 by 12-inch rib stiffened panel specimens were refabricated to eliminate the skin distortion as described in section 3.3. The panels were of satisfactory manufacturing and coating quality. The field repairs applied represent the final development product for the ceramic compositions, lamp spot heater repair method, and the plasma spraying of molybdenum disilicide.

12.4.1 Panel Specimen Preparation - Defects were gritblasted on the skin as described in section 12.3.1. The same defect pattern as shown in 12-5 was selected, except the first and second rows of repairs on each side of the panel centerline were 5/8 and 1-1/4 inches, respectively. Two defect locations were used for each repair, one directly over a rib and a second halfway between two ribs. Table 12-4 presents the type, size, and location of the repair coatings evaluated.

Two panels of each alloy and coating combination had 1/8-inch diameter defects gritblasted at locations d and f. The panels were then sent to Sylvania for repair coating by replacing the fused slurry silicide coating with the focused radiant lamp coating. Sylvania, using the procedures described in section 11, experienced some difficulty in achieving and maintaining the required thermal conditions on the rib stiffened panels due to heat losses from the relatively open structure of the rib side of the panel. A bat-type insulation was used to minimize these heat losses. This is a valid condition as panels in actual service will have insulation on the inside surface. Early failures occurred on panel SYL-72, the first panel to be repaired. Subsequent panels showed a marked improve-

Table 12-4

FIELD REPAIR COATINGS EVALUATED

REPAIR SITE DESIGNATION	DEFECT SIZE (DIAMETER-IN.)	DEFECT LOCATION	REPAIR TYPE	
			Cb-752/R-512E PANELS	C-129Y/VH-109 PANELS
a	1/4	OVER RIB	CERAMIC J-2	CERAMIC E-2
b	1/4	OVER RIB	CERAMIC N-2	--
c	1/4	BETWEEN RIBS	CERAMIC J-2	CERAMIC E-2
d	1/8	BETWEEN RIBS	SYLVANIA R-512E LAMP	SYLVANIA R-512E LAMP
e	NONE	BETWEEN RIBS	-	-
f	1/8	OVER RIB	SYLVANIA R-512E LAMP	SYLVANIA R-512E LAMP
g	1/4	OVER RIB	CERAMIC O-2	CERAMIC H-1
h	1/4	BETWEEN RIBS	CERAMIC N-2	-
i	1/4	BETWEEN RIBS	CERAMIC O-2	CERAMIC H-1
j	1/8	BETWEEN RIBS	METCO-PLASMA $MoSi_2$	METCO-PLASMA $MoSi_2$
k	NONE	OVER RIB	-	-
l	1/8	OVER RIB	METCO-PLASMA $MoSi_2$	METCO-PLASMA $MoSi_2$

457-2857

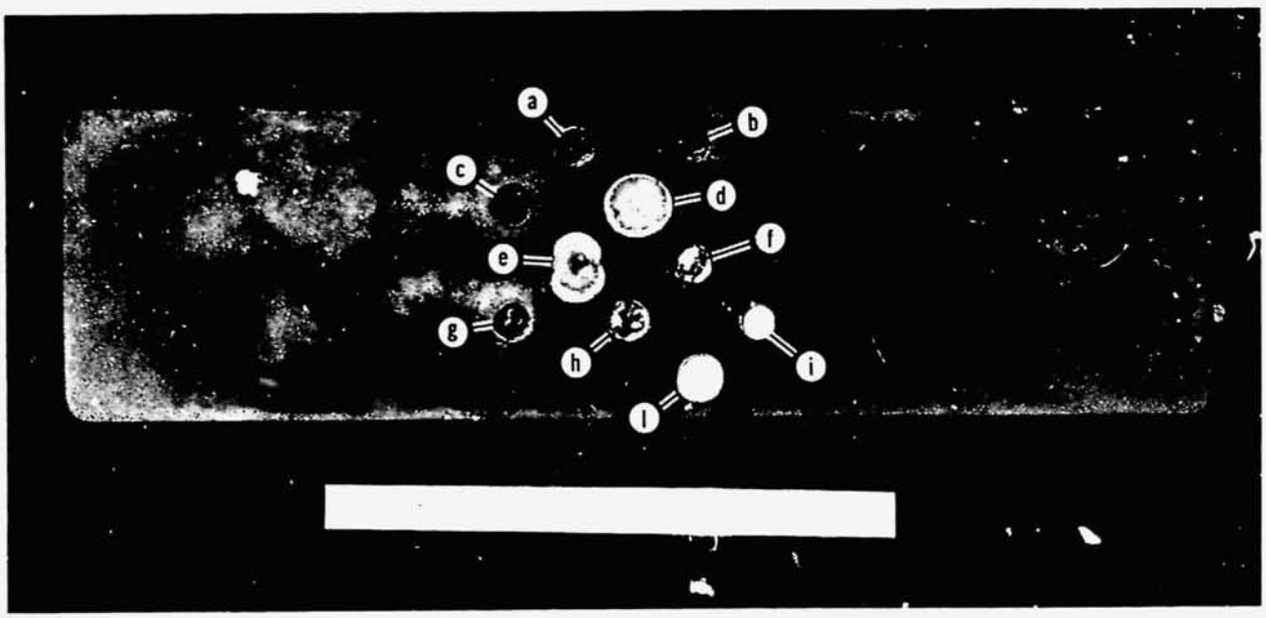

TYPICAL 3 BY 12-INCH RIB STIFFENED PANEL SHOWING FIELD REPAIRS BEFORE FLIGHT SIMULATION TESTING

457-2860

Figure 12-13

ment with proper temperature control maintained by using the insulation behind the repair area.

Defects in the four panel specimens were gritblasted at locations j and l and the panels were sent to Metco, Inc. for plasma sprayed molybdenum disilicide repairs. Metco cleaned the area to be repaired by lightly gritblasting and masking the panel with a 1/8-inch thick piece of steel having a 3/8-inch diameter hole in the desired repair area. The steel mask served to limit the spray to the desired area but also served as a heat sink during spraying to limit the heat input to the panels. The molybdenum disilicide then was applied to a thickness of 8 to 10 mils.

The final repairs to be applied were the ceramic composition repairs. The defect sites for ceramic repair were 1/4-inch diameter and were gritblasted as described above. Three ceramic compositions, J-2, N-2, and O-2, were selected for application to the R-512E-coated Cb-752 panels. The E-2 and H-1 compositions were applied to the VH-109-coated C-129Y alloy panels. The ceramic compositions were applied by the procedures described in appendix C. Each of the field repairs was considered satisfactory as applied. A typical panel after field repairing is shown in figure 12-13.

12.4.2 Results of Panel Evaluation - The field repairs and panels both performed well with a few minor oxidation failures and no structural failures. The results of the field repair performance are summarized in table 12-5. The two types of panels, Cb-752 with R-512E and C-129Y with VH-109 coating, will be discussed separately, since they exhibited similar performance characteristics.

12.4.2.1 Results of Cb-752 Alloy Panels - Three Cb-752 panels with the R-512E protective coating were tested through 110 simulated mission cycles without structural failure. Two panels, SYL-71 and SYL-72, had field repairs on the skin, as shown in table 12-4, and panel SYL-74 was tested without repairs on the skin. To provide a reference standard, panel SYL-70, without repairs, was not exposed to the boost acoustic fatigue exposure cycles.

Panels SYL-71 and 72 were the first to be repaired by Sylvania using the focused radiant lamp. As previously described, some difficulties were experienced. Two repair sites on panel SYL-72 failed after 22 and 44 reentry profile cycles, as illustrated in figure 12-14. Oxidation failure occurred on the periphery of the repair area pproximately 1/4 inch from the original gritblasted defect site. The molten slurry flowed during the repair cycle to the peripheral line in which the failures occurred. The slurry fusion temperature (2350 to 2400°F) was sufficient to dissolve part of original R-512E coating, but the temperature at this point was not high enough to reform the desired intermetallic compound. The

Table 12–5

OXIDATION TEST RESULTS OF FIELD REPAIR COATINGS EXPOSED TO SIMULATED FLIGHT CONDITIONS

PANEL SPEC. NO.	TYPE AND LOCATION OF REPAIR SITES										
	CERAMIC FIELD REPAIR						SYLVANIA R-512E REPLACEMENT REPAIR		METCO PLASMA MOLYBDENUM DISILICIDE		TOTAL PANEL DEFLECTION INCHES
	J–2 (SYL) E–2 (VAC)		N–2		O–2 (SYL) H–1 (VAC)						
	OR	BR	OR	BR	OR	BR	LAMP OR	LAMP BR	OR	BR	
SYL–71	110 NF	110 NF	110 NF	110 NF	88 NF	110 NF	110 NF	22 F	110 NF	110 NF	0.012
SYL–72	110 NF	110 NF	110 NF	110 NF	110 NF	110 NF	44 F	22 F	110 NF	110 NF	0.003
VAC–93	110 NF	110 NF	NOT TESTED	NOT TESTED	110 NF	110 NF	110 NF	110 NF	110 NF	110 NF	0.029
VAC–94	110 NF	110 NF	NOT TESTED	NOT TESTED	110 NF	110 NF	110 NF	110 NF	110 NF	110 NF	0.021

SYMBOLS:

F – FAILURE AFTER INDICATED NUMBER OF REUSE CYCLES

NF – NO FAILURE AFTER INDICATED NUMBER OF REUSE CYCLES

OR – REPAIR OVER RIB

BR – REPAIR BETWEEN RIBS.

457–2858

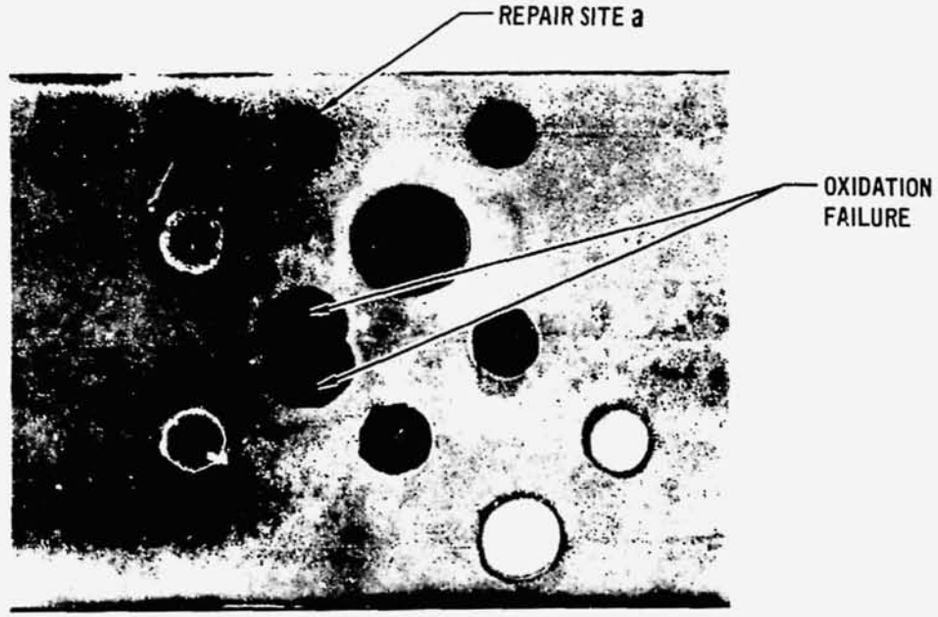

PANEL SYL–72 AFTER 22 REENTRY PROFILE CYCLES SHOWING OXIDATION FAILURES ADJACENT TO LAMP REPAIR SITE f

Figure 12–14

457–3332

problem was satisfactorily resolved by reducing the heat losses from the back of the repair area so that the wetted area of the molten slurry was hot enough to reform the correct protective coating composition. While it was unfortunate that these early failures occurred, it is believed that the problem is understood and has been solved. The good performance of the lamp repair areas supports this conclusion. The premature failures on the periphery of the lamp repairs were field repaired with the U-1 ceramic composition to prevent further oxidation. This procedure of repairing oxidation failures to permit continued evaluation of an adjacent area was employed in all panel evaluations.

One ceramic composition (O-2) at repair site c on panel SYL-71 failed after 88 reentry profile cycles. This particular composition has been found to permit higher rates of oxygen penetration than the other two ceramic compositions (J-2 and N-2) when applied to the R-512E coating. One of the molybdenum disilicide plasma sprayed repairs showed an oxidation failure after 110 profile cycles at repair site 1 on panel SYL-72. The failure was caused by the panel edge curling during testing and putting a deflection of approximately 0.08 inch across the 0.5-inch repair site diameter.

The primary characteristic of panel performance was curling of the edges. This occurred only in the Cb-752 alloy panels and occurred on all three panels of this alloy, including the unrepaired panel. Two coating failures were initiated by this edge curling. The first was discussed in connection with the plasma spray repaired site. The second occurred on panel SYL-72, in which an oxidation failure occurred in the rib to skin weld area on the end of the panel after 66 cycles, as shown in figure 12-15. The skin was trimmed off and the area repair coated with U-1 ceramic repair composition. The panels SYL-71, 72, and 74 are shown in figure 12-16 after 110 reentry profile cycles. The panels and repair areas performed satisfactorily.

Panel SYL-72 was metallographically sectioned to examine each of the repairs. No additional failures or immediately pending failure areas were noted. The zones of contamination were generally lower than had been observed on previous panel or coupon tests. The contamination zones below the ceramic and plasma sprayed repairs were between 2 and 5 mils. Figure 12-17 shows the J-2 ceramic repair composition from repair site c, located on the skin between the ribs. The repair was excellent in all respects and was typical. The repair area in which the R-512E coating was replaced with the Sylvania spot heater is shown in figure 12-18. The coating

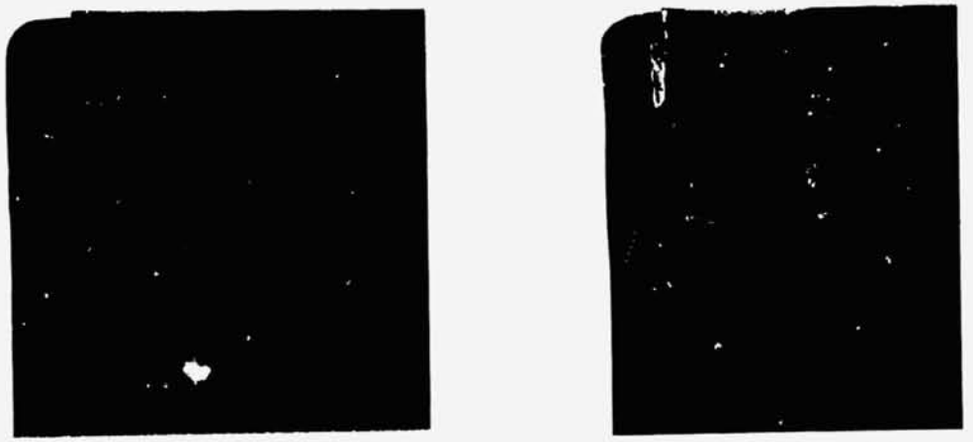

457-2876

OXIDATION FAILURE OF PANEL SYL-72 AFTER 66 REENTRY PROFILE CYCLES CAUSED BY EDGE CURLING

Figure 12-15

thickness was good and the repair area was protective for the 110 reentry profile cycles.

12.4.2.2 Results of C-129Y Alloy Panels - Three C-129Y panels with the VH-109 coating were tested. Two panels, VAC-93 and VAC-94, were tested with repairs on the skin, as shown in table 12-4. Panel VAC-91 was tested without repairs. None of the field repair sites on either panel VAC-93 or panel VAC-94 failed in oxidation. Each of the VH-109 coated panels had a few small oxidation failures, usually on edges. One common area of coating weakness which appeared toward the end of the exposure cycles was on the edge of the ribs. Panel VAC-93 showed numerous coating oxidation failures on the central portion of the rib after 88 profile reentry cycles, as shown in figure 12-19. Both acoustic and profile loading were terminated after 88 profile cycles because of the probability of excessive panel deflections during subsequent cycles. (See section 12.3.2.3 for past experience with C-129Y rib oxidation failures.) The remaining two panels, VAC-91 and VAC-93, showed the same condition after 110 reentry cycles, but the loading did not have to be terminated. Panels VAC-93, 94 and 91 are shown in figure 12-21 after 110 reentry profile cycles.

Metallographic examination of each of the repairs from panel VAC-93 was conducted. The good repair performance observed visually after 110 reentry profile cycles was verified by the metallographic results. No pending failures were noted and the amount of contamination below the repair was very small (1 to 5 mils). Figure 12-20 shows a molybdenum disilicide plasma sprayed repair with only 5 mils

PANEL SYL-72

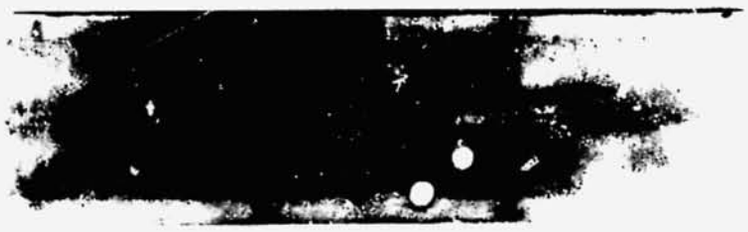

PANEL SYL-71

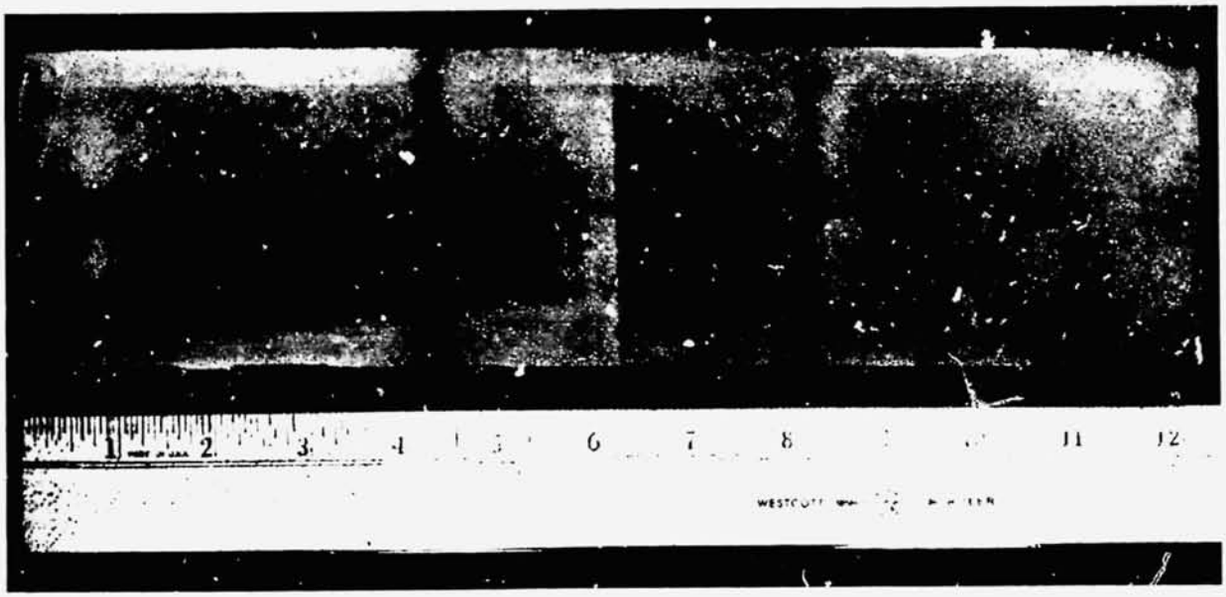

PANEL SYL-74

R-512E COATED Cb-752 ALLOY PANELS AFTER 110 FLIGHT SIMULATION REUSE CYCLES

457-2875

Figure 12-16

of oxygen contamination below a dense adherent repair. Figure 12-22 shows two ceramic repair compositions, E-2 and H-1, with virtually no contaminated zone.

12.5 CONCLUSIONS OF PANEL EVALUATION - The field repairs in all cases performed satisfactorily and were considered ready to be used in service. The repair which passed 110 reentry flight simulation cycles satisfactorily were

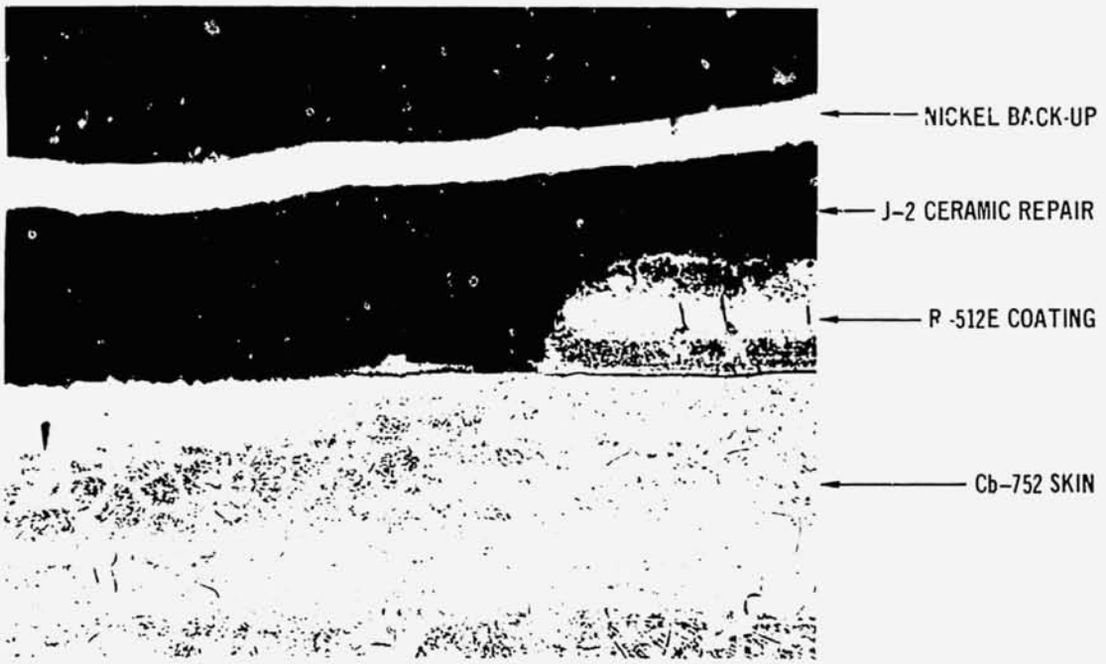

200X

J-2 CERAMIC REPAIR FROM PANEL SYL-72 AFTER 110 REENTRY PROFILE CYCLES

Figure 12 – 17

457 - 3333

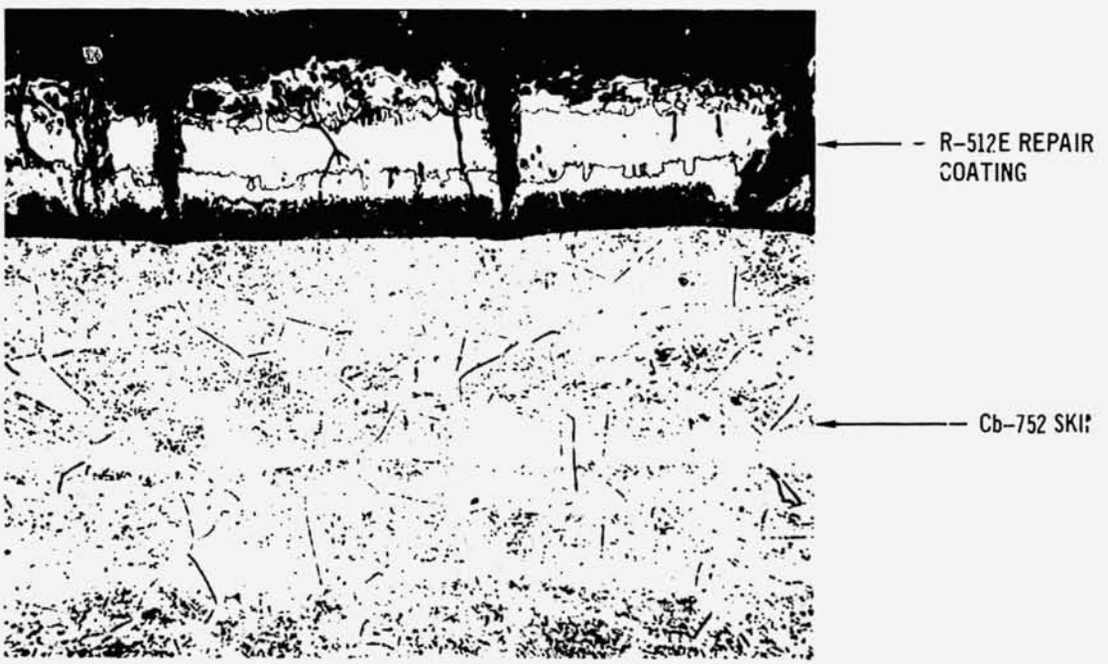

300X

R-512E REPAIR COATING APPLIED WITH SYLVANIA SPOT HEATER ON PANEL SYL-72 AFTER 110 REENTRY PROFILE CYCLES

457 - 3334

Figure 12 – 18

457-2856

0.37X

PANEL VAC-93 AFTER 88 REENTRY PROFILE CYCLES SHOWING OXIDATION FAILURES ON THE RIB EDGES

Figure 12-19

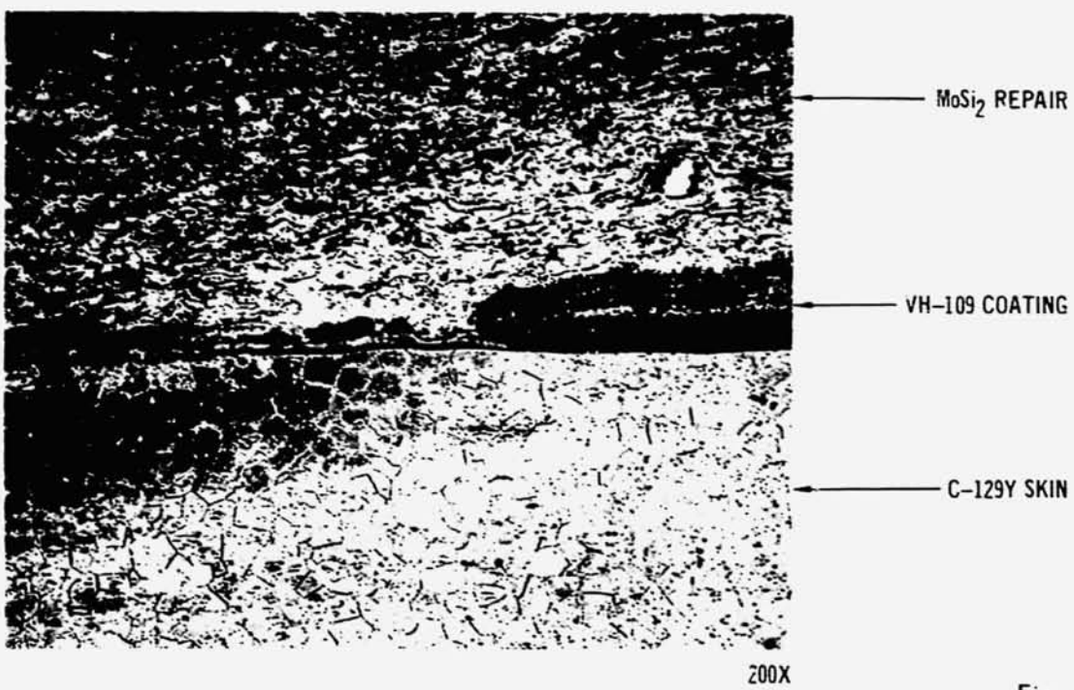

200X

Figure 12-20

$MoSi_2$ PLASMA SPRAYED REPAIR OF PANEL VAC-93 AFTER 110 REENTRY PROFILE CYCLES

457-3335

applied to full-size, 20 by 20-inch, rib stiffened panels, which were supplied to NASA-MSFC for evaluation. The repairs considered to be ready for service and supplied to MSFC were:

a) for the R-512E coated Cb-752
   - o Sylvania lamp replacement of silicide coating
   - o plasma deposited molybdenum disilicide
   - o ceramic composition J-2
   - o ceramic composition N-2

PANEL VAC-93

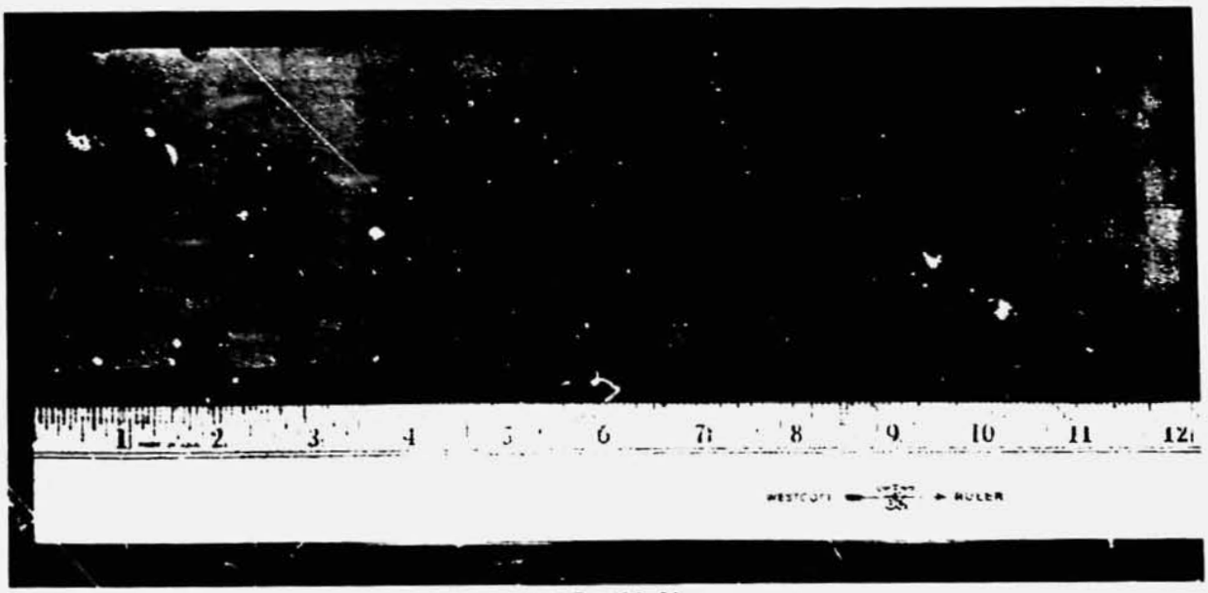

PANEL VAC-94

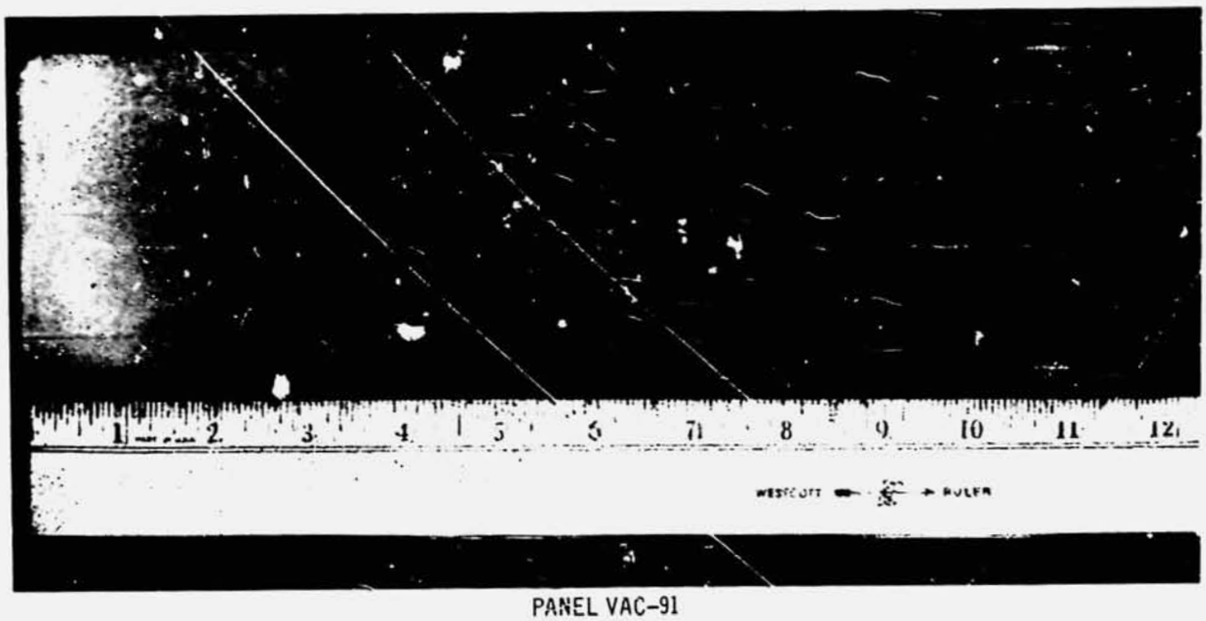

PANEL VAC-91

VH-109 COATED C-129Y ALLOY PANELS AFTER 110 FLIGHT SIMULATION REUSE CYCLES

457-2859

Figure 12-21

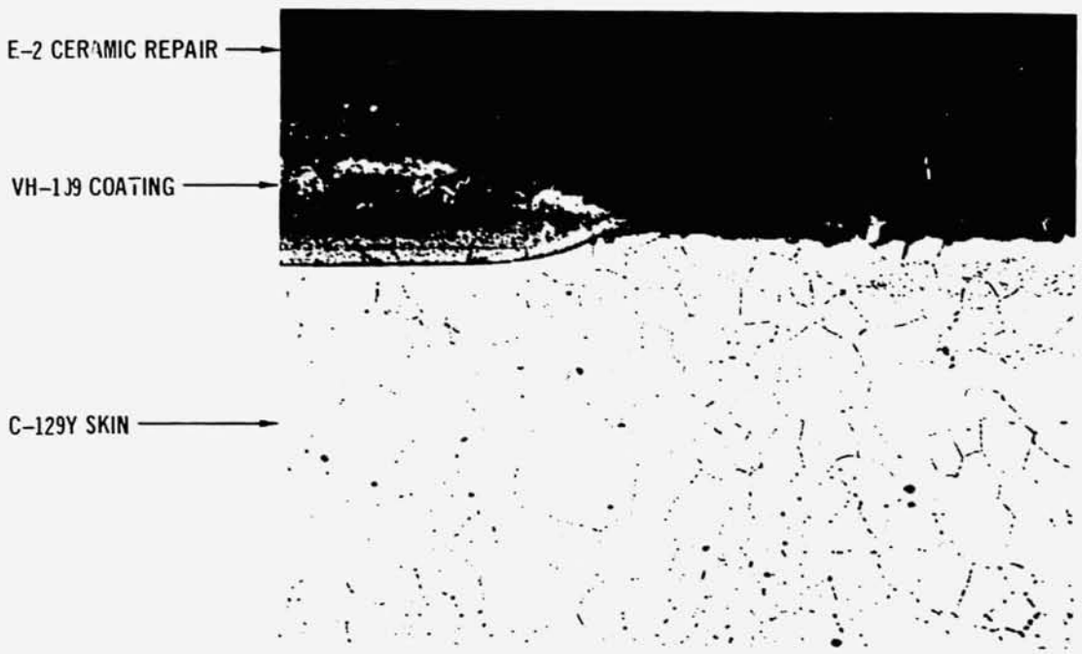

E-2 REPAIR COMPOSITION 250X

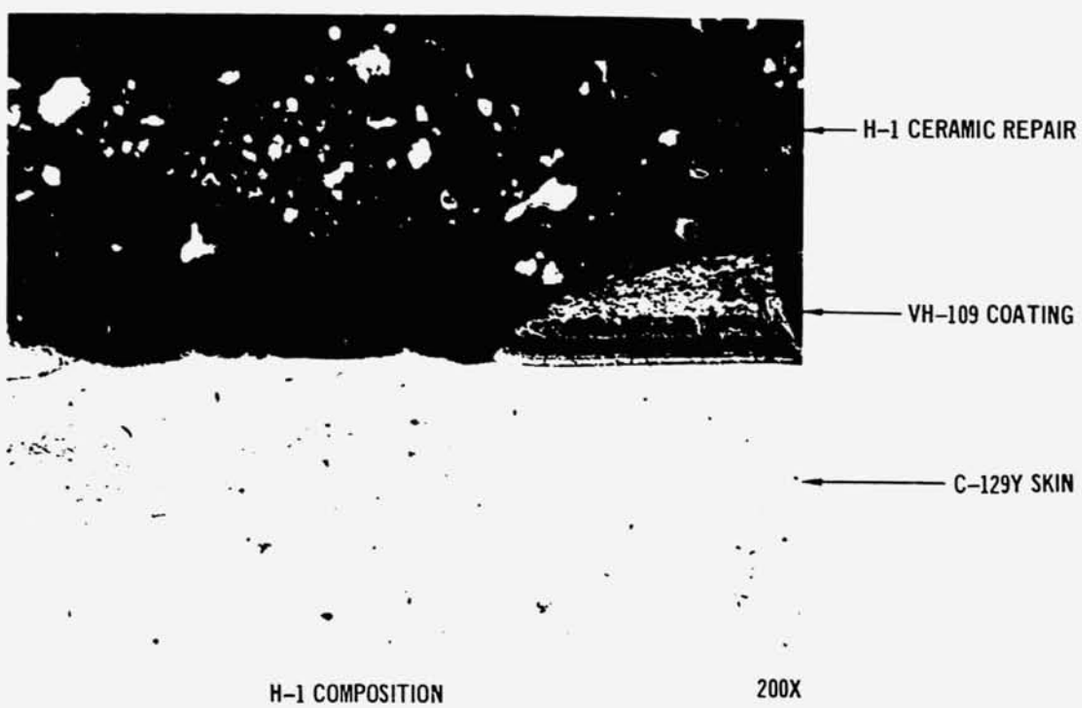

H-1 COMPOSITION 200X

CERAMIC REPAIR ON PANEL VAC-93 AFTER 110 REENTRY PROFILE CYCLES

457-3336

Figure 12-22

b) for the VH-109 coated C-129Y

- o Sylvania lamp replacement of silicide coating
- o plasma deposited molybdenum disilicide
- o ceramic composition E-2
- o ceramic composition H-1.

13. FIELD REPAIR OF FULL SIZE RIB STIFFENED PANELS

A variety of different field repair coatings was developed and the adequacy of these repair systems has been demonstrated on 3 by 12-inch panel specimens subjected to flight simulation testing. The final demonstration was to apply the proven field repairs to full-size rib stiffened panels.

The design of the 20 by 20-inch rib stiffened panels was described in section 4 and the fabrication and coating are covered in section 3. It was decided to apply 4 different types of repairs to a total of 20 different sites on the panel skin. Figure 13-1 shows the repair site locations and type of repair. The defects to be repaired were formed by gritblasting the coating from the skin in the desired locations using 220 mesh aluminum oxide at a pressure of 40 lb/in^2. The defects for the R-512E replacement repairs with the spot heater and the defects for molydbenum disilicide plasma spray were 1/8 inch in diameter. The defects for repair with the ceramic compositions were 1/4 inch in diameter.

The repairs were applied by the methods derived on this program and described in the appropriate sections of this report. (Lamp replacement of R-512E is described in section 11, the plasma spraying in section 10, and the ceramic repairs in section 7 and appendix C.) As a final proof inspection, each of the panels was heated to 2200°F for 10 minutes in an air atmosphere furnace. Each of the 40 repair sites was fully protective and functioning normally. The physical handling involved in defecting, repairing, and inspecting 20 separate areas on each panel produced a general soiling of the skin surface. The panels were cleaned by aluminia gritblasting at 15 lb/in^2 pressure. The surface removal was not measureable by micrometer but is nominally 0.1 to 0.2 mil. The panels in general had a good appearance and are shown in figures 13-2 and 13-3.

REPAIR OF 20 BY 20-IN. RIB STIFFENED PANELS

REPAIR SITE	C-129Y VH-109	Cb-752 R-512E
a	E-2 CERAMIC	J-2 CERAMIC
b	SYLVANIA LAMP	SYLVANIA LAMP
c	H-1 CERAMIC	N-2 CERAMIC
d	H-1 CERAMIC	N-2 CERAMIC
e	$MoSi_2$ PLASMA SPRAY	$MoSi_2$ PLASMA SPRAY
f	$MoSi_2$ PLASMA SPRAY	$MoSi_2$ PLASMA SPRAY
g	E-2 CERAMIC	J-2 CERAMIC
h	SYLVANIA LAMP	SYLVANIA LAMP
i	E-2 CERAMIC	J-2 CERAMIC
j	H-1 CERAMIC	N-2 CERAMIC
k	E-2 CERAMIC	J-2 CERAMIC
l	H-1 CERAMIC	N-2 CERAMIC
m	$MoSi_2$ PLASMA SPRAY	$MoSi_2$ PLASMA SPRAY
n	H-1 CERAMIC	N-2 CERAMIC
o	SYLVANIA LAMP	SYLVANIA LAMP
p	SYLVANIA LAMP	SYLVANIA LAMP
q	E-2 CERAMIC	J-2 CERAMIC
r	E-2 CERAMIC	J-2 CERAMIC
s	$MoSi_2$ PLASMA SPRAY	$MoSi_2$ PLASMA SPRAY
t	H-1 CERAMIC	N-2 CERAMIC

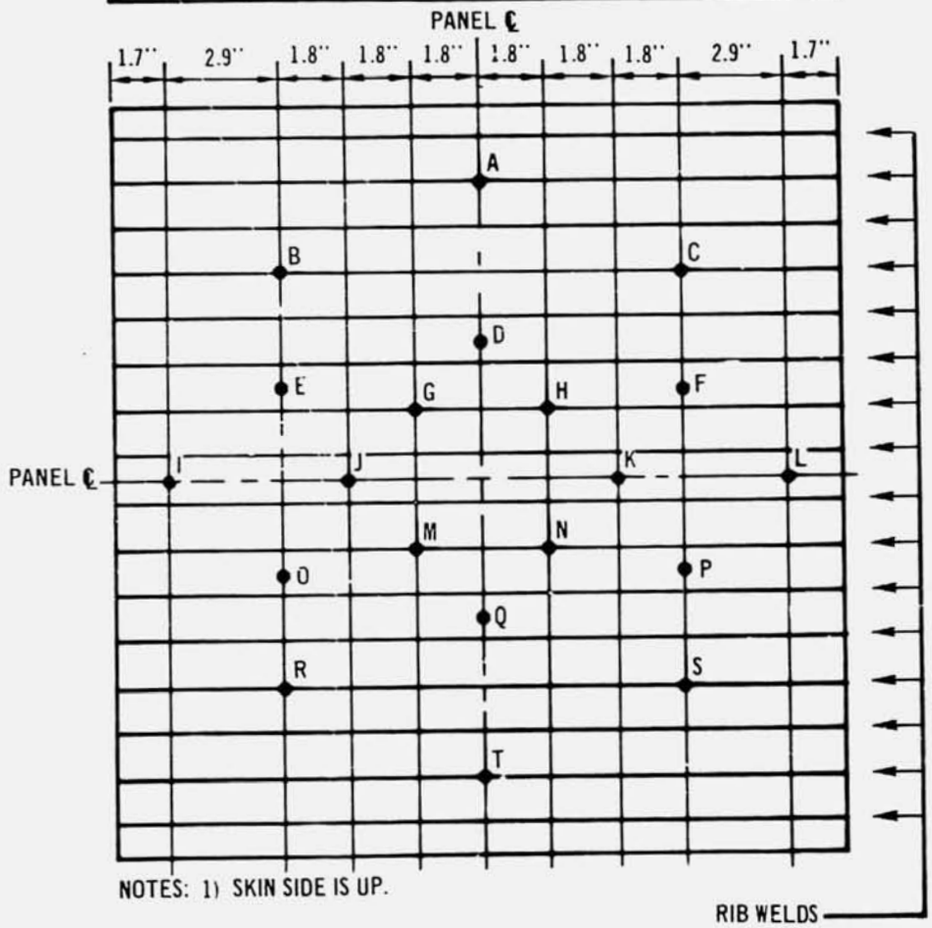

Figure 13-1

REPAIR SITE LOCATIONS FOR 20 BY 20-INCH PANELS

457-3337

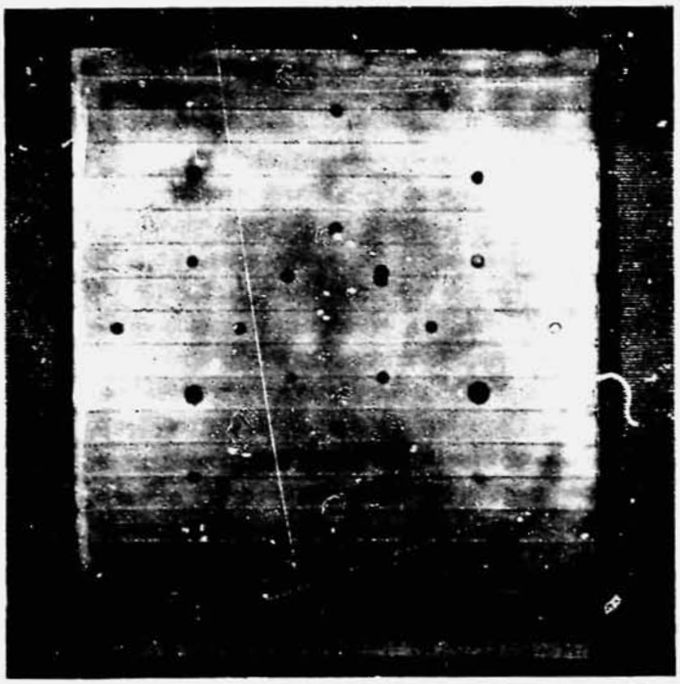

FULL SIZE Cb–752/R–512E RIB STIFFENED PANEL WITH FIELD REPAIR COATINGS

4457–3339

Figure 13–2

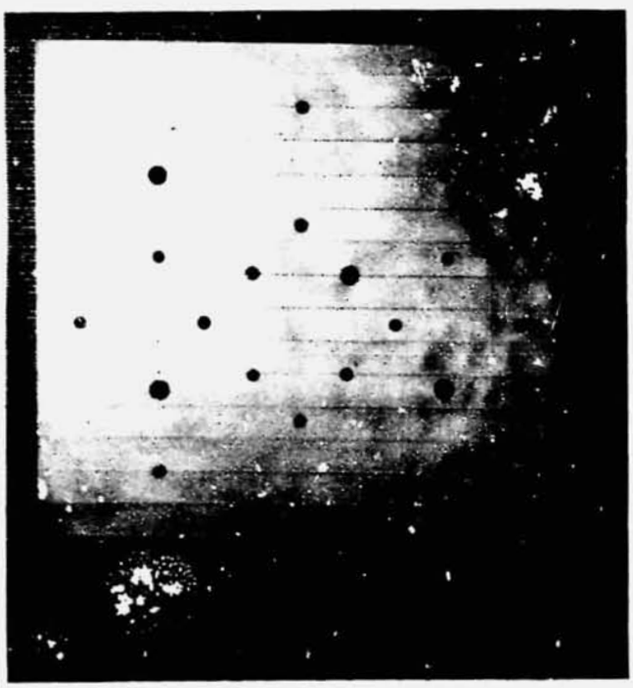

FULL SIZE C–129Y/VH–109 RIB STIFFENED PANEL WITH FIELD REPAIR COATINGS

457–3340

Figure 13–3

14. CONCLUSIONS AND RECOMMENDATIONS

The following conclusions and recommendations were drawn from the results of this field repair program:

14.1 COATING DAMAGE TOLERANCE - It is difficult to assign quantitative values to coating damage tolerance because of the multiplicity of possible conditions causing damage and the variety of hardware configurations. Coated columbium hardware should be handled with reasonable care, but this is equally true for any aerospace metallic material, particularly when used in thin gages. The coatings have a significant amount of damage tolerance and are in no way a hypersensitive material.

When damage does occur, it can easily be assessed by visual inspection. In each of the types of damage studied, levels of damage were demonstrated that did not affect coating life. Therefore, one need not be concerned about not detecting damage that should be repaired. There will be a minor problem in educating inspection personnel to recognize true damage so that excess amounts of needless repairs are not conducted.

The final question of the consequences of sustaining damage to the coating, which is not detected and repaired, was dealt with effectively. If the coating is totally removed from a small area there are no structural or aerodynamic consequences for more than one reentry. Estimates for hole formation through a thin (0.010-inch) skin on a panel range from 3 to 10 reentry cycles reaching 2400°F. Therefore, there is significant time to detect columbium oxidation and terminate it with effective repairs. The formation of holes in a skin is the condition which must be prevented in order to stop hot boundary layer gasses from entering the vehicle. No panel structural failures due to skin oxidation were observed through 50 reentry flight simulation cycles.

14.2 FIELD REPAIRS - Three types of field repair were developed which are ready and qualified for application to an operational columbium system. The first method employs a ceramic composition which is painted or sprayed on. Upon fusion either before or during service, for 5 minutes at 2100°F the repair stops oxidation under reentry conditions for over 100 mission cycles. Associated with the ceramics is a small amount of oxygen solution below the repair which is less than 0.008 inch deep and causes no structural problem.

The second method provides for the reapplication of the original fused slurry silicide coating. An inexpensive focused radiant lamp is the only equipment

14. CONCLUSIONS AND RECOMMENDATIONS

The following conclusions and recommendations were drawn from the results of this field repair program:

14.1 COATING DAMAGE TOLERANCE - It is difficult to assign quantitative values to coating damage tolerance because of the multiplicity of possible conditions causing damage and the variety of hardware configurations. Coated columbium hardware should be handled with reasonable care, but this is equally true for any aerospace metallic material, particularly when used in thin gages. The coatings have a significant amount of damage tolerance and are in no way a hypersensitive material.

When damage does occur, it can easily be assessed by visual inspection. In each of the types of damage studied, levels of damage were demonstrated that did not affect coating life. Therefore, one need not be concerned about not detecting damage that should be repaired. There will be a minor problem in educating inspection personnel to recognize true damage so that excess amounts of needless repairs are not conducted.

The final question of the consequences of sustaining damage to the coating, which is not detected and repaired, was dealt with effectively. If the coating is totally removed from a small area there are no structural or aerodynamic consequences for more than one reentry. Estimates for hole formation through a thin (0.010-inch) skin on a panel range from 3 to 10 reentry cycles reaching 2400°F. Therefore, there is significant time to detect columbium oxidation and terminate it with effective repairs. The formation of holes in a skin is the condition which must be prevented in order to stop hot boundary layer gasses from entering the vehicle. No panel structural failures due to skin oxidation were observed through 50 reentry flight simulation cycles.

14.2 FIELD REPAIRS - Three types of field repair were developed which are ready and qualified for application to an operational columbium system. The first method employs a ceramic composition which is painted or sprayed on. Upon fusion, either before or during service, for 5 minutes at 2100°F the repair stops oxidation under reentry conditions for over 100 mission cycles. Associated with the ceramics is a small amount of oxygen solution below the repair which is less than 0.008 inch deep and causes no structural problem.

The second method provides for the reapplication of the original fused slurry silicide coating. An inexpensive focused radiant lamp is the only equipment

required and the repair is effected in a 2-minute processing cycle at 2700°F. Flight size hardware has been repaired with only minor distortion of the skin due to local heating. The repairs are as effective as the original coating, lasting in excess of 100 reentry cycles.

The final method effects a local repair by applying molybdenum disilicide by plasma spraying. Portable plasma spray equipment can be easily used in the field and the repair is fully protective without heating or fusion. The life of the molybdenum disilicide repair is in excess of 100 cycles and, like the ceramic repairs, a small zone of oxygen solution is formed below the repair which is not detrimental to panel performance.

Each of the repairs is easy to apply, inexpensive, and reliable. They can all be highly recommended and each may have some contrasting subtle advantages or disadvantages for a particular application.

14.3 COLUMBIUM PANEL PERFORMANCE - Rib stiffened panels, with and without field repairs coatings on the skin, successfully performed for 110 reentry flight simulation cycles. The flight simulation included static boost loads, boost acoustic loading, and simultaneous reentry flight conditions of temperatures, air pressure and bending stress as a function of time. These comprehensive evaluations established coated columbium as a viable thermal protection material system.

14.4 COLUMBIUM PANEL FABRICATION - The technology for manufacturing high quality rib stiffened panels was established. The program also employed single faced vee corrugated panels (7 by 7 inches) manufactured by forged upset diffusion joining. This process has the potential of making high quality heatshield panels at an attractive cost. It is recommended that this process be investigated further in conjunction with other design and manufacturing approaches to determine the minimum production costs for fabricating and coating reliable columbium panels.

14.5 COLUMBIUM HEAT SHIELD PANEL REFURBISHMENT - This program has demonstrated that effective coating repairs can be easily applied in the field without removing the panels from the vehicle. In those cases in which damage has been sustained by the underlying columbium and the panel must be removed, there are many potentially applicable repair methods for repairing the substrate and recoating. Thus, panels could be refurbished, either at a factory or at an operational base, and returned to service to effect a cost saving over replacing and discarding the damaged panel. It is therefore recommended that a refurbishment study be initiated to develop and demonstrate repair procedures.

15. REFERENCES

1. Fitzgerald, B. G. and Rusert, E. L., "Evaluation of the Fused Slurry Silicide Coating Considering Component Design and Reuse," Technical Report AFML-TR-70-154 December 1970.
2. Christensen, H. E., "Entry Thermal Environment for Shuttle TPS High Temperature Insulation," Technical Memo E242-324, 29 September 1970.
3. Priceman, S. and Kubick, R., "Development of Protective Coatings for Columbium Alloy Gas Turbine Blades," Progress Report STR69-7175-0194.4, 31 October 1969.
4. DeClue, D. H., "Investigation of the Chipping Tendency in LB-2 Coated Cb-752 " Technical Report E6620-215, 20 February 1967.
5. Wah Chang Albany Technical Data Book, "Columbium, Tantalum and Tungsten Alloys - Technical Information - Volume Three," January 1968.
6. Fitzgerald, B. G., "Fused Slurry Silicide Coatings for Columbium Alloy Reentry Heat Shields," Fifth Quarterly Report for Contract No. NAS 3-14307, dated 30 November 1971.
7. Bartlett, H. E. and Barry, F. R., "ASSET - Volume VIII, Manufacturing Technology," AFFDL-TR-65-31, Volume VIII, dated December 1965.
8. Culp, J. D., Fitzgerald, B. G., and Fitzpatrick, T. H., "Advances in Coated Refractory Metal Hardware," Presented to Refractory Composites Working Group Meeting, dated 25 January 1966.
9. Priceman, S. and Sama, L., "Development of Fused Slurry Silicide Coatings for the Elevated-Temperature Oxidation Protection of Columbium and Tantalum Alloys," AFML-TR-68-210, dated December 1968.
10. Fitzgerald, B. G., "Fused Slurry Silicide Coating for Columbium Alloy Reentry Heat Shields," Seventh Quarterly Report for Contract No. NAS 3-14307, dated 30 April 1972.

APPENDIX A

CERAMIC FIELD REPAIR COMPOSITIONS

A.** 1) 60 gm Pyrex frit, #7740
30 gm Al_2O_3
10 gm Boron
110 ml Cenilac

2) (MRC-3 Composition)

B.* 1) Basecoat
1.0 gm $CbSi_2$
2.5 gm SiC
6.9 gm Sauereisen No. 8
2.1 ml $D.H_2O$

2) 1st Overcoat
40 gm Pyrex frit #7740
40 gm PS-7
20 gm Al_2O_3

3) 2nd Overcoat
30 gm SiC
19 ml Syton
0.5 ml AC-55

4) 1-hour air dry or 1/2 hour @ 170°F.

C.* 1) Basecoat
7.0 gm Sauereisen No. 8
3.0 gm $CbSi_2$
1.7 ml Distilled H_2O

2) Overcoat
2.0 gm Pyrex frit #7740
2.0 gm PS-7
1.0 gm Al_2O_3

D.** 1) 60 gm Pyrex frit, #7740
30 gm Al_2O_3
5 gm Boron
110 ml Cenilac

E.** 1) 2.0 gm Ceramacast 505
1.0 gm Al_2O_3
0.3 gm Boron
2.0 ml Distilled H_2O

F. 1) 0.8 gm Al_2O_3
1.5 gm Pyrex frit #7740
0.3 gm $CbAl_3$
1.5 ml PS-7
2) Air dried, then propane torched (2-1/2 inch distance) for 30 seconds.

G.* 1) Basecoat
2.0 gm Ceramacast 505
1.0 ml Distilled H_2O
2) Overcoat
MRC-3 with 1/2 the amount of Boron.

H.* 1) 2.0 gm Ceramacast 505
1.0 ml Distilled H_2O

I.* 1) 1.0 gm Al_2O_3
1.0 ml Cenilac (binder)

J.* 1) 1.0 gm Al_2O_3
2.0 gm Pyrex frit #7740
0.5 gm $CbSi_2$
3.5 ml Cenilac
2) Air dried, then propane torched (2-1/2 inch distance) for 30 seconds.

K.* 1) 1.0 gm Pyrex frit
1.0 ml Cenilac

L.* 1) 2.0 gm $CbSi_2$
0.2 gm NaF
2.2 ml Syton

M.* 1) 1.0 gm Pyrex frit #7740
1.0 gm $CbSi_2$
2.0 ml Syton

N.* 1) 1.0 gm Pyrex frit #7740
1.0 gm $CbSi_2$
2.0 ml Cenilac

O.* 1) 1.0 gm Pyrex frit #7740
1.0 gm $CbSi_2$
2.0 ml PS-7

P.* 1) 1.0 gm Pyrex frit #7740
1.0 gm $CbSi_2$
0.1 gm Boron
2.1 ml Cenilac

R. 1) 60% Si - 20% Cr - 20% Fe (-325 mesh alloy, 99.9% Purity) Flame Sprayed.

2) O_2 @ 30 psi
Ac @ 30 psi
4 passes for preheat at 3 inches from specimen.
Feed speed set at 18.
25 passes at approximately 2 inches/second and 2-1/2 inches from specimen.

S.** 1) 1.0 gm 60% Si - 20% Cr - 20% Fe (alloy)
1.0 ml Cenilac

T.** 1) 4 gm Sauereisen #8
1 gm $CbSi_2$
1 ml Distilled H_2O

U.** 1) 4 gm Sauereisen #8
1 gm Al_2O_3
1 ml Distilled H_2O

V.** 1) 4 gm Al_2O_3
1 gm Pyrex frit #7740
5.5 ml Cenilac

W.** 1) Basecoat
1.0 gm $CbSi_2$
2.5 gm SiC
6.9 gm Sauereisen #8
2.1 ml Distilled H_2O
2) Overcoat
4.0 gm Al_2O_3
1.0 gm Pyrex frit #7740
5.5 ml Cenilac

X.** 1) 4.0 gm Sauereisen #8
1.0 gm 60% Si - 20% Cr - 20% Fe (alloy)
1.0 ml Distilled H_2O

Y.** 1) 1.0 gm $CbSi_2$
1.0 gm 60% Si - 20% Cr - 20% Fe (alloy)
1.0 gm Pyrex frit #7740
3.3 ml Cenilac

Z.** 1) 4.0 gm Sauereisen #8
1.0 gm 60% Si - 20% Cr - 20% Fe (alloy)
1.0 ml Distilled H_2O

B-1. 1) Basecoat

Liquid gold conversion coat (brush application - 500°F for 1/2 hour).

**2) Overcoat

2.0 gm 60% Si - 20% Cr - 20% Fe (alloy)
3.0 gm SiC
10.0 gm Sauereisen #8
3.0 ml Distilled H_2O

D-1.***
8.0 gm Al_2O_3
4.0 gm Pyrex frit
0.26 gm Boron
13.5 ml Cenilac

E-1.***
4.0 gm Al_2O_3
4.0 gm Pyrex frit #7740
0.26 gm Boron
8.8 ml Cenilac

F-1.***
8.0 gm Al_2O_3
2.0 gm Pyrex frit #7740
0.13 gm Boron
11.0 ml Cenilac

G-1.**
2.0 gm $CbSi_2$
2.0 gm 60% Si - 20% Cr - 20% Fe (alloy)
2.0 gm Pyrex frit #7740
7.0 ml Cenilac

H-1.**
2.0 gm $CbSi_2$
2.0 gm 60% Si - 20% Cr - 20% Fe (alloy)
2.0 gm Pyrex frit #7740
0.33 gm Boron
7.0 ml Cenilac

I-1.** 6.0 gm Pyrex frit #7740
4.0 gm Al_2O_3
1.0 gm Boron
12.0 m. Cenilac

J-1.** 6.0 gm Pyrex frit
4.0 gm Al_2O_3
0.5 gm Boron
12.0 ml Cenilac

K-1.* 1.0 gm Boron
4.0 ml Cenilac

L-1. *1) Basecoat
1.0 gm Boron
4.0 ml Cenilac
**2) Overcoat
1.0 gm Boron
1.0 gm Al_2O_3
4.5 ml Cenilac

M-1. *1) Basecoat
1.0 gm Boron
4.0 ml Cenilac
**2) Overcoat
2.0 gm $CbSi_2$
2.0 gm 60% Si - 20% Cr - 20% Fe (alloy)
2.0 gm Pyrex frit #7740
7.0 ml Cenilac

N-1. *1) Basecoat
1.0 gm Boron
4.0 ml Cenilac

**2) Overcoat

60 gm Pyrex frit #7740

30 gm Al_2O_3

10 gm Boron

110 gm Cenilac

O-1.** 4.0 gm Sauereisen #8

1.0 gm $CbSi_2$

1.0 gm 60% Si - 20% Cr - 20% Fe (alloy)

1.0 gm Pyrex frit #7740

0.17 gm Boron

1.5 ml Distilled H_2O

P-1.* 1.0 gm $CbSi_2$

1.0 gm Pyrex frit #7740

0.17 gm Boron

2.2 ml Cenilac

R-1.* 1.0 gm $CbSi_2$

1.0 gm Pyrex frit #7740

0.17 gm Boron

0.60 gm Silicon (-325 mesh)

3.3 ml Cenilac

S-1.* 1.0 gm $CbSi_2$

1.0 gm Pyrex frit #7740

0.17 gm Boron

0.20 gm Chromium (-325 mesh)

2.6 ml Cenilac

T-1.* 1.0 gm $CbSi_2$

1.0 gm Pyrex frit #7740

0.17 gm Boron

0.20 gm Iron (3 micron)

2.6 ml Cenilac

U-1.* 1.0 gm Pyrex frit #7740
0.17 gm Boron
1.3 ml Cenilac

V-1.** 1) Basecoat
Liquid gold conversion coat (brush application - 500°F for 1/2 hour).
2) Overcoat
4.0 gm Pyrex frit #7740
4.0 gm Al_2O_3
0.10 gm Boron
9.0 ml Cenilac

W-1.*** 8.0 gm Al_2O_3
4.0 gm Pyrex frit #7740
0.53 gm Boron
13.7 ml Cenilac

X-1.** 1.0 gm 60% Si - 20% Cr - 20% Fe, alloy metal powder
0.1 gm Boron, amorphous
1.0 ml Cenilac

Y-1.** 2.0 gm Pyrex frit, #7740
2.0 gm 60% Si - 20% Cr - 20% Fe, alloy metal powder
0.33 gm Boron, amorphous
5.0 ml Cenilac

Z-1.** 0.6 gm Pyrex frit, #7740
0.3 gm 60% Si - 20% Cr - 20% Fe, alloy metal powder
0.1 gm Boron, amorphous
1.1 ml Cenilac

A-2.** 2.0 gm Pyrex frit, #7740
0.34 gm Boron, amorphous
2.0 ml Krylon aluminum spray paint

B-2.** 2.0 gm Pyrex frit #7740
0.34 gm Boron
2.0 ml Krylon spray, clear (No. 1303)

C-2.** 1 gm Boron
2.0 ml Krylon aluminum spray paint (No. 1402)

D-2.** 1.0 gm 60% Si - 20% Cr - 20% Fe (alloyed powder)
1.0 gm Boron
2.0 ml Krylon spray, clear (No. 1303)

E-2.** 1.0 gm Pyrex frit #7740
0.17 gm Boron
2.0 ml Supersaturated solution of Zein in denatured alcohol, herein designated "Alze"

F-2.** U-1, 3 mils thick
H-1, 1st overcoat, 12 mils thick
A-2, 2nd overcoat, 2 mils thick

G-2.** H-1, 3.5 mils thick
A-2, 3.6 mils thick

H-2.** 2.0 gm Pyrex frit #7740
0.34 gm Boron
2.0 ml, Pratt & Lambert aluminum paint (No. 7897)

I-2.** 2.0 gm Pyrex frit #7740
0.34 gm Boron
2.0 ml Phelan's aluminum paint (No. 292)

J-2.** 1.0 gm Pyrex frit #7740
0.17 gm Boron
0.10 gm 3XD aluminum powder
2.0 ml Alze

K-2.** U-1 + 3XD aluminum powder (10:1)

L-2.** A-1 + 3XD aluminum powder (10:1)

M-2.** H-1 + 3XD aluminum powder (10:1)

N-2.** 0.6 gm Pyrex frit #7740
0.3 gm Al_2O_3
0.1 gm Boron
1.1 ml Alze

O-2.** 0.2 gm Pyrex frit #7740
0.2 gm $CbSi_2$
0.2 gm 60% Si - 20% Cr - 20% Fe (alloyed powder)
0.03 gm Boron
1.5 ml Alze

P-2.** 0.6 gm Pyrex frit #7740
0.3 gm Al_2O_3
0.1 gm Boron
0.2 gm 3XD aluminum powder
2.0 ml Alze

R-2.** 0.2 gm Pyrex frit #7740
0.2 gm $CbSi_2$
0.2 gm 60% Si - 20% Cr - 20% Fe (alloyed powder)
0.03 gm Boron
0.01 gm 3XD aluminum powder
1.3 ml Alze

S-2.** 1.0 gm Pyrex frit #7740
0.5 gm Silicon
0.17 gm Boron
2.0 ml Alze

T-2.** 1.0 gm Pyrex frit
0.5 gm Silicon
0.05 gm 3XD aluminum powder
0.17 gm Boron
2.0 ml Alze

U-2.** 0.6 gm Pyrex frit #7740
0.3 gm Al_2O_3
0.1 gm Boron
1.0 ml Krylon spray, clear (no. 1303)

V-2.** 1.0 gm Pyrex frit #7740
0.3 gm B_2O_3
1.0 ml Alze

W-2.** 1.0 gm Pyrex frit #7740
0.05 gm B_4Si
1.0 ml denatured alcohol

X-2.** 0.6 gm Pyrex frit #7740
0.3 gm Al_2O_3
0.3 gm B_4Si
1.2 ml denatured alcohol

Y-2.** 0.5 gm Pyrex frit #7740
0.5 gm $CbSi_2$
0.5 gm 60% Si - 20% Cr - 20% Fe (alloyed powder)
0.025 gm B_4Si
2.0 ml denatured alcohol

Z-2.** 1.0 gm Pyrex frit #7740
0.05 gm B_4Si
1.0 ml Cenilac

A-3.** 1.0 gm Pyrex frit #7740
0.05 gm B_4Si
1.0 ml Alze

* Hand mixed until homogeneous

** Ball-milled 1 hour

*** Ball-milled 2 hours

APPENDIX B - TEST MATERIALS

1. Columbium alloy (Cb-752) R-512E Sylvania coated specimens, 2 x 2.25 x 0.025 inch and 1 x 2.25 x 0.025 inch.
2. Columbium alloy (C-129Y) VH-109 VAC-HYD coated specimens, 2 x 2 x 0.027 inch and 1 x 2 x 0.027 inch.
3. Pyrex frit No. 7740 (-325 mesh).
4. Al_2O_3 (-270 mesh).
5. Boron, amorphous, (-325 mesh).
6. Cenilac (6 parts Cellulose nitrate lacquer to 5 parts TTT 226 lacquer thinner).
7. Columbium silicide (-325 mesh).
8. Silicon Carbide (-325 mesh).
9. Sauereisen No. 8.
10. Distilled water.
11. Positive Sol, (PS-7), AL_2O_3 stabilized colloidal silica.
12. Syton, NH_4^+ stabilized colloidal silica.
13. AC-55 (acrylic emulsion).
14. Ceramacast 505.
15. Columbium Aluminide (-325 mesh).
16. Sodium Fluoride, reagent grade.
17. 60% Si - 20% Cr - 20% Fe (-325 mesh alloy; 99.9% purity).
18. Silicon (-325 mesh).
19. Chromium (-325 mesh).
20. Iron (3 microns).
21. Liquid Bright Gold (conversion), Hanovia.
22. Tungsten metal powder, purified.
23. Tantalum (-325 mesh).

24. Hafnium (8 microns).

25. Sodium Silicate Solution, Technical (40-42° Be').

26. Krylon aluminum spray paint (No. 1402).

27. Krylon spray, clear (No. 1303).

28. Alze, (supersaturated solution of Zein in denatured alcohol).

29. Pratt & Lambert aluminum paint (No. 7897).

30. Phelan's aluminum paint (No. 292).

31. Reynolds 3XD aluminum powder.

32. Silicon (325 mesh).

33. Denatured alcohol.

34. Boron silicide (200 mesh).

APPENDIX C

PROCEDURE FOR APPLICATION OF A CERAMIC REPAIR COAT TO R-512E COATED Cb-752 ALLOY OR VH-109 COATED C-129 ALLOY

1. Damaged area to be prepared and cleaned by grit blasting:
   a. The defect area and 1/32-inch surrounding this area shall be exposed by masking off the surrounding area at least 8 inches from defect with a double thickness of platers tape. A 1/8-inch thick aluminum template may be used instead of the tape.
   b. The exposed area is then subjected to fused aluminum oxide (-220 mesh) grit, using a suction gritblaster with a 40 lbs/in^2 air pressure through a 3/8-inch nozzle at a distance of 3-1/4 inches. The length of grit blasting time is determined by the coating thickness. Initially a color change is noted, from a light gray to a dark gray which indicates the base metal has been exposed. This procedure (depending on coating thickness) requires 12 to 22 seconds, an additional 60 seconds of grit blasting insures complete removal of residual coating and slight entry into the base metal.

      The tape (or template) is then removed and the defect area lightly brushed to remove foreign particles.
2. After the preparatory procedures have been accomplished, the repair slurry is applied with a No. 3 artist brush or sprayed on using a Sprayon Jet Pak. Stirring, shaking or ball milling may be used to insure a homogeneous mixture of this slurry prior to use. After application of repair slurry over defect (and 1/8-inch overlap) by brush, this slurry is air dryed for 5 minutes then gently but firmly pressed with a flat surfaced spatula to dissipate any possible entrapment of bubbles and also to maintain the height of the repair within 10 mils. After compaction of the slurry with the spatula, the repair slurry is air dryed for 30 minutes and then fused, using a spot heater or pyropanel capable of maintaining a temperature of 2050°F for 5 minutes.

   The second method of application of the repair slurry is with the Sprayon Jet Pak unit. After thorough mixing of the repair slurry, it is sprayed over the surface of the defect (and partially on the undamaged coating) until the repair slurry is slightly above the surface of the fused slurry silicide coating. This procedure is performed by maintaining the

nozzle of the "jet pak" approximately 7-8 inches from the defect and making 6 passes over the defect allowing one minute drying time between each pass.

Both of the above mentioned applications of the repair slurry need not be fused immediately. Fusion may be accomplished during service if the temperature obtained is to be equal to or greater than 2050°F.

APPENDIX D

FULL SIZE COLUMBIUM PANEL EVALUATION

TEST PLAN

1.0 INTRODUCTION

The culmination of this program produced two rib stiffened columbium panels, 20 by 20 inches. These panels contain field repair coatings on the exterior skin, as described in section 13, to provide for a final evaluation of the repairs by NASA on full scale hardware. This test plan provides a recommended test procedure and set of environmental parameters to be used to evaluate the field repair coatings developed. The accessory fixture hardware was designed to be used with the MSFC apparatus designed for evaluation of Space Shuttle thermal protection systems as described in reference (1). The accessory fixture design provides for accepting two types of panels, a rib stiffened panel, 20 by 20.1 inches, and a single faced vee corrugated panel, 18.5 by 20.4 inches.

The test conditions recommended are based on the parameters employed in the evaluation of the 3 by 12-inch rib stiffened panels tested to 110 reentry flight simulation cycles described in section 12. The test sequence employs three alternately repeated evaluation test exposures: (1) an acoustic boost simulation cycle, (2) a static room temperature load to simulate boost and landing and (3) a reentry flight simulation exposure which combines temperature, reduced air pressure and loads which are varied simultaneously as a function of time.

2.0 MANUFACTURING AND COATING OF ACCESSORY HARDWARE

The accessory fixture for integrating the MDAC columbium panels into the MSFC test apparatus is shown in figures D-1 and D-2. Most of the accessory fixture is to be fabricated from columbium and then fused slurry silicide coated. The alloy is not designated on the drawing, but any of the group of Cb-752, C-129Y or FS-85 is considered acceptable. The following material properties were employed in the design.

a) Tensile yield strength at R.T. - - - - 55 KSI
b) Tensile ultimate strength at R.T.- - - 70 KSI
c) Tensile elongation at R.T. - - - - - - 20%
d) Tensile yield strength at 2400°F - - - 25 KSI
e) Thermal expansion- - - - - - - - - - - 4×10^{-6}/°F

The fabrication of detail parts involves simple sheet metal cutting and forming operations. The detail parts require fused slurry silicide coating with [illegible]E or equivalent. Total coating thickness should be 3.0 mils per surface or a dimensional change thickness of 2.0 mils per coated surface.

The coated columbium threaded fasteners required are presented in detail on the McDonnell Standard Parts Sheets 3M317 and 3M318 of figures D-3 and D-4. These Standard Parts Sheets furnish all the necessary information to produce the fasteners and sources for procurement found acceptable to MDAC. The TAPCO coating specified can be replaced satisfactorily with the fused slurry silicide coating, but the coating dimensional change thickness of 2.0 plus or minus 0.4 mils per surface must be maintained for proper thread engagement.

3.0 SPECIMEN PREPARATION

The initial step in preparing the specimen for testing should be to attach the support beam, end adapters and side adapters to the test panel specimen. The 0.15-inch thermal expansion gaps on each side and end of the panel must be maintained and the total panel specimen and fixture assembly must be 39 by 39 inches. One drop of a glass matrix sealing compound designated U-1 shall be placed in the expansion joint between the end and side adapters to prevent air leakage during testing. This U-1 sealing compound can be obtained from MDAC or prepared in accordance with appendix C formulation. This material is compatible with the fused slurry silicide coating and can be used, if required, to seal between the panel and -11 edge seal retainer or -8 retention spring clip. The panel support frame should be positioned in the center of the test chamber, the panel assembly located on the support posts and the panel assembly leveled by adjusting the movable floor of the test apparatus. Finally, the apparatus hold-down bar can be bolted into place.

4.0 TEST CONDITIONS

The recommended test conditions include a boost acoustic cycle, a boost static proof loading and a reentry heating and load cycle. One element of the sequence can be employed separately or any combination of the three elements used.

4.1 Acoustic Boost Simulation - It is recommended that the boost acoustic simulation be performed for a total of 3000 seconds (30 seconds per cycle times 100 cycles) at a maximum skin stress of 3020 psi (rms) at room temperature. The panel frequency range and decibel level must be determined with a strain rosette placed in the geometric center of the panel.

4.2 The static boost load, or proof test load, should be applied at room temperature. The criterion for establishing this load level is to achieve a rib tensile stress of 77% of the room temperature yield stress or a limit load. The Cb-752 panel would require a differential pressure load of 1.82 psi to achieve a rib tensile stress of 57,000 psi.

4.3 The reentry simulation testing involves the simultaneous application of temperature and stress at a predetermined skin air pressure. The recommended test conditions for exterior skin air pressure, skin temperature and differential pressure across the panel are presented in figure D-5.

5.0 EVALUATION CRITERIA AND DATA

The primary criterion for evaluating the rib stiffened panels with field repair coatings will be the ability to carry the required loads without structural failure. The following data should be generated as a function of test cycle to evaluate panel performance beyond standard data such as environmental test parameters, etc:

a) Panel deflection should be measured to establish accumulative creep rate of the panels.

b) A photographic record of repair areas would provide the criteria for establishing a visual inspection procedure.

c) A record of coating failures in non-repair area should be kept to establish coating performance. Unscheduled field repairs, if required, should be monitored to obtain data on field repairs made under true field conditions.

6.0 REFERENCE

(1) Research Inc. Fixture Drawing E39051, "Vacuum Test Fixture for TPS Samples," with instruction manual and other supporting drawings, dated 15 January 1971.

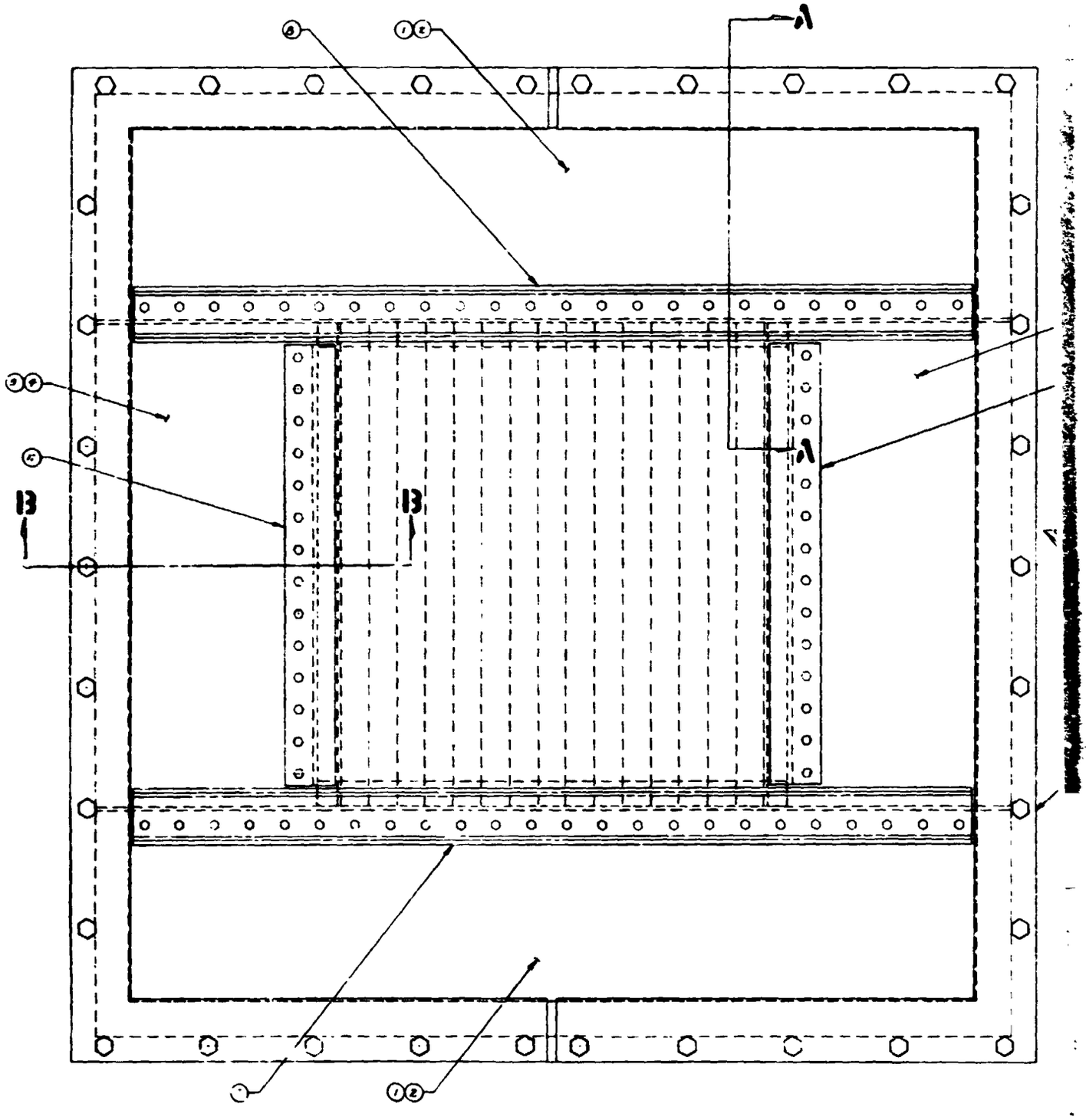

457-3398

FIGURE D-1

FOLDOUT #2

NOTES:

1. DIMENSIONS AFTER COATING (R SIDE) WILL BE 0.008 INCH GREATER PER COATED SURFACE THAN THE DIMENSIONS SHOWN.
2. EXPANSION GAP BETWEEN PANEL AND -1 OR -2 END ADAPTER SHOULD BE .15 INCH ON EACH END OF THE PANEL
3. EXPANSION GAP BETWEEN PANEL SKIN EDGE AND -12 EDGE SEAL SPACER SHOULD BE .15 INCH ON EACH SIDE OF THE PANEL
4. NEOAC GLASS BASED REPAIR COMPOSITION #1 WILL BE PLACED INTO EACH OF FOUR CORNERS AT WHICH END ADAPTERS INTERSECT EDGE ADAPTERS. ONE DROP REQUIRED.
5. THE CAVITY BELOW THE PANEL SHALL BE FILLED WITH A SUITABLE INSULATION TO PREVENT RADIANT HEAT LOSSES FROM PANEL TO TEST CHAMBER.
6. ENTIRE PANEL AND ADAPTER ASSEMBLED WILL BE 39 x 39 INCHES.
7. FABRICATE PANEL SUPPORT FRAME FROM 1 INCH DIAMETER SPECIALITY ROD STOCK AND WELD COMPATIBLE ½ INCH SHEET STOCK.

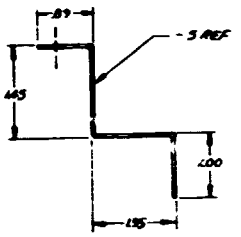

DETAIL C

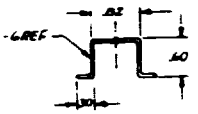

DETAIL D

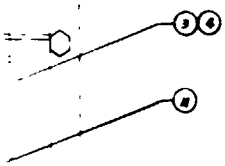

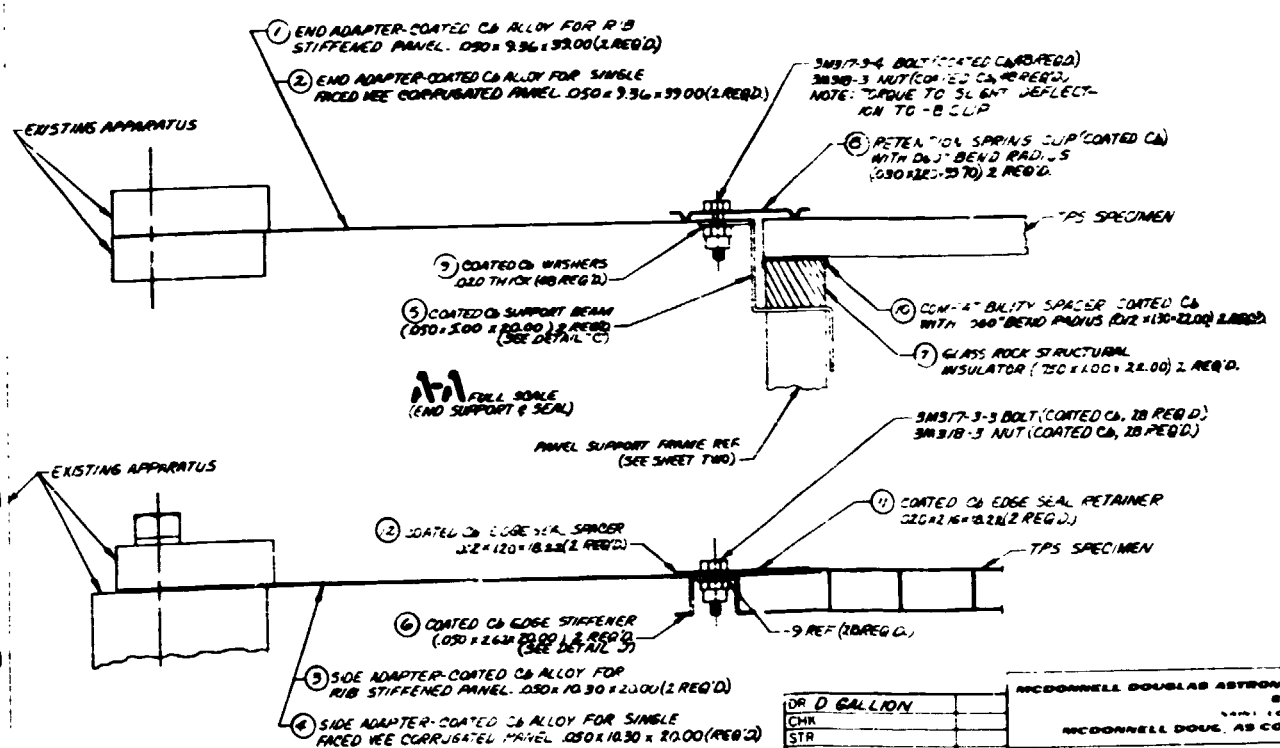

B-B FULL SCALE (LATERAL SEAL)

DR	D GALLION	
CHK		
STR		
GR		

MCDONNELL DOUGLAS ASTRONAUTICS COMPANY
EASTERN DIVISION
MCDONNELL DOUG. AS CORP. "BA." ION

ACCESSORY FIXTURE FOR INTEGRATING Cb PANELS INTO NASA TEST APPARATUS

SIZE	CODE IDENT NO	
	76301	12336H

SCALE ½ | WT | LB | SHEET 1

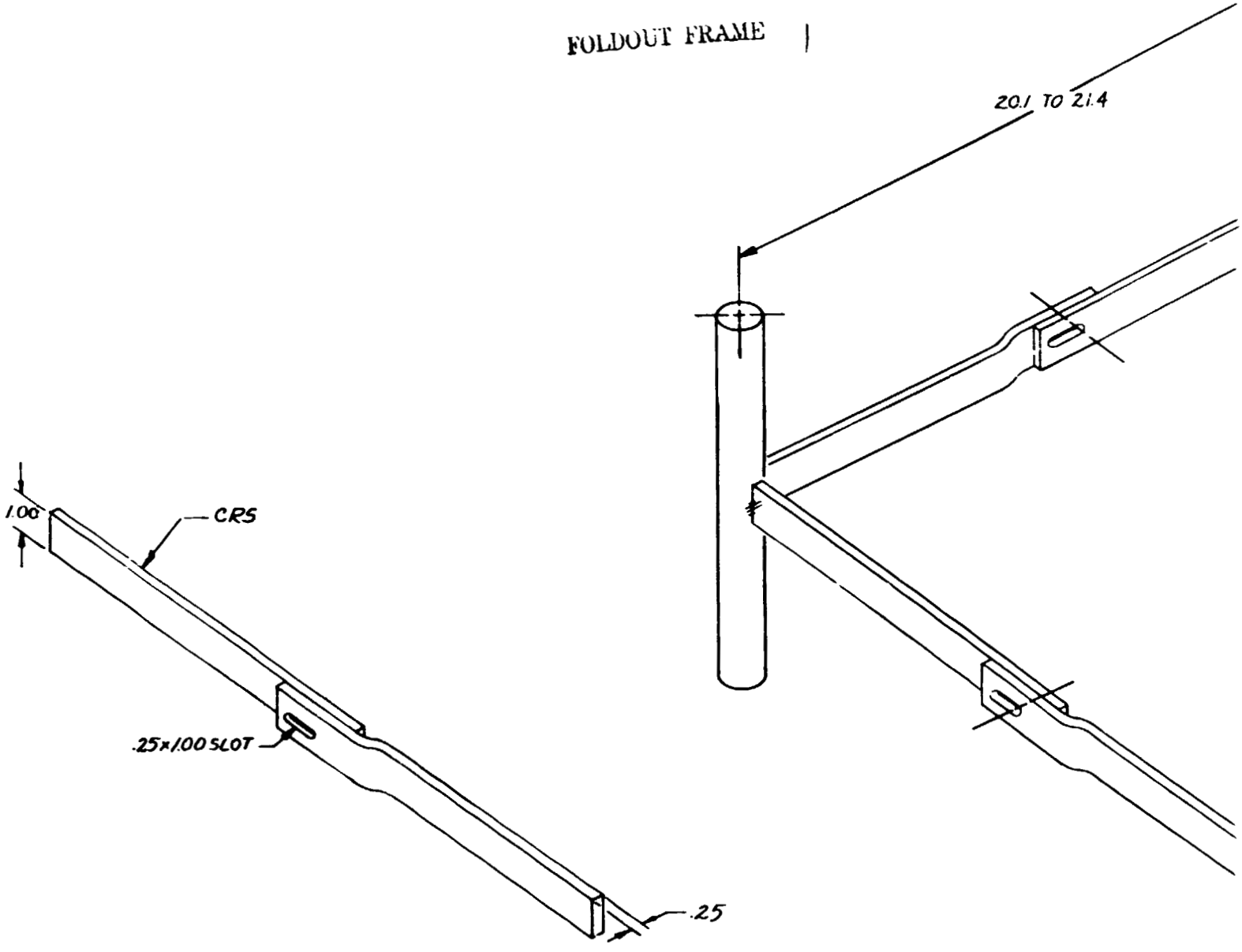

457-3399

PANEL SUPPORT FRAME

FIGURE D-2

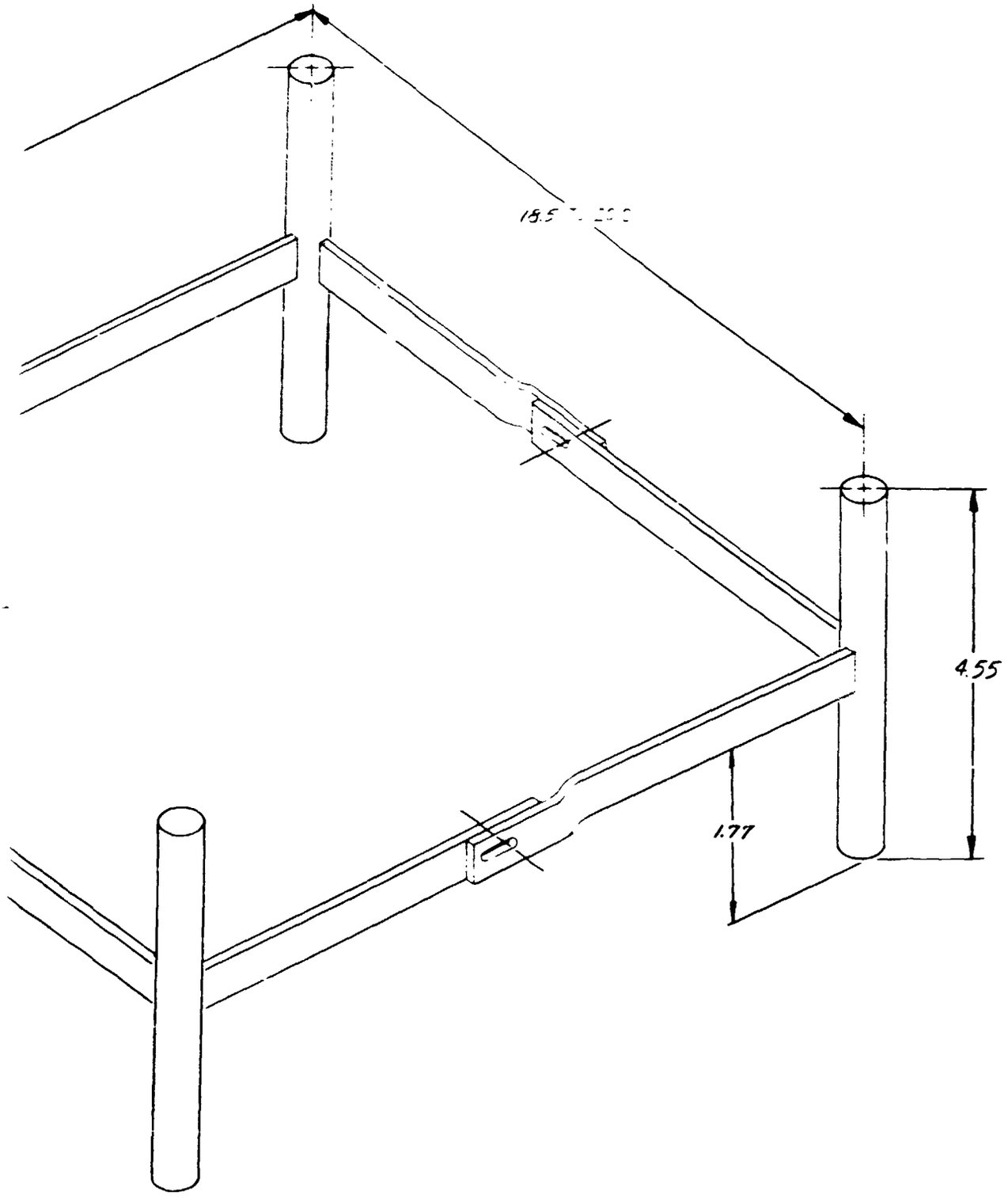

MCDONNELL DOUGLAS ST. LOUIS	SIZE	CODE IDENT NO. 76301	ACCESSORY FIXTURE FOR INTEGRATING C$_b$ PANELS INTO NASA TEST APPARATUS
	SCALE 1/2	REV	SHEET 2

PAGE 86

MCDONNELL

ST LOUIS MISSOURI

JUNE 1967

PAGE 88

STANDARD PARTS

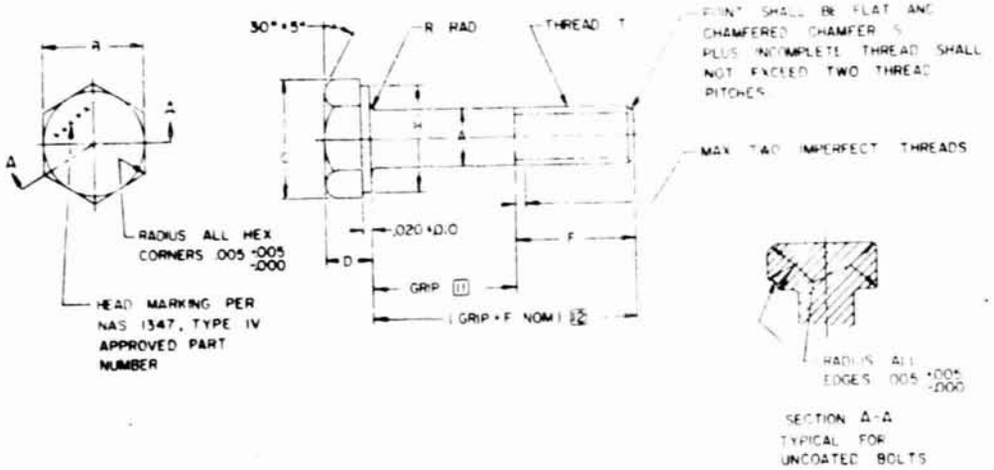

TABLE I

APPROVED PART NUMBER	THREAD T SPECIAL FORM	AFTER COAT DIMENSIONS A DIA.	B	C REF.	D	F REF.	H MIN.	R REF.	S CHAMFER	ROOM TEMP [2] TENSION LB-MIN	APPROX. TENSION 2500°F LBS [3]
3M317-3-( )	.1900-32	.1914 .1899	.377 .365	.43	.142 .125	.468	.359	.008	.032×45°	1072	344
3M317-4-( )	.2500-28	.2519 .2495	.440 .428	.51	.173 .156	.468	.422	.008	.032×45°	2070	662
3M317-5-( )	.3125-24	.3139 .3115	.502 .490	.58	.205 .188	.531	.484	.008	.032×45°	3337	1068

TABLE II

INTERIM [1] PART NUMBER	THREAD T SPECIAL FORM	BEFORE COAT DIMENSIONS A DIA.	B	C REF.	D	F REF.	H [4] MIN.	R RAD	S CHAMFER	ROOM TEMP [2] TENSION LB-MIN
3M317-3-( )U	.1900-32	.1868 .1864	.3724 .3634	.426	.1374 .1724	.466	.3564	.015 .005	.030×45°	1430
3M317-4-( )U	.2500-28	.2473 .2469	.4354 .4254	.506	.1684 .1534	.466	.4194	.015 .005	.030×45°	2760
3M317-5-( )U	.3125-24	.3093 .3089	.4973 .4874	.576	.2004 .1804	.529	.4814	.015 .005	.030×45°	4450

TABLE III

THREAD DIMENSIONS AFTER COAT APPROVED PART NUMBER	MAJ. DIA	PITCH DIA.	MINOR DIA. REF.	ROOT RAD. REF.	CREST RAD. REF.	BEFORE COAT INTERIM [1] PART NUMBER	MAJ. DIA	PITCH DIA.	MINOR DIA	ROOT RAD	CREST RAD.
3M317-3-( )	.1874 .1810	.1687 .1633	.1508	.0060	.0064	3M317-3-( )U	.1878 .1784	.1595 .1501	.1492 .1452	.0084 .0071	.0034 .0019
3M317-4-( )	.2473 .2406	.2258 .2203	.2068	.0070	.0080	3M317-4-( )U	.2427 .2378	.2166 .2151	.2047 .2002	.0095 .0080	.0041 .0024
3M317-5-( )	.3099 .3023	.2914 .2755	.2618	.0082	.0088	3M317-4-( )U	.3053 .2997	.2752 .2736	.2607 .2557	.0108 .0091	.0050 .0030

APPROVED JANUARY 1986	MCDONNELL STANDARD	CODE IDENT NO. 76381
© JUNE 1967	TITLE: BOLT - HEX HEAD, TAPCO COATED, COLUMBIUM ALLOY	3M317
457-3391		SHEET 1 OF 3

Figure D-3

PAGE NO.

MCDONNELL

ST LOUIS MISSOURI

JUNE 1967

PAGE NO

STANDARD PARTS

ENGINEERING INFORMATION

⚠ THIS NUMBER IS TO BE USED FOR PURPOSE OF PROCUREMENT AND STOCKING OF UNCOATED BOLTS ONLY AND SHALL NOT BE SPECIFIED ON PRODUCTION DRAWINGS.

2. THESE BOLTS ARE INTENDED FOR USE IN SINGLE MISSION VEHICLES AT TEMPERATURES UP TO 2700°F.

⚠ TABULATED ROOM TEMPERATURE TENSION STRENGTH *BEFORE COAT VALUES ARE BASED ON VENDOR TESTING AND* ARE FOR INSPECTION PURPOSES ONLY. AFTER COAT VALUES ARE BASED ON TESTING WITH COATED 3M318 SERIES NUTS AND MAY BE CONSIDERED MINIMUM ULTIMATE BOLT STRENGTH FOR PURPOSES OF DEVELOPING DESIGN ALLOWABLES. TABULATED 2500°F TENSION STRENGTH REPRESENTS A PROXIMATIONS BASED ON LIMITED FASTENER TESTING AT TEMPERATURE.

CODE: FIRST DASH NUMBER DESIGNATES NOMINAL DIAMETER IN .062 INCH INCREMENTS. SECOND DASH NUMBER DESIGNATES GRIP LENGTH IN .062 INCH INCREMENTS. "U" AFTER SECOND DASH NUMBER DESIGNATES UNCOATED BOLTS ( ).

EXAMPLE: 3M317-4-8 DESIGNATES A COATED COLUMBIUM 1/4 INCH DIAMETER HEX HEAD BOLT WITH A .500 INCH GRIP LENGTH.

MATERIAL: COLUMBIUM ALLOY PER MAC MMS 175.

COATING: TAPCO COATING PER MAC MMS 573 (.0016 - .0024 INCH THICKNESS PER SURFACE.)

NOTES:

1. PROCUREMENT SPECIFICATION: NONE.
2. THIS STANDARD TAKES PRECEDENCE OVER DOCUMENTS REFERENCED HEREIN.
3. REFERENCED DOCUMENTS SHALL BE OF THE ISSUE IN EFFECT ON DATE OF INVITATION FOR BID.
4. PRE COAT TREATMENT: 3M317-( )-( )U SERIES BOLTS SHALL BE PICKLED .0001 - .0003 INCH PER SURFACE PER MAC P.S. 13154 PRIOR TO COATING (NOT APPLICABLE TO BOLT MFG.)
5. 3M317-( )-( )U SERIES BOLTS AS SUPPLIED BY THE BOLT MANUFACTURER SHALL BE COLOR CODED WITH A BAND AT THE CENTER OF THE SHANK PORTION OF THE BOLT PER MAC P.S. 16007. WIDTH OF BAND NOT TO EXCEED 25% OF THE SHEAR BEARING AREA.
6. BEARING SURFACE SQUARENESS OF 3M317-( )-( )U SERIES BOLTS: WITHIN .002 TIR WITH SHANK.
7. WASHER FACE DIAMETER OF 3M317-( )-( )U SERIES BOLTS: MAXIMUM NOT TO EXCEED WIDTH ACROSS FLATS.
8. CONCENTRICITY OF 3M317-( )-( )U SERIES BOLTS: "H" AND "A" DIAMETERS WITHIN .005 TIR FOR 3/16 SIZE, .006 TIR FOR 1/4 SIZE AND .007 TIR FOR 5/16 SIZE. "A" DIAMETER AND THREAD PITCH DIAMETER WITHIN .0045 TIR ON ALL SIZES.
9. SHANK STRAIGHTNESS OF 3M317-( )-( )U SERIES BOLTS: WITHIN .0040 TIR PER INCH OF LENGTH FOR 3/16 SIZE AND .0030 TIR PER INCH OF LENGTH FOR 1/4 AND 5/16 SIZES.
10. SURFACE ROUGHNESS OF THE 3M317-( )-( )U SERIES BOLTS PER MIL-STD-10: MAXIMUM RMS UNDERSIDE OF HEAD, HEAD TO SHANK FILLET RADIUS, SHANK, AND ALL THREAD ELEMENTS -32. ALL OTHER SURFACES 125.
11. GRIP LENGTH TOLERANCE, *BEFORE COAT* +.013/-.0077, AFTER COAT ±.010.
12. OVERALL LENGTH TOLERANCE BEFORE COAT +.000/-.015, AFTER COAT ± .021/-.016.
13. BOLT HEADS SHALL BE HOT FORGED. THREADS SHALL BE COLD ROLLED BY A SINGLE ROLLING PROCESS.
14. TEST AND DATA REQUIREMENTS: 3M317-( )-( )U SERIES BOLTS ONLY. VENDOR SHALL SUBMIT WITH EACH LOT DATA AS REQUIRED BELOW:
    - A. EXAMINATION OF THE PRODUCT: (EXCLUDING SURFACE CONDITION)
      DATA REQUIRED - CERTIFICATION OF CONFORMANCE.
      SAMPLE SIZE PER LOT - MIL-B-6812 PARAGRAPH 4.3.1
      CLASSIFICATION OF DEFECTS - MIL-B-6812 PARAGRAPH 4.3.1.2.1 AS APPLICABLE
      ACCEPTANCE CONDITION - PER DWG REQUIREMENT.
    - B. EXAMINATION OF THE PRODUCT (SURFACE CONDITION):
      DATA REQUIRED - CERTIFICATION OF CONFORMANCE.
      SAMPLE SIZE PER LOT - 100% INSPECTION.
      ACCEPTANCE CONDITION - BOLTS SHALL BE COMPLETELY FREE OF *SURFACE CONTAMINATION* (NO SURFACE DISCOLORATION ALLOWED.)
    - C. SURFACE DISCONTINUITIES: (FLUORESCENT PENETRANT INSPECTION).
      DATA REQUIRED - CERTIFICATION OF CONFORMANCE.
      SAMPLE SIZE PER LOT - 100% INSPECTION
      ACCEPTANCE CONDITION - NO DISCONTINUITIES ALLOWED.
    - D. MATERIAL CERTIFICATION
      DATA REQUIRED - VENDOR REPORTS PER MMS 175, PARAGRAPH 4.4 (MATERIAL SUPPLIER LAB REPORTS MAY BE SUBMITTED IN LIEU OF VENDOR REPORTS.)
      SAMPLE REQUIRED - A SUITABLE LENGTH OF RAW MATERIAL *FROM THE ENDS OF THE SPOOL (COIL)* OF WIRE ROD USED SHALL BE TAKEN AT THE START AND AT THE COMPLETION OF EACH MACHINE RUN. SAMPLE LENGTHS SHALL BE ANALYZED AND CERTIFIED. ADDITIONAL SAMPLE LENGTHS SHALL BE INCLUDED WITH THE DELIVERY OF FASTENERS.
    - E. ROOM TEMPERATURE TENSION TEST
      DATA REQUIRED - ACTUAL FAILING VALUES AND MODE OF FAILURE. SAMPLE SIZE - 3 PER LOT. $R_e = 1$
      TEST NUT SHALL BE OF SUFFICIENT STRENGTH TO INSURE BOLT FAILURE. (Rc 43 MAX.)
      THREAD FORM OF TEST NUTS SHALL CONFORM TO THE DIMENSIONS OF COATED 3M318 NUTS.
      MINIMUM ACCEPTANCE VALUE - PER DRAWING TABULATION.
15. PACKAGING 3M317-( )-( )U SERIES BOLTS ONLY. ALL FASTENERS SHALL BE *INDIVIDUALLY* PACKAGED IN POLYETHYLENE BAGS, MANILA ENVELOPES, (OR EQUIVALENT) AND IDENTIFIED BY EXTERIOR MARKING OF THE CONTAINER AS FOLLOWS:
    VENDOR NAME _____
    PART NUMBER _____
    MATERIAL TYPE-COMPOSITION _____
    LOT NUMBER _____
16. PACKAGING 3M317-( )-( ) FASTENERS ONLY. ALL FASTENERS SHALL BE INDIVIDUALLY PACKAGED IN POLYETHYLENE BAGS, MANILA ENVELOPES, (OR EQUIVALENT) AND IDENTIFIED BY EXTERIOR MARKING OF THE CONTAINER AS FOLLOWS:
    COATING APPLICATOR NAME AND ADDRESS _____
    COATING RUN LOT NUMBER _____
    PROJECT CONCERNED _____

INTERMEDIATE PACKAGING SHALL INCLUDE PROVISIONS FOR INHIBITING MOVEMENT OF UNIT PACKAGES WHICH COULD RESULT IN DAMAGE TO THE COATED FASTENER.

APPROVED JANUARY 1966 REVISED © JUNE 1967	MCDONNELL STANDARD	CODE IDENT NO. 78381
	TITLE: BOLT - HEX HEAD, TAPCO COATED, COLUMBIUM ALLOY	3M317 SHEET 2 OF 3

457-3392

Figure D-3 (Continued)

PAGE NO.

MCDONNELL

ST. LOUIS, MISSOURI

JUNE 1967

STANDARD PARTS

PAGE NO.

INFORMATION BELOW THIS LINE NOT PERTINENT TO ENGINEERING DESIGN

PART NUMBER ◆	APPROVED VENDOR	SUPERSEDED PARTS (NOT APPROVED FOR PROCUREMENT) DISPOSITION DIRECTIONS
3M317-( )( )U	▲	NONE
3M317-( )( )	■	NONE

PROCUREMENT REQUIREMENTS: 3M317 REV. C

RECEIVING INSPECTION REQUIREMENTS: 3M317 REV. C
43M138 [3M317-( )( )U AND 3M317-( )( ) SERIES]
MMS573 SECTION 4 [3M317-( )( ) SERIES ONLY]

▲ APPROVED VENDORS AND IDENT NO'S: STANDARD PRESSED STEEL COMPANY JENKINTOWN, PENNSYLVANIA (03681)
VOI SHAN MFG. COMPANY, CULVER CITY, CALIFORNIA (92215)

NOTES:
■ 1. SEE MMS 573 FOR APPROVED SOURCES FOR APPLICATION OF COATING.
◆ 2. MAC SHALL PROCURE UNCOATED BOLTS ONLY, AND ONLY FROM THE SOURCES INDICATED BY "▲". MAC SHALL THEN SHIP UNCOATED BOLTS TO SOURCES INDICATED BY "■" FOR COATING.

THE ABOVE LISTED VENDORS ARE THE ONLY SOURCES FOR NUTS SHOWN HEREON APPROVED FOR PROCUREMENT AND/OR USE ON MCDONNELL PRODUCTS. VENDORS OF COMPETITIVE ARTICLES MAY APPLY TO THE MCDONNELL STANDARDS ENGINEERING DEPARTMENT FOR APPROVAL AS A SOURCE OF SUPPLY.

APPROVED JANUARY 1966 REVISED © JUNE 1967	MCDONNELL STANDARD	CODE IDENT NO. 70331
	TITLE: BOLT - HEX HEAD, TAPCO COATED, COLUMBIUM ALLOY	3M317 SHEET 2 OF 2

457-3393

Figure D-3 (Continued)

PAGE NO.

MCDONNELL

ST LOUIS MISSOURI

JUNE 1967

PAGE NO.

STANDARD PARTS

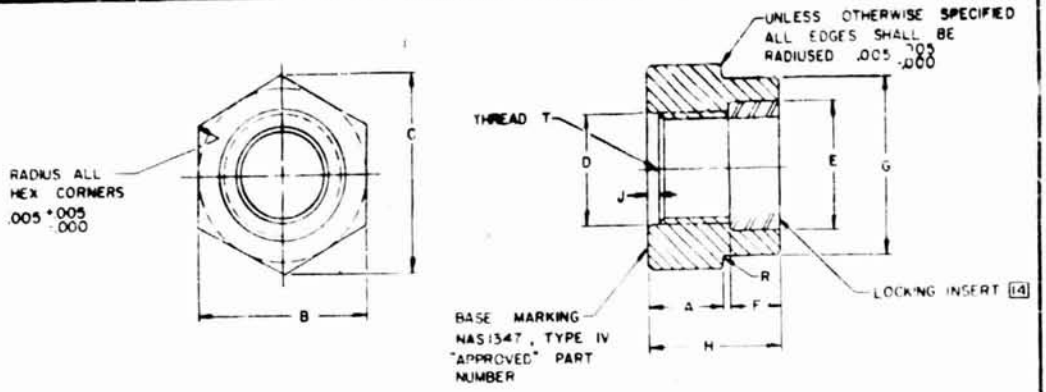

TABLE I

AFTER COAT DIMENSIONS WITH/WITHOUT INSERT															
APPROVED PART NUMBER	INTERIM PART NUMBER (SEE CODE)	THREAD T SPECIAL FORM	A	B	C REF.	D DIA. MIN.	E DIA.	F	G DIA. MIN.	H MAX.	J C'BORE MIN.	R RAD REF.	ROOM TEMP TENSILE LBS - MIN.	APPROX. TENSION 2500°F LBS.
3M318-3	3M318-3L	.1900-32	.151 .141	.377 .365	.430	.1986	.3134 .3064	.110 .100	.3650	.3550	.062	.013	1072	344
3M318-4	3M318-4L	.2500-28	.197 .187	.440 .428	.506	.2595	.3684 .3614	.110 .100	.4280	.3730	.062	.013	2070	662
3M318-5	3M318-5L	.3125-24	.265 .255	.502 .490	.580	.3231	.4226 .4171	.110 .100	.4900	.3980	.062	.013	3337	1068

TABLE II

BEFORE COAT DIMENSIONS												
INTERIM PART NUMBER (SEE CODE)	THREAD T SPECIAL FORM	A	B	C REF.	D DIA. MIN.	E DIA.	F	G DIA. MIN.	H MAX.	J C'BORE MIN.	R RAD MIN.	ROOM TEMP TENSILE LBS-MIN
3M318-3LU	.1900-32	.146 .136	.3734 .3634	.436	.2032	.3210 .3110	.110 .100	.3634	.2504	.062	.0200 .0100	1470
3M318-4LU	.2500-28	.192 .184	.4354 .4254	.502	.2641	.3710 .3660	.110 .100	.4254	.3684	.062	.0200 .0100	2760
3M318-5LU	.3125-24	.240 .232	.4974 .4874	.576	.3277	.4250 .4200	.110 .100	.4874	.3914	.063	.0200 .0100	4450

TABLE III

THREAD DIMENSIONS											
AFTER COAT WITH/WITHOUT INSERT						BEFORE COAT					
APPROVED PART NUMBER	INTERIM PART NUMBER (SEE CODE)	MAJ. DIA REF.	PITCH DIA.	MINOR DIA.	MAJ. DIA. RAD. TYP.	INTERIM PART NUMBER (SEE CODE)	MAJ. DIA.	PITCH DIA.	MINOR DIA.	MAJOR DIA. RAD.
3M318-3	3M318-3L	.1963	.1753 .1697	.1649 .1599	.0017	3M318-3LU	.2032 .1964	.1805 .1789	.1675 .1645	.0048 .0022
3M318-4	3M318-4L	.2566	.2326 .2268	.2215 .2165	.0020	3M318-4LU	.2641 .2563	.2378 .2360	.2241 .2111	.0053 .0025
3M318-5	3M318-5L	.3197	.2914 .2854	.2788 .2730	.0024	3M318-5LU	.3277 .3189	.2966 .2946	.2814 .2784	.0059 .0025

APPROVED JANUARY 1966 REVISION © JUNE 1967	MCDONNELL STANDARD TITLE NUT - HEX, TAPCO COATED, COLUMBIUM ALLOY	CODE IDENT NO. 81205 3M318 SHEET 1 OF 3

457 3394

Figure D-4

PAGE NO.

MCDONNELL

ST. LOUIS, MISSOURI

JUNE 1967

PAGE NO.

STANDARD PARTS

ENGINEERING INFORMATION:

⚠1 THESE "INTERIM PART NUMBER" ARE TO BE USED FOR PROCUREMENT AND STOCKING OF NUTS SUBJECT TO SUBSEQUENT PROCESSING. SPECIFY ONLY THE "APPROVED PART NUMBER" ON PRODUCTION DRAWINGS.

⚠2 TABULATED ROOM TEMPERATURE TENSION STRENGTH BEFORE COAT VALUES ARE BASED ON VENDOR TESTING AND ARE FOR INSPECTION PURPOSES ONLY. AFTER COAT VALUES ARE BASED ON TESTING WITH COATED 3M317 SERIES BOLTS AND MAY BE CONSIDERED MIN. ULTIMATE NUT STRENGTHS FOR PURPOSES OF DEVELOPING DESIGN ALLOWABLES. TABULATED 2500°F TENSION STRENGTH REPRESENTS APPROXIMATIONS BASED ON LIMITED FASTENER TESTING AT TEMPERATURE.

3 THESE NUTS ARE INTENDED FOR USE WITH 3M316, 3M317, 3M328, AND 3M329 COATED COLUMBIUM BOLTS.

4 PRODUCTION DRAWINGS SHALL SPECIFY "INSTALL PER MAC P.S. 19111."

CODE:

DASH NUMBER SUFFIXED BY "LU" DESIGNATES AN UNCOATED NUT WITHOUT LOCKING INSERT. ⚠1

DASH NUMBER SUFFIXED BY "L" DESIGNATES A COATED NUT WITHOUT LOCKING INSERT. ⚠1

DASH NUMBER WITHOUT SUFFIXED CODE LETTER DESIGNATES THE COMPLETED NUT, COATED, WITH INSERT INSTALLED.

EXAMPLE:

3M318-4 DESIGNATES A COATED COLUMBIUM SELF-LOCKING HEX NUT TO BE USED WITH 1/4 INCH DIAMETER COATED COLUMBIUM BOLT.

MATERIAL:

NUT BODY - COLUMBIUM ALLOY PER MAC MMS 175.
INSERT - DUPONT POLYMER VESPEL SP1.

COATING:

NUT BODY - TAPCO COATING PER MAC MMS 573. (.0016 - .0024 INCH PER SURFACE).

NOTES:

1. PROCUREMENT SPECIFICATION - NONE.
2. THIS STANDARD TAKES PRECEDENCE OVER DOCUMENTS REFERENCED HEREIN.
3. REFERENCED DOCUMENTS SHALL BE OF THE ISSUE IN EFFECT ON DATE OF INVITATION FOR BID.
4. PRE-COAT TREATMENT - 3M318-( )LU SERIES NUTS SHALL BE PICKLED .0001 TO .0003 INCH PER SURFACE PER MAC P.S. 13154 PRIOR TO COATING (NOT APPLICABLE TO NUT MANUFACTURER).
5. BEARING SURFACE SQUARENESS, RELATIVE TO PITCH DIAMETER CENTERLINE, FOR 3M318-( )LU SERIES NUTS, SHALL CONFORM TO MIL-N-25027.
6. "E" DIMENSION FOR 3M318-( )L SERIES NUTS MAY BE REAMED AFTER COATING TO ORIGINAL DIAMETER BY NUT MANUFACTURER PRIOR TO INSTALLATION OF THE LOCKING INSERT.
7. "H" DIMENSION MINIMUM AND "J" DIMENSION MAXIMUM ARE LIMITED TO THE THREAD LENGTH NECESSARY TO INSURE TENSION FAILURE OF THE 3M317 SERIES BOLTS.
8. "D" DIAMETER MAXIMUM SHALL NOT EXCEED "B" WIDTH.
9. TEST AND DATA REQUIREMENTS - 3M318-( )LU SERIES NUT ONLY. VENDOR SHALL SUBMIT WITH EACH LOT DATA AS REQUIRED BELOW.
   - A. EXAMINATION OF THE PRODUCT (EXCLUDING SURFACE CONDITION)
     DATA REQUIRED - CERTIFICATION OF CONFORMANCE.
     SAMPLE SIZE PER LOT - MIL-N-25027, PARAGRAPH 4.4.1.2.
     CLASSIFICATION OF DEFECTS - MIL-N-25027, PARAGRAPH 4.4.1.2.1 AS APPLICABLE.
     ACCEPTANCE CONDITION - PER DRAWING TABULATION.
   - B. EXAMINATION OF THE PRODUCT (SURFACE CONDITION)
     DATA REQUIRED - CERTIFICATION OF CONFORMANCE.
     SAMPLE SIZE PER LOT - 100% INSPECTION.
     ACCEPTANCE CONDITION - NUTS SHALL BE COMPLETELY FREE OF SURFACE CONTAMINATION. (NO SURFACE DISCOLORATION ALLOWED.)
   - C. SURFACE DISCONTINUITIES (FLUORESCENT PENETRANT INSPECTION)
     DATA REQUIRED - CERTIFICATION OF CONFORMANCE.
     SAMPLE SIZE PER LOT - 100% INSPECTION.
     ACCEPTANCE CONDITION - NO DISCONTINUITIES ALLOWED.
   - D. MATERIAL CERTIFICATION
     DATA REQUIRED - VENDOR REPORTS PER MMS 175, PARAGRAPH 4.4. (MATERIAL SUPPLIER LAB REPORTS MAY BE SUBMITTED IN LIEU OF VENDOR REPORTS)
     SAMPLE REQUIRED - A SUITABLE LENGTH OF RAW MATERIAL FROM THE ENDS OF THE ROD OR BAR USED SHALL BE TAKEN AT THE START AND AT THE COMPLETION OF EACH MACHINE RUN. SAMPLE LENGTHS SHALL BE ANALYZED AND CERTIFIED. ADDITIONAL SAMPLE LENGTHS SHALL BE INCLUDED WITH THE DELIVERY OF FASTENERS.
   - E. ROOM TEMPERATURE TENSION TESTS
     DATA REQUIRED - ACTUAL FAILING RESULTS AND MODE OF FAILURE.
     SAMPLE SIZE - 3 SAMPLES PER LOT, $R_R = 1$
     TEST BOLTS SHALL BE OF SUFFICIENT STRENGTH TO INSURE NUT FAILURE. (Rc 43 MAX)
     THREAD FORM OF TEST BOLT SHALL CONFORM TO THE COATED 3M317 BOLT.
     MINIMUM ACCEPTANCE VALUES - PER DWG. TABULATION.
10. TEST AND DATA REQUIREMENTS: 3M318-( )L SERIES NUTS ONLY. VENDOR SHALL SUBMIT WITH EACH LOT DATA AS REQUIRED BELOW.
    - A. LOCKING TORQUE TEST - ROOM TEMPERATURE.
      DATA REQUIRED - ACTUAL TORQUE VALUES (MAX. LOCKING - MIN. BREAKAWAY)
      SAMPLE SIZE PER LOT - 3 SAMPLES PER LOT, $R_R = 1$
      TEST CONDITION - MIL-N-25027, PARAGRAPH 4.5.3.2.2.1, EXCEPT 7 INSTALLATION AND REMOVAL CYCLES.
      TEST BOLT - THREAD FORM OF TEST BOLTS SHALL CONFORM TO THE DIMENSIONS OF THE COATED 3M317 BOLTS.
      ACCEPTANCE CONDITION - TORQUE VALUES PER MIL-N-25027 TABLE III, EXCEPT MAX. LOCKING TORQUES SHALL BE ONE-HALF MIL-N-25027 VALUES 14.

APPROVED JANUARY 1966	MCDONNELL STANDARD	CODE IDENT NO. 71331
REVISED © JUNE 1967	TITLE NUT—HEX, TAPCO COATED, COLUMBIUM ALLOY	3M318 SHEET 2 OF 3

Figure D-4 (Continued)

PAGE 00.

MCDONNELL

ST. LOUIS MISSOURI

JUNE 1967

PAGE 00.

STANDARD PARTS

11. PACKAGING: 3M318-( )LU SERIES NUTS ONLY.
ALL NUTS SHALL BE INDIVIDUALLY PACKAGED IN POLYETHYLENE BAGS, MANILA ENVELOPES (OR EQUIVALENT) AND IDENTIFIED BY EXTERIOR MARKING OF THE CONTAINER AS FOLLOWS
VENDOR NAME _____
PART NUMBER _____
MATERIAL TYPE _____
LOT NUMBER _____

12. PACKAGING: 3M318-( )L SERIES NUTS ONLY.
ALL NUTS SHALL BE INDIVIDUALLY PACKAGED IN POLYETHYLENE BAGS, MANILA ENVELOPES (OR EQUIVALENT) AND IDENTIFIED BY EXTERIOR MARKING OF THE CONTAINER AS FOLLOWS
COATING APPLICATOR NAME AND ADDRESS _____
COATING RUN LOT NUMBER _____
PROJECT CONCERNED _____
INTERMEDIATE PACKAGING SHALL INCLUDE PROVISIONS FOR INHIBITING MOVEMENT OF UNIT PACKAGES WHICH COULD RESULT IN DAMAGE TO THE COATED FASTENER.

13. PACKAGING: 3M318-( ) SERIES NUTS ONLY.
ALL NUTS SHALL BE INDIVIDUALLY PACKAGED IN POLYETHYLENE BAGS, MANILA ENVELOPES (OR EQUIVALENT) AND IDENTIFIED BY EXTERIOR MARKING OF THE CONTAINER AS FOLLOWS
INSERT MATERIAL TYPE _____
INSERT INSTALLATION PROCESS LOT NUMBER _____
BONDING AGENT _____

14. IN THOSE INSTANCES WHERE THE MAX. LOCKING TORQUE ACCEPTANCE CONDITION PER NOTE 10 IS EXCEEDED, AN ACCEPTABLE MEANS OF PRODUCT MODIFICATION SHALL BE TO CHAMFER THE INSERT I.D. .050 MAX. BY 80°.

INFORMATION BELOW THIS LINE NOT PERTINENT TO ENGINEERING DESIGN

PART NUMBER ◆	APPROVED VENDOR	SUPERSEDED PARTS (NOT APPROVED FOR PROCUREMENT) DISPOSITION DIRECTIONS
3M318-( )LU	▲	NONE
3M318-( )L	■	NONE
3M318-( )	▲	NONE

PROCUREMENT REQUIREMENTS: 3M318 (REV C)

RECEIVING INSPECTION REQUIREMENTS: 3M318 (REV C)
63M139 - (3M318-( )LU, 3M318-( )L AND 3M318-( ) SERIES NUTS).
MMS 373 SECTION 4 - (3M318-( )L SERIES NUTS ONLY).

APPROVED VENDORS AND IDENT NO'S: STANDARDS PRESSED STEEL, JENKINTOWN, PENNSYLVANIA (00660)
VOI SHAN MANUFACTURING COMPANY, CULVER CITY, CALIFORNIA (92215)
ELASTIC STOP NUT CORPORATION, UNION, NEW JERSEY (72962)
KAYNAR MANUFACTURING COMPANY, LOS ANGELES, CALIFORNIA (75237)

NOTES:
■ 1. SEE MMS [illegible] FOR APPROVED SOURCE FOR APPLICATION OF COATINGS.
◆ 2. MAC SHALL PROCURE UNCOATED NUTS ONLY, AND ONLY FROM THE SOURCES INDICATED BY "▲". MAC SHALL THEN SEND UNCOATED NUTS TO SOURCE INDICATED BY "■" FOR COATING. AFTER RECEIPT OF THE COATED PARTS MAC SHALL RETURN THE NUTS TO THE ORIGINAL SOURCE "▲" FOR INSTALLATION OF THE INSERT.

THE ABOVE LISTED VENDORS ARE THE ONLY SOURCES FOR PARTS SHOWN HEREON APPROVED FOR PROCUREMENT AND/OR USE ON MCDONNELL PRODUCTS. VENDORS OF COMPETITIVE ARTICLES MAY APPLY TO THE MCDONNELL STANDARDS ENGINEERING DEPARTMENT FOR APPROVAL AS A SOURCE OF SUPPLY.

APPROVED JANUARY [illegible] © JUNE 1967	MCDONNELL STANDARD	CODE IDENT NO. 81205
	TITLE: NUT - HEX, TAPCO COATED, COLUMBIUM ALLOY	3M318 SHEET 3 OF 3

457-3396

Figure D-4 (Continued)

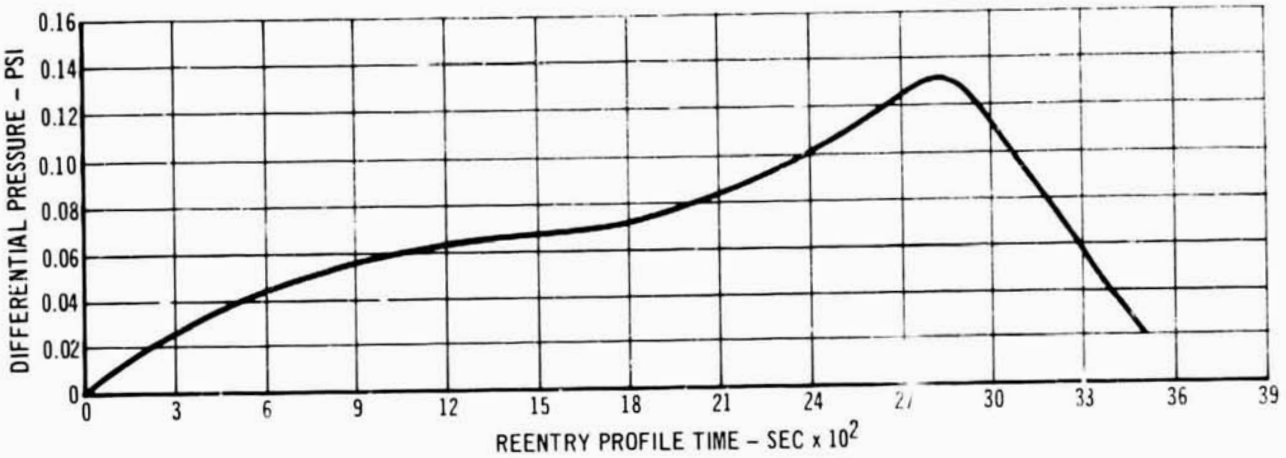

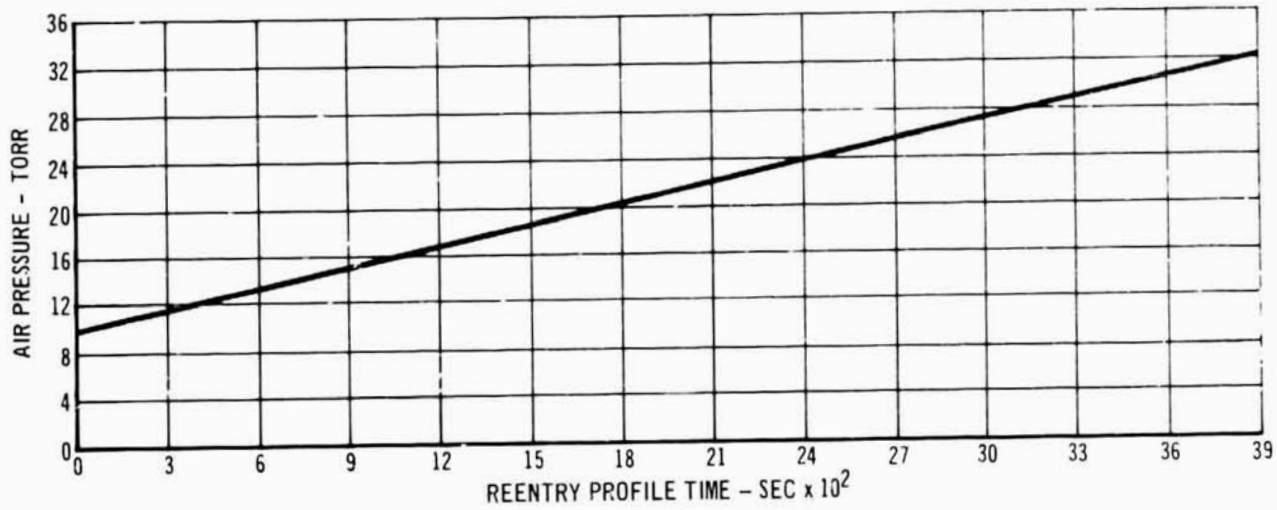

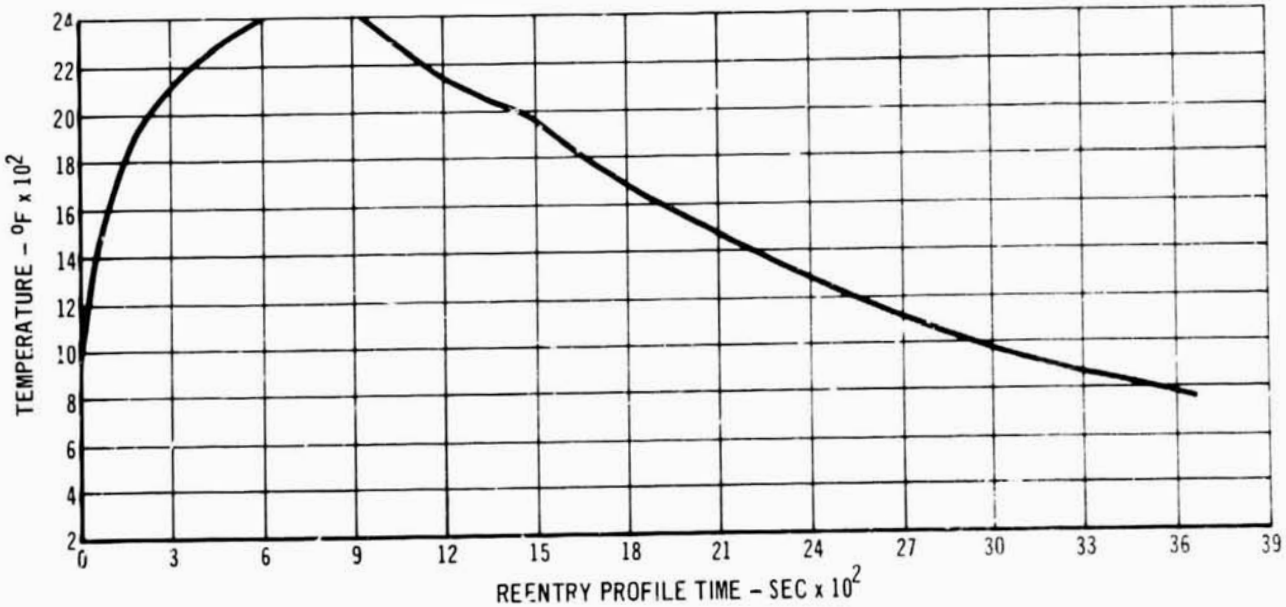

457-3397

RECOMMENDED REENTRY PROFILE TEST CONDITIONS

FIGURE D-5